The University of Sydney

RARE BOOKS LIB

Copyright in relation to this thesis*

Under the Copyright Act 1968 (several provision of which are referred to below), this thesis must be used only under the normal conditions of scholarly fair dealing for the purposes of research, criticism or review. In particular no results or conclusions should be extracted from it, nor should it be copied or closely paraphrased in whole or in part without the written consent of the author. Proper written acknowledgement should be made for any assistance obtained from this thesis.

Under Section 35(2) of the Copyright Act 1968 'the author of a literary, dramatic, musical or artistic work is the owner of any copyright subsisting in the work'. By virtue of Section 32(1) copyright 'subsists in an original literary, dramatic, musical or artistic work that is unpublished' and of which the author was an Australian citizen, an Australian protected person or a person resident in Australia.

The Act, by Section 36(1) provides: 'Subject to this Act, the copyright in a literary, dramatic, musical or artistic work is infringed by a person who, not being the owner of the copyright and without the licence of the owner of the copyright, does in Australia, or authorises the doing in Australia of, any act comprised in the copyright'.

Section 31(1)(a)(i) provides that copyright includes the exclusive right to 'reproduce the work in a material form'. Thus, copyright is infringed by a person who, not being the owner of the copyright, reproduces or authorises the reproduction of a work, or of more than a reasonable part of the work, in a material form, unless the reproduction is a 'fair dealing' with the work 'for the purpose of research or study' as further defined in Sections 40 and 41 of the Act.

Section 51(2) provides that "Where a manuscript, or a copy, of a thesis or other similar literary work that has not been published is kept in a library of a university or other similar institution or in an archives, the copyright in the thesis or other work is not infringed by the making of a copy of the thesis or other work by or on behalf of the officer in charge of the library or archives if the copy is supplied to a person who satisfies an authorized officer of the library or archives that he requires the copy for the purpose of research or study'.

*'Thesis' includes 'treatise', dissertation' and other similar productions.

A FRAMEWORK FOR ADVANCED/INTELLIGENT OPERATION OF EMULSION COPOLYMERISATION REACTORS

by

Bassam Alhamad

B.Sc (Chemical Engineering) Hons,
M.Sc (Instrumentation and Analytical Science) Hons

A thesis submitted in fulfilment of the requirements for the degree of Doctor of Philosophy

Ph.D.

In Process Systems Engineering
Department of Chemical Engineering

The University of Sydney
Australia

2005

Declarations

I declare that the entire contents of this thesis are, to the best of my knowledge and belief, original, unless otherwise acknowledged in the text. I have not submitted this, in whole or part, for another degree at this or any other institution.

BASSAM MOH'D ALHAMAD

Oct 2004

ACKNOWLEDGEMENTS

Beginning, I would like to highly thank my supervisor Prof. Jose Romagnoli, for his guidance and support throughout the thesis. I highly appreciate his knowledge that added a lot to mine. It was a great pleasure for me to study under a well knowledgeable and highly skilled person.

Then, I would like to thank my co-supervisors, Dr. Joseph Zeaiter and Dr. Vincent Gomes for their ongoing assistance and their high inspirations. I also thank Prof. Robert Gilbert for his suggestions and inputs of knowledge in emulsion copolymerisation kinetics. Other are also not to be forgotten, Dr. Reza Mahidasht, Dr. Chris Fergusson, Mrs Jelica Strauch are all acknowledged for their assistance and endurance within the laboratory.

The financial support to the project from the Australian Postgraduate Award scheme and the Key Centre for Polymer Colloids established under the Australian Research Council's Research Centres Program was a high encouragement towards success.

I also acknowledge the University of Bahrain for being a continuous financial support for my studies in Australia. I gained the knowledge, and now I should deliver it, and I'll deliver it all over the world, starting from Bahrain.

My friends in the PSE group are considered as a part of my family, and members of family do not forget each other. We had nice times and memories that will never be forgotten. I would like to hand special thanks to Dr. Joseph Zeaiter, Dr. Ali Abbas, Dr. David Wang, Dr. Hassan Alhammadi, Pablo Rolandi, Shahla Ghaffari, Robert Willis, Mustafa Nowee, Murtada Srour, Abdul Halim Maulud, Bharat Bhushan and Ronald Chew.

The technical and administrative staff in the department had their input towards the success of many students, especially Denis Trevaskis, Annette, Ellen, Javier, Linda, Liz, Jeffrey.

Finally, I would like to thank my parents for their effort, encouraging words, cheering and love feelings, endurance from the time I was young till the time came for them to be proud

of their son, and on my side I am always proud of my parents. My parents, parents in law, my brothers, and brother in law, my sisters in law have always been cheering and helpful with their encouragement and nice words.

I would like to sincerely, with all love to address the best support to my wife Suha, who proved to be a great wife and a special one too, that I had been gifted. My son Yusuf, you are also counted to be a part of my research support.

To My Parents, Wife, Kid, Brothers and Sisters

ABSTRACT

Emulsion copolymerisation processes are of significant industrial importance. Since these processes use water instead of solvents, they are attractive from an environmental point of view. Despite the fact that these processes have been studied for more than 50 years, there are still aspects which are not completely understood due to the complexities of these systems. Emulsion copolymerisation permits the synthesis of an almost unlimited number of polymer types and therefore highlights its advantages in being used in obtaining a better balance of properties for commercial application of polymers.

The industrial importance of emulsion copolymerisation is evident by examining the size of the market and societies constant demand for materials with improved or novel properties. In Western countries alone, the current production of all polymers is in excess of 10^8 tonnes per year, with approximately 30% of this by free radical means. The major applications of polymer latex's are for use in synthetic rubber, high impact polymers, latex foam, latex paints, sealants, adhesives and many other applications. Therefore, the manufacture of polymers with more desirable properties is an important are of research and study. Although emulsion polymerisation processes have been studied extensively since the First World War as noted through large volumes of literature, there are very few papers useful for design and operation of emulsion copolymerisation processes. It is the purpose of this thesis to survey and verify earlier models and to introduce a new model with experimental verification to the particle size distribution (PSD) and molecular weight distribution (MWD), of the produced polymer.

In this thesis, a framework for the optimization and advanced control operation of emulsion copolymerisation reactors was developed. This required covering several areas starting from modelling, optimization and then control. The framework would help in producing a soft sensor that would measure the molecular weight and particle size online. Since there is no online technology that can be used to know the key polymer properties of an emulsion copolymerisation process, the development of a soft sensor is crucial. A detailed dynamic model was developed, which is applied to a system exhibiting zero-one kinetics to the emulsion copolymerisation of styrene and MMA. The model comprised a set of rigorously developed population balance equations to predict the monomer

conversion, PSD and MWD. Diffusion-controlled kinetics at high monomer conversion were also combined with numerous elementary chemical and physical mechanisms which operate in both the organic particle phase and the aqueous continuous phase The model has the ability to predict MWD, number and weight average molecular weight (M_n and M_w), average particle size, PSD, conversion, etc. The model had been tested to match the experimental results at variable temperatures, different feed rates and variable co-monomer composition varying at 75/25, 50/50 and 25/75 feed composition. The model had been validated against the experimental results in a newly constructed state-of-the-art automated reactor facility.

The model was then used to determine the optimal feed rates to maximize the polydispersity index for particle size and molecular weight (PSPI and MWPI). Monomers feed rate showed a small change on maximizing, but the surfactant and initiator feed rates and the temperature showed significance on maximizing the PSPI and MWPI.

An online calorimetry model was also developed to inferentially determine the conversion of each monomer. The model was based on the heat balance equations, and on the heat of loss calculations, to determine the heat transfer coefficient.

A multivariable model predictive control (MPC) was formulated to solve the control problems associated with regulatory control and the final specifications (setpoint). The simultaneous control of the PSPI and MWD by manipulating the monomers flow rates of styrene and MMA, surfactant flow rate, initiator flow rate and the reactor temperature was therefore considered. A 4×4 formulation was defined for the multi-constrained optimal control problem for maximising the breadth of the PSD while maintaining the M_n, conversion, average particle size and PSPI at set points. Another case of an online multivariable constrained MPC was tested to maximize the M_n by defining a 5x4 formulation. The MPC formulation was tested and showed good control to obtain the required properties in the product. The temperature, as an added variable in the controlling process, increased the dimensions of control, especially regarding the molecular weight.

The whole strategy has been developed within a gPROMS-API-DCS environment to allow for real-time implementation of a model-based control strategy and consequently direct

transfer of the technology to a general industrial application. The optimal control problem was obtained via an interface to the gOPT dynamic optimisation code. The MPC was developed in MATLAB. For online MPC, a mex function was created using C++, enabling MATLAB to communicate with the Honeywell PlantScape DCS via means of a dynamic link library (dll).

TABLE OF CONTENTS

DECLARATIONS ..... **II**

ACKNOWLEDGEMENTS ..... **III**

ABSTRACT ..... **VI**

TABLE OF CONTENTS ..... **IX**

LIST OF FIGURES ..... **XIII**

LIST OF TABLES ..... **XVII**

GLOSSARY OF SYMBOLS ..... **XVIII**

CHAPTER 1: INTRODUCTION

1.1 THESIS INCENTIVE 1.3
1.2 RESEARCH AIMS 1.5
1.3 THESIS CONTRIBUTIONS 1.6
1.4 THESIS STRUCTURE 1.7
1.5 AUTHOR PUBLICATIONS 1.9
1.6 REFERENCES 1.10

CHAPTER 2: MATHEMATICAL MODELLING

2.1 INTRODUCTION 2.2
2.2 EMULSION COPOLYMERISATION SYNTHESIS 2.3
2.2.1 Emulsion Copolymerisation Overview *2.3*
2.3 PARTICLE SIZE DISTRIBUTION 2.5
2.4 MOLECULAR WEIGHT DISTRIBUTION 2.7
2.5 EMULSION COPOLYMERISATION REACTOR MODELS 2.7
2.6 MODEL DEVELOPMENT 2.14
2.6.1 Modelling the Zero-one System *2.16*
2.6.1.1 Initiator Balance 2.21
2.6.1.2 Surfactant Balance 2.22
2.6.1.3 PSD Model 2.24

2.6.1.3.1 Kinetic Coefficients:.....2.27
2.6.1.4 Reactor Balance Equations.....2.38
2.6.1.5 MWD Model.....2.42
2.6.1.5.1 Molecular weight distribution functions.....2.42
2.6.1.5.2 Instantaneous and cumulative MWDs.....2.42
2.6.1.5.3 Number and weight averages and polydispersity.....2.43
2.6.1.5.4 Rate parameters determining the MWD.....2.43
2.6.1.5.5 Modelling the MWD.....2.44
2.7 NUMERICAL SOLUTION IN gPROMS.....2.44
2.7.1 Numerical Solution in gPROMS for PSD.....2.45
2.8 MODELLING RESULTS.....2.47
2.9 CONCLUSION.....2.59
2.10 REFERENCES.....2.60

CHAPTER 3: EXPERIMENTAL EMULSION COPOLYMERISATION

3.1 INTRODUCTION.....3.2
3.2 AUTOMATED REACTOR FACILITY.....3.2
3.2.1 1L Polymerisation Reactor.....3.2
3.2.2 5L Polymerisation Reactor.....3.5
3.2.2.1 Monomer Feed Line.....3.7
3.2.2.2 Heating/Cooling System.....3.7
3.2.2.3 Nitrogen Line.....3.9
3.3 EXPERIMENTAL VALIDATION.....3.12
3.3.1 Conversion Analysis.....3.14
3.3.2 Particle Sizing.....3.15
3.3.2.1 Particle Sizing using CHDF.....3.15
3.3.2.2 Particle Sizing Using PCS.....3.16
3.3.3 Molecular Weight Analysis.....3.17
3.3.4 Results.....3.21
3.3.4.1 Monomer Conversion.....3.21
3.3.4.2 Particle Size Distribution.....3.24
3.3.4.3 Molecular Weight Distribution.....3.28
3.4 CONCLUSION.....3.38
3.5 REFERENCES.....3.39

CHAPTER 4: PROCESS OPTIMISATION

4.1 INTRODUCTION.....4.2
4.2 OPTIMISATION: INTRODUCTION.....4.3
4.2.1 Formulation of Optimization Problems.....4.4
4.2.2 Topics in Optimization.....4.5
4.2.3 Method of Attack.....4.8
4.2.4 Dynamic Optimisation in gPROMS.....4.9

4.2.4.1 The objective function 4.10
4.2.4.2 Bounds on the optimisation decision variables 4.10
4.2.4.3 Other constraint types 4.11
4.2.4.4 Classes of control variable profile 4.12
4.2.4.5 Optimisation report file 4.13
4.3 OPTIMISATION OF THE EMULSION COPOLYMERISATION PROCESS 4.14
4.3.1 Strategy Development *4.15*
4.3.2 Experimental Validation of the Optimal Control Strategy *4.21*
4.4 CONCLUSION 4.27
4.5 REFERENCES 4.29

CHAPTER 5: INFERENTIAL MONITORING OF CONVERSION

5.1 INTRODUCTION 5.2
5.2 CONVERSION MONITORING THROUGH REACTOR CALORIMETRY 5.3
5.2.1 Heat Transfer Analysis *5.6*
5.2.2 Data Acquisition and Parameter Estimation *5.11*
5.3 EXPERIMENTAL SETUP 5.12
5.4 RESULTS AND ANALYSIS 5.13
5.4.1 Relationship between overall conversion and process conditions *5.13*
5.4.2 Comparison between experiment and simulation result *5.14*
5.4.3 Optimisation results *5.15*
5.5 CONCLUSION 5.17
5.6 REFERENCES 5.18

CHAPTER 6: REAL TIME OPTIMAL CONTROL OF EMULSION COPOLYMERISATION

6.1 INTRODUCTION 6.2
6.2 OVERALL ARCHITECTURE 6.5
6.3 MODEL PREDICTIVE CONTROL ALGORITHM 6.7
6.3.1 Model Identification *6.8*
6.3.2 Multivariable Case (MIMO) *6.10*
6.3.3 Tuning in MPC *6.11*
6.3.4 MPC setup *6.12*
6.3.4.1 MPC Controller Block 6.14
6.4 REAL-TIME IMPLEMENTATION ARCHITECTURE 6.15
6.4.1 MATLAB – gPROMS – Honeywell Link *6.18*
6.4.1.1 MATLAB – gPROMS Link 6.18
6.4.1.2 MATLAB – Honeywell Link (DCS Interface Options) 6.18
6.4.2 Two Way Data Communication *6.20*
6.5 REAL TIME CONTROL OF SEMI-BATCH EMULSION COPOLYMERISATION REACTOR 6.21

6.5.1 MPC Application *6.22*
6.5.1.1 Multivariable Control: PSD and MWD (MIMO) 6.23
6.5.1.2 Multivariable MPC: MWD Control 6.33
6.6 CONCLUSION 6.40
6.7 REFERENCES 6.42

CHAPTER 7: CONCLUSIONS AND FUTURE DIRECTIONS

7.1 CONCLUSIONS 7.2
7.2 FUTURE WORK 7.3

LIST OF FIGURES

FIGURE 2.1 EFFECT OF COMPARTMENTALISATION ON TERMINATION. 2.16
FIGURE 2.2 MECHANISMS OCCURRING IN EMULSION POLYMERISATION 2.18
FIGURE 2.3 PARTICLE SIZE 2.48
FIGURE 2.4 AVERAGE NUMBER OF RADICALS PER PARTICLE 2.48
FIGURE 2.5 CONVERSION OF MONOMER TO COPOLYMER 2.49
FIGURE 2.6 TOTAL NUMBER OF PARTICLES 2.49
FIGURE 2.7 NUMBER AVERAGE MOLECULAR WEIGHT (M_n) 2.50
FIGURE 2.8 WEIGHT AVERAGE MOLECULAR WEIGHT (M_w) 2.50
FIGURE 2.9 CONCENTRATION OF STYRENE IN WATER PHASE 2.51
FIGURE 2.10 CONCENTRATION OF MMA IN WATER PHASE 2.51
FIGURE 2.11 CONCENTRATION OF STYRENE IN PARTICLE PHASE 2.52
FIGURE 2.12 CONCENTRATION OF MMA IN PARTICLE PHASE 2.52
FIGURE 2.13 RATE OF REACTION OF STYRENE (A) AND MMA (B) IN WATER PHASE 2.53
FIGURE 2.14 RATE OF REACTION OF STYRENE AND MMA IN PARTICLE PHASE 2.53
FIGURE 2.15 SEQUENCE NUMBER OF STYRENE AND MMA 2.54
FIGURE 2.16 MOLAR FRACTION OF STYRENE AND MMA 2.54
FIGURE 2.17 PROBABILITIES OF PROPAGATION OF STYRENE AND MMA 2.55
FIGURE 2.18 WEIGHT FRACTION OF STYRENE AND MMA 2.55
FIGURE 2.19 PARTICLE SIZE DISTRIBUTION (PSD) 2.56
FIGURE 2.20 MOLECULAR WEIGHT DISTRIBUTION (MWD) 2.56

FIGURE 3.1 SIDE-VIEW SCHEMATIC OF THE REACTOR SYSTEM (PDC MACHINES INC.). 3.3
FIGURE 3.2 FRONT-VIEW SCHEMATIC OF THE REACTOR SYSTEM (PDC MACHINES INC.). 3.4
FIGURE 3.3 TOP-VIEW SCHEMATIC OF THE REACTOR SYSTEM (PDC MACHINES INC.). 3.4
FIGURE 3.4 SCHEMATIC DIAGRAM OF THE AUTOMATED REACTOR FACILITY 3.5
FIGURE 3.5 THE 5L EMULSION COPOLYMERISATION REACTOR 3.6
FIGURE 3.6 MAGNETIC DRIVER 3.6
FIGURE 3.7 PITCHED BLADE IMPELLER 3.7
FIGURE 3.8 TEMPERATURE PROFILE 3.8
FIGURE 3.9 CONTROL BUILDER – TEMPERATURE CONTROL 3.8
FIGURE 3.10 COPOLYMERISATION PLANT 3.9

FIGURE 3.11 SCHEMATIC DIAGRAM OF THE AUTOMATED 5L REACTOR FACILITY. 3.10

FIGURE 3.12 COPOLYMERISATION REACTION ENGINEERING CONTROL.....3.11

FIGURE 3.13 PRINCIPLE OF SIZE EXCLUSION CHROMATOGRAPHY. 3.17

FIGURE 3.14 PATH OF POLYMER CHAINS AROUND POROUS COLUMN PACKING.....3.18

FIGURE 3.15 MONOMER CONVERSION OBTAINED IN EMULSION COPOLYMERISATION OF STYRENE AND MMA (50/50) MIXTURE AT 75°C FOR MONOMER FEED RATES OF: (A) BATCH (0 g/s), (B) 0.064 g/s, (C) 0.032 g/s, (D) 0.016 g/s, (E) 0.008 g/s 3.22

FIGURE 3.16 MONOMER CONVERSION OBTAINED IN EMULSION COPOLYMERISATION OF STYRENE AND MMA OF A MONOMER FEED RATE OF 0.064 G/S FOR A MONOMER FEED RATIO AND TEMPERATURE OF: (A) TEMP = 75°C, 75/25 STYRENE/MMA, (B) TEMP = 75°C, 25/75 STYRENE/MMA, ...3.23

FIGURE 3.17 PARTICLE DIAMETER OBTAINED IN EMULSION COPOLYMERISATION OF STYRENE AND MMA (50/50) MIXTURE AT 75°C FOR MONOMER FEED RATES OF: (A) BATCH (0 g/s), (B) 0.064 g/s, (C) 0.032 g/s, (D) 0.016 g/s 3.24

FIGURE 3.18 PARTICLE DIAMETER OBTAINED IN EMULSION COPOLYMERISATION OF STYRENE AND MMA OF A MONOMER FEED RATE OF 0.064 g/s FOR A MONOMER FEED RATIO AND TEMPERATURE OF:.....3.25

FIGURE 3.19 PARTICLE SIZE DISTRIBUTION OBTAINED IN EMULSION COPOLYMERISATION OF STYRENE AND MMA (50/50) MIXTURE AT 75°C FOR MONOMER FEED RATES OF: (A) BATCH (0 g/s), (B) 0.064 g/s, (C) 0.032 g/s, (D) 0.016 g/s 3.26

FIGURE 3.20 PARTICLE SIZE DISTRIBUTION OBTAINED IN EMULSION COPOLYMERISATION OF STYRENE AND MMA OF A MONOMER FEED RATE OF 0.064 g/s FOR A MONOMER FEED RATIO AND TEMPERATURE OF:.....3.27

FIGURE 3.21 EXPERIMENTAL AVERAGE GROWTH RATE OF THE POLYMER PARTICLES AT DIFFERENT MONOMER FEED RATES. 3.28

FIGURE 3.22 NUMBER AVERAGE MOLECULAR WEIGHT (M_n) OBTAINED IN EMULSION COPOLYMERISATION OF STYRENE AND MMA (50/50) MIXTURE AT 75°C FOR VARIABLE MONOMER FEED RATES.....3.30

FIGURE 3.23 NUMBER AVERAGE MOLECULAR WEIGHT OBTAINED (M_n) IN EMULSION COPOLYMERISATION OF STYRENE AND MMA OF A MONOMER FEED RATE OF 0.064 G/S FOR A MONOMER FEED RATIO AND TEMPERATURE OF:.....3.31

FIGURE 3.24 WEIGHT AVERAGE MOLECULAR WEIGHT (M_w) OBTAINED IN EMULSION COPOLYMERISATION OF STYRENE AND MMA (50/50) MIXTURE AT 75°C FOR VARIABLE MONOMER FEED RATES.....3.32

FIGURE 3.25 WEIGHT AVERAGE MOLECULAR WEIGHT (M_w) OBTAINED IN EMULSION COPOLYMERISATION OF STYRENE AND MMA OF A MONOMER FEED RATE OF 0.064 g/s FOR A MONOMER FEED RATIO AND TEMPERATURE OF:.....3.33

FIGURE 3.26 MOLECULAR WEIGHT DISTRIBUTION OBTAINED IN EMULSION COPOLYMERISATION OF STYRENE AND MMA (50/50) MIXTURE AT 75°C FOR MONOMER FEED RATES OF: (A) BATCH (0 g/s), (B) 0.064 g/s, (C) 0.032 g/s, (D) 0.016 g/s, (E) 0.008 g/s 3.34

FIGURE 3.27 MOLECULAR WEIGHT DISTRIBUTION OBTAINED IN EMULSION COPOLYMERISATION OF STYRENE AND MMA OF A MONOMER FEED RATE OF 0.064 g/s FOR A MONOMER FEED RATIO AND TEMPERATURE OF:.....3.35

FIGURE 3.28 PREDICTED MOLECULAR WEIGHT DISTRIBUTIONS AT 75°C. 3.37

FIGURE 3.29 EXPERIMENTAL MOLECULAR WEIGHT DISTRIBUTIONS AT 75°C. 3.37

FIGURE 4.1 PROFILES OF TYPICAL CLASSES OF CONTROL VARIABLE (PSE LTD., 2000A). 4.12

FIGURE 4.2 CASE 1: VALIDATION OF OPTIMISATION RESULTS, (A) OPTIMAL PROFILE, (B) PSD, (C) PARTICLE DIAMETER, (D) CONVERSION, (E) MWD 4.22

FIGURE 4.3 CASE 2: VALIDATION OF OPTIMISATION RESULTS TO MAXIMIZE M_N (A) MANIPULATED VARIABLES OPTIMAL PROFILE; (B) PARTICLE DIAMETER; (C) MWD; (D) M_n 4.23

FIGURE 4.4 CASE 3: VALIDATION OF OPTIMISATION RESULTS TO MAXIMIZE M_n. (A) MANIPULATED VARIABLES OPTIMAL PROFILE; (B) PARTICLE DIAMETER; (C) MWD (D) M_n 4.24

FIGURE 4.5 CASE 1: MAXIMISING PSPI 4.26

FIGURE 4.6 PROFILE OF THE PARTICLE NUMBER UNDER OPTIMUM CONDITIONS. 4.26

FIGURE 5.1 RELATION BETWEEN RATE OF REACTION BETWEEN STYRENE AND MMA 5.9

FIGURE 5.2 COMPARISON OF OVERALL CONVERSION BETWEEN EXPERIMENTAL, AND CALORIMETRY SIMULATION FOR (A) RUN 1, (B) RUN 2, (C) RUN3 (D) RUN 3, CONVERSION OF EACH MONOMER 5.16

FIGURE 5.3 OPTIMISATION RUN (A) NUMBER AVERAGE MOLECULAR WEIGHT (M_n), (B) OVERALL CONVERSION WITH THE OPTIMAL PROFILES 5.18

FIGURE 6.1 MODEL FRAMEWORK 6.6
FIGURE 6.2 BASIC CONCEPT FOR MODEL PREDICTIVE CONTROL 6.8
FIGURE 6.3 MODEL USED FOR MPC 6.13
FIGURE 6.4 MPC SIMULINK LIBRARY 6.14
FIGURE 6.5 REAL-TIME IMPLEMENTATION ARCHITECTURE 6.16
FIGURE 6.6 ROBAS ARCHITECTURE 6.17
FIGURE 6.7 SIMPLE FORM OF ROBAS ARCHITECTURE 6.20
FIGURE 6.8 MPC OF EMULSION COPOLYMERISATION OF STYRENE AND MMA 6.25
FIGURE 6.9 EXPERIMENTAL PSPI USING ON-LINE MPC 6.26
FIGURE 6.10 OPTIMAL FEED PROFILE OBTAINED BY ONLINE MPC. 6.26
FIGURE 6.11 OPTIMAL PARTICLE SIZE DISTRIBUTION OF THE COPOLYMER WITH TIME (EXPERIMENTAL) 6.28
FIGURE 6.12 OPTIMAL PARTICLE SIZE DISTRIBUTION OF THE COPOLYMER WITH TIME (SIMULATION) 6.28
FIGURE 6.13 OPTIMAL PARTICLE SIZE DISTRIBUTION OF THE FINAL PRODUCT (SDS) 6.29
FIGURE 6.14 OPTIMAL PARTICLE SIZE DISTRIBUTION OF THE FINAL PRODUCT (AMA – SURFACTANT) 6.29
FIGURE 6.15 PARTICLE SIZE USING ON-LINE MPC. 6.30
FIGURE 6.16 OVERALL CONVERSION USING ON-LINE MPC. 6.30
FIGURE 6.17 M_N USING ONLINE MPC 6.31
FIGURE 6.18 TOTAL NUMBER OF PARTICLES (SIMULATION) 6.31
FIGURE 6.19 MPC OF EMULSION COPOLYMERISATION OF STYRENE AND MMA 6.34
FIGURE 6.20 EXPERIMENTAL M_N USING ON-LINE MULTIVARIABLE CONSTRAINED MPC. 6.36
FIGURE 6.21 OPTIMAL FEED PROFILE USING OFF-LINE MULTIVARIABLE CONSTRAINED MPC 6.36
FIGURE 6.22 OPTIMAL FEED PROFILE USING ON-LINE MULTIVARIABLE CONSTRAINED MPC. 6.37
FIGURE 6.23 EXPERIMENTAL PARTICLE SIZE USING ON-LINE MULTIVARIABLE CONSTRAINED MPC 6.37
FIGURE 6.24 PSD UNDER OPTIMAL OPERATION (CONSTRAINED MIMO MPC). 6.38
FIGURE 6.25 EXPERIMENTAL OVERALL CONVERSION USING ON-LINE MULTIVARIABLE CONSTRAINED MPC. 6.38

LIST OF TABLES

TABLE 2.1 EMULSION COPOLYMERISATION MODELS.....2.8

TABLE 3.1 COPOLYMER STYRENE AND MMA EMULSION COPOLYMERISATION RECIPE...3.13
TABLE 3.2 LIST OF PARAMETERS USED FOR STYRENE AND MMA COPOLYMERISATION..3.20

TABLE 4.1 AREAS AND TOPICS IN OPTIMISATION.....4.6
TABLE 4.2 OPTIMISATION DETAILED RESULTS (MAXIMISING M_N).....4.20
TABLE 4.3 OPTIMISATION DETAILED RESULTS (MAXIMISING PSPI).....4.20

TABLE 5.1 REACTOR DIMENSIONS AND TYPICAL OPERATING PARAMETERS.....5.14
TABLE 5.2 OPERATION PROCESS MODES.....5.14

GLOSSARY OF SYMBOLS

a_i	step-response coefficients at sample 'i'
a_s	Minimum area occupied by a single surfactant molecule on a particle surface, dm^2
A	dynamic matrix
A_s	Actual area taken up by one surfactant molecule when adsorbed onto a surface, dm^2
A_{tot}	Total surface area of latex particles, dm^2
$B(V',V')$	rate coeff. for coagulation of two particles of volume V and V', $L.mol^{-1}.s^{-1}$
$C_{micelle}$	concentration of micelles, $mol.L^{-1}$
C_P	monomer concentration in the latex particles, $mol.L^{-1}$
C_{P_sat}	saturated monomer concentration in the latex particles, $mol.L^{-1}$
C_W	monomer concentration in the water phase, $mol.L^{-1}$
C_{pm}	heat capacity of the monomer, $J/g.^oC$
C_{pw}	heat capacity of water, $J/g.^oC$
D	inner reactor diameter, m
d	process disturbance
DHp	heat of polymerisation, J/mol
d_m	density of monomer, $kg.L^{-1}$
d_p	density of polymer, $kg.L^{-1}$
D_W	diffusion coefficient for monomer in water, dm^2
e	error
$[E]$	aqueous phase concentration of desorbed radicals, $mol.L^{-1}$

F_m	monomer feed to the reactor, mol.s^{-1}
$F_{m,in}$	inlet monomer feed rate, mol.s^{-1}
G	Number of radial intervals into which the particle size distribution is split
$[IM_i]$	aqueous phase concentration of oligomeric radicals of degree 'i', mol.L^{-1}
J	objective function
j_{crit}	critical degree of polymerisation for homogeneous nucleation
k	current sample
K	rate of propagation volume growth per particle, L.s^{-1}
K_a	Equilibrium constant for adsorption of surfactant at the air/water interface, L.mol^{-1}
k_d	rate coefficient for initiator decomposition, s^{-1}
$k_{des,A}$	rate coefficient for desorption of monomeric radicals of terminal A from particles, s^{-1}
$k_{des,B}$	rate coefficient for desorption of monomeric radicals of terminal B from particles, s^{-1}
k_{des}	Average rate coefficient for desorption of monomeric radicals from particles, s^{-1}
k_e^i	average rate coefficient for entry of an oligomeric radical of degree 'i' into an existing particle, L.mol^{-1}.s^{-1}
$k_{e,A}^i$	rate coefficient for entry of an oligomeric radical of degree 'i' with terminal A into an existing particle, L.mol^{-1}.s^{-1}
$k_{e,B}^i$	rate coefficient for entry of an oligomeric radical of degree 'i' with terminal B into an existing particle, L.mol^{-1}.s^{-1}
k_{eE}	average rate coefficient for re-entry of desorbed radicals, L.mol^{-1}.s^{-1}
$k_{eE,A}$	rate coefficient for re-entry of desorbed radicals with terminal A, L.mol^{-1}.s^{-1}
$k_{eE,B}$	rate coefficient for re-entry of desorbed radicals with terminal B, L.mol^{-1}.s^{-1}

$k^i_{e,micelle}$	average rate coefficient for entry of an oligomeric radical of degree 'i' into a micelle, $L.mol^{-1}.s^{-1}$
$k^i_{e,micelle,A}$	rate coefficient for entry of an oligomeric radical of degree 'i' with terminal A into a micelle, $L.mol^{-1}.s^{-1}$
$k^i_{e,micelle,B}$	rate coefficient for entry of an oligomeric radical of degree 'i' with terminal B into a micelle, $L.mol^{-1}.s^{-1}$
k_p	long chain limiting propagation rate coeff. in the latex phase, $L.mol^{-1}.s^{-1}$
k^1_p	monomeric radical propagation rate coeff. in the latex phase, $L.mol^{-1}.s^{-1}$
$k^i_{p,aq}$	average aqueous phase propagation rate coefficient for oligomeric radicals of degree 'i', $L.mol^{-1}.s^{-1}$
$k^i_{p,aqA}$	aqueous phase propagation rate coefficient for oligomeric radicals of degree 'i' of monomer A (styrene), $L.mol^{-1}.s^{-1}$
$k^i_{p,aqB}$	aqueous phase propagation rate coefficient for oligomeric radicals of degree 'i' of monomer B (MMA), $L.mol^{-1}.s^{-1}$
$K_{wp,A}$	partition coefficient for styrene between the water phase and particle phase
$K_{wp,B}$	partition coefficient for MMA between the water phase and particle phase
$K_{mp,A}$	partition coefficient for styrene between the monomer phase and particle phase
$K_{mp,B}$	partition coefficient for MMA between the monomer phase and particle phase
$K_{mw,A}$	partition coefficient for styrene between the monomer and water phase
$K_{mw,A}$	partition coefficient for MMA between the monomer and water phase
$k_{o,i}$	rate of exit of a monomeric radical of type *i* from the polymer particles.

$k_{t,aq}^{i,j}$	Average rate coefficient for termination reaction between oligomeric radicals of degree 'i' and 'j' in the aqueous phase, $L.mol^{-1}.s^{-1}$
$k_{t,aq,A}^{i,j}$	rate coefficient of terminal A for termination reaction between oligomeric radicals of degree 'i' and 'j' in the aqueous phase, $L.mol^{-1}.s^{-1}$
$k_{t,aq,B}^{i,j}$	rate coefficient of terminal B for termination reaction between oligomeric radicals of degree 'i' and 'j' in the aqueous phase, $L.mol^{-1}.s^{-1}$
k_{tr}	Average rate coefficient for radical transfer to monomer, $L.mol^{-1}.s^{-1}$
$k_{tr,A}$	rate coefficient of monomer A for radical transfer to monomer, $L.mol^{-1}.s^{-1}$
$k_{tr,B}$	rate coefficient of monomer B for radical transfer to monomer, $L.mol^{-1}.s^{-1}$
M_o	monomer molecular weight, $kg.mol^{-1}$
$\overline{n}$	average number of radicals per particle
$n(r)$	molar concentration density of particles of unswollen radius r, $mol.L^{-1}.dm^{-1}$
$n_a(r)$	molar concentration density of particles of terminal A of unswollen radius r, $mol.L^{-1}.dm^{-1}$
$n_b(r)$	molar concentration density of particles of terminal B of unswollen radius r, $mol.L^{-1}.dm^{-1}$
$n_0(r)$	molar concentration density of particles of unswollen radius r containing no radicals, $mol.L^{-1}.dm^{-1}$
$n_1^M(r)$	molar concentration density of particles of unswollen radius r, containing monomeric radicals, $mol.L^{-1}.dm^{-1}$
$n_1^P(r)$	molar concentration density of particles of unswollen radius r, containing polymeric radicals, $mol.L^{-1}.dm^{-1}$
N_A	Avogadro's constant, mol^{-1}
$N_{m,i}$	number of moles of monomer of monomer type "i"
$N_{m,T}$	total number of moles of monomer

N_{tot}	total number concentration of particles, L^{-1}
P_i	molar concentration of species of length i
P_s	power input by the stirrer, W
$Q_{j,loss}$	heat losses from the jacket, W
$Q_{r,loss}$	heat losses from the reactor, W
r	radius of latex particle, dm
Δr	size of radial interval, dm
$< r >$	number mean particle radius, nm
$< r^2 >$	number mean squared radius, nm^2
R_{pAp}	rate of reactions of the polymer for monomer A in the particle phase, mol.L-1.s-1
R_{pBp}	rate of reactions of the polymer for monomer B in the particle phase, mol.L-1.s-1
R_{pAw}	rate of reactions of the polymer for monomer A in the water phase, mol.L-1.s-1
R_{pBw}	rate of reactions of the polymer for monomer B in the water phase, mol.L-1.s-1
r_s	swollen radius of latex particle, dm
S	concentration of added surfactant per unit volume of the aqueous phase, $mol.L^{-1}$
S_W	concentration of free surfactant in the aqueous phase, $mol.L^{-1}$
T_{amb}	ambient temperature, °C
T_{reac}	reactor temperature, °C
$T_{j,in}$	inlet jacket temperature, °C
$T_{j,out}$	outlet jacket temperature, °C
u	process input
U	heat transfer coefficient, $W/m^2.K$
V	reaction volume, m^3

V_d	volume of monomer in the droplets, L
V_{org}	volume of the organic phase, L
V_M	volume of monomer in the system, L
V_P	volume of polymer in the system, L
V_r	total reaction volume, L
V_W	volume of water in the system, L
X	instantaneous monomer conversion
y	process output
z	critical degree of polymerisation for entry

Greek Symbols

α	coefficient for heat losses , $W/^oC^\beta$
β	power coefficient
β_A	probability that a monomeric radical of type *i* reacts in the aqueous phase by either propagation or termination with terminal A
β_B	probability that a monomeric radical of type *i* reacts in the aqueous phase by either propagation or termination with terminal B
λ	weighting factor
τ	process time constant
δ	Stern layer thickness, dm
$\delta_{N,Z}$	Kronecker delta
ϕ_m	monomer volume fraction
ϕ_p	polymer volume fraction
γ	surface tension of aqueous phase of the emulsion, $dyn.cm^{-1}$
γ_{cmc}	critical surface tension of the aqueous phase, $dyn.cm^{-1}$

γ_i	polydispersity index
γ_o	surface tension of pure water, $dyn.cm^{-1}$
Π	surface pressure,$dyn.cm^{-1}$
ρ	pseudo rate coefficient for all entry events (oligomeric radicals and exited radicals) into existing particles, s^{-1}
ρ_{init}	pseudo rate coefficient for entry of an oligomeric radical into an existing particle, s^{-1}

Chapter 1

Introduction

1.1 THESIS INCENTIVE 1.3
1.2 RESEARCH AIMS 1.5
1.3 THESIS CONTRIBUTIONS 1.6
1.4 THESIS STRUCTURE 1.7
1.5 AUTHOR PUBLICATIONS 1.9
1.6 REFERENCES 1.10

Polymerisation is defined as the bonding of two or more monomers to form a polymer. Knowledge and understanding of this process involve a great deal of fundamental science, the investigation of which reveals much new fundamentals scientific knowledge; moreover, knowledge is readily to be applied, because this is an industrially important process. The fundamentals of this field are now sufficiently well understood that new products can be made, with the specified properties meeting customer needs. Intelligent, knowledge based design is the way of the future for this important technology. While much of the science and the basis of the field are now scientifically secure, there is still much to be done in the advanced control operation of theses processes.

Polymers are divided into two distinct groups: thermoplastics and thermosets. The majority of polymers are thermoplastic, meaning that once the polymer is formed it can be heated and reformed over and over again. This property allows for easy processing and recycling. The other group, the thermosets, can not be remelted. Once these polymers are formed, reheating will cause the material to scorch. Every polymer has very distinct characteristics, but most polymers have the following general attributes.

1. Polymers can be very resistant to chemicals. All the cleaning fluids in home that are packaged in plastic are polymers. Reading the warning labels that describe what happens when the chemical comes in contact with skin or eyes or is ingested emphasizes the chemical resistance of these materials.

2. Polymers can be both thermal and electrical insulators. The appliances, cords, electrical outlets, and wiring, are made or covered with polymeric materials. Thermal resistance is evident in the kitchen with pot and pan handles made of polymers, the coffee pot handle, the foam core of refrigerators and freezers, insulated cups, coolers, and microwave cookware. The thermal underwear that many skiers wear is made of polypropylene and the fibrefill in winter jackets is acrylic.

3. Generally, polymers are very light in mass with varying degrees of strength. The range of applications varies from dime store toys to the frame structure of space stations, or from delicate nylon fibre in pantyhose to Kevlar, which is used in bullet-proof vests.

4. Polymers can be processed in various ways to produce thin fibres or very intricate parts. Plastics can be moulded into bottles or the body of a car or be mixed with solvents to become an adhesive or paint. Elastomers and some plastics stretch and are very flexible.

Other polymers can be foamed like polystyrene and urethane, to name just two examples. Polymers are materials with a seemingly limitless range of characteristics and colours. Polymers have many inherent properties that can be further enhanced by a wide range of additives to broaden their uses and applications.

1.1 Thesis Incentive

In industry, polymer engineers used to form theory polymers based on fixed recipes that they believed was most suitable through experience, but however it lacked the optimising factor and the requirements to produce a new product. The other problem was the knowledge the process engineer had was limited in that emulsion polymerisation chemistry and its techniques. Moreover, the reactor control and operation was limited to temperature, level and reagents flow rates. Nowadays, there are many polymer industries that compete with each other to produce polymers of different properties to the different needs that meet the demand of the market. This need leaded to the development of new theories based on a scientific thought. Today, the industry that has the scientific basis producing its products will lead the market, because it will be able to produce a huge range of products from adhesives, surface coatings, plastics, barriers etc.

Polymerisation reactors usually exhibit complex nonlinear dynamic behaviour, because of the complexity of the physicochemical interactions and the kinetics of the polymerisation reactions. In these reactors many important variables, often related to end-use polymer properties, cannot be measured on-line or can only be measured at very low sampling frequencies. Furthermore end-use polymer properties are usually related to the molecular weight and its distribution, particle size and its distribution, composition distribution in the polymerisation reactor. Finally, a typical industrial polymer reactor is used to manufacture a variety of grades of the same basic product necessitating frequent start-ups, online transitions, and shutdowns.

Because of these reasons effective process monitoring and control of these reactors has been very challenging and has been the focus of active research programs in academia which has resulted in many publications. From an industrial perspective there are significant incentives for efficient polymer and copolymer reactor monitoring and control

which include the production of higher quality products, safer processes, minimization of transition losses, and higher production rates.

The dependence on molecular weight of mechanical properties is an important area of polymer physics. Polymer properties such as maximum stress at break have a typical dependence on the average molecular weight of the polymer. Another illustration of the influence of the molecular weight is seen in the way the susceptibility of a material to stress cracking decreases with increasing average molecular weight. Similar correlations arise with properties such as impact behaviour, glass transition temperature, rate of crack propagation, adhesion, and many others. Mechanical properties of a polymer depend both on average molecular weight and on the molecular weight distribution (Gilbert, 1995).

For theses reasons, the need to controlling the molecular weight distribution (MWD) of polymers will help to control the properties of the demanded targeted polymer. The copolymer to be produced would require the control of the operating conditions of the reaction. On the other hand, knowledge of particle size and particle size distribution (PSD) is of primary importance in virtually all particulate systems, which includes aerosols, emulsions, suspensions, dispersions and powders. The importance and significance of this physical characteristic of a system is realized when one examines the chemical, physical and mechanical properties affected by particle size and its distribution. This includes the bulk density of powders, powder flow, the rheological properties of emulsions, suspensions and dispersions which strongly affect processing and end-use applications, suspension, viscosity and emulsion stability, coagulum formation, film formation, reaction rates, solubility rates, magnetic properties, opacity, gloss and others. (Collins, 1997)

In order to produce accurate predictions of the copolymers produced, knowledge and skills in physical chemistry, colloid and surface science, reaction engineering and kinetics, programming are needed. This knowledge is used to model the emulsion copolymerisation reactors to predict the PSD and MWD. On the other hand, the process is very sensitive to the operating conditions which increase the complexity of the operation. The operating conditions include the temperature, pressure, level, flow rate and the proportions of the reagents. Moreover, during the reaction many disturbances occur, which should be adjusted by the system, which will only do if it is controlled using advanced control techniques. There had been a considerable advance in the reactions of polymer kinetics

and sensor technology, which is still developing. Nowadays, the offline measurement of the PSD and MWD of the copolymers is still in demand; on the other hand, online measurements are much more demanded.

The online measurements of PSD and MWD would require a model that will incorporate the non-linear behaviour of the copolymerisation reaction, and all of the operating conditions that would influence the copolymer properties. The need of a model is vital, since industries would not allow applying our knowledge in their process, except when they see the evidence of its influence towards higher productivity. Now, with the new model of accurate predictions, would act as a sensor, and on the other hand could be used to obtain new recipes for new products. Moreover, advanced control techniques should be developed to overcome the unexpected disturbances in the emulsion copolymerisation process, and to maintain product consistency and optimum productivity.

1.2 Research Aims

Emulsion copolymerisation is widely used in the formation of variety of products. It is a heterogeneous polymerisation reaction and encompasses complex mechanisms and two monomers. This makes the achievement of the desired copolymer properties difficult, especially that the key polymer properties are sensitive to the operating conditions. The predicted copolymer properties should be accurate for the model to act as a soft sensor. Advances process control techniques are developed to ensure the applicability of the model into a real practice plant.

Therefore, the aim of this thesis is to develop a comprehensive model and a novel framework that would be able to predict accurately the key polymer properties, and used to determine the optimal operation conditions and under advanced control techniques. The thesis can be divided into the following objectives:

- To develop a comprehensive dynamic model that has the capability to accurately predict the average radius and the particle size distribution (PSD), number and weight average and the molecular weight distribution (MWD), and conversion, over a wide range of operating conditions. For control purposes, that is to have the

process in closed loop control (online), the model has to be fast and computationally efficient.

- The reactor facility has to be launched and prepared to undergo the copolymerisation reactions which will assist in validating the model predictions under different process operating conditions. The reactor facility should be automated with the computer for advanced control operations.

- The sophisticated model will be incorporated within an optimal control policy to produce desired polymer PSD and MWD for off-line and on-line applications.

- A calorimetric model is developed to infer conversion through calorimetric measurements that includes detailed reactor energy/mass balance of the process operation.

- To develop an advanced control strategy that is model based for on-line optimal operation of the copolymerisation reactor.

The novelty of this comprehensive model is its power to predict the key polymer properties online, and its practicality and applicability to be implemented online under advanced control techniques.

1.3 Thesis Contributions

There had several contributions through this thesis. The main contributions are:

- The development of a mathematical model, using the real kinetics, with no data fitting used, of the copolymerisation reactor that is suitable for real-time applications. The mathematical model is very efficient in accuracy and time, hence able to predict most of the key polymer properties including PSD and MWD, despite of the complexity in the reaction process, which includes a high number of partial and normal differential equations.

- The mathematical model of the emulsion copolymerisation reactor was made reliable by validating it under different operating conditions, using the monomer feed, surfactant feed, initiator feed and the reaction temperature as primary variables to control the PSD and MWD.

- The dynamic model was used to generate off-line optimal profiles, and for on-line soft-sensing of the PSD and MWD.

- An intelligent control hierarchy is formulated for such distributed parameter system incorporating three different levels; offline optimization, on-line Dynamic matrix control (DMC) and regulatory control successively. The novelty of this approach is the incorporation of a validated high order dynamic model as a soft sensor for on-line feedback of the PSD and MWD.

- An architecture is developed to control the emulsion copolymerisation process. This architecture can be applied to generic complex particle systems. The architecture has been developed within a gPROMS-API-DCS environment allowing for direct transfer of the technology to a general industrial application.

- The model developed was validated in a 1L reactor and then scaled up to a 5L reactor, for optimisation and control. This shows the possibility of scaling up the model to larger plant scales.

1.4 Thesis Structure

The thesis structure is organised as follows:

- Chapter 2 describes the dynamics of a styrene and MMA semi-batch emulsion copolymerisation reactor. The mathematical model equations and kinetics are included in this chapter. Simulation results are shown at the end of the chapter.

- Chapter 3 shows the reactor facility of the 1L and the 5L reactor. The instrumentation and the automated facility used with each reactor are discussed. The validation of the model with the experimental results is also discussed.

- Chapter 4 describes the process optimisation for molecular weight and particle size control. The two monomers, surfactant and initiator feed trajectories, along with the temperature of the reaction are used to develop the optimal profiles for two cases. The first case is when a polymer with a broad particle size distribution is required, and the second case is when a high molecular weight is required to be produced.

- Chapter 5 demonstrates the development of an inferential calorimetric model that includes mass/energy balances of the reactor, which is used to infer the rate of reaction and conversion through the calorimetric measurements.

- Chapter 6 includes the real-time implementation architecture used to control the emulsion copolymerisation system. It addresses the overall framework for the on-line optimal control of the emulsion copolymerisation process. The MPC is applied for on-line PSD & MWD control, both MIMO systems with different control formulations. Soft and hard constraints are also included in the control formulation to cover for process limitations. The novel approach of using the dynamic model as a soft-sensor for on-line feedback of the PSD and MWD is also explained. The architecture developed includes the data link between the plant and the model under control. This architecture, developed by BASsam Alhamad and ROB Willis, so called "ROBAS", was robust and reliable in controlling the plant. The "ROBAS" architecture is also discussed including the explanation of data link through the DCS system.

- Finally, Chapter 7 includes a number of conclusions and recommendations, where an expert system environment is recommended that assists in the decision support and the use of computational fluid dynamics tools that will assist in understanding the profile of the fluid dynamics in the reactor.

1.5 Author Publications

Alhamad, B., V.G. Gomes, and J.A. Romagnoli, *Inferential conversion monitoring in emulsion copolymerisation through calorimetric measurements.* International Journal of Chemical Reactor Engineering, 2005, *in press.*

Alhamad, B., V.G. Gomes, and J.A. Romagnoli, *Inferential Conversion Monitoring through Calorimetric Measurements in Emulsion Copolymerisation.* CHEMECA, 2004

Alhamad, B., J.A. Romagnoli, and V.G. Gomes, *Particle Evolution in Batch and Semi-Batch Emulsion Copolymerisation.* in *31st Australasian Chemical Engineering Conference CHEMECA,* 2003, Adelaide, South Australia.

Alhamad, B., et al. *A Model-Based Framework for Advanced Optimal Operation of Polymerisation processes: Application to Emulsion Copolymerisation of Styrene/MMA*, in *ESCAPE-14,* 2004, Lisbon.

Alhamad, B., J.A. Romagnoli, and V.G. Gomes, *Optimal Control for Emulsion Copolymerisation: Application within a DCS environment.* in *7th International Symposium on Dynamics and Control of Process Systems.* July 5 -7, 2004, Boston, USA

Alhamad, B., J.A. Romagnoli, and V.G. Gomes, *A Model-Based Framework for Advanced Optimal Operation of Copolymerisation processes: Application to Emulsion Copolymerisation of Styrene/MMA,* Journal of Chemical Engineering Science, *60, 10, 2005, 2795-2813.*

Alhamad, B., J.A. Romagnoli, and V.G. Gomes, *A modelling framework based on population balances for optimum operation and advanced control of emulsion polymerization*, CHISA, 2004

Alhamad, B., J. A. Romagnoli, and V. Gomes, On-line Multivariable Predictive Control of Molar Mass and Particle Size Distributions in Free-Radical Emulsion Copolymerization., Journal of Chem. Eng. Science, 2005, *in Press, Corrected Proof*

Alhamad, B., R. Willis, J. Romagnoli, and V. Gomes, A Model Based Framework for online MPC Control of Emulsion Copolymerization of Styrene and MMA, *7th World Congress of Chemical Engineering*, 10 - 14 July 2005, Glasgow, Scotland

1.6 References

Collins E.A. (1997), Emulsion Polymerisation and Emulsion Polymers, ed. Lovell, P.A. and El-Aasser, M.S., John Wiley & Sons Ltd, England, Ch: 12.

Gilbert R.G. (1995), Emulsion polymerisation: A Mechanistic Approach, London: Academic Press, Ch: 6

Chapter 2

Mathematical Modelling

2.1 INTRODUCTION 2.2
2.2 EMULSION COPOLYMERISATION SYNTHESIS 2.3
2.2.1 Emulsion Copolymerisation Overview 2.3
2.3 PARTICLE SIZE DISTRIBUTION 2.5
2.4 MOLECULAR WEIGHT DISTRIBUTION 2.7
2.5 EMULSION COPOLYMERISATION REACTOR MODELS 2.7
2.6 MODEL DEVELOPMENT 2.14
2.6.1 Modelling the Zero-one System 2.16
2.6.1.1 Initiator Balance 2.21
2.6.1.2 Surfactant Balance 2.22
2.6.1.3 PSD Model 2.24
2.6.1.3.1 Kinetic Coefficients: 2.27
2.6.1.4 Reactor Balance Equations 2.38
2.6.1.5 MWD Model 2.42
2.6.1.5.1 Molecular weight distribution functions 2.42
2.6.1.5.2 Instantaneous and cumulative MWDs 2.42
2.6.1.5.3 Number and weight averages and polydispersity 2.43
2.6.1.5.4 Rate parameters determining the MWD 2.43
2.6.1.5.5 Modelling the MWD 2.44
2.7 NUMERICAL SOLUTION IN gPROMS 2.44
2.7.1 Numerical Solution in gPROMS for PSD 2.45
2.8 MODELLING RESULTS 2.47
2.9 CONCLUSION 2.59
2.10 REFERENCES 2.60

2.1 Introduction

The emulsion copolymerization process is a complex process that would require an accurate model with efficient computation capabilities in order to predict accurately the polymer properties, and be able for real-time applications. Mathematical model enhances the understanding of the process and allows the process engineer to make predictions, and possibly informs how to control the part of the real world (the system) that is under investigation. An important part of the mathematical model is to collect the consequent data, kinetic equations, rate reactions, population balance equations, mass and energy balance equations, feeding all that into the mathematical model, to predict the key polymer properties and validated against the experiments.

Over the years, the focus was on kinetic studies of batch emulsion copolymerisation and many detailed publications have been reported in the literature. These studies helped to developing models able to estimate the key polymer properties. These models include those described by (Broadhead et al., 1985, Dougherty, 1986b, Dougherty, 1986a, Gugliotta et al., 1995, Liotta et al., 1998, Penlidis et al., 1986, Richards et al., 1989, Zeaiter et al., 2002a, Zeaiter et al., 2002b, Gerrens, 1969, Krackler and Naidus, 1969, Urquiola et al., 1991, Crowley et al., 2000, Coen et al., 1998). The control of particle size and molecular weight distribution described by a population balance model of semibatch emulsion polymerisation of styrene was developed by (Zeaiter et al., 2002b). For emulsion copolymerisation of styrene and MMA, a recent paper (Alhamad et al., 2003) published showing good agreement between the model simulation and experimental results on predicting conversion, average particle size and particle size distribution (PSD), where the model was based on population balance equations, and assumed to obey zero-one kinetics. Only recently, the control of particle size and molecular weight distribution described by a population balance model of semibatch emulsion polymerisation was developed (Zeaiter et al., 2002b). However, in a recent work, (Sajjadi and Brooks, 2001) observed an increase in the particle number with a decrease in the monomer feed rate in semibatch emulsion polymerisation. (Zeaiter et al., 2002b) observed that increasing the feed rate would result in a bigger particle size, and at a very low rate, a bimodal distribution is produced. The work by Saldivar and co-workers (Saldivar et al., 1998b, Saldivar et al., 2001, Saldivar et al., 2002) provided extensive information on developing a comprehensive model for emulsion copolymerisation. A computational mechanistic model written in Fortran was

developed by (Coen et al., 1998) that showed good results for PSD, but was and found to take a significant amount of time in tracking the particle size distribution. However, the model is slow for real time applications.

In this chapter, a dynamic reactor model is developed for a styrene and MMA emulsion copolymerisation batch/semi-batch reactor to predict the evolution of the PSD and MWD over the entire range of monomers conversion. The kinetics adopted were obtained from (Coen et al., 1998), (Clay and Gilbert, 1995), (Dougherty, 1986a), (Maxwell and Russell, 1993, Maxwell et al., 1992, Verdurmen et al., 1993, Casey et al., 1994, Noel et al., 1994b, Noel et al., 1994a). A more accurate prediction is obtained by adopting the most suitable kinetics to the process based on knowledge and the predictions, since many of the kinetics obtained through theory were found to be controversial.

2.2 Emulsion Copolymerisation Synthesis

Emulsion copolymerisation is a heterogeneous reaction process in which unsaturated comonomer or comonomer solutions are dispersed in a continuous phase with the aid of an emulsifier system and polymerised with free radical initiators.

2.2.1 Emulsion Copolymerisation Overview

Free radical polymerisation processes involve four basic kinetic steps. These are:

- *Initiation:* The breakdown of initiator molecules, followed by the reaction of the free radicals with the comonomers
- *Propagation:* The addition of comonomer molecules to growing oligomeric radical chains
- *Termination:* The stoppage of polymer growth due to free radicals obtaining their satisfied electron pairing due to the combining of two radical chains
- *Chain transfer:* A second means of chain stoppage resulting from the polymeric free radicals losing their radical, which is transferred to another species.

The main ingredients in an emulsion copolymerisation reaction are water insoluble monomers, water, surfactant and water-soluble initiator. (Gilbert, 1995) explains their roles as follows:

- *Water insoluble monomers:* The major polymerisable component of an emulsion copolymerisation is the chosen monomers, that is of limited solubility in water and that swells its product copolymer. Thus are the building blocks of copolymerisation reactions. They primarily consist of small molecules containing carbon-carbon double bonds. Styrene and methyl methacrylate (MMA) are the monomers utilised for experimental work here, producing poly (styrene-MMA).
- *Water:* The continuous phase in the process. Water provides a medium of transfer of comonomers from droplets to particles; it separates the polymerisation loci, being the medium where the initiator and oligomer formation occurs; it also acts to maintain a low viscosity and provide good heat transfer.
- *Surfactant:* undertakes two roles, providing particle nucleation sites as well as impart colloidal stability to the growing particles as a result of their absorption at the particle water interface.

Prior to examining the kinetic events, a thorough understanding of the sequence of events as they occur in emulsion copolymerisation process is required. An original description of events is taken from (Harkins, 1947) qualitative outlook on emulsion polymerisation, which can be translated to emulsion copolymerisation, (Hagiopol, 1999). The description is based on splitting the process into three intervals. Interval I encompass particle formation, while intervals II and III are concerned with the particle growth.

A conventional emulsion copolymerisation, over the course of the reaction, will consist of as many as three phases. The first, most abundant, is the aqueous, or continuous phase. This phase initially contains the initiator, surfactant micelles and a small amount of the slightly soluble monomer and is present in all intervals of the reaction. The second phase consists of the emulsion/monomer droplets that are concentrated with the slightly insoluble monomer. It is from here that the reaction is fed with the required measure of monomer to facilitate propagation. The monomers droplets are present in intervals I and II only, after which the latex particles, which form the third phase, are found in high concentration. The

latex particles form early in the reaction and are present through the reaction in various sizes. They contain the formed polymer and some (Intervals I and II) or all (Interval III) of the un-polymerised monomer.

2.3 Particle Size Distribution

Knowledge of particle size and particle size distribution is of primary importance in virtually all particulate systems, which includes aerosols, emulsions, suspensions, dispersions and powders. The importance and significance of this physical characteristic of a system is realised when one examines the chemical, physical and mechanical properties affected by particle size and particle size distribution.

In the real world situation, it is difficult to prepare or maintain a totally dispersed latex system. If all the particles of a latex or dispersion were the same size, there would be no need to consider average. The concept of average allows distinction to be made among the different sizes and shapes that prevail in real systems. The most familiar average is the number average, defined as:

$$r_{avg} = \frac{\sum r_i n_i}{\sum n_i} \qquad \text{(Eq. 2.1)}$$

A kinetic model was developed by Coen et al. (1998) developed a kinetic model which included the kinetic events such as the aqueous phase propagation, transfer, entry, re-entry and termination, micellar nucleation, secondary nucleation, coagulation and diffusion. A zero-one system was applied. The population balance equations developed are:

$$\frac{\partial n_o(V,t)}{\partial t} = \rho\left[n_1^p + n_1^m - n_o\right] + k_{dM} n_1^m - n_o(V)\int_o^\infty B(V,V')[n_o(V') + n_1^p(V')]dV'$$

(entry) + (desorption) − (coagulation)

$$+ \int_o^\infty B(V, V-V')[n_o(V')n_o(V-V') + n_1^p(V')n_1^p(V-V')]dV' \qquad \text{(Eq. 2.2)}$$

(coagulation)

$$\frac{\partial n_1^p(V,t)}{\partial t} = \rho_{init}(V)n_o - \rho(V)n_1^p - k_{tr}C_p n_1^p - \frac{\partial}{\partial V}(Kn_1^p) + k_p^1 C_p n_1^M$$

(entry) − (termination) − (growth) + (propagation)

$$+ \int_o^\infty B(V, V-V')[n_o(V')n_1^p(V-V') + n_1^p(V')n_o(V-V')]dV'$$

$$- n_1^p \int_o^\infty B(V,V')[n_o(V') + n_1^p(V')]dV' + \delta(V-V_o) \qquad \text{(Eq. 2.3)}$$

+ (coagulation)

$$\times\left([IM_{j_{crit}-1}]k_{p,w}^{j_{crit}-1}C_w + \sum_{i=z}^{j_{crit}-1}[IM_i]k_{e,micelle}^i[micelle]\right)$$

+ (homogeneous nucleaction) + (micellar nucleation)

$$\frac{\partial n_1^M(V,t)}{\partial t} = -(\rho + k_p^1 C_p + k_{dM})n_1^M + k_{eE}[E]n_o + k_{tr}C_p n_1^p \qquad \text{(Eq. 2.4)}$$

(entry) + (propagation) + (desorption) + (entry) + (termination)

where n_o, n_1^p and n_1^M are the number of particles containing no radicals, one polymeric radical and one monomeric radical respectively. The total number of particles in the system is then calculated from,

$$N_c = N_A \int_0^\infty (n_o + n_1^M + n_1^p)dV \qquad \text{(Eq.2.5)}$$

$$\text{and } \bar{n} = \frac{\int_0^\infty (n_1^M + n_1^p)dV}{\int_0^\infty (n_o + n_1^M + n_1^p)dV} \qquad \text{(Eq. 2.6)}$$

2.4 Molecular Weight Distribution

An important factor determining the physical properties of a polymer is its molecular weight. Since a polymer sample is composed of a large number of individual chains, and since it is unlikely that these will have the similar molecular weight, these physical properties depend on the average molecular weight and the molecular weight distribution. Several methods were developed to obtain the MWD model. The first theoretical method of these models is the 'kinetic rate model', which uses the kinetics to determine the molecular weight. The second method utilised is the "moments" method, which makes use of the theory of moment analysis to determine the molecular weight distribution. The third model is the Monte Carlo simulation method, which uses random sampling to obtain numerical solutions to the mathematical problem.

2.5 Emulsion Copolymerisation Reactor Models

However, the nature of emulsion copolymerisation is heterogeneous, having different phases. The system comprises water, surfactant, monomer and water soluble initiator, with the principal site for copolymerisation being monomer-swollen particles and newly nucleated micelles at surfactant concentrations near or above the critical micelle concentration. The monomer is dispersed in the water phase in the form of droplets, and it acts as a reservoir supplying the growing particles with monomer. It is stabilised by the surfactant molecules, so-called "micelles". Copolymerisation may be carried out in seeded batch, semi-batch or continuous stirred tank reactors. Batch and semibatch process are typically used for low volume, high value products, whereas continuous processes are employed for large-scale production.

The works of Saldivar and co-workers (Araujo et al., 2001, Bonilla et al., 2002, Saldivar and Ray, 1997, Saldivar et al., 1998b, Saldivar et al., 2001, Saldivar et al., 2002) have provided a good source of information and ideas that have contributed extensively to the work presented in this thesis. They have presented a comprehensive model applicable to batch, semibatch and continuous operations based on the experimental analysis of ten binary and three ternary polymerisations.

As can be seen in Table 2.1, there are several models that are available in literature for the simulation of emulsion copolymerisation reactors; however, most models have been tested to limited conditions and types of reactors. There are very few models that have the comprehensive nature. In the following subsections, more details are put towards the analysis of earlier models with their contributions and limitations pointed out.

Table 2.1 **Emulsion Copolymerisation Models**

	Property modelled				Experimental Verification		
Authors	Kinetics	MWD	PSD	Average Size	Batch	Semi-Batch	CSTR
(Arzamendi et al., 1994)	X	X		X	X	X	
(Ballard et al., 1981)	X						
(Show-An and Kuo-Wei, 1988)			X				
(Dougherty, 1986a, Dougherty, 1986b)	X	X	X		X		
(Forcada and Asua, 1985)	X						
(Forcada and Asua, 1991, Forcada and Asua, 1990)	X	X		X	X		
(Haskell and Settlage, 1971)	X						
(Gevorkova et al., 1970, T. A. Gevorkova, 1972)	X						
(Giannetti et al., 1988)	X	X					
(Giannetti, 1989)	X		X				
(Guillot, 1980, Guillot, 1981, Guillot, 1990, Guillot, 1993)	X				X		
(Hamielec et al., 1987, Hamielec et al., 1983, Broadhead et al., 1985, Dube et al., 1997)	X	X	X		X		

Authors	Kinetics	MWD	PSD	Average Size	Batch	Semi-Batch	CSTR
(Lin et al., 1981)	X	X			X		
(Noel et al., 1994b)	X				X		
(Nomura et al., 1983, Nomura et al., 1981, Nomura et al., 1982)	X			X	X		
(Nomura and Fujita, 1985)	X	X		X	X		
(Omi et al., 1987)	X	X			X	X	
(Mead and Poehlein, 1988)	X		X				X
(Quarderer and Katti, 1993)	X	X	X				
(Richards et al., 1989)	X	X	X		X		X
(Storti et al., 1989a, Storti et al., 1989b)	X		X		X		
(Cociani et al., 1989, Storti et al., 1992b, Storti et al., 1992a)		X					X
(Urretabizkaia et al., 1992)	X			X		X	
(van`Doremaele et al., 1992)	X	X			X		
(Araujo et al., 2001, Saldivar and Ray, 1997, Saldivar et al., 1998b, Saldivar et al., 1998a, Saldivar et al., 2001, Saldivar et al., 2002)	X	X	X	X	X	X	
(B. Alhamad et al.)	X	X	X	X	X	X	X

Table 2.1 Emulsion Copolymerisation Models

One of the first attempts to generalize the ideas of Smith-Ewart to the copolymer case was the model developed by Haskell and Settlage (Haskell and Settlage, 1971). A monodisperse population of particles was described in the model, but no account for the desorption of radicals was considered. The system was applied to the batch and semibatch copolymerisation of vinylidene chloride with other unspecified monomers, and was mentioned to have a qualitative agreement of the model predictions with the experimental data.

The first successful attempt to generalize the Smith-Ewart recurrence equation of emulsion homopolymerisation to the copolymer case was the model developed by Ballard, Napper and Gilbert (Ballard et al., 1981). A zero-one kinetics system was used, and the work suggests the use of apparent rate constants to treat the copolymer system as a pseudo-homopolymer system.

Nomura and coworkers (Nomura et al., 1983, Nomura et al., 1981, Nomura et al., 1982) used the "average" rate constants to extend previous emulsion polymerisation results to the copolymerisation case. The great contribution by the authors was the development of the desorption rate coefficient for the case of emulsion copolymerisation. The account for the monomer partitioning in emulsion copolymerisation was introduced by Guillot (Guillot, 1980, Guillot, 1981, Guillot, 1990, Guillot, 1993, Broadhead et al., 1985, Hamielec et al., 1987, Hamielec et al., 1983) using rigorous thermodynamic models.

(Forcada and Asua, 1985) developed a simple model for the sequence length distribution in binary copolymers based on Markov chains. The issue was that no experimental data was shown to verify the model. A kinetic model to predict the number of monodispersed particles was presented by (Urretabizkaia et al., 1992). An important point to mention is that the use of apparent rate constants for treating the copolymer systems as pseudo-homopolymer systems has become a well-established practice in free radical polymerisation modelling. This approach has been identified in several ways: apparent rate constants (Arriola, 1989), pseudo-homopolymer approach (Tobita and Hamielec, 1991), or pseudo-kinetic approach (Fitch and Tsai, 1971b).

Most of the models for MWD are a set of population balance equations having the discrete internal coordinate the chain length instead of the number of growing chains. Some of these models include a simple description of nucleation for an average particle size.

One of the earliest attempts to calculate the MWD in emulsion copolymerisation is the work done by (Lin et al., 1981), which intended the molecular weight based on a known experimental particle size. (Nomura and Fujita, 1985) added simple equations to their previous models (Nomura et al., 1983, Nomura et al., 1981, Nomura et al., 1982) to describe molecular weight. (Omi et al., 1987) introduced a model that predicts kinetics and composition of the copolymer, as well as the sequence lengths and average molecular weights. The model is compared with experimental data for batch and semibatch copolymerisations. The PSD was not calculated, and the numbers of particles, as well as other parameters were estimated empirically from experimental measurements.

More recently papers, is a set of papers, Storti and coworkers (Cociani et al., 1989, Storti et al., 1992b, Storti et al., 1992a) presented a model for MWD alone using a stochastic approach. Their model uses Markov chains to estimate the probabilities of transitions of a polymeric chain based on kinetic parameters. Accurate MWD and sequence distributions can be calculated, avoiding the need for long-chain assumption. Some important restrictions to the model to work with no branching reactions allowed and no chain length dependent effect, taking into consider that the only example was the prediction of polydispersity in the CSTR homopolymerisation of styrene.

(Forcada and Asua, 1991, Forcada and Asua, 1990) presented a more complex model to calculate kinetics, number of average size particles, and MWD for the batch emulsion copolymerisation of styrene-methyl methacrylate. The kinetics and MWD were calculated using population balance equations with two discrete internal coordinates, number of radicals per particle and per length, but the PSD was not calculated. The effect of feed composition over conversion profiles and final M_w were successfully compared with experimental data after parameter fitting.

(Show-An and Kuo-Wei, 1988) presented one of the first papers dealing explicitly with the PSD for emulsion copolymerisation systems. They used the population balance approach,

extending the model of (Ballard et al., 1981) to consider size dependence. No experimental verification of the model was provided.

(Storti et al., 1989a, Storti et al., 1989b) presented a population balance equation model for describing the kinetics and particle size distribution for a general n-component emulsion copolymerisation. Poehilin and coworkers (Mead and Poehlein, 1988) modelled the PSD and kinetics for the steady state operation of seed-fed CSTRs. The PSD calculation was based in the known form of the residence time distribution of CSTRs.

Hamielec and coworkers (Hamielec et al., 1987, Hamielec et al., 1983, Broadhead et al., 1985, Dube et al., 1997) presented the first comprehensive model for emulsion copolymerisation. The model includes kinetics to predict PSD, MWD and copolymer conversion, and in one version includes a kinetic scheme that allows the prediction of branching and cross-linking. As with Storti et al. models, the MWD was calculated for a monodisperse PSD. In the case of the more complete kinetic scheme, the method of moments was employed to get only the leading moments of the MWD. The PSD calculations were not based on a full population balance equation, but used ordinary differential equations. The model does not account for the different histories of monomer concentrations. The model was fitted to experimental data for conversion versus time in batch reactions for the system butadiene-styrene.

Another comprehensive model for emulsion copolymerisation was published by Dougherty (Dougherty, 1986a, Dougherty, 1986b).The model predicts kinetics, MWD and PSD; however, it makes many simplifying assumptions and lacks detail. The PSD was modelled using what Dougherty calls a "histogram" approach. The MWD was calculated assuming an average number of radicals independent of particle size and adapting expression taken from bulk polymerisation. The model predicted qualitatively well the experimental data of (Nomura and Fujita, 1985) for the system methyl methacrylate-styrene at 50°C in batch reactors, but failed in quantitative predictions.

There is general agreement in the literature on the fact that there are two nucleation mechanisms in emulsion polymerisation: micellar and homogeneous. It is generally recognized that micellar nucleation is operating and predominant when the emulsifier is present in concentrations above the critical micelle concentration (CMC). For monomers

with relatively high water solubility, and especially if the emulsifier is present in low concentration, it is accepted that homogeneous nucleation may also be significant, being one of the postulated nucleation mechanisms for emulsion polymerisation below the CMC.

In the homogeneous nucleation mechanism, particles are created by oligomeric radicals reaching a critical length in the water phase and precipitating as new polymer particles. This mechanism was originally proposed by (Fitch and Tsai, 1971a) and then extended by (Hansen and Ugelstad, 1982) and (Feeney et al., 1984).

(Richards et al., 1989) proposed a comprehensive model for binary emulsion copolymerisation for CSTR, batch and semibatch reactors based entirely on the extended homogeneous nucleation mechanism of Feeney et al., assuming that no micellar nucleation takes place even above the CMC of the emulsifier. The main criticism for this model is its lack of a micellar nucleation mechanism. After this publication, a new body of experimental evidence (Hansen, 1992a, Morrison et al., 1992, Gilbert et al., 1991, Hansen, 1992b) again shows that micellar nucleation is the predominant mechanism for particle formation above the CMC.

It is important to notice that in all the more comprehensive models analysed, the MWD was calculated decoupled from the PSD. This does not allow calculation of broadening effects on the MWD, which may be important in CSTRs in which the PSDs are mainly broad.

Saldivar et al. (Araujo et al., 2001, Saldivar and Ray, 1997, Saldivar et al., 1998b, Saldivar et al., 1998a, Saldivar et al., 2001, Saldivar et al., 2002) proposed a comprehensive model for the emulsion copolymerisation process. Simpler forms of the PSD model are derived, since the PSDs are computationally intractable. Further dimensionally reduction of the models for MWD is obtained using the technique of moments. The mass of polymer in the particle has been chosen as the internal coordinate to write the population balance equations. The main theoretical disadvantage of the polymer mass representation is that it is difficult to describe phenomena that depend strictly on the history of the particle.

It is important to note that in the models analysed, the MWD was calculated decoupled from the PSD. This does not allow calculation of broadening effects on the MWD, which

may be important in CSTRs in which the PSDs are broad. In our work, two families of models are presented: (1) the PSD and reactor models to describe the conversion evolution, composition and PSD in stirred tank reactors; and (2) the MWD models including M_n and M_w, which are coupled to the PSD models. The instantaneous MWD are calculated by considering the live and dead polymers, as proposed by (Clay and Gilbert, 1995).

From the practical point of view, detailed comprehensive models, suitable for use in flow sheet simulation for process design and analysis, are necessary.

2.6 Model Development

The kinetic rate model for emulsion polymerisation and copolymerisation is based on a system with zero-one kinetics (Gilbert, 1995) which is employed for straight chain addition polymerisation combining the effects of radical transfer, particle growth and molecular weight distribution (MWD). When modelling the emulsion polymerisation processes, there are two mechanisms used for particle growth, zero-one and pseudo-bulk kinetics (Gilbert, 1995).

In an emulsion polymerization system, the latex particles can differ in size as well as in the number of radicals per particle, and in the degree of polymerization of these radicals. The growth rate of a particle obviously depends on the number of radicals, but is also affected by their degree of polymerization since the termination rate coefficient depends on the length of the terminating chains. This is the so-called chain-length-dependent (CLD) termination. Because, in general, both the number and the degree of polymerization of the radicals affect the particle growth rate, such parameters should be included as additional internal coordinates in the population balance equations (PBE). Unfortunately, this leads to an intractable multidimensional PBE. The only way to overcome this difficulty is to reduce the dimensionality of the problem by making some approximations. The most common alternatives are:

- To neglect CLD termination. In this way we can remove the degree of polymerization of the radicals from the PBE.

• To neglect particles with two or more radicals: zero-one model. This automatically eliminates the problems related with termination and reduces the dimensionality of the equations since the number of radicals is limited to zero or one.

• To neglect compartmentalization effects (i.e. the isolation of radicals in separate particles): pseudo-bulk model. The number of radicals is no longer an internal coordinate, since particles of the same size are assumed to have the same (average) number of radicals. One may or may not account for CLD termination, but in either case the chain length distribution of the growing chains does not appear as an internal coordinate in the PBE.

Using the first hypothesis, we are still left with two internal coordinates: particle size and number of radicals per particle. This remains a complex problem, but it had been showed how to solve it by defining an infinite set of particle density functions, each accounting for the PSD of the particles having a given number of radicals. For a general case involving nucleation, coagulation, variable coefficients, etc., the infinite set of integro-hyperbolic partial differential equations can only be solved by numerical methods, at the expense of large computation times. Consequently, this approach (even if approximate) is rarely used to compute the PSD. In fact, analytic solutions are available. In particular, (Giannetti, 1989(a), 1989 (b)) derived a solution applicable to the Interval II of emulsion polymerization (no nucleation, no coagulation, constant coefficients, etc.) and later extended it to the Interval I. This kind of solutions may be used to gain insight into system behaviour and to check numerical results, but they are of limited interest for reactor simulation.

The other two alternatives to handle the kinetics, i.e. the zero-one and the pseudo-bulk model, are substantially simpler and thus widely used in Emulsion Polymerisation models.

In a zero-one system, the entry of a radical into a particle already contains a radical causing termination at a rate much higher than that of the overall polymerization. Therefore, a particle can have either zero or one radicals. For zero-one systems, it becomes feasible to use an exact mathematical formulation because: i) the number of PBEs is reduced given that termination does not have to be taken into consideration. There are two alternative treatments for zero-one systems. One possibility is to distinguish only between

particles having zero or one radicals. Another possibility, more frequently consists in further dividing particles having one radical in two populations, according to whether the radical is monomeric or polymeric. Since only monomeric radicals are assumed to desorb, this facilitates the description of radical desorption

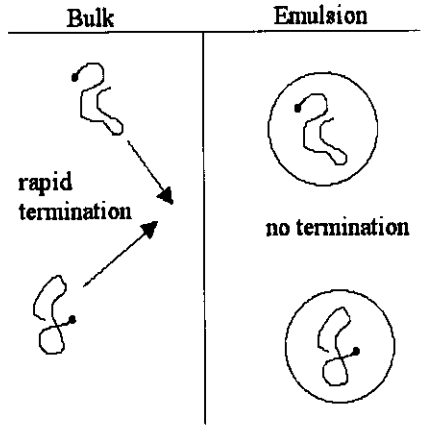

Figure 2.1. Effect of compartmentalisation on termination.

In contrast, a pseudo-bulk system has a relatively high number of free radicals per particle, which means that there could be more than one radical in a particle with no instantaneous termination occurring.

The latex particles are less than 100nm, and hence the zero-one model is considered to be more accurately and more suitable to this operation process.

2.6.1 Modelling the Zero-one System

(Gilbert, 1995) and (Coen et al., 1998) were the first to present the PBEs (including coagulation) for this version of the zero-one model. However, note that in these works the terms accounting for particle formation due to coagulation were incorrectly transcribed in press. These PBEs can easily be derived if recognized that termination being instantaneous, both the entry of a radical into a particle already containing a radical and the coagulation between two active particles lead to a dead particle. Concerning the coagulation terms, note that the factor 2 to 1 must only be included in the rate of particle

formation due to coagulation when the same particle density function appears twice in the kernel (to avoid double counting).

A necessary but not sufficient condition is that $n \leq 0.5$. Nevertheless, it is necessary to make a clear distinction between the applicability of the zero-one model for the prediction of the kinetic behaviour of the system (i.e. n) and the prediction of PSD. This problem was discussed in detail by (Giannetti, 1989) and is of primary importance for the modeling of PSD. According to this author, even if the contribution of particles with more than one radical is negligible for the kinetic behaviour of the system when $n << 0.5$, the same is not true for the PSD. Actually, the fact that particles with more than one radical do exist, increases the broadness of the PSD with respect to that predicted by the zero-one model. This is a shortcoming to bear in mind when using this approach to compute the PSD. Since this approach is only suitable for systems following zero-one kinetics, its applicability is somewhat limited. In fact, zero-one systems generally concern small particles (for which the rate of radical entry is low and the rates of radical desorption and termination are high) and low conversions (as to avoid a significant Trommsdorff effect). Despite its inherent limitations, the zero-one model can be of great value in interpreting mechanistic studies. In particular, it has been used by Gilbert's workgroup to investigate the mechanisms of particle formation in the emulsion polymerization of styrene. This approach has also been used in a few reaction engineering studies. (Zeaiter et al., 2002b) extended (Coen et al., 1998) to predict the evolution of PSD and MWD during the semi-batch emulsion polymerization of styrene. The model was used to study the possibility of controlling PSD and MWD by manipulation of the reactor temperature and monomer flow rate.(Crowley et al., 2000) simplified the model proposed by (Coen et al., 1998), by neglecting particle coagulation, and used it to investigate the optimization of the surfactant feed profile given a target bimodal PSD. (Meadows et al., 2003) extended the model by (Coen et al., 1998) to non-isothermal conditions, neglecting particle coagulation, and used it to explore methods for controlling the PSD.

A general description of a zero-one system is illustrated in Figure 2.2 below,

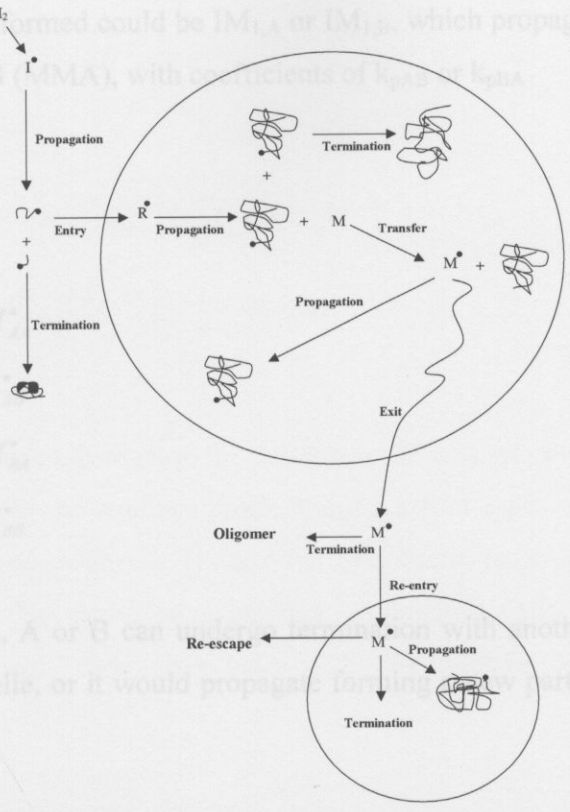

Figure 2.2. Mechanisms occurring in emulsion polymerisation.

The copolymerisation process begins with the decomposition of the initiator in the water phase, which then reacts with monomers A and B to generate oligomeric radicals according to the following reactions:

$$I - I \xrightarrow{k_d} 2I^{\bullet}$$

$$I^{\bullet} + M \xrightarrow{k_{p1}} IM_1^{\bullet}$$

where k_d is the dissociation coefficient (s^{-1}) and k_p is the propagation coefficient (l/mol.s)

These oligomeric radicals then undergo a sequence of reactions as outlined below:

$$IM_i^{\bullet} + M \xrightarrow{k^i_{p,aq}} IM_{i+1}^{\bullet}$$

The oligomeric radical formed could be $IM_{1,A}$ or $IM_{1,B}$, which propagate with monomer A (styrene) or monomer B (MMA), with coefficients of k_{pAB} or k_{pBA}

$$I^{\bullet} + M_A \xrightarrow{kp_A} IM_A^{\bullet}$$

$$I^{\bullet} + M_B \xrightarrow{kp_B} IM_B^{\bullet}$$

$$IM_A^{\bullet} + M_A \xrightarrow{kp_{AA}} IM_{AA}^{\bullet}$$

$$IM_A^{\bullet} + M_B \xrightarrow{kp_{AB}} IM_{AB}^{\bullet}$$

$$IM_B^{\bullet} + M_A^{\bullet} \xrightarrow{kp_{BA}} IM_{BA}^{\bullet}$$

$$IM_B^{\bullet} + M_B^{\bullet} \xrightarrow{kp_{BB}} IM_{BB}^{\bullet}$$

The oligomeric radical, A or B can undergo termination with another radical, entry to a latex particle or a micelle, or it would propagate forming a new particle by homogeneous nucleation.

$$IM_i^{\bullet} + T^{\bullet} \xrightarrow{k_{t,aq}} inert\ products,\ i < z$$

$$IM_i^{\bullet} + latex\ particle \xrightarrow{k_e^i} entry\ ,\ i = z,\ldots,j_{crit} - 1$$

$$IM_i^{\bullet} + micelle \xrightarrow{k_{e,micelle}^i} new\ particle\ ,\ i = z,\ldots,j_{crit} - 1$$

$$IM_{jcrit}^{\bullet} \longrightarrow new\ particle$$

Mass balances on the various aqueous radical species leads to the following set of rate equations:

$$\frac{d[I^{\bullet}]}{dt} = 2k_d[I] - k_{p1}[I^{\bullet}]C_w \qquad \text{(Eq. 2.7)}$$

$$\frac{d[IM_1^{\bullet}]}{dt} = k_{p1}[I^{\bullet}]C_w - k_{p,aq}^1[IM_1^{\bullet}]C_w - k_{t,aq}[IM_1^{\bullet}][T^{\bullet}] \qquad \text{(Eq. 2.8)}$$

$$\frac{d[IM_i^\bullet]}{dt} = k_{p,.aq}^{i-1}[IM_{i-1}^\bullet]C_w - k_{p,aq}^{i}[IM_i^\bullet]C_w - k_{t,aq}[IM_i^\bullet][T^\bullet] \;,\; i < z \qquad \text{(Eq. 2.9)}$$

$$\frac{d[IM_i^\bullet]}{dt} = k_{p,.aq}^{i-1}[IM_{i-1}^\bullet]C_w - k_{p,aq}^{i}[IM_i^\bullet]C_w - k_{t,aq}[IM_i^\bullet][T^\bullet] - k_e^i[IM_i^\bullet]\frac{N_{tot}}{N_A} - k_{e,micelle}^i C_{micelle}[IM_i^\bullet], \quad i = z,....,j_{crit}-1 \qquad \text{(Eq. 2.10)}$$

No radicals are fed to or removed from the system, so the overall balance of radicals in the aqueous phase is zero. In the aqueous phase, there are four types of radical species that need to be addressed and balanced. The are the oligomeric radicals of degree 1; degree greater than 1 and less than z; degree greater than or equal to z and less than $j_{crit} - 1$; and exited monomeric radicals. These can be balanced by the following set of rate equations,

$$IM_1 = \frac{2k_d[I]}{k_{p,aq}^1 \cdot C_w + k_{t,aq} \cdot T} \qquad \text{(Eq. 2.11)}$$

$$IM_i = \frac{k_{p,aq}^{i-1} \cdot IM_{i-1} \cdot C_w}{k_{p,aq}^i \cdot C_w + k_{t,aq} \cdot T}, \qquad \text{for i = 2 to (z-1)} \qquad \text{(Eq. 2.12)}$$

$$IM_{(i)} = \frac{k^{(i-1)}{}_{paq} \cdot IM_{(i-1)} \cdot C_w}{k^i{}_{paq} \cdot C_w + \sum(k_e^{\,i} \cdot n) \cdot \Delta r + k^i{}_{e,micelle} \cdot C_{micelle} + k_{taq} \cdot T}, \text{ for i = z to } (j_{crit}\text{-}1) \qquad \text{(Eq. 2.13)}$$

$$IM_{jcrit} = \frac{k_{p,aq}^{jcrit-1} \cdot IM_{jcrit-1} \cdot C_w}{k_{t,aq} \cdot T} \qquad \text{(Eq. 2.14)}$$

Defining the terms, C_w is the monomer concentration in the water phase, N_{tot} is the total number of latex particle per litre of aqueous phase, and N_A is Avogadro's number. Furthermore, the monomeric radicals formed by radical transfer to the monomer, $M^\bullet$, which either could be styrene or MMA, $M^\bullet_A$ or $M^\bullet_B$, may desorb from the particle with such "exited" radicals denoted by $E^\bullet_A$, or $E^\bullet_B$. It is important to note that, $M^\bullet_A$ means that the terminal monomer is A, and so as for the other terms. Once such a desorbed radical

meets the surface of a particle, it will immediately penetrate the particle due to its high lipophilic nature. This adsorption-desorption process is reversible, as illustrated below:

$$E_A^{\bullet} + particle \underset{k_{dM}}{\overset{k_{eE}}{\rightleftharpoons}} (particle - M^{\bullet})$$

$$E_B^{\bullet} + particle \underset{k_{dM}}{\overset{k_{eE}}{\rightleftharpoons}} (particle - M^{\bullet})$$

Hence, the total radical concentration in the aqueous phase [T•] becomes:

$$[T^{\bullet}] = \sum_{i=1}^{z-1} [IM_i^{\bullet}] + [E^{\bullet}] \qquad \text{(Eq. 2.15)}$$

An important point to be pointed out is that oligomeric radicals for each monomer A and B could not be taken individually for several reasons:

(a) The reaction taking place has the probability of reacting either with A or with B, and that is for one particle to 10^{17} particles.

(b) Monomer A does not react individually from monomer B

2.6.1.1 Initiator Balance

The consumption of initiator is only apparent in the aqueous phase of the reaction. The concentration of initiator, $[I]$, is the number of moles of initiator present at any time, t, divided by the volume of the aqueous phase (V_w), F_I is the flow rate of the initiator. As shown previously, the rate of consumption by decomposition of the initiator is given by,

$$\frac{d[I]}{dt} = -2fk_d\left([I] + \frac{F_I}{V_w}\right) \qquad \text{(Eq. 2.16)}$$

The above equation also represents the rate of radical production. The decomposition coefficient, k_d, for persulfate and in terms of Arrhenius parameters, is given by,

$$k_d = 8 \times 10^{15} e^{-135/RT} \qquad \text{(Eq. 2.17)}$$

From the above expression, it can be seen that this parameter is temperature dependant and increases with an increase in temperature, as with all other rate coefficients.

2.6.1.2 Surfactant Balance

A material balance can also be carried out on the surfactant over the aqueous and dispersed phases of the polymerisation. The latex particles and sparingly soluble monomer droplets are stabilised by the adsorption of surfactant molecules onto their surface. The actual amount that is adsorbed is in equilibrium with the amount in the aqueous phase and the dispersed phases, expressed as,

$$S_T = V_W S_W + K_S S_W V_P + \frac{\Gamma_S K_{ad} S_W A_P}{1 + K_{ad} S_W} \qquad \text{(Eq. 2.18)}$$

The first term accounts for the surfactant in the aqueous phase, the second term for the surfactant absorbed into the particle, S_b, and the third term for the surfactant adsorbed onto the surface of the particle, S_a. V_W is the Volume fraction of the water in the aqueous phase; S_W is the amount of surfactant in the aqueous phase and determines $[S]_w$, the surfactant concentration in the aqueous phase; K_S and K_{ad} are the absorption and adsorption coefficients for the surfactant, respectively; Γ_S is the interfacial tension between the particle and the surfactant. A_P is the area of the particle. The last term in Equation 2.19 resembles the Langmuir-type isotherm, for adsorption.

The area occupied by one surfactant molecule when adsorbed onto a surface is given by,

$$A_m = a_{ms}\left(1 + \frac{1}{S_W K_{ad}}\right) \qquad \text{(Eq. 2.19)}$$

where a_s is the minimum area of a micelle covered by a surfactant molecule. The free surfactant in the water phase, can be calculated using the following relationship (Coen et al., 1998),

$$S_W = [S] - \frac{A_P}{N_A A_m} \qquad \text{(Eq. 2.20)}$$

Here, $[S]$ is the total moles of added surfactant per unit volume of the aqueous phase. The total surface area of the latex particles is found by,

$$A_P = \int_0^\infty 4\pi r_s^2 n(r) dr \qquad \text{(Eq. 2.21)}$$

$$= \sum_0^\infty 4\pi r^2 N_r \qquad \text{(Eq. 2.22)}$$

where N_r is the number of particles with unswollen radius, r.

If A_m is unknown or unable to be calculated, the aqueous phase concentration of surfactant can be calculated using the following expression,

$$[S]_w^2 + [S]_w\left(\frac{A_p}{a_s N_A} + \frac{1}{K_{ad}} - [S]\right) - \frac{1}{K_{ad}}[S] = 0 \qquad \text{(Eq. 2.23)}$$

Finally, the micelle concentration can be found using the maximizing function,

$$C_{micelle} = MAX\left(0, \frac{[S]_w - cmc}{n_{agg}}\right) \qquad \text{(Eq. 2.24)}$$

Where cmc is the *critical micelle concentration* and n_{agg} is the aggregation number for the surfactant.

The micelle concentration, $C_{micelle}$ is determined by the rate of surfactant consumption. The amount of adsorbed surfactant onto the particle surface is defined as,

$$S_{ads} = \frac{4\pi r_s^2 N_{tot}}{N_A a_s} \qquad \text{(Eq. 2.25)}$$

and therefore,

$$C_{micelle} = \max imum\left[0, \frac{[S_{added}] - S_{ads} - [cmc]}{n_{agg}}\right] \qquad \text{(Eq. 2.26)}$$

where $[S_{added}]$ is the total concentration of surfactant added, n_{agg} is the average number of surfactant molecules in a micelle (known as the micellar aggregation number), [cmc] is the critical micelle concentration, and a_s is the area occupied by an adsorbed surfactant molecule,. From Equation 2.27, it is observed that the concentration of the micelles is none when the surfactant concentration is below the cmc. Another relation could also be seen, that is the critical relationship existing between the number of particles, N_{tot} and the surfactant concentration.

When surfactant is added on to the reactor on a semi-batch reaction, the following additional equations are used:

$$\frac{dN_s}{dt} = F_s \qquad \text{(Eq. 2.27)}$$

$$S = \frac{N_s}{V_w} \qquad \text{(Eq. 2.28)}$$

$$\frac{dV_w}{dt} = F_w \qquad \text{(Eq. 2.29)}$$

where *s* denotes to the surfactant, w denotes to the water, N is the number of moles. F is the flow rate, where F_s is in mol/s and F_w is in l/s.

2.6.1.3 PSD Model

Given assumptions as in (Zeaiter et al., 2002b), the population balance equations for the three particle types (n_1^p, n_o and n_1^M) are as follows:

$$\frac{\partial n_1^p(V,t)}{\partial t} = \frac{\delta(V-V_o)}{\Delta r}\left(k_{p,aq}^{jcrit-1} C_w IM_{jcrit-1} + \sum_1^{jcrit-1} k_{e,micelle} C_{micelle} IM_i\right) + k_p C_p n_1^m + \rho_{init} n_1^o$$

$$- \rho n_1^p - k_{tr} C_p n_1^p - \frac{\partial(Kn_1^p)}{\partial V} + \int_0^\infty B(V,V-V')\left[n_o(V')n_1^p(V-V') + n_1^p(V')n_o(V-V')\right]dV'$$

$$- n_1^p(V)\int_0^\infty B(V,V')\left[n_o(V') + n_1^p(V')\right]dV' \qquad \text{(Eq. 2.30)}$$

$$\frac{\partial(Kn_{1,1}^p)}{\partial V} = \frac{K}{8\pi\Delta r}\frac{n_{1,2}^p}{\left(r_{uns,2}\right)^2} \qquad \text{(Eq. 2.31)}$$

$$\frac{\partial n_1^m(V,t)}{\partial t} = k_{tr} C_p n_1^p + k_{eE}[E] n_o - (k_p C_p + \rho + k_{dm}) n_1^m \qquad \text{(Eq. 2.32)}$$

$$\frac{\partial n_o(V,t)}{\partial t} = \rho\left(n_1^p + n_1^m - n_o\right) + k_{dm} n_1^m + \int_0^\infty B(V,V-V')\left[n_o(V')n_o(V-V') + n_1^p(V')n_1^p(V-V')\right]dV'$$

$$- n_o(V)\int_0^\infty B(V,V')\left[n_o(V') + n_1^p(V')\right]dV' \qquad \text{(Eq. 2.33)}$$

The solutions to the above equations, known as the evolution equations is used for the particle size distribution as a function of unswollen volume, V, otherwise known as the volume distribution. As mentioned previously, to reduce the computational load in the implementation of the model, it is suggested (Fitzroy, 2000) to discretise the model into the corresponding equations as a function of unswollen radius.

The population balance for particles containing zero radicals incorporates entry and exit events of monomeric radicals of type i (monomer A, styrene or monomer B, MMA). That is, n_o particles are formed through the entry of radicals into particles containing both polymeric and monomeric radicals. Also, they are formed via the desorption of monomeric radicals form particles that contain only monomeric radicals, n_i^m. The population decreases, when the particle is entered by an oligomeric radical to form a n_i^p particle or by the event of re-entry of a monomeric radical to form a n_i^m particle. k_{dm} is the desorption coefficient of monomeric radicals from particles.

Particles that contain polymeric radicals of type i, n_i^p, are formed through the nucleation mechanisms of micellar and homogeneous, with entry to micelles or through propagation; through the entry event of an oligomeric radical into a n_o particle; and when particles with monomeric radicals propagate the monomeric radical converts to a polymeric radical. The population of n_i^p type particles decreases via termination when either an oligomeric or exited radical enters or due to the event of chain transfer to a monomer.

The growth of a particle only affects n_i^p type particles since firstly, there must be radicals to facilitate growth and secondly, a monomeric radical becomes a polymeric radical once growth is initiated. Therefore, the growth component only appears in the equation relating to polymeric radicals with the propagational growth rate.

A Dirac delta function is used (Coen et al., 1998). It assumes that volume is no longer constant (due to the growth term) and thus, this function ensures that all particles nucleate with constant volume.

For particles that contain only monomeric radicals, n_1^m, the evolution equation is slightly less complicated due to the lack of events that need to be represented. Generation of these particles is the result of re-entry of exited monomeric radicals as well as chain transfer events within particles containing polymeric radicals. They are consumed via the propagation of radicals inside the particle, desorption of the monomeric radical and the entry of any radical.

The above set of coupled-partial integro-differential equations is the set of evolution equations that describe the volume-based distribution for the latex particles in an emulsion copolymerisation. The overall balance is represented by,

$$n(V,t) = n_o(V,t) + n_1^m(V,t) + n_1^p(V,t) \qquad \text{(Eq. 2.34)}$$

However, to make this set comprehensive, the incorporation of the coagulation effects must be realized. Coagulation effects in emulsion polymerisation reactions are neglected The incorporation of coagulation effects into the model increases the size of the model considerably, in terms of variables (Fitzroy, 2000). However, the assumptions of compartmentalisation and having the particle size of the latex produced less than 100 nm validates the assumption of neglecting the coagulation effect.

After discretising the particle volume-base distribution, the average number of radicals per particle, $\bar{n}(V)$, can be expressed by,

$$\bar{n}(V) = \frac{1}{\sum_{l=1}^{G} n(V_l)} \left[\sum_{i=1}^{2} \left(\sum_{l=1}^{G} n_{1,i}^{P}(V_l) \right) + \sum_{i=1}^{2} \left(\sum_{l=1}^{G} n_{1,i}^{M}(V_l) \right) \right] \qquad \text{(Eq. 2.35)}$$

where G is the number of increments that have been assigned to accommodate the discrete function in V.

The average number of radicals per particle, $\bar{n}$, is given by,

$$\bar{n} = \frac{1}{\sum_{i=1}^{G} n(V_i)} \left(\sum_{i=1}^{G} n_1^P(V_i) + \sum_{i=1}^{G} n_1^M(V_i) \right) \qquad \text{(Eq. 2.36)}$$

while the total number of particles per unit volume, N_{tot} , can be calculated from,

$$N_{tot} = N_A \int_0^{\infty} n(V) dV \qquad \text{(Eq. 2.37)}$$

2.6.1.3.1 Kinetic Coefficients:

In order to form the mathematical model for the emulsion copolymerisation, the mass and energy balances were required. Then the population balance equations were developed. The population balance equations require the rate coefficients and associated parameters. First of all, empirical formulas by (Gilbert, 1995) are used to determine the critical degree for micellar (z) and homogeneous (j_{crit}) nucleation.

$$z = 1 + \frac{-23\text{kJ.mol}^{-1}}{RT \ln C_W^{sat}} \qquad j_{crit} = 1 + \frac{-55\text{kJ.mol}^{-1}}{RT \ln C_W^{sat}} \qquad \text{(Eq. 2.38)}$$

For a styrene emulsion with an anionic surfactant, z = 3 and j_{crit} = 5.
For a MMA emulsion with an anionic surfactant, z = 5 and j_{crit} = 10.

K in the population balance equations is the propagational growth rate, and is given by:

$$K_A = \frac{(k_{pAA} C_{p,A} + k_{pAB} C_{P,B}) M_{w,A}}{d_{p,A} \cdot N_a} \qquad \text{(Eq. 2.39)}$$

$$K_B = \frac{(k_{pBB} C_{p,B} + k_{pBA} C_{P,A}) M_{w,B}}{d_{p,B} \cdot N_a} \qquad \text{(Eq. 2.40)}$$

$$K = P_A K_A + P_B K_B \qquad \text{(Eq. 2.41)}$$

or similarly can be found by the following relation:

$$K = \frac{k_{pBA}C_{p,A}K_A + k_{pAB}C_{p,B}K_B}{k_{pBA}C_{p,A} + k_{pAB}C_{p,B}} \quad \text{(Eq. 2.42)}$$

Growth only significantly affects n_1^p type particles, as radicals propagate without changing the particle's identity. The entry processes to the particle and to the micelle, and hence the rate coefficients, k^i_e and $k^i_{e,micelle}$, are assumed to be diffusion controlled. Given that oligomeric radicals can only enter a micelle or pre-existing particle, the entry coefficients for monomers A and B to the micelles (Clay and Gilbert, 1995) is calculated as follows

$$k^i_{e,micelle,A}(V) = 4\pi r_{micelle} \cdot Na \cdot \frac{D_{w,A}}{i}, i \geq z; k^i_{e,micelle}(V) = 0, i < z, \quad \text{(Eq. 2.43)}$$

$$k^i_{e,micelle,B} = 4\pi r_{micelle} \cdot Na \cdot \frac{D_{w,B}}{i}, i \geq z; k^i_{e,micelle}(V) = 0, i < z, \quad \text{(Eq. 2.44)}$$

where $r_{micelle}$ is the radius of the micelle, $D_{w,A}$, $D_{w,B}$ are the diffusion coefficients in the water phase, respectively, N_A is the Avogadro's number, i is the degree of polymerisation.

The average entry to the micelle (Vicente et al., 2002, Sayer et al., 2001) is given as:

$$k^i_{e,micelle} = k^i_{e,micelle,A} \cdot f_A \cdot \phi_A + k^i_{e,micelle,B} \cdot f_B \cdot \phi_B \quad \text{(Eq. 2.45)}$$

The entry rate coefficients to the particle (Clay and Gilbert, 1995) for monomers A and B are:

$$k^{i,j}_{e,A} = 4\pi r^j_s \cdot Na \cdot \frac{D_{w,A}}{i}, i \geq z; k^i_e(V) = 0, i < z, \ , \quad \text{(Eq. 2.46)}$$

$$k^{i,j}_{e,B} = 4\pi r^j_s \cdot Na \cdot \frac{D_{w,B}}{i}, i \geq z; k^i_e(V) = 0, i < z, \quad \text{(Eq. 2.47)}$$

where r_s is the radius of the particle swollen with monomer. Note that r_s is related to the unswollen radius, r_{uns}, as follows:

$$r_s^j = r_{uns}^j \times \left(\frac{d_{avg}}{d_{avg} - C_p \cdot M_w} \right)^{1/3} \quad \text{(Eq. 2.48)}$$

The overall rate of entry, ρ^j is derived from the following equation:

$$\rho^j = \rho_{init}^j + k_{eE} E \quad \text{(Eq. 2.49)}$$

where ρ_{init}^j is the rate of formation of 'z-mers' obtained from

$$\rho_{init}^j = \sum_1^G \left(k_e^{(i,j)} \cdot IM_i \right) \quad \text{(Eq. 2.50)}$$

where G is the number of radius increments for the system to be integrated.

The copolymer mole fractions are

$$f_A = \frac{N_{m,A}^{fed}}{N_{m,A}^{fed} + N_{m,B}^{fed}} \quad \text{(Eq. 2.51)}$$

$$f_B = 1 - f_A \quad \text{(Eq. 2.52)}$$

where $N_{m,A}^{fed}$ and $N_{m,B}^{fed}$ are the number of moles fed for A and B.

$F_1$and F_2 are the propagational probabilities in the water phase.

$$F_1 = \frac{r_A f_A^2 + f_A f_B}{r_A f_A^2 + 2 f_A f_B + r_B f_B^2} \quad \text{(Eq. 2.53)}$$

$$F_2 = 1 - F_1 \quad \text{(Eq. 2.54)}$$

The average entry (Vicente et al., 2002, Sayer et al., 2001) is given as

$$k_e^{i,j} = f_A \cdot \phi_A \cdot k_{e,A}^{i,j} + f_B \cdot \phi_B \cdot k_{e,B}^{i,j} \quad \text{(Eq. 2.55)}$$

where f_A is the fraction of monomer A, and f_B is the fraction of monomer B, and Φ_A and Φ_B are the probability of the reaction of radicals in the water phase, and they are defined as follows (Maxwell and Russell, 1993, Russell et al., 1992):

$$\phi_A = \frac{k_{pBA} \cdot f_A}{k_{pBA} \cdot f_A + k_{pAB} f_B} \quad \text{(Eq. 2.56)}$$

$$\phi_B = 1 - \phi_A \quad \text{(Eq. 2.57)}$$

where k_{pBA}, k_{pAB} are the propagation coefficients when A propagates with B, and B propagates with A (Clay and Gilbert, 1995), respectively, and they are obtained by the following relations:

$$k_{pAA} = k^1_{p,aq,A} \quad \text{(Eq. 2.58)}$$

$$k_{pBB} = k^1_{p,aq,B} \quad \text{(Eq. 2.59)}$$

$$k_{pAB} = \frac{k_{pAA}}{r_A} \quad \text{(Eq. 2.60)}$$

$$k_{pBA} = \frac{k_{pBB}}{r_B} \quad \text{(Eq. 2.61)}$$

where k_{pAA}, k_{pBB} are the propagation coefficients when A propagates with A, and B propagates with B, respectively, and r_A and r_B are the reactivity ratios for monomers A and B, respectively.

The propagation constant for monomer A and monomer B obtained from (Clay and Gilbert, 1995) are given as follows:

$$k_{po,A} = 10^{7.63} e^{\frac{-32500}{RT_r}} \quad \text{(Eq. 2.62)}$$

$$k_{po,B} = 10^{6.4} e^{\frac{-22200}{RT_r}} \quad \text{(Eq. 2.63)}$$

Theses propagation coefficients are diffusion controlled at high conversions, relating the propagation rate constant being chemically and diffusion controlled (Maxwell and Russell, 1993, Russell et al., 1992).

$$\frac{1}{k_{p,A}} = \frac{1}{k_{po,A}} + \frac{1}{k_{diff,A}} \quad \text{(Eq. 2.64)}$$

$$\frac{1}{k_{p,B}} = \frac{1}{k_{po,B}} + \frac{1}{k_{diff,B}} \qquad \text{(Eq. 2.65)}$$

where $k_{po,A}$, $k_{po,B}$ are the propagation rate coefficient at low conversion, while $k_{diff,A}$, $k_{diff,B}$, are the diffusion controlled rate coefficients given as:

$$k_{diff,A} = 4\pi\sigma N_A (D_{mon,A} + D_{rd,A}) \qquad \text{(Eq. 2.66)}$$

$$k_{diff,B} = 4\pi\sigma N_A (D_{mon,B} + D_{rd,B}) \qquad \text{(Eq. 2.67)}$$

where $D_{rd,A} = \frac{1}{6} k_{p,A} C_{p,A} \alpha^2$ (Eq. 2.68)

and $D_{rd,B} = \frac{1}{6} k_{p,B} C_{p,B} \alpha^2$ (Eq. 2.69)

The diffusion coefficients for styrene and MMA (Gilbert, 1995, Faldi et al., 1994, Clay and Gilbert, 1995) change at high conversion, which in turn results in the decrease of the propagation and termination coefficient, which becomes diffusion controlled at high conversion. The diffusion coefficient for both monomers A and B, were expressed as a function of the polymer volume fraction inside the particle:

$$D_{mon,A} = 10^{0.417 - 29.51\phi_{p,A} + 53.14\phi_{p,A}^2 - 36.03\phi_{p,A}^3} \; for \phi_{p,A} < 0.8,$$
$$D_{mon,A} = 9 \times 10^{-8} e^{-19.16\phi_{p,A}} \; for \phi_{p,A} \geq 0.8 \qquad \text{(Eq. 2.70)}$$

$$D_{mon,B} = 10^{-4.386 - 3.2\phi_{p,B} + 9.049\phi_{p,B}^2 - 12.079\phi_{p,B}^3} \; for \phi_{p,B} < 0.8$$
$$D_{mon,B} = 75.651 * e^{-42.271\phi_{p,B}} \; for \phi_{p,B} < 0.8 \qquad \text{(Eq. 2.71)}$$

An additional entry phenomenon can be brought forward at high ϕ_p, that is, entry of a z-mer into a glassy particle, is impeded, e.g. because of slow diffusion through the interface. The "frustrated" z-mer then desorbs back into the aqueous phase and may propagate to a j_{crit}-mer and cause secondary nucleation. Therefore, an empirical equation for the entry efficiency, $e_e = ((1-\phi_p)^{Cp,sat}$, could be used to model these changes.

The further propagation coefficients (Clay and Gilbert, 1995) were taken as follows:

$$k^1_{p,aq,A} = 2k_{p,A} \quad \text{(Eq. 2.72)}$$

$$k^2_{p,aq,A} = 1.753k_{p,A} \quad \text{(Eq. 2.73)}$$

$$k^3_{p,aq,A} = k_{p,A} \quad \text{(Eq. 2.74)}$$

$$k^1_{p,aq,B} = 3.15k_{p,B} \quad \text{(Eq. 2.75)}$$

$$k^2_{p,aq,B} = 2k_{p,B} \quad \text{(Eq. 2.76)}$$

$$k^3_{p,aq,B} = k_{p,B} \quad \text{(Eq. 2.77)}$$

$$k^i_{p,aq} = k^3_{p,aq} \quad \text{(Eq. 2.78)}$$

The average propagation coefficient (Vicente et al., 2002, Sayer et al., 2001) was given as:

$$k^i_{p,aq} = k^i_{p,aq,A} \cdot f_A \cdot \phi_A + k^i_{p,aq,B} \cdot f_B \cdot \phi_B \quad \text{(Eq. 2.79)}$$

Probabilities for oligomeric radicals to propagate or terminate in the particle phase are defined as follows:

$$P_A = \frac{k_{pBA} \cdot C_{p,A}}{k_{pBA} \cdot C_{p,A} + k_{pAB} \cdot C_{p,B}} \quad \text{(Eq. 2.80)}$$

$$P_B = 1 - P_A \quad \text{(Eq. 2.81)}$$

The average propagation coefficient in the particle phase is calculated as follows:

$$k_p = k_{pAA} \cdot P_A^2 + k_{pAB} \cdot P_A \cdot P_B + k_{pBA} \cdot P_B \cdot P_A + k_{pBB} \cdot P_B^2 \quad \text{(Eq. 2.82)}$$

There have been different methods of obtaining the average propagation coefficient in the aqueous phase, which had very similar effects on the model.

$$k_{p,aq}^{1} = \frac{\left(k_{pAA}f_A + k_{pAB}f_B\right)\cdot k_{pBA}f_A}{k_{pBA}f_A + k_{pAB}f_B} + \left(k_{pBB}f_B + k_{pBA}f_A\right)\cdot\left(1 - \frac{k_{pBA}f_A}{k_{pBA}f_A + k_{pAB}f_B}\right) \quad \text{(Eq. 2.83)}$$

$$k_{p,aq}^{1} = \frac{r_A f_A^2 + 2f_A f_B + r_B f_B^2}{f_A / k_{pAB} + f_B / k_{pBA}} \quad \text{(Eq. 2.84)}$$

Within the particle phase, transfer to monomeric radicals takes place. The assumption of no transfer to polymeric radicals is applicable, since there are no transfer agents. The transfer coefficient for both styrene and MMA are given as follows

$$k_{tr,A} = k_{p,A} \times 10^{-0.658} e^{\frac{-23400}{RT_r}} \quad \text{(Eq. 2.85)}$$

$$k_{tr,B} = 4 \times 10^{5.3} e^{\frac{-45900}{RT_r}} \quad \text{(Eq. 2.86)}$$

The average transfer coefficient is given as follows

$$k_{tr} = k_{tr,AA}P_A^2 + k_{tr,BB}P_B^2 + k_{tr,AB}P_A P_B + k_{tr,BA}P_B P_A \quad \text{(Eq. 2.87)}$$

The particles with a radical could undergo termination reactions, which may further be activated and propagate again, and then terminate and so on. The termination coefficient at high conversions is subjected to an effect known as the gel effect. The termination rate coefficient and the gel effect are calculated by:

$$k_{t,aq,A} = 1.703 \times 10^{9} e^{\frac{-2263*4.182}{RT_r}} \quad \text{(Eq. 2.88)}$$

$$k_{t,aq,B} = 9.8\times10^{7} e^{\frac{-701*4.182}{RT_r}} \quad \text{(Eq. 2.89)}$$

$$k_{to} = k_{t,aq,A} f_A + k_{t,aq,B} f_B \quad \text{(Eq. 2.90)}$$

$$k_t = k_{to} \cdot g^2 \quad \text{(Eq. 2.91)}$$

$$g^2 = \left(g_A^2 \cdot g_B^2\right)^{1/2} \quad \text{(Eq. 2.92)}$$

$$g_A^2 = \left[\frac{1}{1-x}\exp\left(-6.59x - 1.896x^2\right)\right]^2 \quad \text{(Eq. 2.93)}$$

$$g_B^2 = \left[\exp\left(-0.94x - 3.87x^2 + 0.49x^3\right)\right]^2 \quad \text{(Eq. 2.94)}$$

while k_t, average termination coefficient in the particle phase is given as:

$$k_t = k_{tAA} P_A^2 + 2k_{tAB} P_A P_B + k_{tBB} P_B^2 \quad \text{(Eq. 2.95)}$$

There are three phases in the copolymerisation reaction, the water (w), particle (p) and monomer (m) droplets phase. The Partition Coefficient (K) between each two phases is taken into consideration and given as follows:

$$K_{A,wp} = \frac{C_{w,A}^{sat}}{C_{p,A}^{sat}} \quad \text{(Eq. 2.96)}$$

$$K_{A,mp} = \frac{d_{m,A} \cdot K_{A,wp}}{M_{w,A} \cdot C_{w,A}^{sat}} \quad \text{(Eq. 2.97)}$$

$$K_{B,wp} = \frac{C_{w,B}^{sat}}{C_{p,B}^{sat}} \quad \text{(Eq. 2.98)}$$

$$K_{B,mp} = \frac{d_{m,B} \cdot K_{B,wp}}{M_{w,B} \cdot C_{w,B}^{sat}} \quad \text{(Eq. 2.99)}$$

$$K_{A,mw} = \frac{K_{A,mp}}{K_{A,wp}} \quad \text{(Eq. 2.100)}$$

$$K_{B,mw} = \frac{K_{B,mp}}{K_{B,wp}} \quad \text{(Eq. 2.101)}$$

where $d_{m,B}$ is the density of monomer B, $M_{w,B}$ is the molecular weight of monomer B, and $C_{w,B}^{sat}$ is the saturated concentration of monomer B in the water phase.

The polymer fraction in the particle phase is calculated by knowing the number of moles of polymers of each A and B.

$$F_{bar,A} = \frac{N_{pol,A}}{N_{pol,B} + N_{pol,B}} \quad \text{(Eq. 2.102)}$$

$$F_{bar,B} = \frac{N_{pol,B}}{N_{pol,B} + N_{pol,B}} \quad \text{(Eq. 2.103)}$$

The area of the particle is given as:

$$Area_{particle} = (36\pi \times Ntot)^{1/3} \times V_p^{2/3} \quad \text{(Eq. 2.104)}$$

The average diameter or average radius of the particles is determined by the following:

$$Diameter_{particle} = \left(\frac{Area_{particle}}{\pi N_{tot}} \right)^{1/2} \quad \text{(Eq. 2.105)}$$

or

$$Average_{radius} = \frac{\sum (r_{uns} \cdot n)}{\sum n} \quad \text{(Eq. 2.106)}$$

The particle size polydispersity index, PSPI gives an indication of the width of the distribution. The PSPI is defined as the mean squared radius divided by the mean radius squared,

$$PSPI = \frac{< r^2 >}{< r >^2} \quad \text{(Eq. 2.107)}$$

where the mean squared radius is defined by:

$$< r^2 >= \frac{\sum_{i=1}^{G} n(i) r(i)^2}{\sum_{i=1}^{G} n(i)} \qquad \text{(Eq. 2.108)}$$

If all particles are identical, the mean squared radius and mean radius squared will be equal. This corresponds to a polydispersity index of 1, and the distribution is said to be mono-dispersed. As the distribution widens, the larger particles will more heavily influence the numerator (due to the r^2 term) and hence the index will increase.

The volume of the organic phase is determined by:

$$\frac{dV_{org}}{dt} = \frac{F_{mA,in} \cdot M_{w,A}}{d_{m,A}} + \frac{F_{mB,in} \cdot M_{w,B}}{d_{m,B}} - shrinkage$$

$$shrinkage = \sum_{i=A}^{B} \left\{ M_i (R_{pip} V_p + R_{piw} V_w) \left(\frac{1}{d_{m,i}} - \frac{1}{d_{p,i}} \right) \right\} \qquad \text{(Eq. 2.109)}$$

The volume of the monomer can be calculated by the difference between the volume of the organic phase and the sum of the volumes of polymer particles and of monomer in the aqueous phase. Here, F_m is the monomer feed rate. Notice that the molecular weight is still that of the monomer unit as the polymerisation reaction does not completely decompose the molecule, rather it joins them together in series. Thus for every mole of monomer consumed, the mass of polymer formed is equivalent to the mass of monomer consumed. The density of the polymer is however higher than that of the monomer, as the monomer units are brought closer together during polymerisation. Hence the first term in the right hand side of the previous equation represents the volume shrinkage caused by the polymerisation of the monomer.

The number of particles having a terminal of A or B is estimated using the parameter AA:

$$AA = \frac{k_{pAA}}{k_{pBB}} \frac{r_B}{r_A} \frac{C_{pB}}{C_{pA}} \qquad \text{(Eq. 2.110)}$$

$$n_a = \left(\frac{1}{1+AA}\right)\cdot n \qquad \text{(Eq. 2.111)}$$

$$n_b = \left(\frac{AA}{1+AA}\right)\cdot n \qquad \text{(Eq. 2.112)}$$

The sequence length distribution is estimated by the following two equations:

$$S_a = 1 + r_A \frac{N_{m,A}}{N_{m,B}} \qquad \text{(Eq. 2.113)}$$

$$S_b = 1 + r_B \frac{N_{m,B}}{N_{m,A}} \qquad \text{(Eq. 2.114)}$$

The probability that a monomeric radical of type i reacts in the aqueous phase by either propagation or termination is given by

$$\beta_A(j) = \frac{k_{pAA}\cdot C_{wA} + k_{pAB}\cdot C_{wB} + (k_{tAA}\cdot P_A + kt_{AB}\cdot P_B)\cdot T}{k_{pAA}\cdot C_{wA} + kp_{AB}\cdot C_{wB} + (k_{tAA}\cdot P_A + k_{tAB}\cdot P_B)\cdot T + \sum k_e(j)\cdot N_{tot}\cdot \frac{\phi_w}{N_a} + \sum k_{e,micelle}} \qquad \text{(Eq. 2.115)}$$

$$\beta_B(j) = \frac{k_{pBA}\cdot C_{wA} + k_{pBB}\cdot C_{wB} + (k_{tBA}\cdot P_A + kt_{BB}\cdot P_B)\cdot T}{k_{pBA}\cdot C_{wA} + kp_{BB}\cdot C_{wB} + (k_{tBA}\cdot P_A + k_{tBB}\cdot P_B)\cdot T + \sum k_e(j)\cdot N_{tot}\cdot \frac{\phi_w}{N_a} + \sum k_{e,micelle}} \qquad \text{(Eq. 2.116))}$$

k_{oi} is the rate of exit of a monomeric radical of type i from the polymer particles. Assuming a diffusion mechanism and no additional resistance at the interface, (Nomura, 1982) derived the following equation for k_{oi}:

$$k_{o,A} = \frac{12\cdot D_{w,A}\ K_{A,wp}\cdot d^2}{1 + 2\cdot D_{w,A}\ K_{A,wp}\cdot D_{p,A}} \qquad \text{(Eq. 2.117)}$$

$$k_{o,B} = \frac{12\cdot D_{w,B}\ K_{B,wp}\cdot d^2}{1 + 2\cdot D_{w,B}\ K_{B,wp}\cdot D_{p,B}} \qquad \text{(Eq. 2.118)}$$

where $D_{w,A}$ and $D_{p,A}$ are the diffusion coefficients of a monomeric radical of type i in the aqueous phase and the polymer particles, respectively, $K_{A,wp}$ is the partition coefficient of

such a radical between polymer particles and the aqueous phase, and d is the diameter of the particles.

(Asua et al., 1989) showed that termination only has a significant effect on the probability of desorption for small particle sizes. The overall desorption coefficients are calculated by:

$$k_{des,A}(j) = \frac{(k_{tr,AA} \cdot P_A + k_{tr,BA} \cdot P_B) \cdot C_{p,A} \cdot k_{o,A}}{\beta_A(j) \cdot k_{oA} + k_{pAA} \cdot C_{p,A} + k_{pAB} \cdot C_{p,B}} \quad \text{(Eq. 2.119)}$$

$$k_{des,B}(j) = \frac{(k_{tr,AB} \cdot P_A + k_{tr,BB} \cdot P_B) \cdot C_{p,B} \cdot k_{o,B}}{\beta_B(j) \cdot k_{o,B} + k_{pBA} \cdot C_{p,A} + k_{pBB} \cdot C_{p,B}} \quad \text{(Eq. 2.120)}$$

$$k_{des}(j) = k_{des,A}(j) + k_{des,B}(j) \quad \text{(Eq. 2.121)}$$

If all particles are identical, the mean squared radius and mean radius squared will be equal. This corresponds to a polydispersity index of 1, and the distribution is said to be mono-dispersed. As the distribution widens, the larger particles will more heavily influence the numerator (due to the r^2 term) and hence the index will increase.

2.6.1.4 Reactor Balance Equations

For a semi-batch process (as being considered here), the rate of accumulation of monomer in the reaction vessel can be obtained from a molar balance equation,

$$\frac{dN_{m,A}}{dt} = F_{mA,in} - R_{pAp}V_p - R_{pAw}V_w \quad \text{(Eq. 2.122)}$$

$$\frac{dN_{m,B}}{dt} = F_{mB,in} - R_{pBp}V_p - R_{pBw}V_w \quad \text{(Eq. 2.123)}$$

$$\frac{dN_{pol,A}}{dt} = R_{pAp}V_p + R_{pAw}V_w \quad \text{(Eq. 2.124)}$$

$$\frac{dN_{pol,B}}{dt} = R_{pBp}V_p + R_{pBw}V_w \quad \text{(Eq. 2.125)}$$

where $N_{pol,A}$ and $N_{pol,B}$ are the number of moles of copolymer having its terminal as A and B, respectively.

The conversion of monomer to polymer is calculated by the following equations:

$$\frac{dN_{m,A}^{fed}}{dt} = F_{mA,in} \quad \text{(Eq. 2.126)}$$

$$\frac{dN_{m,B}^{fed}}{dt} = F_{mB,in} \quad \text{(Eq. 2.127)}$$

where $F_{mA,in}$, $F_{mB,in}$ are the flow rates of monomer A and B, respectively.

$$x_A = 1 - \frac{N_{m,A}}{N_{m,A}^{fed}} \quad \text{(Eq. 2.128)}$$

$$x_B = 1 - \frac{N_{m,B}}{N_{m,B}^{fed}} \quad \text{(Eq. 2.129)}$$

$$x = \frac{x_A M_{w,A} + x_B M_{w,B}}{M_{w,A} + M_{w,B}} \quad \text{(Eq. 2.130)}$$

where x_A and x_B are the conversions of monomers A and B to a copolymer, and x is the overall conversion.

The average density of the monomer phase and polymer, and the average molecular weight are calculated by:

$$d_{avg} = f_A \cdot d_{m,A} + f_B \cdot d_{m,B} \quad \text{(Eq. 2.131)}$$

$$d_p = f_A \cdot d_{p,A} + f_B \cdot d_{p,B} \quad \text{(Eq. 2.132)}$$

$$M_w = f_A \cdot M_{w,A} + f_B \cdot M_{w,B} \quad \text{(Eq. 2.133)}$$

The volume of the water phase is given by:

$$V_w = \frac{V_{wo}}{1 - \frac{M_{w,A}}{C_{w,A}} - \frac{M_{w,B}}{C_{w,B}}} \quad \text{(Eq. 2.134)}$$

The volume of the monomer phase is given as follows

$$V_m = \frac{N_{m,avg} \cdot M_w}{d_{avg}} \quad \text{(Eq. 2.135)}$$

where, $N_{m,avg}$ is the average number of moles given as:

$$N_{m,avg} = f_A N_{m,A} + f_B N_{m,B} \quad \text{(Eq. 2.136)}$$

and d_{avg} is the average density of the monomers styrene and MMA.

The concentration of styrene and MMA in the particle phase is calculated as follows:

$$C_p = P_A \cdot C_{p,A} + P_B \cdot C_{p,B} \quad \text{(Eq. 2.137)}$$

where $C_{p,A}$ and $C_{p,B}$ are the concentrations of monomers A and B in the particle phase. A clear relation can be seen that the concentration in the particle phase is dependent on the probabilities, which are functions of the propagation coefficient in the particle phase, with either monomer A, or monomer B.

$C_{p,A}$ and $C_{p,B}$ may reach a maximum of the saturated value of monomer concentration, in the particle phase, and are calculated using the following equations. The concentration in the water is calculated using the partition coefficients between the three different phases.

$$C_{p,A} = MIN\left(C_{p,A}^{sat}, \frac{N_{m,A}}{K_{A,mw} \cdot K_{A,wp} \cdot V_m + K_{A,wp} \cdot V_w + V_p} \right) \quad \text{(Eq. 2.138)}$$

$$C_{p,B} = MIN\left(C_{p,B}^{sat}, \frac{N_{m,B}}{K_{B,mw} \cdot K_{B,wp} \cdot V_m + K_{B,wp} \cdot V_w + V_p} \right) \quad \text{(Eq. 2.139)}$$

$$C_{w,A} = MIN\left(C_{w,A}^{sat}, C_{p,A} \cdot K_{A,wp} \right) \quad \text{(Eq. 2.140)}$$

$$C_{w,B} = MIN\left(C_{w,B}^{sat}, C_{p,B} \cdot K_{B,wp} \right) \quad \text{(Eq. 2.141)}$$

$$C_w = C_{w,A} + C_{w,B} \quad \text{(Eq. 2.142)}$$

where $C_{p,A}^{sat}$, $C_{p,B}^{sat}$ are the saturated concentrations of A and B in the particle phase, respectively, $N_{m,A}$ and $N_{m,B}$ are the number of moles of A and B, respectively, V_m, V_w and V_p are the volumes of the monomer, water and particle phase, respectively. The volume of polymer particles (V_p) is defined for two separate regimes: when monomer droplets exits and when there are no longer any droplets. So the copolymer particle volume is calculated by two different equations in two stages. The first stage is when the conversion is about 40%, i.e. when interval II of the reaction ends at the commencement of the Interval III, where the monomer droplets start to decrease. The V_p for first regime is calculated by:

$$\frac{dV_p}{dt} = \frac{M_{w,A} \cdot (R_{p,A,p} \cdot V_p + R_{p,A,w} \cdot V_w) + M_{w,B} \cdot (R_{p,B,p} \cdot V_p + R_{p,B,w} \cdot V_w)}{d_p} \qquad \text{(Eq. 2.143)}$$

whereas for the second regime, V_p is given by:

$$\frac{dV_p}{dt} = \frac{M_{w,A} \cdot (R_{p,A,p} \cdot V_p + R_{p,A,w} \cdot V_w) + M_{w,B} \cdot (R_{p,B,p} \cdot V_p + R_{p,B,w} \cdot V_w)}{d_p} - \left[M_{w,A} \cdot R_{p,A,p} \cdot V_p \cdot \left(\frac{1}{d_{m,A}} - \frac{1}{d_{p,A}} \right) + M_{w,B} \cdot R_{p,B,p} \cdot V_p \cdot \left(\frac{1}{d_{m,B}} - \frac{1}{d_{p,B}} \right) \right] \qquad \text{(Eq. 2.144)}$$

where $R_{p,A,p}$ and $R_{p,A,w}$ are the rate of reactions of the polymer for monomer A and B in the particle and water phase, respectively. The rates of the reactions are calculated by the following equations:

$$R_{pAp} = \frac{\left(kp_{AA} \cdot kp_{BB} \cdot (r_A \cdot C_{pA}^{\ 2} + C_{pA} \cdot C_{pB})\right)}{k_{pBB} \cdot r_A \cdot C_{pA} + k_{pAA} \cdot r_B \cdot C_{pB}} \bullet \frac{\bar{n} \cdot N_{tot}}{N_a \cdot V_p} \qquad \text{(Eq. 2.145)}$$

$$R_{pBp} = \frac{\left(kp_{AA} \cdot kp_{BB} \cdot (r_B \cdot C_{pB}^{\ 2} + C_{pA} \cdot C_{pB})\right)}{k_{pBB} \cdot r_A \cdot C_{pA} + k_{pAA} \cdot r_B \cdot C_{pB}} \bullet \frac{\bar{n} \cdot N_{tot}}{N_a \cdot V_p} \qquad \text{(Eq. 2.146)}$$

$$R_{pAw} = \frac{\left(kp_{AA} \cdot kp_{BB} \cdot (r_A \cdot C_{wA}^{\ 2} + C_{wA} \cdot C_{wB})\right)}{k_{pBB} \cdot r_A \cdot C_{wA} + k_{pAA} \cdot r_B \cdot C_{wB}} \bullet T \qquad \text{(Eq. 2.147)}$$

$$R_{pBw} = \frac{\left(kp_{AA} \cdot kp_{BB} \cdot (r_B \cdot C_{wB}{}^2 + C_{wA} \cdot C_{wB})\right)}{k_{pBB} \cdot r_A \cdot C_{wA} + k_{pAA} \cdot r_B \cdot C_{wB}} \bullet T \qquad \text{(Eq. 2.148)}$$

2.6.1.5 MWD Model

The number molecular weight distribution is the number of non growing (dead) chains with a given molecular weight. The population of dead chains is controlled both by the number distribution of living (growing, i.e. propagating) chains, by the rate at which chains grow, and by the kinetic events that stop these chains growing. The distributions of living and dead chains will not necessarily be the same. The number distribution of living chains is denoted by R(M), and that of dead chains by P(M), where M is the molecular weight. N is sometimes used instead of N, which is the degree of polymerisation and they are related through the following equation:

$$N = \frac{M}{M_o} \qquad \text{(Eq. 2.149)}$$

where M_0 is the molecular weight of a monomer unit.

2.6.1.5.1 Molecular weight distribution functions

The number MWD is defined as P(M). P(M) is then defined such that P(M)d M is the number of polymer chains with molecular weight in the range M to M+dM, in the limit of vanishingly small increment of molecular weight dM. With this definition, P(M) is proportional to the amount of non growing polymer present, and formally has dimensions equal to (number of chains)/(molecular weight). The weight MWD, W(M) is defined as:

$$W(M) = M\,P(M) \qquad \text{(Eq. 2.150)}$$

2.6.1.5.2 Instantaneous and cumulative MWDs

Any experimental measurement of the molecular weight distribution in a polymer sample will measure the cumulative distribution of lengths of all chains formed throughout the whole history of that sample. The lifetime of an average chain is much more smaller than that of a typical period of polymerisation. For instance, the slowest chain-stopping event is

usually "transfer event" to monomer. The timescale foe styrene or MMA is ca. 1-10 s, whereas a polymerisation process lasts for hours. This means that the concentration of the polymer in the particle phase and the rate coefficients will be essentially constant during the life of a particular chain, but will vary over the lifetime of a polymerisation run. Because of this variation over the lifetime of a run, the distribution of molecular weights formed at any time will also vary during the course of the reaction (Gilbert, 1995).

The instantaneous molecular weight distribution at time t is denoted by *P(M,t)*, and the cumulative one is denoted by $\overline{P}(M,t)$. The relationship between the two is:

$$\overline{P}(M,t) = \int_0^t P(M,\tau)d\tau \qquad \text{(Eq. 2.151)}$$

$$P(M,t) = \frac{\partial \overline{P}(M,t)}{\partial t} \qquad \text{(Eq. 2.152)}$$

2.6.1.5.3 Number and weight averages and polydispersity

Although the full number or weight MWD represents the most complete description of the molecular weight, more compact measures are obviously more convenient (Gilbert, 1995). The number average molecular weight, M_n is defined as:

$$M_n = \frac{\sum M \cdot P(M)}{\sum P(M)} \qquad \text{(Eq. 2.153)}$$

The weight average molecular weight, M_w is defined as:

$$M_w = \frac{\sum M^2 \cdot P(M)}{\sum M \cdot P(M)} \qquad \text{(Eq. 2.154)}$$

The Molecular weight polydispersity index (MWPI) gives an indication of the width of the distribution.

$$MWPI = \frac{M_w}{M_n}$$

2.6.1.5.4 Rate parameters determining the MWD

In order to determine the molecular weight distribution, one must take into account all the events that can start, continue and stop the growth of polymer chains. These events are

entry, propagation and termination, and in addition for emulsion copolymerisation is the transfer event. Transfer can be both to monomer ($k_{tr,M}$) and to added chain transfer agent (with concentration [A]), $k_{tr,A}$. The total transfer rate is given by the pseudo first order coefficient (Gilbert, 1995):

$$\textit{Total transfer rate} = C_p k_{tr,M} + [A]\, k_{tr,A} \qquad \text{(Eq. 2.155)}$$

The total entry rate coefficient is the sum of the three individual events:

$$\rho = \rho_I + \rho_{th} + \rho_{re} \qquad \text{(Eq. 2.156)}$$

2.6.1.5.5 Modelling the MWD

The absolute number of polymer chains formed per unit time per particle is given as:

$$\frac{\partial \bar{P}(M,t)}{\partial t} = P(M) = (k_{tr}C_p + \rho_{avg})\bar{n} \cdot \exp\left(\frac{-(\rho + k_{tr}C_p)}{k_p C_p}\frac{M}{M_o}\right) \qquad \text{(Eq. 2.157)}$$

where M is the molecular weight of the polymer chain P(M) is the instantaneous MWD, and $\bar{P}(M)$ is the cumulative MWD.

2.7 Numerical Solution in gPROMS

gPROMS®, for general **PRO**cess **M**odelling **S**ystem, is the most advanced general purpose process modelling, simulation and optimisation software available today. At its heart gPROMS is an equation-based system, meaning that processes are described by their underlying physical and chemical relationships and the operational task sequences superimposed on them. gPROMS analyses the relationships governing the process and then performs your solution of choice - dynamic or steady-state simulation, optimisation or parameter estimation. All of the complexity of the underlying equations and their solution is hidden from the user.

This enables process designers and operations personnel to quantify process design and operation as never before, leading to real increases in revenue and savings on capital and operational costs. Powerful modelling language, robust and fast solution technology, and a modular, well-designed underlying software structure means that users experience a high

degree of success in applications, however complex the underlying process or operating procedures.

gPROMS is widely recognised as a 'best-in-class' simulation package. It is designed to be both a fully-fledged simulation environment in its own right, and a simulation engine which can be embedded in vendor applications or combined with other 'best-in-class' applications to provide a comprehensive design and operations tool. Similarly, gPROMS' unprecedented level of openness allows models to link to external components, for example, physical properties packages or control system software - with ease.

Advanced features such as dynamic optimisation allow simultaneous optimisation of equipment sizes and operating procedures. This not only has the potential to shorten the design period significantly, it creates capital and operational savings which will be realised over the lifetime of the plant.

Algebraic, ordinary differential and partial differential equations can be written in gPROMS language almost as they appear on paper, leaving the user to concentrate on the accuracy of the modelling equations and not the complexity of the solution techniques. There are no limits to the size of the system to be modelled (other than machine memory), dynamic simulation models have commonly been performed with 100,000 differential-algebraic equations. The gPROMS process model library contains generic models of common process units which can be adapted freely by the user. gPROMS is unique amongst commercial simulators in its facilities for describing processes with discontinuities. This provides significant advantages to solution robustness and speed in situations where they may prove to be a considerable obstacle to solution in other simulators. These capabilities make it possible to model almost any process in gPROMS.

2.7.1 Numerical Solution in gPROMS for PSD

The population balance equations were discretised with respect to radius to convert the evolution equations into a set of coupled ordinary differential equations for each radius r(i). The continuous distribution was broken down into 'G' discrete groups of particles as developed by (Zeaiter et al., 2002b). Having discretised the evolution equations, there is one ordinary differential equation (at constant radius) describing the particle population in each of the groups (increments). Discretising the evolution equations by radius and not

volume is computationally more efficient, since the particle radius increases much more slowly than particle volume (Zeaiter et al., 2002b). Discretising converts the partial differential evolution equations to ordinary differential equations. Moreover, discretisation allows the integro-differential components of the equations to be expressed as finite difference approximations in equally spaced radius increments (Δr) (Zeaiter et al., 2002b). The differential growth term can also be approximated by the finite difference method (Zeaiter et al., 2002b).

$$-\frac{\partial(Kn_1^P)}{\partial V} = \frac{-K}{8\pi\Delta r}\left(\frac{n_1^P(r_{i+1})}{r_{i+1}^2} - \frac{n_1^P(r_{i-1})}{r_{i-1}^2}\right) \qquad \text{(Eq. 2.158)}$$

The following equations are recommended for the endpoints (Gilbert, 1995).

$$i = 1; \quad \frac{-K}{8\pi\Delta r}\left(\frac{n_1^P(r_2)}{r_2^2}\right) \qquad \text{i = G;} \quad \frac{-\mathrm{K}}{8\pi\Delta \mathrm{r}}\left(-\frac{\mathrm{n}_1^{\mathrm{P}}(\mathrm{r}_{\mathrm{G}-1})}{\mathrm{r}_{\mathrm{G}-1}^2}\right) \qquad \text{(Eq. 2.159)}$$

The endpoints effectively assume there is a increment on either end of the discretised distribution that contains no particles. Thus, in each case, one of the terms drops out of the finite difference approximation.

$$-\frac{\partial(Kn_1^P)}{\partial V} = \frac{-K}{4\pi\Delta r}\left(\frac{n_1^P(r_{i+1})}{r_{i+1}^2} - \frac{n_1^P(r_i)}{r_i^2}\right) \qquad \text{(Eq. 2.160)}$$

$$-\frac{\partial(\mathrm{Kn}_1^{\mathrm{P}})}{\partial \mathrm{V}} = \frac{-\mathrm{K}}{4\pi\Delta \mathrm{r}}\left(\frac{\mathrm{n}_1^{\mathrm{P}}(\mathrm{r}_i)}{\mathrm{r}_i^2} - \frac{\mathrm{n}_1^{\mathrm{P}}(\mathrm{r}_{i-1})}{\mathrm{r}_{i-1}^2}\right) \qquad \text{(Eq. 2.161)}$$

The forward finite difference produced an unstable particle number, approximately. A more stable PSD was obtained by using the backward approximation (Zeaiter et al., 2002b). Consequently, the backward finite difference approximation was chosen to be adopted for the discretisation of the PBEs.

2.8 Modelling Results

The simulation results from the model developed as shown throughout this chapter are shown in this section. It is important to note that the model is solely based on the real kinetics of the system. This means that all the results obtained by the simulation should be reasonably explaining the real fact of the process. This will be clearly seen from the results showing the true evidence of the obedience to kinetics.

The key polymer properties are validated against the experimental results in the next chapter. This section is to show the results obtained by the model simulation well obeying the kinetics.

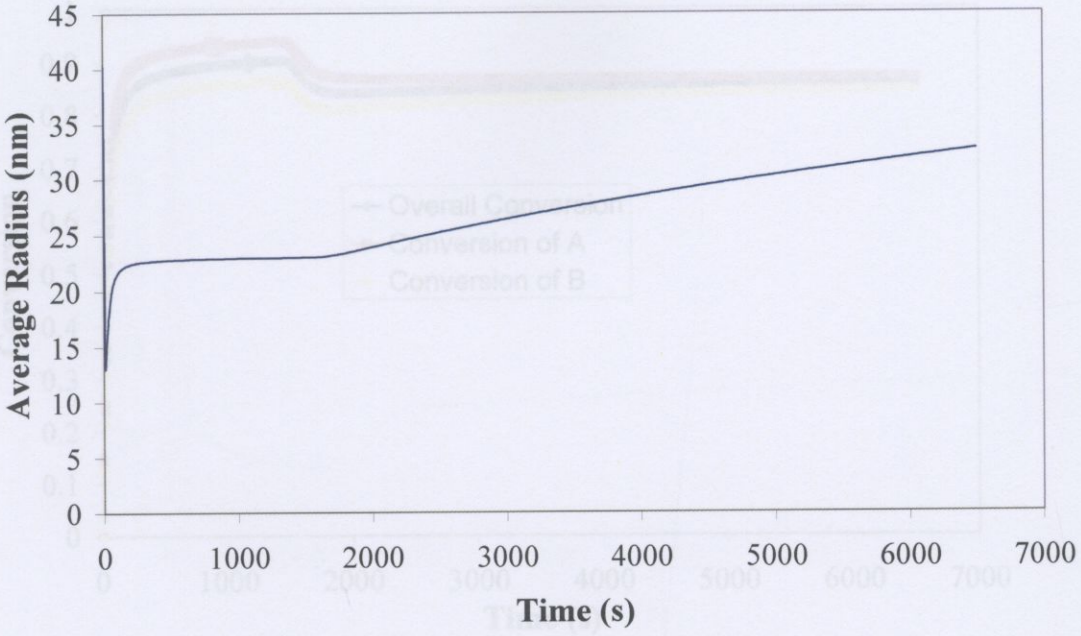

Figure 2.3 Particle Size

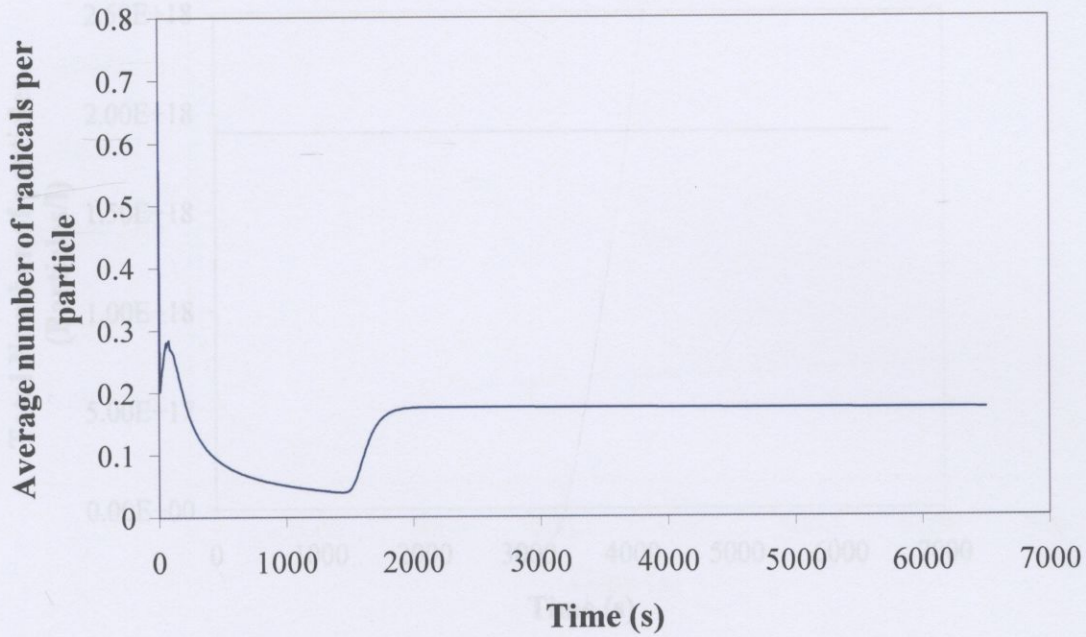

Figure 2.4 Average number of radicals per particle

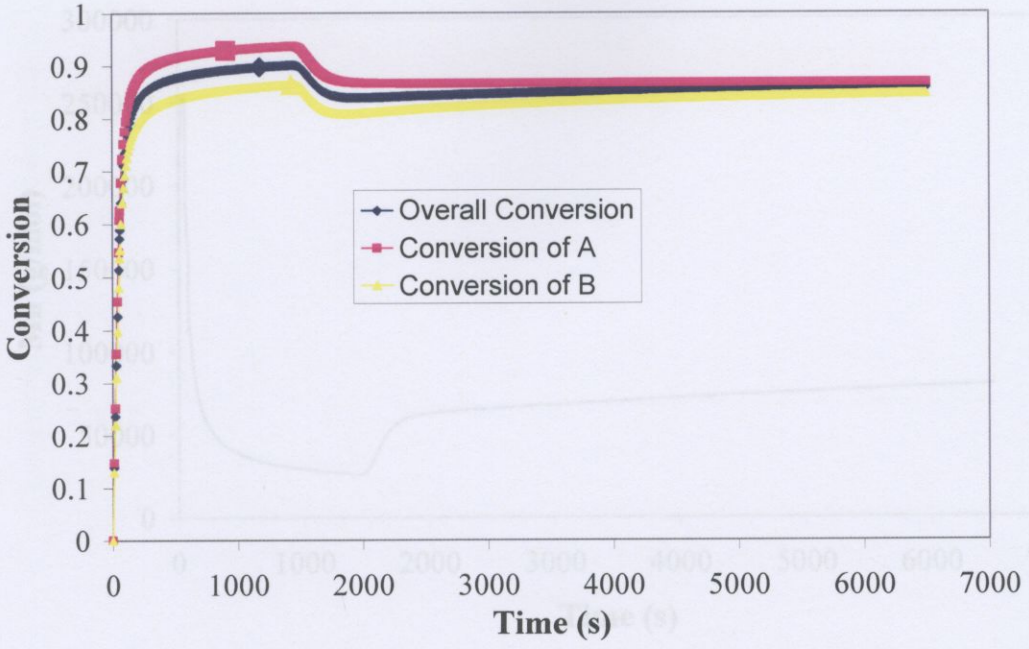

Figure 2.5 Conversion of Monomer to Copolymer

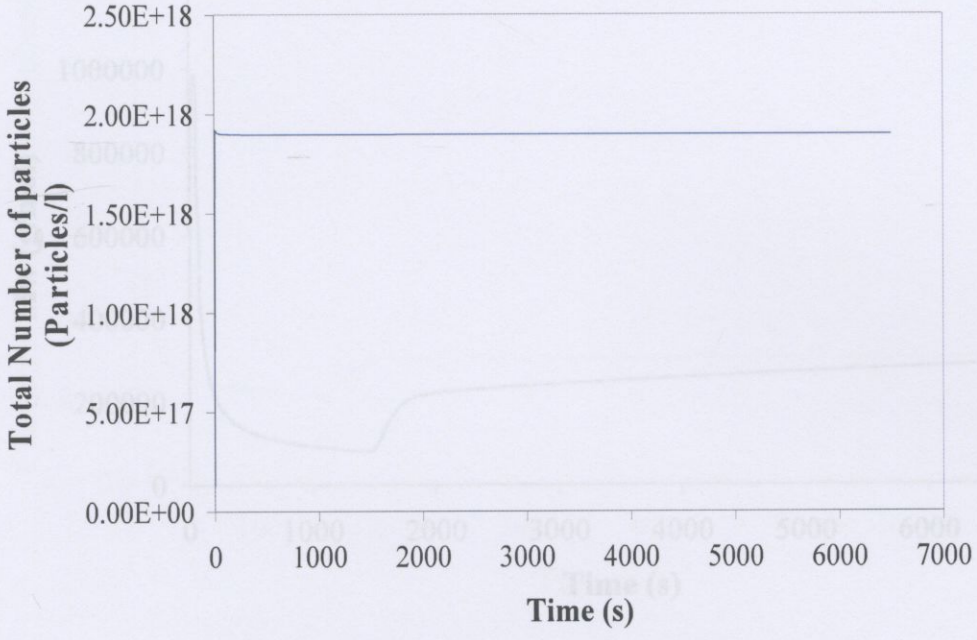

Figure 2.6 Total number of Particles

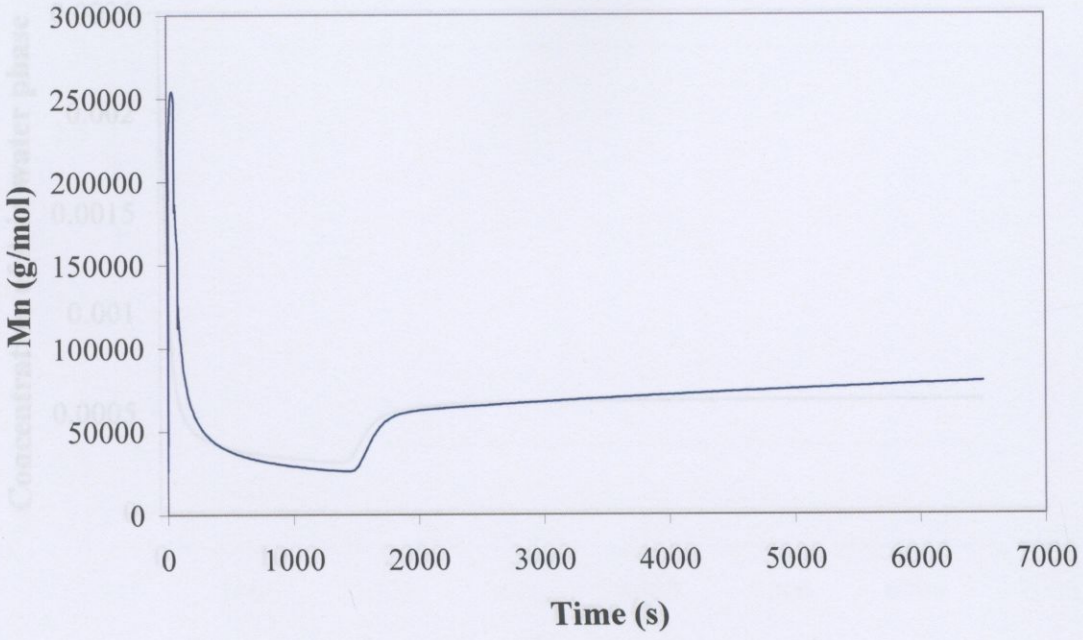

Figure 2.7 Number average molecular weight (M_n)

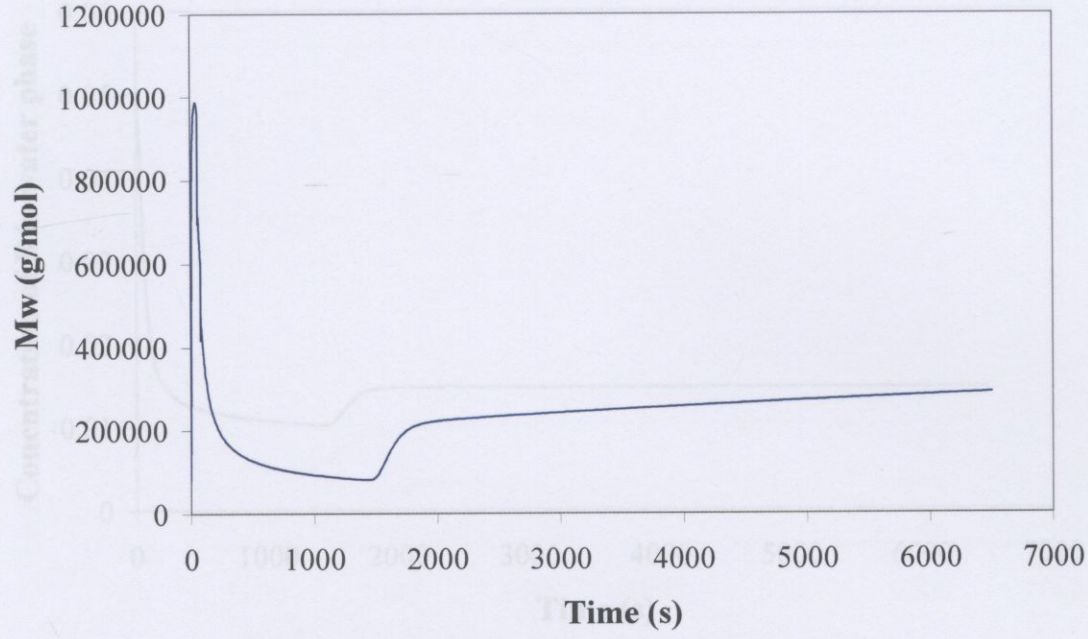

Figure 2.8 Weight average molecular weight (M_w)

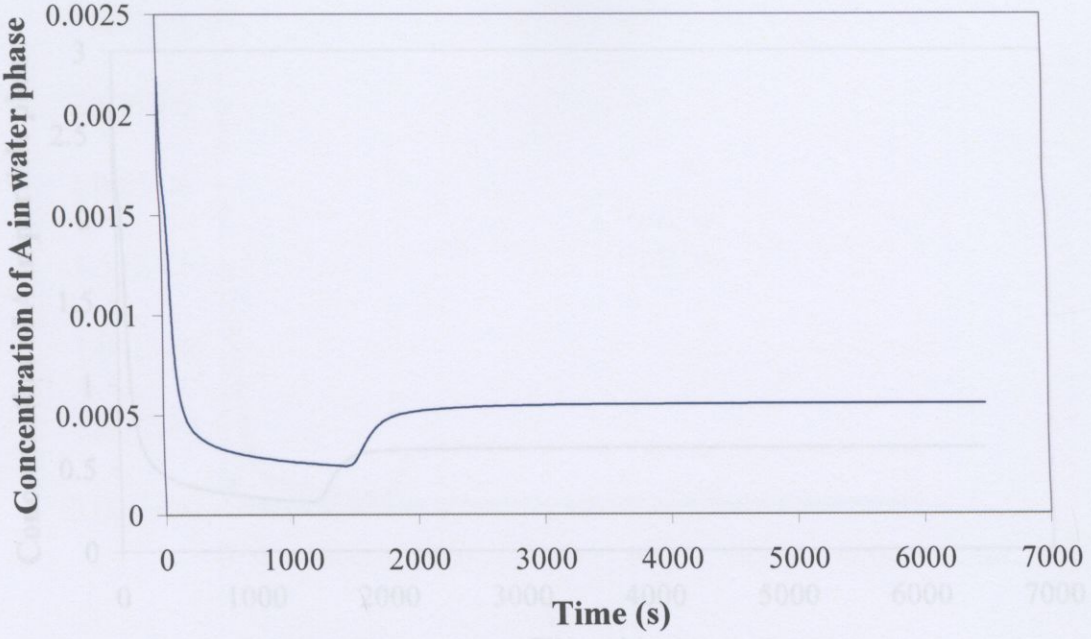

Figure 2.9 Concentration of styrene in water phase

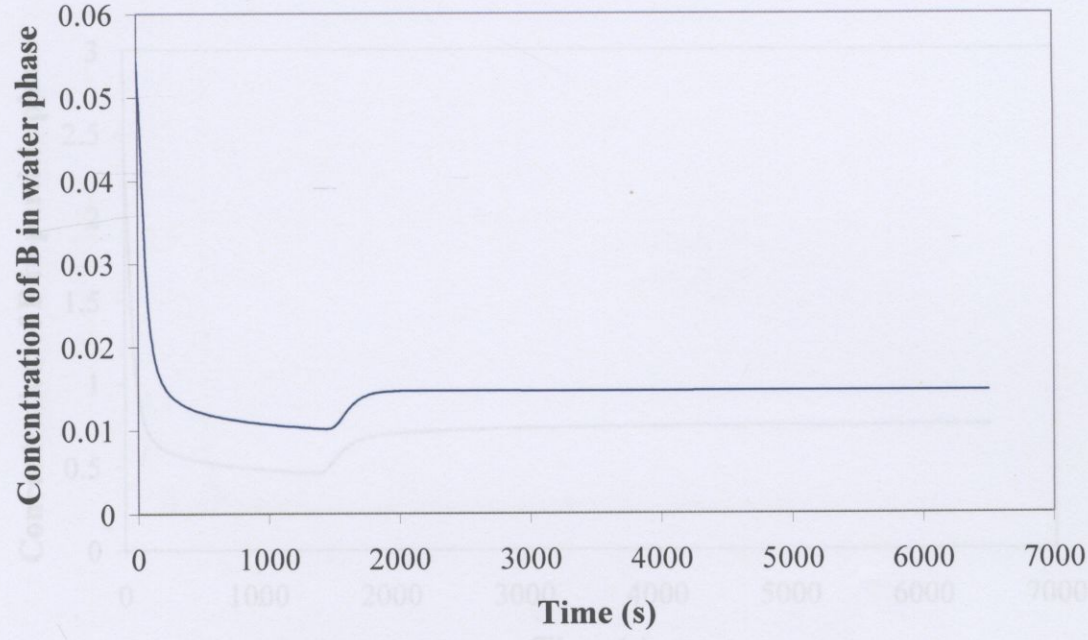

Figure 2.10 Concentration of MMA in water phase

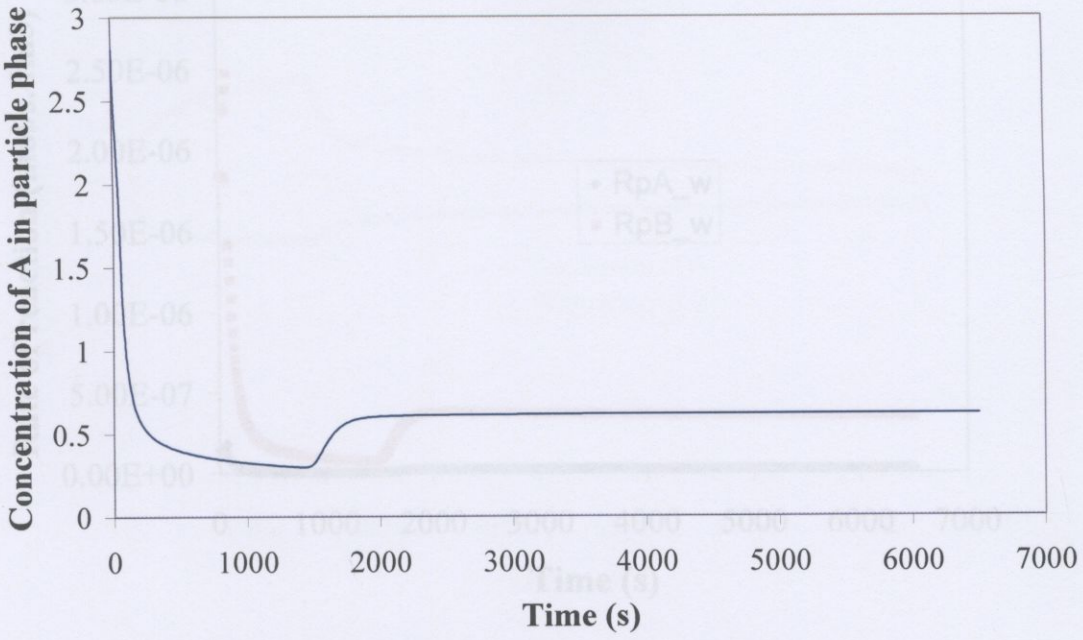

Figure 2.11 Concentration of styrene in particle phase

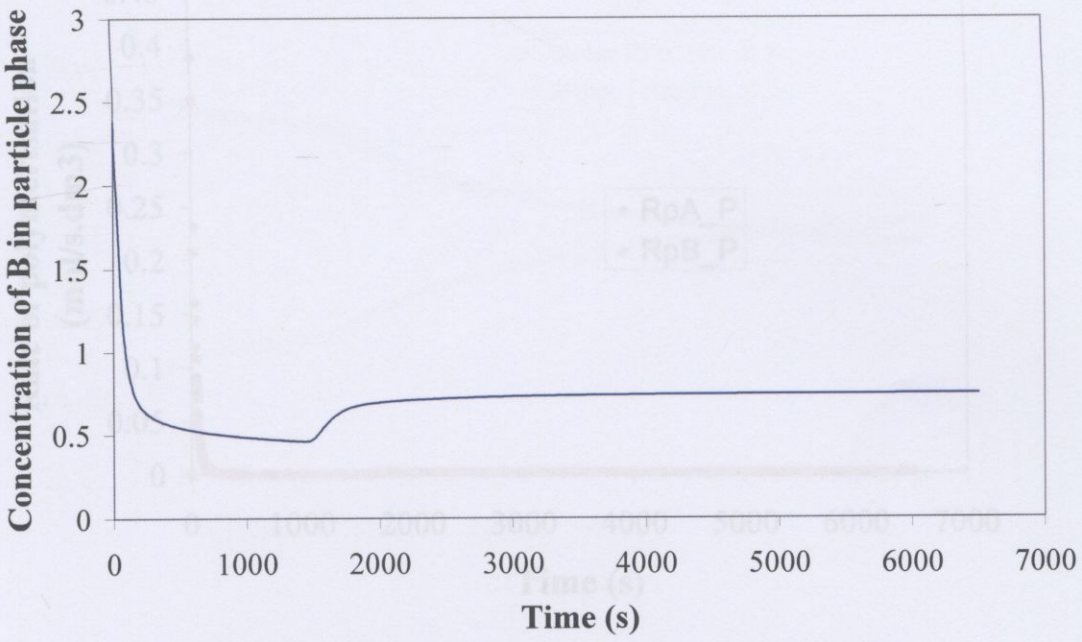

Figure 2.12 Concentration of MMA in particle phase

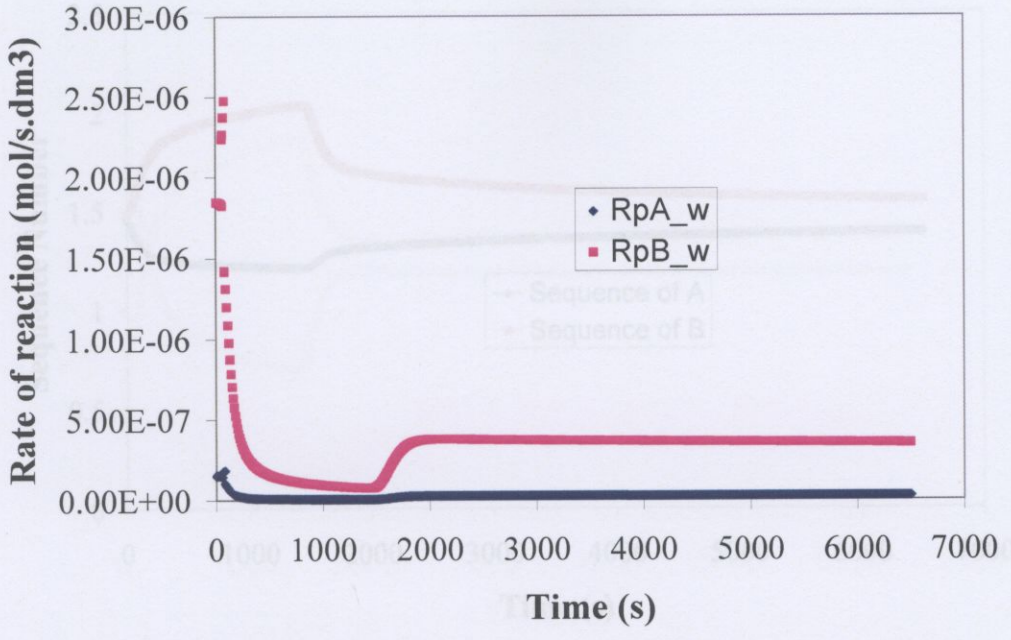

Figure 2.13 Rate of reaction of styrene (A) and MMA (B) in water phase

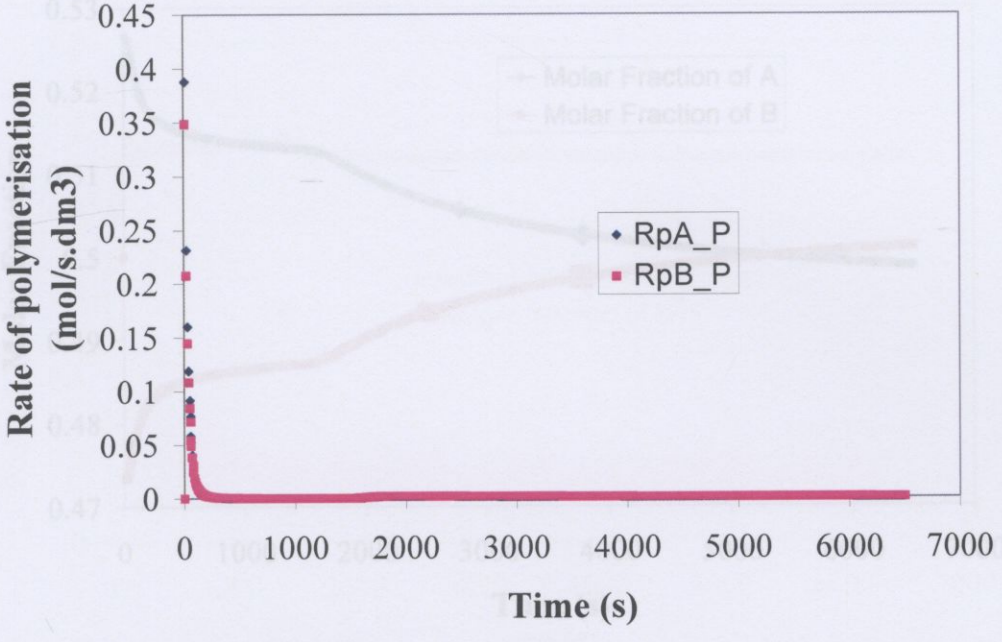

Figure 2.14 Rate of reaction of styrene and MMA in particle phase

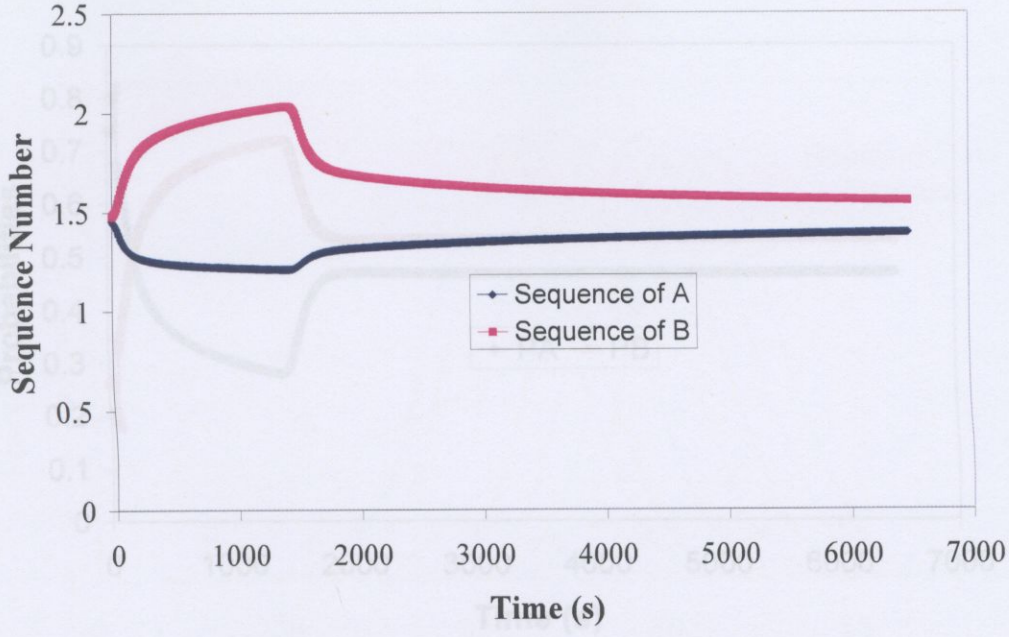

Figure 2.15 Sequence Number of styrene and MMA

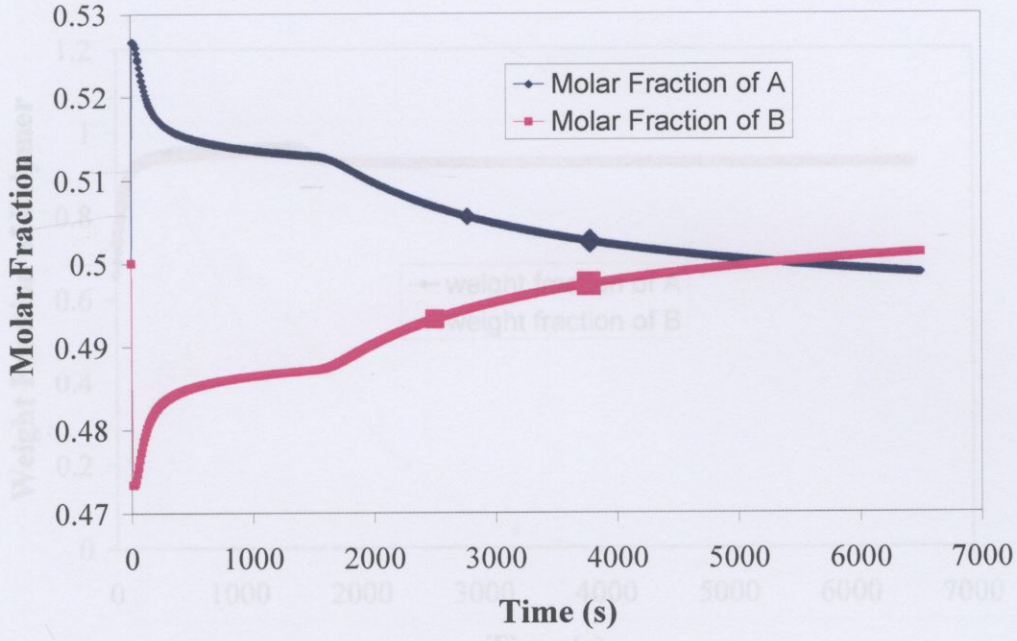

Figure 2.16 Molar fraction of styrene and MMA

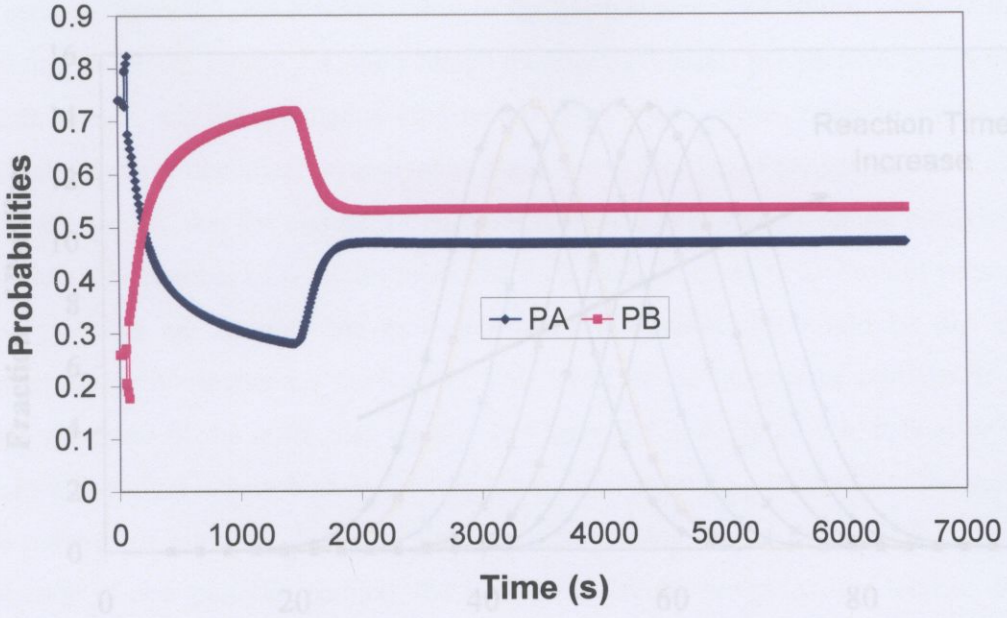

Figure 2.17 Probabilities of propagation of styrene and MMA

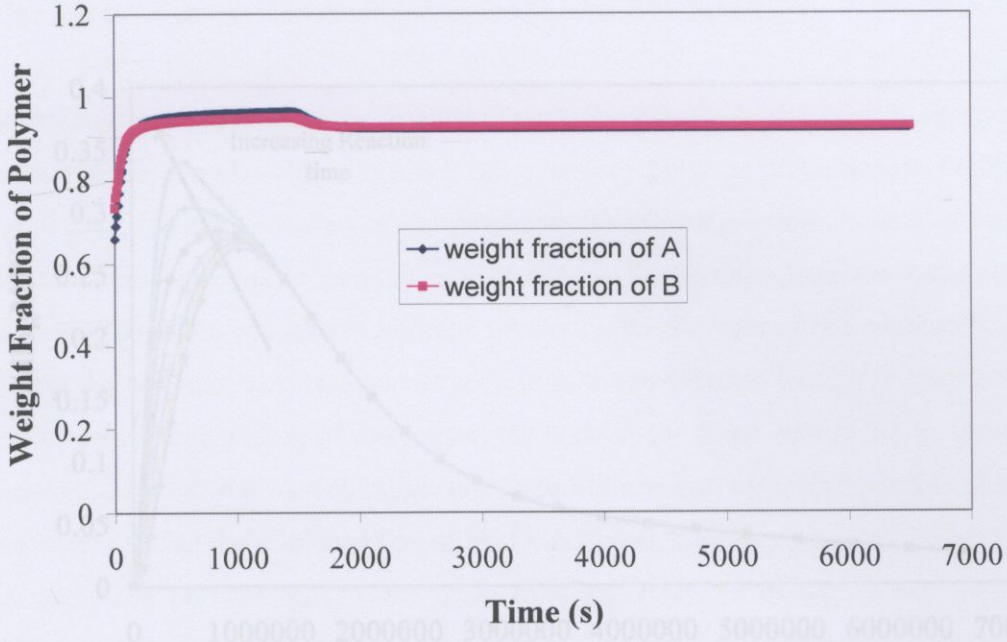

Figure 2.18 Weight fraction of styrene and MMA

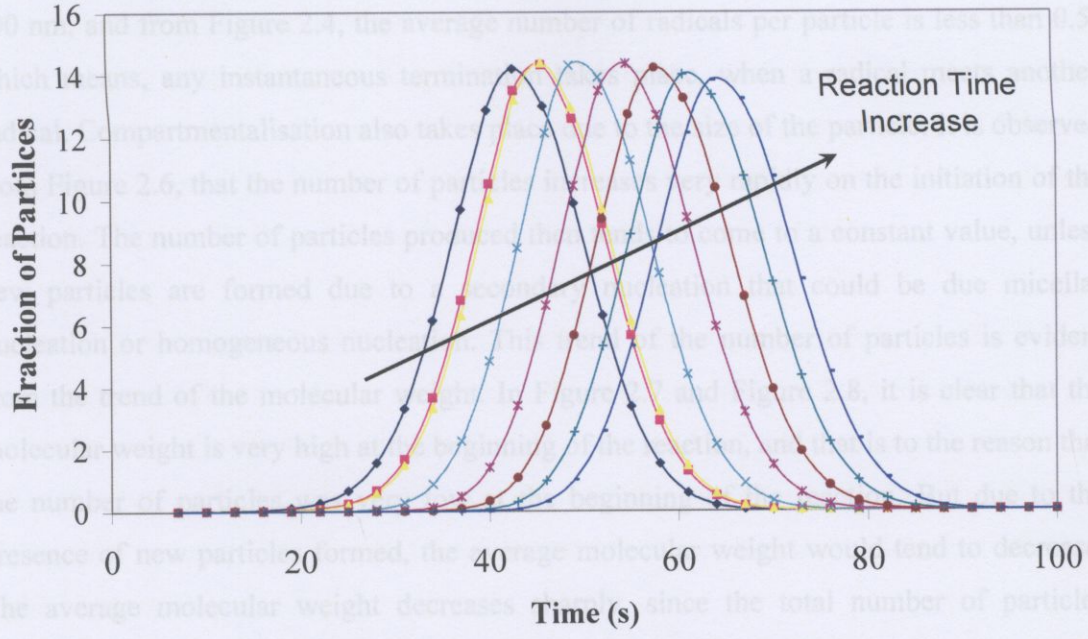

Figure 2.19: Particle Size Distribution (PSD)

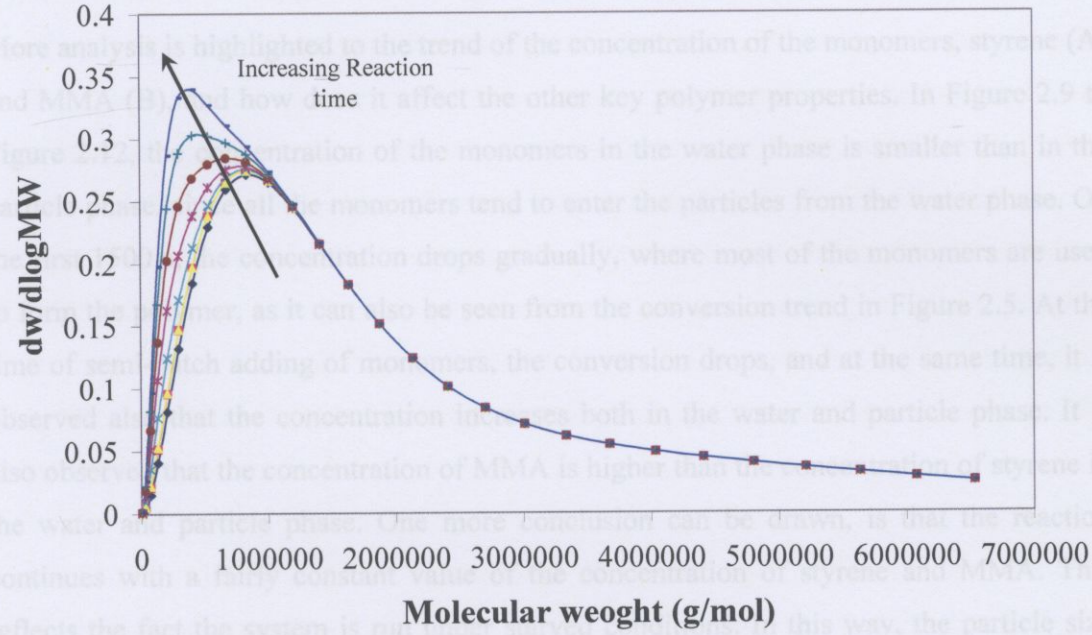

Figure 2.20 Molecular Weight Distribution (MWD)

In Figure 2.3 and Figure 2.4, the obeying of zero-one kinetics is clearly observed. As it can be seen in Figure 2.3, the average radius of the particle size is 40-50 nm, which is less than 200 nm, and from Figure 2.4, the average number of radicals per particle is less than 0.5, which means, any instantaneous termination takes place, when a radical meets another radical. Compartmentalisation also takes place due to the size of the particle. It is observed from Figure 2.6, that the number of particles increases very rapidly on the initiation of the reaction. The number of particles produced then tends to come to a constant value, unless new particles are formed due to a secondary nucleation that could be due micellar nucleation or homogeneous nucleation. This trend of the number of particles is evident from the trend of the molecular weight. In Figure 2.7 and Figure 2.8, it is clear that the molecular weight is very high at the beginning of the reaction, and that is to the reason that the number of particles was very low at the beginning of the reaction. But due to the presence of new particles formed, the average molecular weight would tend to decrease. The average molecular weight decreases sharply, since the total number of particles increases sharply, and then it starts moving gradually, where the number of particles produced is constant. The M_n and M_w have a similar trend, since no branches are expected in the emulsion copolymerisation process of styrene with MMA.

More analysis is highlighted to the trend of the concentration of the monomers, styrene (A) and MMA (B), and how does it affect the other key polymer properties. In Figure 2.9 to Figure 2.12, the concentration of the monomers in the water phase is smaller than in the particle phase, since all the monomers tend to enter the particles from the water phase. On the first 1500 s, the concentration drops gradually, where most of the monomers are used to form the polymer, as it can also be seen from the conversion trend in Figure 2.5. At the time of semi-batch adding of monomers, the conversion drops, and at the same time, it is observed also that the concentration increases both in the water and particle phase. It is also observed that the concentration of MMA is higher than the concentration of styrene in the water and particle phase. One more conclusion can be drawn, is that the reaction continues with a fairly constant value of the concentration of styrene and MMA. This reflects the fact the system is run under starved conditions. In this way, the particle size can be controlled easily. This is exactly what can be seen in Figure 2.3, where the size rises gradually, and in Figure 2.5, where the conversion is fairly constant.

Figure 2.5 shows the conversion of each monomer, styrene and MMA. The figures reveal that the conversion of MMA is lower than the conversion of MMA. This is true, for several reasons. The concentration of MMA is greater than the concentration of styrene. Moreover, the entry of styrene is 3, and of MMA is 10, which means that there will be more styrene entering to the particle, even though the propagation coefficient of MMA is larger than styrene. The difference in the conversion between styrene and MMA is close to each other, due to the fact of the high propagation coefficient of MMA.

Figure 2.13 and Figure 2.14 demonstrate that the rate of polymerisation in the particle phase is much higher than in the water phase. This is true, with no doubt, since most of the polymerisation reaction occurs in the particle phase, and any homogeneous nucleation is counted to be very small. The figures also show that the rate of polymerisation of MMA is higher than styrene. This is clear to the fact that the propagation coefficient of MMA is higher than styrene.

In Figure 2.15, the sequence number at the commence of the reaction of styrene is lower than the sequence number of MMA, because MMA propagation coefficient is larger than styrene, which can be seen from the Figure 2.17. The probability is a function of both the reactivity ratios and the propagation coefficient. The reactivity ratios of both monomers are very close, and that what pushes the sequence of the copolymer to be looking like an alternating sequence. The other factor is the propagation coefficient, which pushes MMA to have a higher probability in propagating than styrene. Figure 2.16 clarifies that concept even more by showing that the molar fraction of styrene is higher than the molar fraction of MMA, due to the fact that the entry for styrene is before the entry of MMA, which is incorporated to the hydrophobicity of styrene. Figure 2.18 reveals that the weight fraction of styrene is similar to MMA, where equal amounts of styrene and MMA are used, and the reactivity ratios are similar.

Figure 2.19 and Figure 2.20 demonstrate the PSD and MWD of the emulsion copolymerisation process with time. In Figure 2.19, it can be seen that the distribution is shifted to the right, giving a higher average of particle size, due to the addition of the monomer. The distribution's height goes lower, since the distribution is becoming broader, and the area under the distribution should be constant, reflecting the constant number of particles that had been formed. In Figure 2.20, the MWD distribution is showed with the

increase in reaction time. It can be seen that the MWD distribution shifts to the left at the beginning of the reaction, (as it had been explained earlier), the particles formed at the beginning of the reaction are few in number, and with time increases, which results in the reduction of the molecular weight. This is followed with the addition of the monomers, which will push the molecular weight to increase. As it can be seen, the whole distribution of the particle size and the molecular weight can be obtained through out the reaction.

2.9 Conclusion

A challenge is to be faced due to the heterogeneous phase possessed by the polymer properties due to the two main key polymer properties, PSD and MWD. These distributions however, represent the complete kinetic history of a polymerisation process and constitute a unique tool for analysing emulsion copolymerisation systems. The more challenging issue is to have the model to act as a soft sensor, where it measures the PSD, MWD, and other key polymer properties on real time.

In this chapter, a detailed dynamic model was developed for a styrene and MMA emulsion copolymerisation reactor to be able to predict the PSD and MWD of the product, thoroughly through the reaction. The kinetic equations included diffusion-controlled kinetic terms at high monomer conversion, where the transition from the 'zero-one' regime to a 'pseudo-bulk' regime occurs. The reactor mass and energy balances, which comprise differential equations, were developed to describe the system transients for batch and semi-batch operation. The population balance equations, describing ab initio particle evolution, include formalisms for particle birth and death processes are included in the model. The model predictions included the polymerization rate for each of styrene and MMA, the copolymer composition, individual monomer conversion and comonomer conversion to copolymer, the particle number, M_n and M_w, MWD, PSD and the average particle size. The complex model equations comprising sets of integro-partial differential and nonlinear algebraic equations were solved using an efficient finite difference scheme within the gPROMS environment. The model was simulated and numerically solved in gPROMS package, which a strong computer simulation software with high efficient capabilities to be used for real time applications.

The simulation results were demonstrated to reflect the applicability of the mathematical model developed. In the next chapter, the model will be validated against the experimental results under different operating conditions. It will then be seen in the next chapters that the model will be used for optimisation and control purposes.

2.10 References

Alhamad, B., Romagnoli, J. A. and Gomes, V. G. (2003) In 31st Australasian Chemical Engineering Conference CHEMECA, Adelaide, South Australia, pp. 138.

Araujo, O., Giudici, R., Saldivar, E. and Ray, W. H. (2001) In Journal of Applied Polymer Science, Vol. 79 John Wiley and Sons Inc.,New York,NY,USA, pp. 2360-2379.

Arriola, D. J. (1989) PhD Thesis, University of Wisconsin, Madison.

Arzamendi, G., Forcada, J. and Asua, J. M. (1994) Macromolecules, 27, 6068-6079.

Asua, J. M., Sudol, E. D. and El-Aaser, M. S. (1989) Journal of Polymer Science, Part A: Polymer Chemistry, 27, 3903-3913.

Ballard, M. J., Napper, D. H. and Gilbert, R. G. (1981) J. Polym. Chem. Ed., 19, 939-954.

Bonilla, J., Saldivar, E., Flores-Tlacuahuac, A., Vivaldo-Lima, E., Pfaendner, R. and Tiscareno-Lechuga, F. (2002) In Polymer Reaction Engineering, Vol. 10 Marcel Dekker Inc., pp. 227-263.

Broadhead, T. O., Hamielec, A. E. and MacGregor, J. F. (1985) Makromol. Chem., Suppl., 10/11, 105-128.

Casey, B. S., Morrison, B. R., Maxwell, I. A., Gilbert, R. G. and Napper, D. H. (1994) Journal of Polymer Science Part a-Polymer Chemistry, 32, 605-630.

Clay, P. A. and Gilbert, R. G. (1995) Macromolecules, 28, 552-569.

Cociani, M., Canu, P., Storti, G., Carra, S. and Morbidelli, M. (1989) Molecular Weight Distribution in Emulsion Polymerization, VCH, Berlin.

Coen, E. M., Gilbert, R. G., Morrison, B. R., Leube, H. and Peach, S. (1998) Polymer, 39, 7099-7112.

Crowley, T. J., Meadows, E. S., Kostoulas, E. and Doyle, F. J. I. (2000) In Journal of Process Control, Vol. 10 Elsevier Science Ltd,Exeter,Engl, Beijing,China, pp. 419-432.

Dougherty, E. P. (1986a) Journal of Applied Polymer Science, 32, 3051-3078.

Dougherty, E. P. (1986b) Journal of Applied Polymer Science, 32, 3079-3095.

Dube, M. A., Soares, J. B. P., Penlidis, A. and Hamielec, A. E. (1997) In Industrial & Engineering Chemistry Research, Vol. 36 ACS,Washington,DC,USA, pp. 966-1015.

Faldi, A., Tirrell, M., Lodge, T. P. and von Meerwall, E. (1994) Macromolecules, 27, 4184-4192.

Feeney, P. J., Napper, D. H. and Gilbert, R. G. (1984) Macromolecules, 17, 2520-2529.

Fitch, R. M. and Tsai, C. H. (1971a) Polymer Colloids I, 103-116.

Fitch, R. M. and Tsai, C. H. (1971b) Polymer Colloids I, 73-102.

Fitzroy, S. (2000) Modeling & Control of the Particle Size Distribution in Emulsion Polymerisation, University of Sydney, Department of Chemical Engineering, Undergraduate Thesis.

Forcada, J. and Asua, J. M. (1985) J. Polym. Sci., Polym. Chem. Ed., 23, 1955-1962.

Forcada, J. and Asua, J. M. (1990) Journal of Polymer Science, Part A: Polymer Chemistry, 28, 987-1009.

Forcada, J. and Asua, J. M. (1991) Journal of Polymer Science, Part A: Polymer Chemistry, 29, 1231-1242.

Gerrens, H. (1969) Journal Of Polymer Science, Part C, 27, 77.

Gevorkova, T. A., Zlantia, S. A. and Zhigareva, K. M. (1970) Teoreticheskie Osnovy Khimicheskoi Tekhnologii, 4, 567-572.

Giannetti, E. (1989) Macromolecules, 22, 2094-2102.

Giannetti, E., Storti, G. and Morbidelli, M. (1988) J. Polym. Sci., Polym. Chem. Ed., 26, 2307-2343.

Gilbert, R. G. (1995) Emulsion Polymerization: A mechanistic approach, Academic Press, London.

Gilbert, R. G., Morrison, B. R. and Napper, D. H. (1991) In Proceedings of the American Chemical Society, Spring Meeting,Apr 15-19 1991, Vol. 64 Publ by ACS,Washington,DC,USA, Atlanta,GA,USA, pp. 308-309.

Gugliotta, L. M., Brandolini, M. C., Vega, J. R., Iturralde, E. O., Azum, J. L. and Meira, G. R. (1995) Polymer Reaction Engineering, 3, 201-233.

Guillot, J. (1980) Makromol. Chem., Rapid Commun, 1, 697-702.

Guillot, J. (1981) Acta Polymerica, 32, 593-600.

Guillot, J. (1990) Makromol. Chem., Macromol Symp., 35, 269-289.

Guillot, J. (1993) Comp. Chem. Eng., 17, S189-S194.

Hagiopol, C. (1999) Copolymerization: Toward a Systematic Approach, Plenum Press.

Hamielec, A. E., MacGregor, J. F. and Penlidis, A. (1983) Polymer Reaction Engineering, 21-71.

Hamielec, A. E., MacGregor, J. F. and Penlidis, A. (1987) Makromol. Chem., Macromol. Symp., 10/11, 521-570.

Hansen, F. K. (1992a) Chem. Eng. Sci., 48, 437-444.

Hansen, F. K. (Ed.) (1992b) Is There Life Beyond Micelles? Mechanisms of Latex Particle Nucleation, ACS Symposium Series No. 492.

Hansen, F. K. and Ugelstad, J. (Eds.) (1982) Particle Formation Mechanisms, Academic Press, New York.

Harkins, W. D. (1947) J. Am. Chem. Soc., 69, 428-444.

Haskell, V. C. and Settlage, P. H. (1971) Polymer Colloids I, 163-172.

Krackler, J. and Naidus, H. (1969) Journal of Polymer Science, Part C, 27, 207.

Lin, C. C., Ku, H. C. and Chiu, W. Y. (1981) J. Appl. Polym. Sci., 26, 1327-1342.

Liotta, V., Sudol, E. D., El-Aasser, M. S. and Georgakis, C. (1998) Journal of Polymer Science Part a-Polymer Chemistry, 36, 1553-1571.

Maxwell, I. A., Morrison, B. R., Gilbert, R. G., Sangster, D. F. and Napper, D. H. (1992) Makromolekulare Chemie-Macromolecular Symposia, 53, 233-242.

Maxwell, I. A. and Russell, G. T. (1993) Makromolekulare Chemie-Theory and Simulations, 2, 95-128.

Mead, R. N. and Poehlein, G. W. (1988) Ind. Eng. Chem. Res., 27, 2283-2293.

Meadows, E. S., Crowley, T. J., Immanuel, C. D. and Doyle III, F. J. (2003) In Industrial and Engineering Chemistry Research, Vol. 42 American Chemical Society, pp. 555-567.

Morrison, B. R., Maxwell, I. A., Gilbert, R. G. and Napper, D. H. (1992) Acs Symposium Series, 492, 28-44.

Noel, L. F. J., Van Zon, J. M. A. M., Maxwell, I. A. and German, A. L. (1994a) Journal of Polymer Science, Part A: Polymer Chemistry, 32, 1009-1026.

Noel, L. F. J., Vanzon, J., Maxwell, I. A. and German, A. L. (1994b) Journal of Polymer Science Part a-Polymer Chemistry, 32, 1009-1026.

Nomura, M. (Ed.) (1982) in Emulsion Polymerization, Academic, Newyork.

Nomura, M. and Fujita, K. (1985) Makromol. Chem., Suppl., 10/11, 25-42.

Nomura, M., Horie, I., Kubo, M. and Fujita, K. (1983) In AIChE Spring National MeetingHouston.

Nomura, M., Kubo, M. and Fujita, K. (1981) Mem. Fac. Eng. Fukui Univ., 29, 167-174.

Nomura, M., Yamamoto, K., Horie, I. and Fujita, K. (1982) J. Appl. Polm. Sci., 27, 2483-2501.

Omi, S., Kushibiki, K. and Iso, M. (1987) Polym. Eng. Sci., 27, 470-482.

Penlidis, A., Macgregor, J. F. and Hamielec, A. E. (1986) Acs Symposium Series, 313, 219-240.

Quarderer, G. J. and Katti, S. S. (1993) Polym. Eng. Sci., 33, 564-572.

Richards, J. R., Congalidis, J. P. and Gilbert, R. G. (1989) J. Appl. Polym. Sci., 37, 2727-2756.

Russell, G. T., Gilbert, R. G. and Napper, D. H. (1992) Macromolecules, 25, 2459-2469.

Sajjadi, S. and Brooks, B. W. (2001) In Journal of Applied Polymer Science, Vol. 79 John Wiley and Sons Inc.,New York,NY,USA, pp. 582-597.

Saldivar, E., Araujo, O., Giudici, R. and Guerrero-Sanchez, C. (2002) In Journal of Applied Polymer Science, Vol. 84 John Wiley and Sons Inc., pp. 1320-1338.

Saldivar, E., Araujo, O., Giudici, R. and Lopez-Barron, C. (2001) In Journal of Applied Polymer Science, Vol. 79 John Wiley and Sons Inc.,New York,NY,USA, pp. 2380-2397.

Saldivar, E., Dafniotis, P. and Ray, W. H. (1998a) Journal of Macromolecular Science - Reviews in Macromolecular Chemistry and Physics, C38, 207-325.

Saldivar, E., Dafniotis, P. and Ray, W. H. (1998b) In Journal of Macromolecular Science - Reviews in Macromolecular Chemistry and Physics, Vol. C38 Marcel Dekker Inc,New York,NY,USA, pp. 207-325.

Saldivar, E. and Ray, W. H. (1997) Journal of Engineering and Applied Science, 43, 2021-2033.

Sayer, C., Arzamendi, G., Asua, J. M., Lima, E. L. and Pinto, J. C. (2001) Computers and Chemical Engineering, 25, 839-849.

Show-An, C. and Kuo-Wei, W. (1988) Journal of Polymer Science: Part A: Polymer Chemistry, 26, 1487-1506.

Storti, G., Carra, S., Morbidelli, M. and Vita, G. (1989a) J. Polym. Sci., Polym. Chem. Ed., 37, 2443-2467.

Storti, G., Morbidelli, M. and Carra, S. (1989b) In Computer Applications in Applied Polymer Science II: Automation, Modeling and Simulation(Ed, T. Provder, E.) ACS Symposium Series No. 404, Washington, DC, pp. 379-402.

Storti, G., Polotti, G., Canu, P. and Morbidelli, M. (1992a) J. Polym. Sci., Polym. Chem. Ed., 30, 751-777.

Storti, G., Polotti, G., Cociani, M. and Morbidelli, M. (1992b) J. Polym. Sci., Polym. Chem. Ed., 30, 731-750.

T. A. Gevorkova, S. A. Z., and K. M. Zhigareva (1972) Teoreticheskie Osnovy Khimicheskoi Tekhnologii, 9, 926-929.

Tobita, H. and Hamielec, A. E. (1991) Polymer, 32, 2641-2647.

Urquiola, B., Arzamendi, G., Leiza, J. R., Zamora, A., Asua, J. M., Delgado, J., El-Aasser, M. S. and Vanderhoff, J. W. (1991) In Journal of Polymer Science, Part A: Polymer Chemistry, Vol. 29, pp. 169-186.

Urretabizkaia, A., Arzamendi, G. and Asua, J. M. (1992) Chemical Engineering Science 12th International Symposium on Chemical Reaction Engineering - ISCRE 12, Jun 28-Jul 1 1992, 47, 2579-2584.

van`Doremaele, G. H. J., van`Herk, A. M. and German, A. L. (1992) Polym. Int., 27, 95-108.

Verdurmen, E. M., Dohmen, E. H., Verstegen, J. M., Maxwell, I. A., German, A. L. and Gilbert, R. G. (1993) Macromolecules, 26, 268-275.

Vicente, M., Sayer, C., Leiza, J. R., Arzamendi, G., Lima, E. L., Pinto, J. C. and Asua, J. M. (2002) Chemical Engineering Journal, 85, 339-349.

Zeaiter, J., Gomes, V. G., Romagnoli, J. A. and Barton, G. W. (2002a) Chemical Engineering Journal, 89, 37-45.

Zeaiter, J., Romagnoli, J. A., Barton, G. W., Gomes, V. G., Hawkett, B. S. and Gilbert, R. G. (2002b) In Chemical Engineering Science, Vol. 57 Elsevier Science Ltd, pp. 2955-2969.

Chapter 3

Experimental Emulsion Copolymerisation

3.1 INTRODUCTION 3.2
3.2 AUTOMATED REACTOR FACILITY 3.2
3.2.1 1L Polymerisation Reactor *3.2*
3.2.2 5L Polymerisation Reactor *3.5*
3.2.2.1 Monomer Feed Line 3.7
3.2.2.2 Heating/Cooling System 3.7
3.2.2.3 Nitrogen Line 3.9
3.3 EXPERIMENTAL VALIDATION 3.12
3.3.1 Conversion Analysis *3.14*
3.3.2 Particle Sizing *3.15*
3.3.2.1 Particle Sizing using CHDF 3.15
3.3.2.2 Particle Sizing Using PCS 3.16
3.3.3 Molecular Weight Analysis *3.17*
3.3.4 Results *3.21*
3.3.4.1 Monomer Conversion 3.21
3.3.4.2 Particle Size Distribution 3.24
3.3.4.3 Molecular Weight Distribution 3.28
3.4 CONCLUSION 3.38
3.5 REFERENCES 3.39

3.1 Introduction

The dynamic reactor model for the emulsion copolymerisation process is developed and needs to be validated. The validation of the model against experimental results is performed at different reactor conditions. A 1L reactor facility was used in the Department of Chemical Engineering to validate the process, while the 5L reactor was launched. The optimisation and the optimal control of the process was developed and validated within the 5L reactor

In this chapter, the automated reactor facility of the 1L and the 5L reactor for the emulsion copolymerisation process is explained. The validation of the process with the experimental results is also shown. Styrene and MMA were chosen, due to the availability of the kinetics and their importance in the formation of many products.

3.2 Automated Reactor Facility

3.2.1 1L Polymerisation Reactor

The 1L reactor system is provided by Pressure Dynamic Consultants (PDC Machines, Inc.), which is a world leader in the design, engineering, manufacture, installation, commissioning, service, and support of equipment for the chemical, petrochemical, pharmaceutical, and specialty gas industries. The reactor includes the reactor vessel, an agitation assembly and a supporting aluminium stand (illustrated in Figure 3.1-3.2). The parts of the reactor vessel are the 1-litre glass cylinder (Büchiglas Uster) with a jacket around the circumference held together between two steel plates (SA 182/316 SS). Stirred glass reactors are ideal for visual observation of chemical reactions under pressure. The glass reactor is a complete system including the glass vessel, supporting stand, agitation assembly (magnetic stirrer, drive motor, belt, belt guard and impeller), multiple process connection ports, drain port, sample tube, temperature sensor, cooling coil, gas line and a rupture disc assembly along with an agitation control panel to adjust and monitor the speed of the stirrer. The maximum operating pressure and temperature of the reactor are 6 bar and 200°C respectively. The reactor vessel has a pneumatic actuation system that can be used to lower the vessel for cleaning and maintenance purposes. Three Pt-100 RTDs (i.e. resistance temperature detectors) were installed to the reactor for on-line temperature

monitoring. Moreover, the reactor vessel had a six-blade impeller for adequate mixing and a proper agitation rate to minimize coagulation.

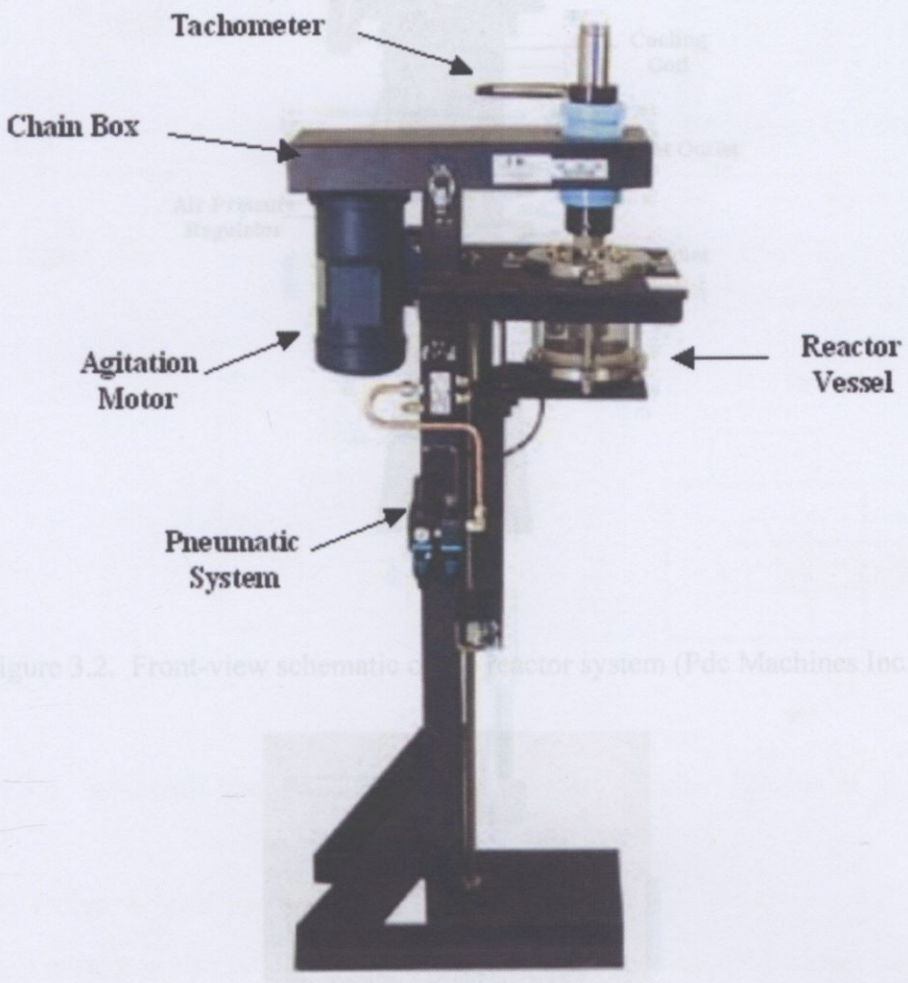

Figure 3.1. Side-view schematic of the reactor system (Pdc Machines Inc.).

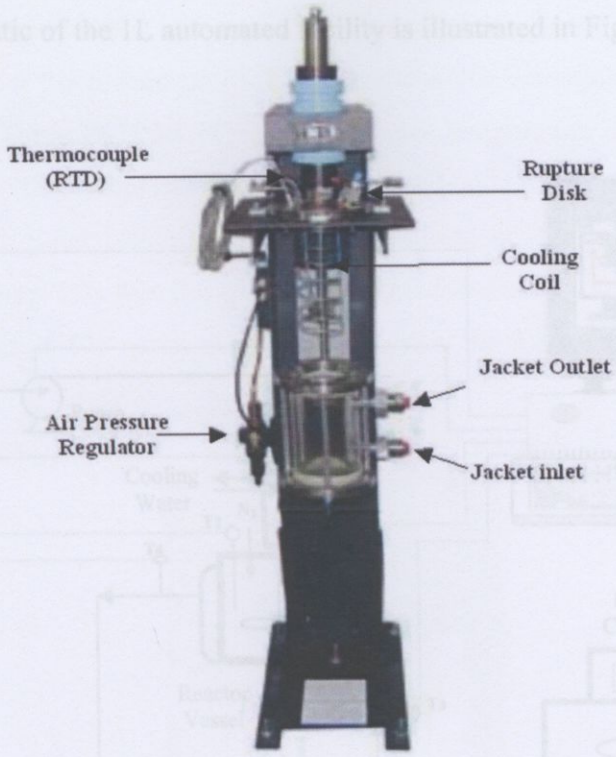

Figure 3.2. Front-view schematic of the reactor system (Pdc Machines Inc.).

Figure 3.3 Top-view schematic of the reactor system (Pdc Machines Inc.).

The overall schematic of the 1L automated facility is illustrated in Figure 3.4.

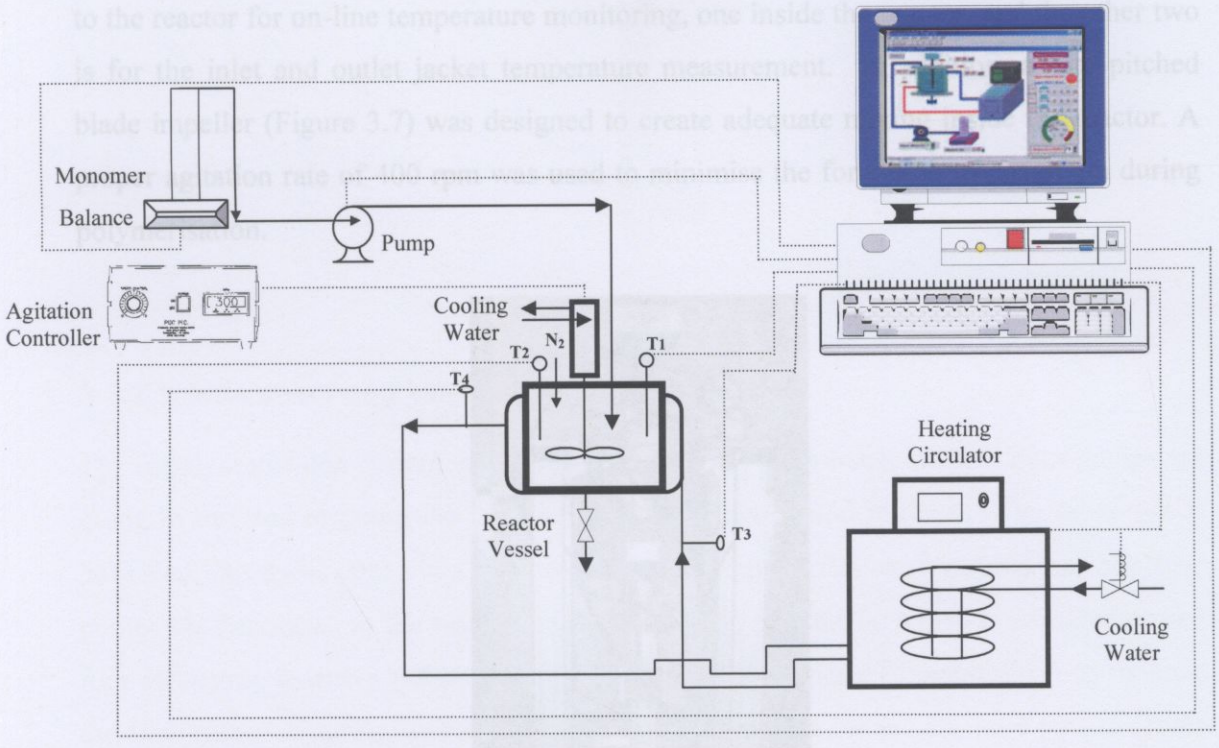

Figure 3.4. Schematic diagram of the automated reactor facility (Zeaiter et al., 2002)

3.2.2 5L Polymerisation Reactor

The reactor system is also provided by PDC Machines, Inc., where it includes an agitation assembly and a supporting metal stand (illustrated in Figure 3.5). It is featured with simple bolted closure, liquid sampling, internal cooling, over-pressure and over-temperature protection, temperature sensor and custom control systems. It has a capacity of 5L, with a watch glass. The design pressure is to 300 psig, and the design temperature is to 200°C. The reactor is floor mounted. The magnetic drivers (Figure 3.6) utilise a design where an outer magnet turns and is magnetically coupled with an inner magnet. The high energy between these two magnets results in torque transmission via a lower shaft. The speed of the agitation is 20 – 1500 rpm. The 5L reactor is therefore, a complete system including the vessel, supporting stand, agitation assembly (magnetic stirrer, drive motor, belt, belt guard and impeller), multiple process connection ports, drain port, sample tube, temperature sensor, cooling coil, gas line and a rupture disc assembly along with an

agitation control panel to adjust and monitor the speed of the stirrer. The reactor vessel can also be lowered from the locked position, via a pneumatic actuation system, for cleaning and maintenance. Three Pt-100 RTDs (i.e. resistance temperature detectors) are installed to the reactor for on-line temperature monitoring, one inside the reactor, and the other two is for the inlet and outlet jacket temperature measurement. In addition, a four-pitched blade impeller (Figure 3.7) was designed to create adequate mixing inside the reactor. A proper agitation rate of 400 rpm was used to minimise the formation of coagulum during polymerisation.

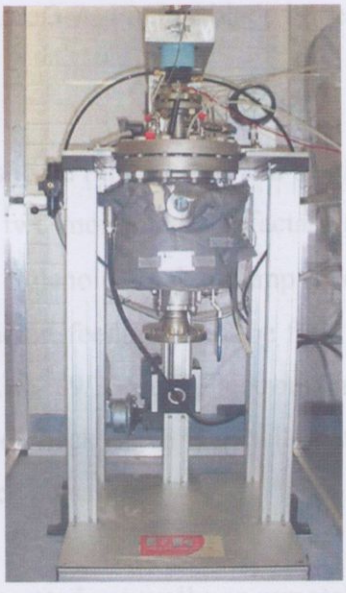

Figure 3.5 The 5L Emulsion Copolymerisation Reactor

Figure 3.6 Magnetic Driver

Figure 3.7 Pitched blade impeller

3.2.2.1 Monomer Feed Line

The copolymerisation system is to be run in batch and semi-batch modes. Four pumps are going to be used to pump the two monomers, surfactant and initiator. The monomer is delivered into the reactor via a Solenoid Dosing pump (ProMinent® gamma/L). The four pumps are connected to the reactor, feeding from the four tanks, which is mounted on the four electronic balances (OHAUS 89/336/EC Electromagnetic Compatibility) to monitor the flow rates. A spring-loaded check valve is installed at the reactor inlet port to create enough head pressure and reduce pulsation.

The monomer pump can be operated manually or remotely from a computer through an "analogue" operating mode, sending (4-20 mA), and receiving (0-10V) to the Distributed Control System (DCS) system.

3.2.2.2 Heating/Cooling System

As had been said in the previous sections, the reaction temperature plays an important role in many kinetic events in the emulsion copolymerisation process, and so it is essential to control the temperature. Two temperature sensors (Pt-100) are installed inside the reactor to continuously monitor the reaction temperature. There are two other temperature sensors (Pt-100) located on the inlet and outlet of the jacket. The Refrigerated and Heating Circulator (Julabo) provides a constant high water flow rate of 40 L/min through the jacket. The circulator is used to heat the reactor contents to the desired reaction temperature. The circulator is equipped with a PID controller built in it for temperature

adjustment to the setpoint. The temperature and the flow rate of the pumps profiles can be seen in the Control Station Software. Typical temperature profile is shown in Figure 3.8.

Figure 3.8 Temperature Profile

The heating circulator can be operated manually or remotely via a computer and is equipped with a PID controller within the Control Builder Software for internal and external temperature control Figure 3.9. A fume hood had been designed to cover the whole copolymerisation plant Figure 3.10.

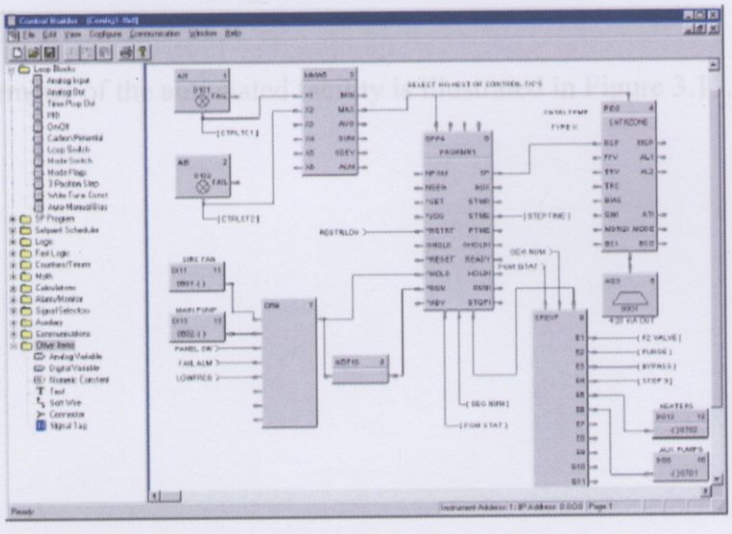

Figure 3.9 Control Builder – Temperature Control

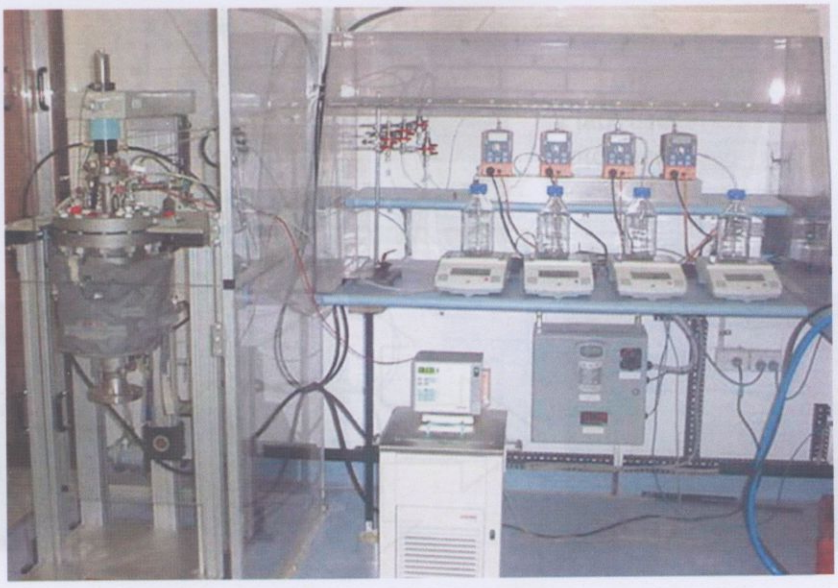

Figure 3.10 Copolymerisation Plant

3.2.2.3 Nitrogen Line

Nitrogen is also used as a blanket with a very slight positive pressure preventing oxygen that acts as an inhibitor during the copolymerisation reaction. A valve had been used to shift between the 1L reactor and the 5L reactor. All the feed that is to be fed to the reactor as a semi-batch process is also cleaned up with Nitrogen.

The overall schematic of the automated facility is illustrated in Figure 3.11.

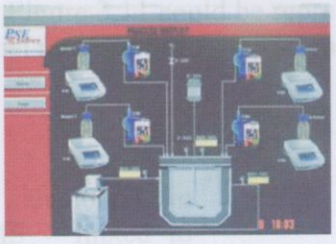

Plant user
Interface

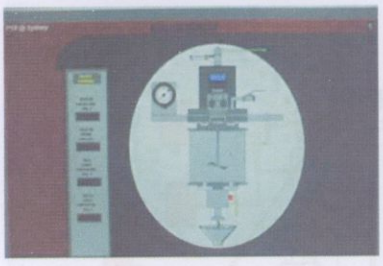

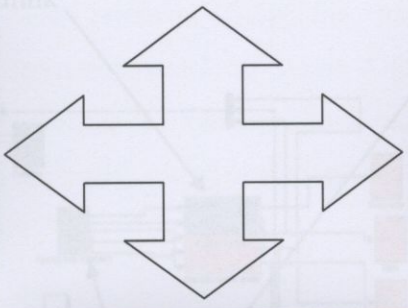

Reactor User
Interface

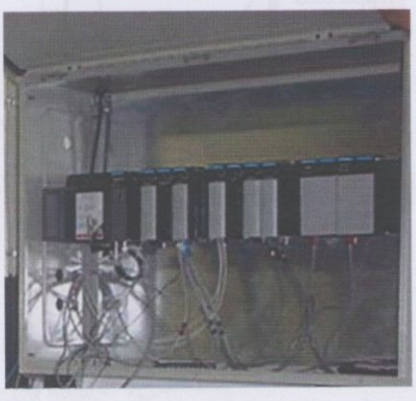

Polymer
Reaction
Engineer

Distributed
Control
System (DCS)

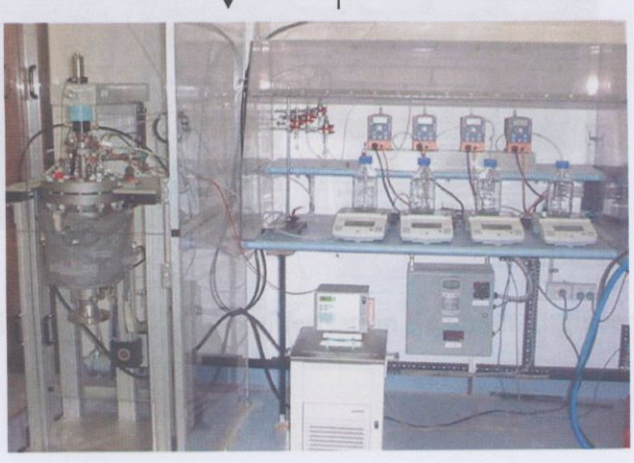

Figure 3.11 Schematic diagram of the automated 5L reactor facility.

The schematic diagram in Figure 3.11 could be represented in another form in Figure 3.12. This figure shows the model that had been used to control the reaction.

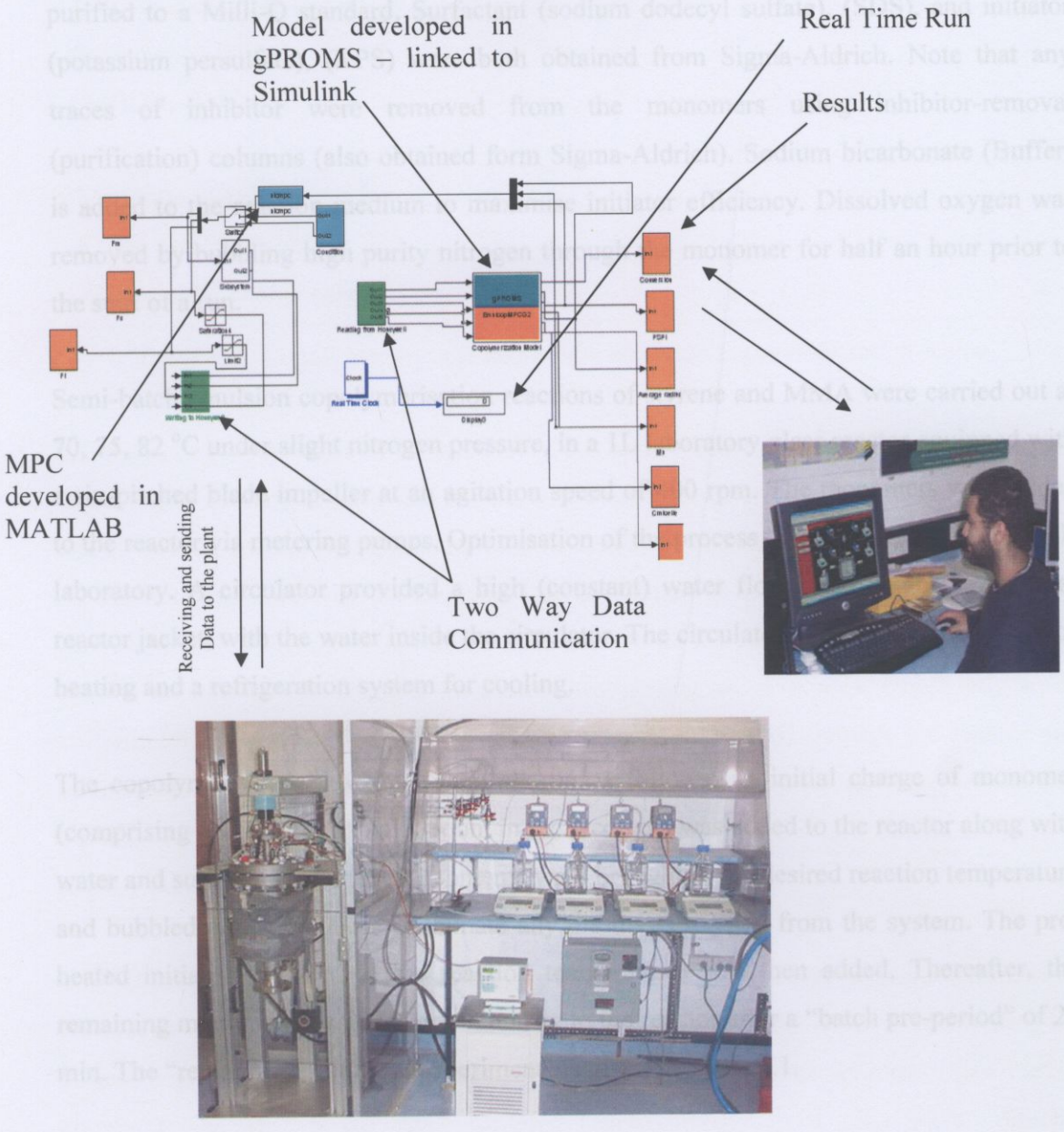

Figure 3.12 Copolymerisation Reaction Engineering Control

3.3 Experimental Validation

Styrene (99% purity, inhibited with 4-tert-butylcatechol) and MMA (99% purity, inhibited with hydroquinone) monomers were obtained from Fluka, while the water used was purified to a Milli-Q standard. Surfactant (sodium dodecyl sulfate), (SDS), and initiator (potassium persulfate), (KPS) were both obtained from Sigma-Aldrich. Note that any traces of inhibitor were removed from the monomers using inhibitor-removal (purification) columns (also obtained form Sigma-Aldrich). Sodium bicarbonate (Buffer) is added to the reaction medium to maximise initiator efficiency. Dissolved oxygen was removed by bubbling high purity nitrogen through the monomer for half an hour prior to the start of a run.

Semi-batch emulsion copolymerisation reactions of styrene and MMA were carried out at 70, 75, 82 °C under slight nitrogen pressure, in a 1L laboratory glass reactor equipped with a six-pitched blade impeller at an agitation speed of 400 rpm. The monomers were added to the reactor via metering pumps. Optimisation of the process is being carried out in a 5 L laboratory. A circulator provided a high (constant) water flowrate through the external reactor jacket, with the water inside the circulator. The circulator is supplied with a coil for heating and a refrigeration system for cooling.

The copolymerisation reactions were all run as follows: an initial charge of monomer (comprising 17.1% of the total amount in the "recipe") was added to the reactor along with water and surfactant. The reactor contents were brought to the desired reaction temperature and bubbled with nitrogen to eliminate any dissolved oxygen from the system. The pre-heated initiator solution (at the reaction temperature) was then added. Thereafter, the remaining monomer was added continuously to the reactor after a "batch pre-period" of 25 min. The "recipe" used in these experiments is given in Table 3.1.

Monomer conversion was gravimetrically determined off-line by taking samples from the reactor. The MWD of the polymer samples was determined off-line by GPC, while most of the PSDs were obtained using the Zetasizer and the CHDF. The CHDF instrument is incapable of reporting on particles smaller than 30 nm in size. This is a limitation of CHDF which is still widely used and considered to be one of the best currently available. The recipe used in this work is shown in Table 3.1.

Styrene Monomer (g)	62.5
MMA Monomer (g)	62.5
Water (g)	531.66
Initiator-Persulfate $K_2S_2O_8$ (g)	0.375
Surfactant-SDS (g)	1.078
$NaHCO_3$-Buffer (g)	1.00
Monomer feed:	
82.9% semibatch charge	
17.1% initial charge (seeding process)	

Table 3.1. Copolymer styrene and MMA emulsion copolymerisation recipe.

The beginning of the reaction should start in the batch mode to produce the seeds. In batch mode, the monomers, styrene and MMA, surfactant and water were carefully added to the reactor (with the water being used to rinse all vessels clean). The hot water bath was set to the desired temperature by the Julabo, while the agitator was turned on at 400 rpm. The tank that has 82.9% (remaining) of the monomers to be fed to the reactor after the seeding process is pumped with nitrogen for 20 minutes, getting rid of oxygen, which may act as an inhibitor. Once the reactor was sealed, nitrogen was passed through the reactor and bubbled through the reaction medium. The flow rate was set such that the nitrogen bubbled 2 to 3 bubbles per second through the oil in the dreschell bottle, ensuring a slightly positive pressure was maintained in the vessel.

The initiator solution was then heated separately to the desired reactor temperature while the reactor contents were allowed to reach a steady state in temperature. On reaching the desired temperature, the initiator was added to the reactor and time set to zero (the start of copolymerisation). Small latex samples (approximately 5-10 mL) were collected periodically and immediately cooled in ice for further analysis. Copolymerisation was assumed to cease with exposure to oxygen and cooling to low temperature.

This procedure was repeated for a number of monomer feed rates, variable reactor temperatures, and different feed ratios.

3.3.1 Conversion Analysis

After weighing out the prescribed dosages of monomer and surfactant, they were charged into the reactor using the water to backwash any residue left behind in the flasks. The initiator was dissolved in a small amount of water and slightly submerged in the water bath to bring the contents to the initial reaction temperature. The flask was also kept covered to minimise the oxygen concentration. Time zero commenced at the addition of the initiator into the reactor. The first sample was taken at this point (usually worked out to be ~10 to 20 seconds after the initiator was charged). Samples were then taken at ten-minute intervals for the first hour and then 15 minute intervals for the second hour. The reactor temperature was recorded every minute for the first 30 minutes, then at each sample time thereafter.

The latex samples were extracted by syringe and needle that was inserted through a tightly sealed stopper. Since perfect mixing was assumed for the model, samples were taken at no particular depth or place in the reactor. This will provide completely random data to analyse. These samples, of about 6 ml, were placed in glass vials, and placed in ice to cease polymerisation of the contents. It is often suggested to add a small amount of inhibitor (e.g. low concentration hydroquinone solution) to the vial to cease the polymerisation at the exact time of extraction.

Once the samples had cooled sufficiently (>5 minutes), gravimetric analysis was carried out to determine the conversion. To do this, a small portion was deposited into a pre-weighed pan, an aluminium pie-dish. The pan and the contents were then weighed and left to dry-out in a fume hood overnight. These samples were then transferred to an oven, at 60°C, for a further 6-8 hours, after which the pan was weighed again. This process proved to be quite efficient in producing a very dry polymer product, and ultimately a determination of the conversion using a derivation of the formula given by (Saldívar and Ray, 1997),

$$x = \frac{\left(\frac{m_{PDS} - m_P}{m_{PS} - m_p} \right) M_T - M_E - M_I}{M_M} \tag{3.1}$$

where m_{PDS}, m_{PS} and m_P are the mass of the pan and dry sample, mass of pan and new sample and mass of pan, respectively. M_T is the total weight inside the reactor at time zero, M_E is the weight of the emulsifier, M_I is the weight of the initiator and M_M is the total weight of the monomer fed to the reactor.

The source of errors, accumulated throughout the course of the experiment, were not confined to just one piece of equipment or procedure. Some were deemed insignificant through the establishment of justified assumptions (e.g., perfect mixing), while others were inherent to the process, such as the accuracy limits of the mass balances, temperature gauge, etc.

3.3.2 Particle Sizing

The particle sizing was undertaken on the latex samples using photon-correlation spectroscopy (PCS) initially and then Capillary Hydrodynamic Fractionator (CHDF). Both methods are relatively simple to operate and produce accurate results, except that the PCS is unable to provide a bimodal distribution.

3.3.2.1 Particle Sizing using CHDF

This technique for the sizing of particles uses fractionation technology as the determining mechanism. The procedure for operation is:

- After the machine and computer have been switched on, turn on the pump and ensure that the pump is operating at between 490kPa and 550kPa.
- To set-up a run, click the icon "Run" in the toolbar. Make sure that it is operating under the condition that the sample is UV-Yes. The problem encountered for this system is the styrene is UV-absorbing and MMA is not. The final copolymer would be UV-absorbing.
- The port for injecting the samples boasts two positions: one for loading and one for injecting. Begin sequence by cleaning the port using the CHDF eluant solution in both positions.
- Prepare sample by diluting it to approximately 2 vol% (determine by sight) with the CHDF eluant. Deposit sample in the port in the load position until the line is

full. This is determined by the overflow line which should release about 10 to 15 drops.

- Repeat step 3.
- Repeat step 4 using the marker solution instead of the sample. The marker solution is 0.003g sodium benzoate in 50g of CHDF eluant. Using the on-line timer, the marker solution is injected 50 seconds after the injection time of the sample, which is deemed t = 0.
- The analysis takes approximately 6 minutes to complete. After the marker has appeared on the fractogram, click on Stop and print results.

The results from the CHDF analysis include the PSD as a function of intensity and the corresponding number- and weight-average diameters of the samples are determined.

3.3.2.2 Particle Sizing Using PCS

The mechanism behind the successful operation of photon-correlation spectroscopy (PCS) is based on the scattering of light to ascertain the particle size. The operating procedure of the Malvern Zetasizer 5000 is,

- Prepare sample by diluting in deionised water to about 2 vol%, determined by sight, in the PCS sampling vial.
- Allow the solution to settle and only proceed once monodispersity has been obtained. This usually occurs after initially agitating the vial to achieve a perfect-mixing environment and then a short wait to allow the solution to stabilise.
- Place the vial in the holder of the PCS and close the cover to protect the eyes from exposure to the laser.
- Enter the relative information pertaining to the sample into the computer program and run the sample.
- Adequate dilution of the sample is perceived to be achieved by the parameter Kcps, which is an indication of the number of particles that are counted per second. The required range for this value is suggested to be between 300 and 700. This parameter also indicates the relative dispersity of the sample.
- The duration of each sample is approximately 2 minutes including the preparation and analysis.

- The output of the analysis indicates the quality of the test and declares whether the test satisfies Malvern's quality criterion by signifying a Pass or Check. If Check is indicated, repeat procedure from step 1.

Due to the scepticism surrounding PCS, it is often suggested to repeat the procedure even for tests that have been passed in order to determine the reproducibility. Each sample was analysed up to 3 times to ascertain this, and, in most cases the tests proved conclusively the relatively accuracy of the results.

3.3.3 Molecular Weight Analysis

The technique of gel permeation chromatography (GPC) is utilised to find the molecular weight experimentally. Gel permeation chromatography will provide answers on the molar mass i.e. number, weight and z-averages (M_n, M_w, M_z) as well as the molar mass distribution (polydispersity) of a polymer sample. Separation in GPC is governed by entropic effects unlike other modes of liquid chromatography where enthalpy effects are predominant.

The principal of GPC is explained best by a schematic representation which shows the first part of an analysis by GPC: from the sample to a chromatogram (Figure 3.13).

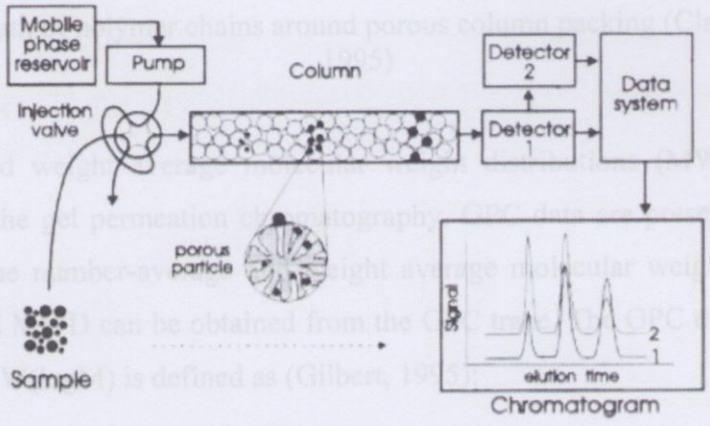

Figure 3.13: Principle of size exclusion chromatography.

When a sample is injected into the column, the polymer molecules are separated according to their hydrodynamic volumes; hence polymer molecules larger than the pores of the

packing material cannot enter the pores and are eluted at the interstitial volume. It should be noted that no fraction of the sample can be eluted before the interstitial volume has passed through the column. Small molecules, however, have access to the pores and will therefore elute at the sum of both the interstitial and pore volume. Molecules which have sizes between the above two extreme values will have access to only a part of the pore volume and will therefore be eluted at an elution volume. It should also be noted that to obtain an absolute molecular mass value of a sample, standards with known molecular masses must be used to obtain a suitable calibration curve.

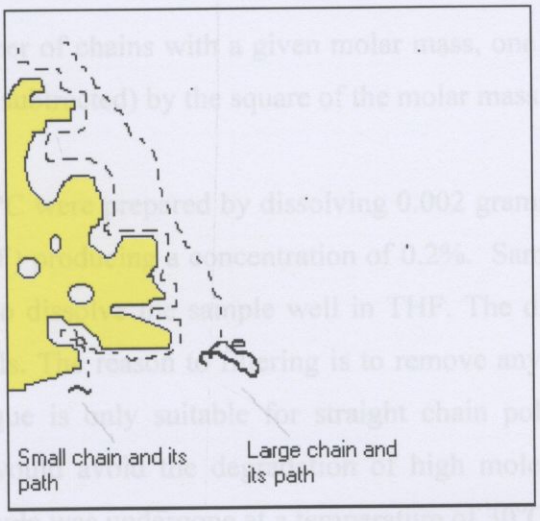

Figure 3.14 Path of polymer chains around porous column packing (Clay and Gilbert, 1995)

The number and weight average molecular weight distributions (MWDs) are readily obtained using the gel permeation chromatography. GPC data are presently largely used just to obtain the number-average and weight average molecular weights, M_n and M_w; however the full MWD can be obtained from the GPC trace. The GPC distribution, X(M) denoted also by W(logM) is defined as (Gilbert, 1995):

$$GPC\ distribution = X(M) = MW(M) = M^2P(M) \tag{3.2}$$

GPC trace is a function of the elution volume V_{el}; it is assumed that the baseline has been subtracted. Appropriate calibration with monodisperse standards yields the GPC calibration curve, which is the volume at which monodisperse standards elute as a function

of the molar mass of the standard denoted by *V(M')*. It is emphasized that the GPC trace is not the MWD. The cumulative number MWD, $\overline{P}(M)$ is the total number of chains in a sample with molar mass *M*, $\overline{W}(M)$. If the calibration curve is linear, which is often the case, them the number distribution $\overline{P}(M)$ and the GPC trace are related by (Gilbert, 1995):

$$\overline{P}(M) = \frac{G(V_{el})}{M^2} \tag{3.3}$$

Hence to find the number of chains with a given molar mass, one should divide the GPC trace (with background subtracted) by the square of the molar mass.

The samples for the GPC were prepared by dissolving 0.002 grams of dry latex in 1 gram of tetrahydrofuran (THF) producing a concentration of 0.2%. Samples are left for at least eight to twelve hours to dissolve the sample well in THF. The dissolved sample is then filtered to the GPC vials. The reason to filtering is to remove any cross-linked polymers, since the GPC technique is only suitable for straight chain polymers. Moreover, the complete dissolution would avoid the degradation of high molecular weight polymers. The analysis of the sample was undergone at a temperature of 30°C and at a THF flow rate of 0.6 ml/min. The general parameters used in modelling styrene and MMA emulsion copolymerisation, which include the reaction rate coefficients for propagation, transfer and termination, surfactant and initiator physical properties, as well as styrene and MMA data are shown in Table 3.2.

Parameter	Value (Styrene)	Value (MMA)	Reference
k_{po}	$k_{po,A} = 10^{7.63} e^{\frac{-32500}{RT_r}}$	$k_{po,B} = 10^{6.4} e^{\frac{-22200}{RT_r}}$	(Clay and Gilbert, 1995)
k_{tr}	$k_{tr,A} = k_{p,A} \times 10^{-0.658} e^{\frac{-23400}{RT_r}}$	$k_{tr,B} = 4 \times 10^{5.3} e^{\frac{-45900}{RT_r}}$	
k_{to}	$k_{to} = k_{t,aq,A} f_A + k_{t,aq,B} f_B$	$k_{to} = k_{t,aq,A} f_A + k_{t,aq,B} f_B$	(Nomura et al., 1983)
$K_{t,aq}$	$k_{t,aq,A} = 1.703 \times 10^9 e^{\frac{-2263*4.182}{RT_r}}$	$k_{t,aq,B} = 9.8 \times 10^7 e^{\frac{-701*4.182}{RT_r}}$	(Nomura et al., 1981), (Nomura et al., 1983)
d_p	1050.1-0.621T	1.178	(Clay and Gilbert, 1995)
d_m	923.6-0.887T	0.909	
z	3	5	
j_{crit}	5	10	
k_{mwp}	C_{W_sat}/C_{p_sat}	C_{W_sat}/C_{p_sat}	(Clay and Gilbert, 1995), (Nomura et al., 1983)
$k_p^1{}_{aq}$	$k^1_{p,aq,A} = 2k_{p,A}$	$k^1_{p,aq,B} = 3.15k_{p,B}$	(Clay and Gilbert, 1995)
$k_p^2{}_{aq}$	$k^2_{p,aq,A} = 1.753k_{p,A}$	$k^2_{p,aq,B} = 2k_{p,B}$	
$k_p^3{}_{aq}$	$k^3_{p,aq,A} = k_{p,A}$	$k^3_{p,aq,B} = k_{p,B}$	
$k_p^4{}_{aq}$	$k^i_{p,aq} = k^3_{p,aq}$	$k^i_{p,aq} = k^3_{p,aq}$	
D_w	1.55×10^{-7}	1.7×10^{-7}	(Coen et al., 1998)
M_o	0.104	0.101	
C_{p_sat}	5.5	6.6	(Gilbert, 1995)
C_{W_sat}	exp(-1.514-1259/(T+273))	0.15	
CMC	3×10^{-3}	3×10^{-3}	
n_{agg}	60	60	
a_s	42×10^{-18}	42×10^{-18}	
σ	0.602×10^{-8}	0.602×10^{-8}	(Clay and Gilbert, 1995)
α	0.74×10^{-8}	0.74×10^{-8}	

Table 3.2. List of parameters used for styrene and MMA copolymerisation.

3.3.4 Results

3.3.4.1 Monomer Conversion

Conversion of the comonomer to copolymer, was calculated on a mass basis, which was determined by the gravimetric analysis, explained in section 3.3.1.

The experimental results for the overall conversion had a good agreement with the model simulation. In Figure 3.15(a), the experiment was run for a batch reaction, and the rest three Figure 3.15(b-d) for a semibatch reaction at different feed rates. The first section of the Figure 3.15(b-d) look like the batch process, since for a semibatch reaction, the first 25 minutes is actually a batch reaction. Then, at the moment of adding monomers to the reaction, the overall conversion drops. This is due to the reason that most of the monomers had only converted to polymer, and at the time of adding, there is more monomer in the reactor at a moment than what it usually had, and therefore the overall conversion drops. Then, the monomers start to propagate converting to a polymer. The drop in the overall conversion is different for different feed rates, where it is a larger drop for a higher flow rate, and a smaller drop for a lower flow rate, proportional to the amount added. A high monomer conversion of 90 % was achieved. At high conversion, the particles are expected to be glassy. Subsequent addition of the monomer at a lower feed rate kept the conversion high. This is related to the point that had been explained previously, that at high feed rate, more monomers are fed to the reactor, and so a larger drop is expected. In other words, by comparison, the addition of monomer at a high feed rate resulted in a sudden decrease in the instantaneous conversion due to the monomer concentration in the aqueous phase increasing, thus causing an increase in the monomer concentration inside the particles. In fact, at a high feed rate, the process resembled 'Interval II' as seen in a batch copolymerisation run (that is the presence of monomer droplets and flooded conditions). The monomer concentration inside the polymer particles increases with an increase in feed rate; eventually reaching values close to the saturation concentration. The growth rate which depends on the monomer concentration will be relatively high under these conditions. It is also observed that the time to get to a high conversion of about 95% is longer for a lower feed rate.

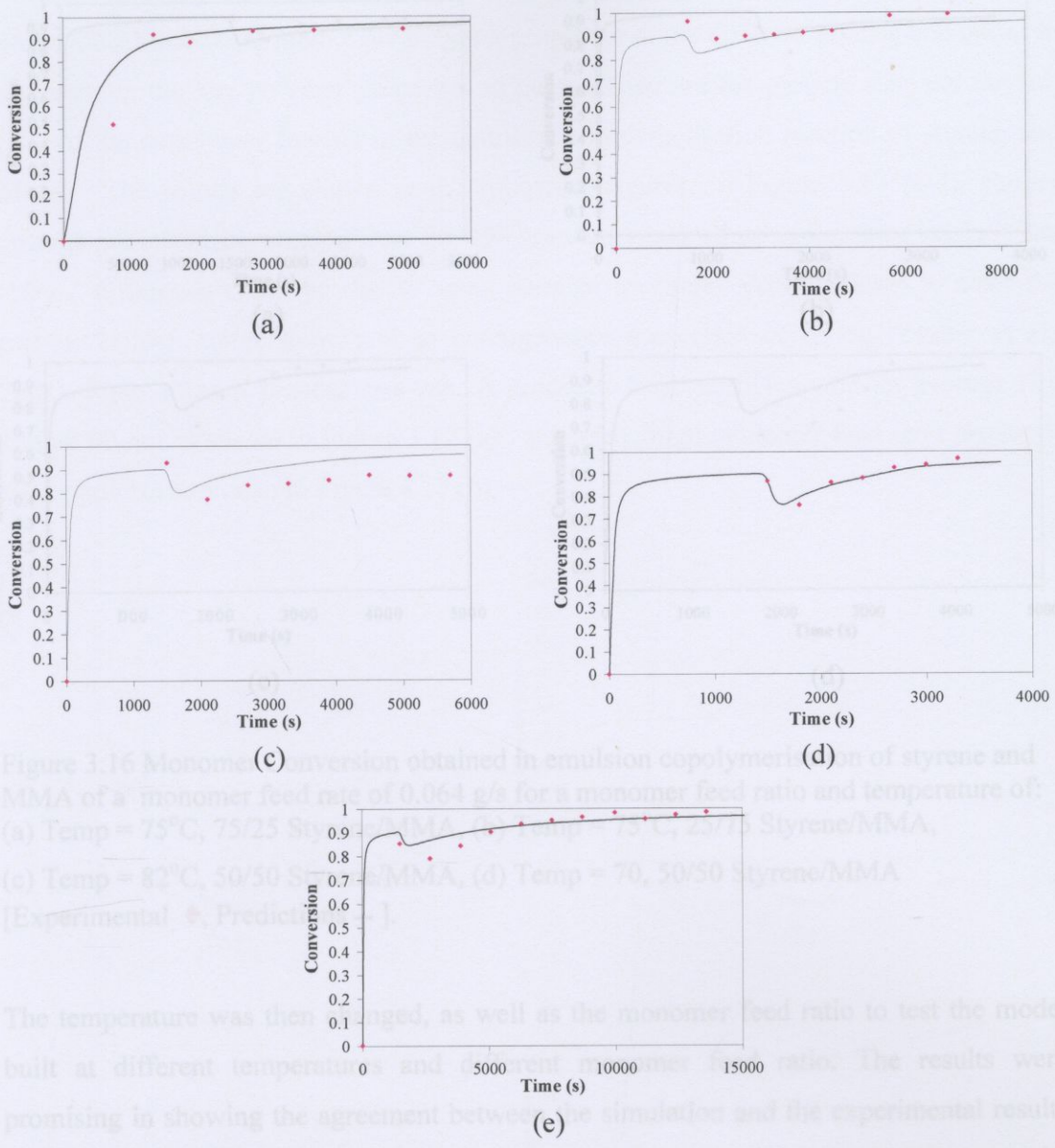

Figure 3.15 Monomer Conversion obtained in emulsion copolymerisation of styrene and MMA (50/50) mixture at 75°C for monomer feed rates of: (a) Batch (0 g/s), (b) 0.064 g/s, (c) 0.032 g/s, (d) 0.016 g/s, (e) 0.008 g/s [Experimental ♦, Predictions ▲].

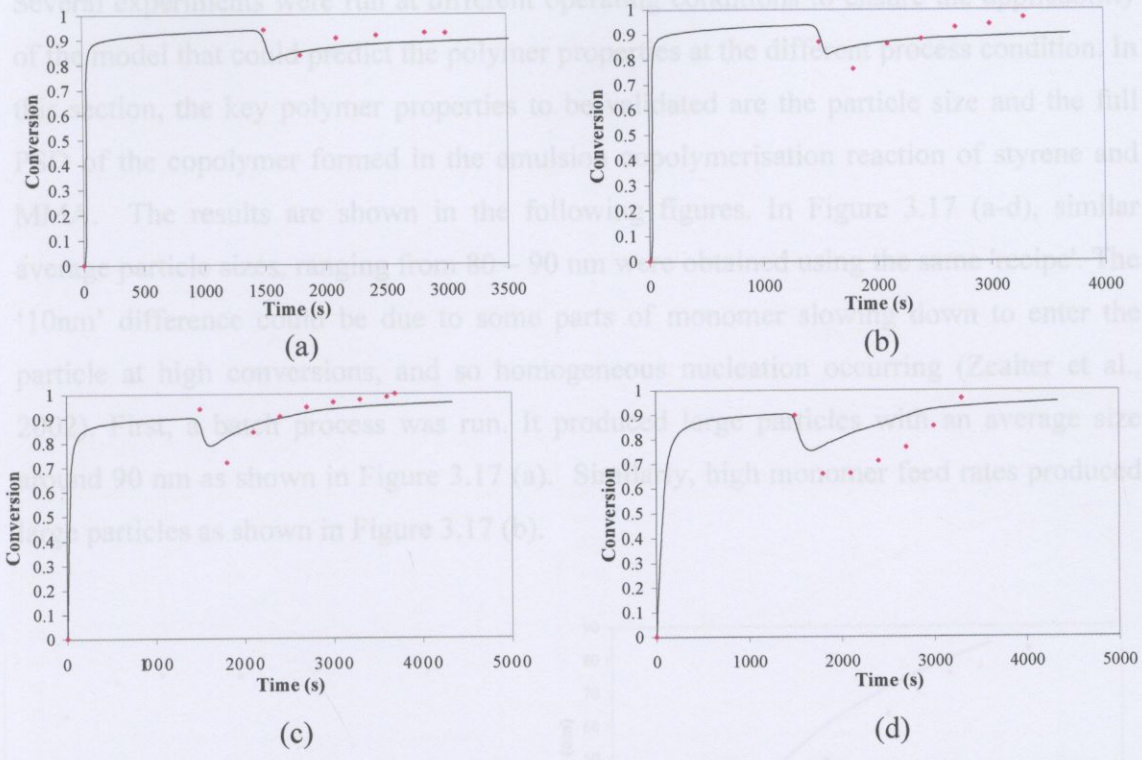

Figure 3.16 Monomer Conversion obtained in emulsion copolymerisation of styrene and MMA of a monomer feed rate of 0.064 g/s for a monomer feed ratio and temperature of: (a) Temp = 75°C, 75/25 Styrene/MMA, (b) Temp = 75°C, 25/75 Styrene/MMA, (c) Temp = 82°C, 50/50 Styrene/MMA, (d) Temp = 70, 50/50 Styrene/MMA [Experimental ♦, Predictions –].

The temperature was then changed, as well as the monomer feed ratio to test the model built at different temperatures and different monomer feed ratio. The results were promising in showing the agreement between the simulation and the experimental results as shown in Figure 3.16(a-d). It can be observed that on raising the temperature, the conversion is faster and goes to over 90 % faster than lower temperature. This returns to the fact that the propagation coefficients increase on rising up temperature, and so as the conversion. On testing the process at two three proportions from 50/50 to 75/25 and 25/75 Styrene/MMA, the conversion reached to 90 % faster for a 25/75 Styrene/MMA feed ratio. The reason is that the propagation coefficient is greater for the MMA monomer than for styrene, and therefore, it propagates faster and more monomers are converted faster to polymer.

3.3.4.2 Particle Size Distribution

Several experiments were run at different operating conditions to ensure the applicability of the model that could predict the polymer properties at the different process condition. In this section, the key polymer properties to be validated are the particle size and the full PSD of the copolymer formed in the emulsion copolymerisation reaction of styrene and MMA. The results are shown in the following figures. In Figure 3.17 (a-d), similar average particle sizes, ranging from 80 – 90 nm were obtained using the same 'recipe'. The '10nm' difference could be due to some parts of monomer slowing down to enter the particle at high conversions, and so homogeneous nucleation occurring (Zeaiter et al., 2002). First, a batch process was run. It produced large particles with an average size around 90 nm as shown in Figure 3.17 (a). Similarly, high monomer feed rates produced large particles as shown in Figure 3.17 (b).

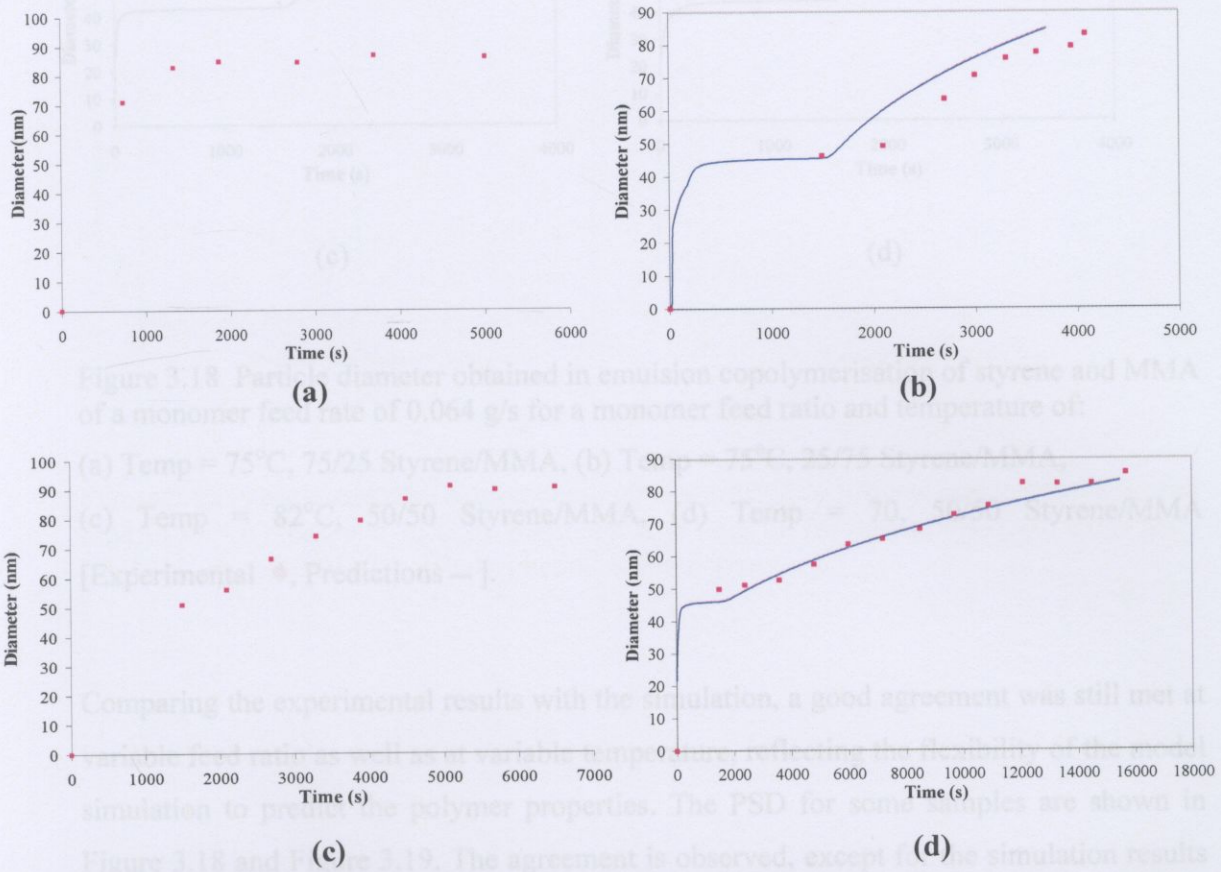

Figure 3.17 Particle diameter obtained in emulsion copolymerisation of styrene and MMA (50/50) mixture at 75°C for monomer feed rates of: (a) Batch (0 g/s), (b) 0.064 g/s, (c) 0.032 g/s, (d) 0.016 g/s[Experimental ■, Predictions —].

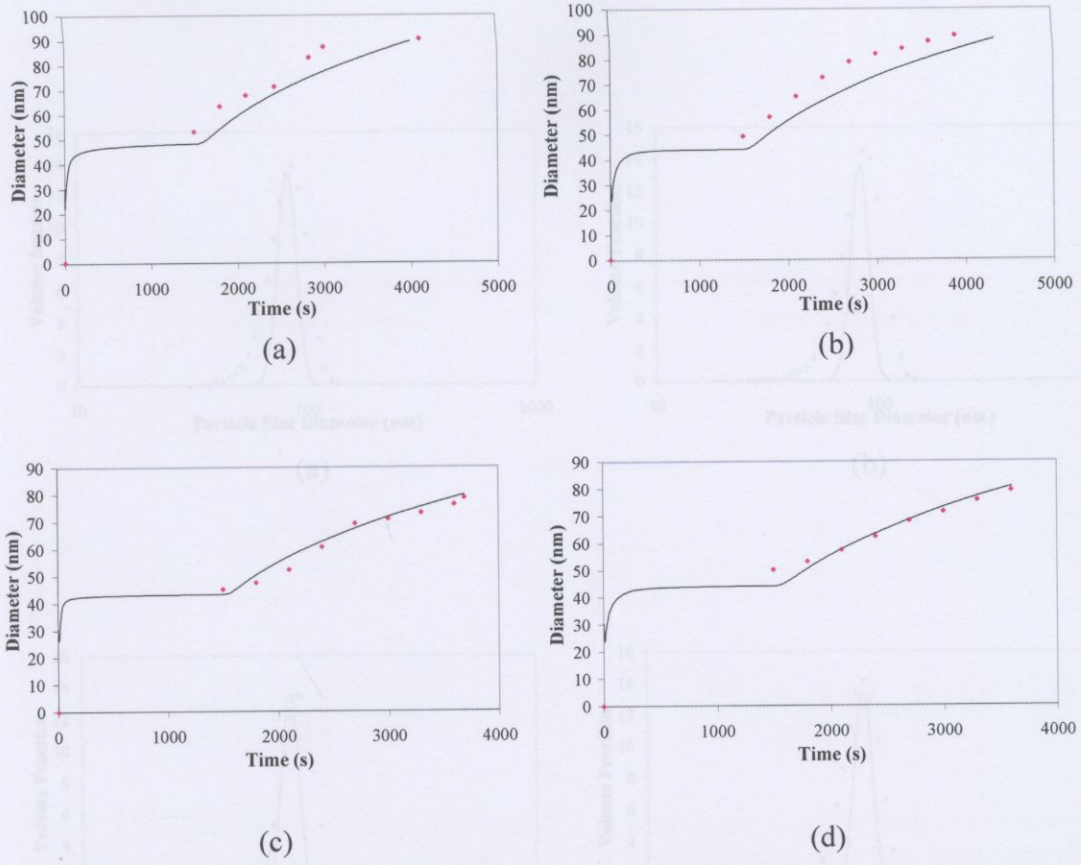

Figure 3.18 Particle diameter obtained in emulsion copolymerisation of styrene and MMA of a monomer feed rate of 0.064 g/s for a monomer feed ratio and temperature of:
(a) Temp = 75°C, 75/25 Styrene/MMA, (b) Temp = 75°C, 25/75 Styrene/MMA,
(c) Temp = 82°C, 50/50 Styrene/MMA, (d) Temp = 70, 50/50 Styrene/MMA
[Experimental ♦, Predictions —].

Comparing the experimental results with the simulation, a good agreement was still met at variable feed ratio as well as at variable temperature, reflecting the flexibility of the model simulation to predict the polymer properties. The PSD for some samples are shown in Figure 3.18 and Figure 3.19. The agreement is observed, except for the simulation results giving narrower distributions.

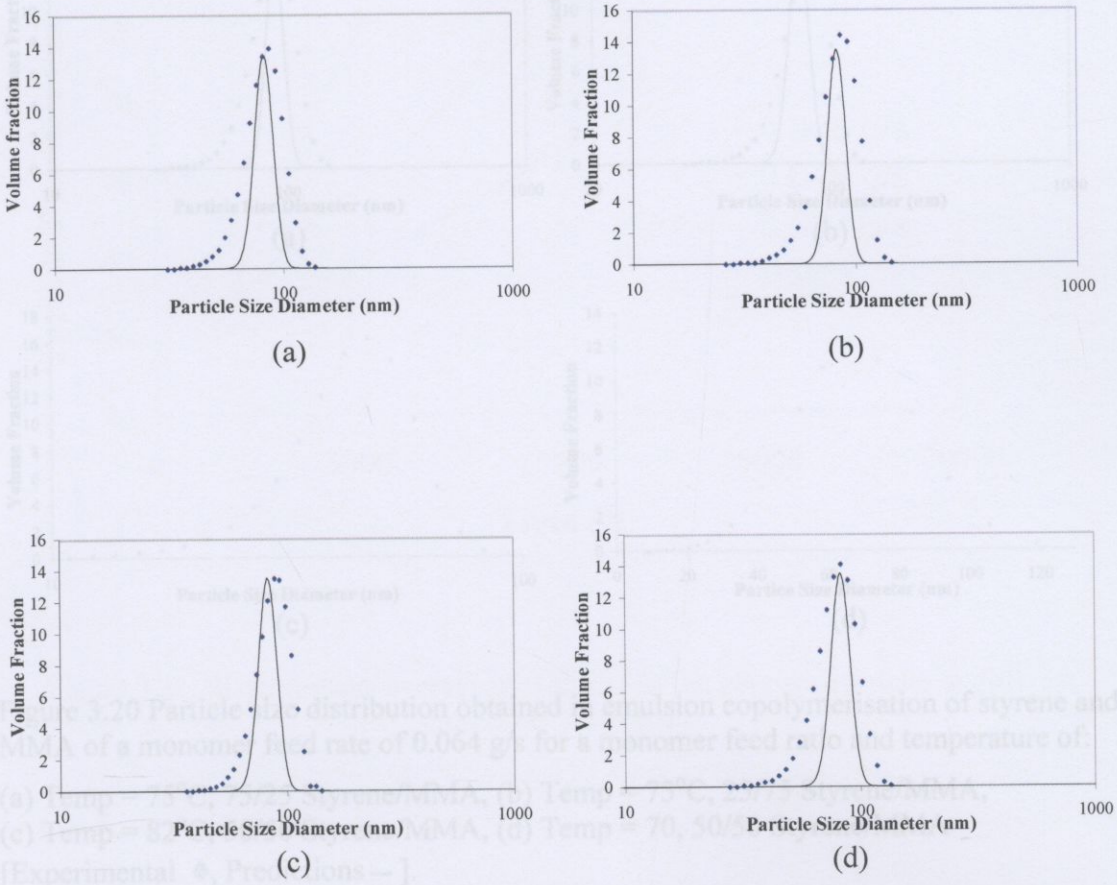

Figure 3.19 Particle size distribution obtained in emulsion copolymerisation of styrene and MMA (50/50) mixture at 75°C for monomer feed rates of: (a) Batch (0 g/s), (b) 0.064 g/s, (c) 0.032 g/s, (d) 0.016 g/s, [Experimental ♦, Predictions –].

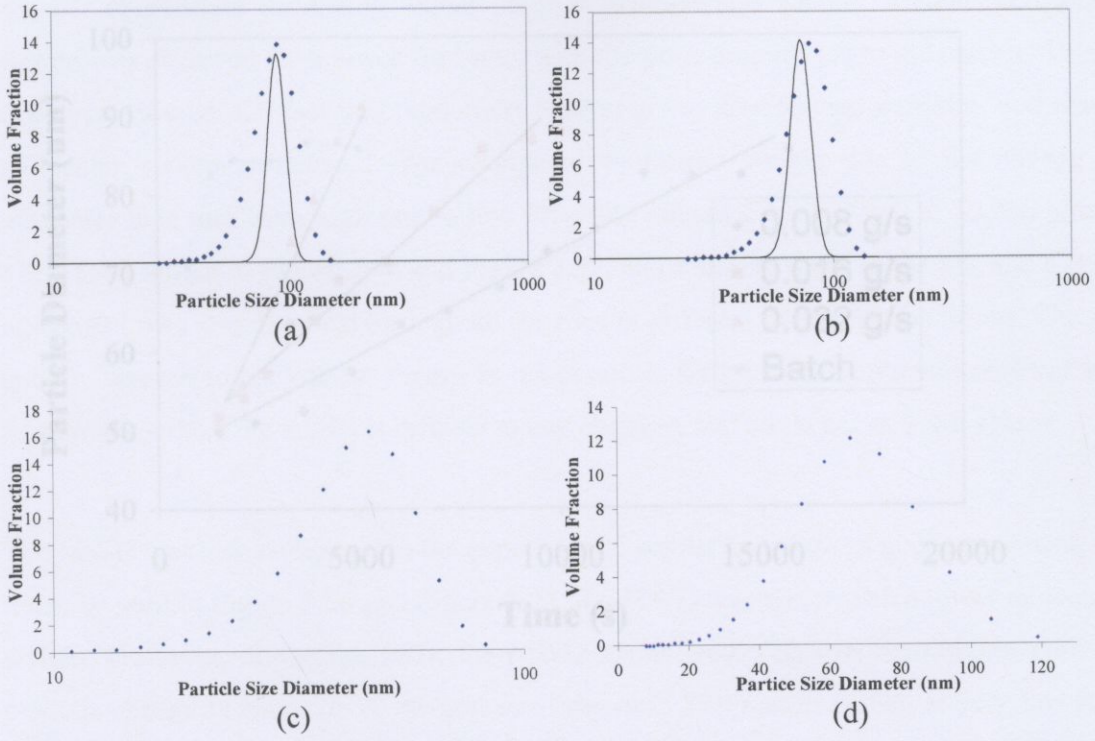

Figure 3.20 Particle size distribution obtained in emulsion copolymerisation of styrene and MMA of a monomer feed rate of 0.064 g/s for a monomer feed ratio and temperature of:

(a) Temp = 75°C, 75/25 Styrene/MMA, (b) Temp = 75°C, 25/75 Styrene/MMA,
(c) Temp = 82°C, 50/50 Styrene/MMA, (d) Temp = 70, 50/50 Styrene/MMA
[Experimental ♦, Predictions –].

A good agreement can be clearly observed from the figures. At low monomer feed rates, however, smaller particles were produced of a diameter of 80 nm. This could be related to the phenomenon of the glassy effect at high monomer conversion, explained and verified by (Zeaiter et al., 2002).

From Figure 3.21, it can be observed that different monomer feed rates has a proportional effect on the growth rate, i.e. increasing the monomer feed rate would increase the growth rate, and on decreasing the monomer feed rate, the growth rate decreases to a point, where the particle needs monomers to grow, and does not get find one, hence it will rather undergo homogeneous nucleation rather than the micelle nucleation.

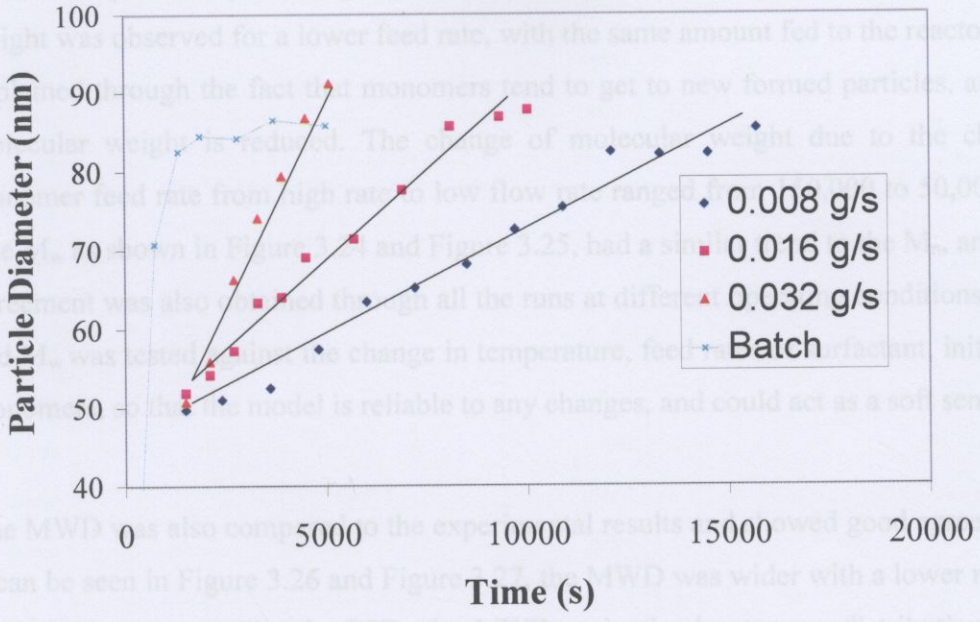

Figure 3.21. Experimental average growth rate of the polymer particles at different monomer feed rates.

3.3.4.3 Molecular Weight Distribution

The molecular weight of the polymer formed was estimated theoretically and compared to the experimental results, as shown in Figures (3.22 – 3.27) in a similar fashion to the PSD comparisons. The model predictions were found to be in good agreement with the experimental data. The M_n was affected by changes in the monomer feed rate, surfactant feed, initiator feed rate and the temperature of the reaction as can be seen in Figure 3.22 and Figure 3.23. The temperature of the reaction had the greater effect onto the molecular weight. This can be explained by the fact that higher temperatures generally cause an increase in the rate of radical transfer, and thus resulting in the formation of shorter chains which means lower molecular weight polymers. The molecular weight was also affected mainly by the surfactant feed rate due to the fact that surfactant would produce new micelles resulting to the state where the monomer would enter the new particles (easier to

diffuse), rather than getting into the larger particles, and hence producing new particles. In other words, the monomers are distributed into more particles rather than getting into less number of particles producing higher number of molecular weight. A lower molecular weight was observed for a lower feed rate, with the same amount fed to the reactor. This is explained through the fact that monomers tend to get to new formed particles, and hence molecular weight is reduced. The change of molecular weight due to the change of monomer feed rate from high rate to low flow rate ranged from 150,000 to 50,000 g/mol. The M_w as shown in Figure 3.24 and Figure 3.25, had a similar trend to the M_n, and a good agreement was also obtained through all the runs at different operating conditions. The M_n and M_w was tested against the change in temperature, feed rates of surfactant, initiator and monomers, so that the model is reliable to any changes, and could act as a soft sensor.

The MWD was also compared to the experimental results and showed good agreement. As it can be seen in Figure 3.26 and Figure 3.27, the MWD was wider with a lower molecular weight. However, unlike the PSD, the MWD maintained a narrow distribution with no obvious change in shape, over the course of the run. The reason is that, at very low feed rates, new particles are tend to be formed, taking a part of the monomers, and hence lower molecular weight is obtained. It is important to note that in terms of surfactant concentration, additional surfactant resulted in a reduction of the rate of polymerisation and also reduced the particle size. An indication of an increase in temperature of 10°C and by halving the molar surfactant concentration, a similar rate of polymerisation and particle size is achieved.

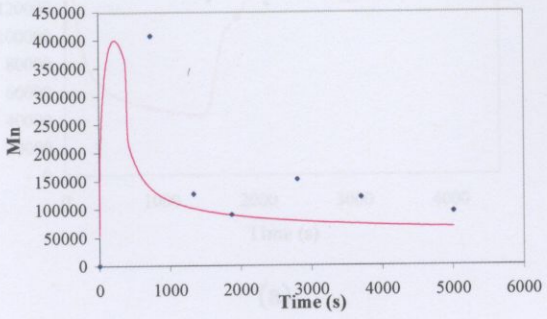

(a)

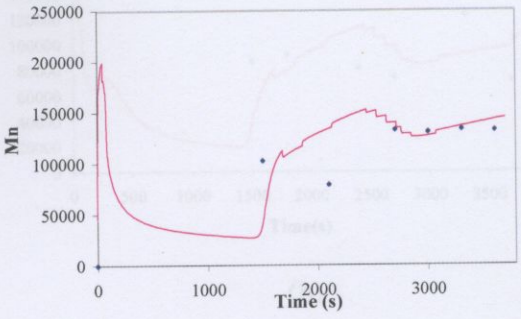

(b)

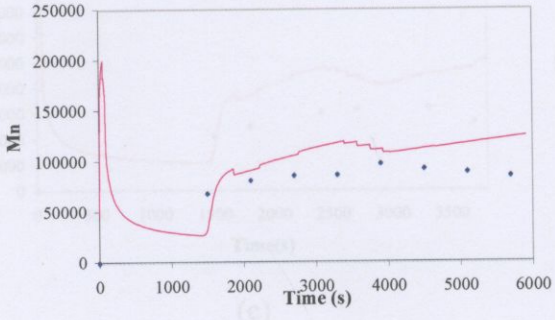

(c)

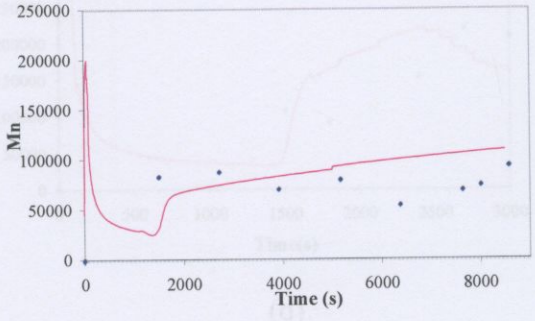

(d)

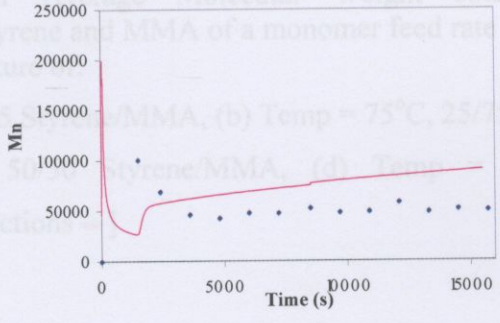

(e)

Figure 3.22 Number Average Molecular Weight (M_n) obtained in emulsion copolymerisation of styrene and MMA (50/50) mixture at 75°C for monomer feed rates of: (a) Batch (0 g/s), (b) 0.064 g/s, (c) 0.032 g/s, (d) 0.016 g/s, (e) 0.008 g/s [Experimental ♦, Predictions –]

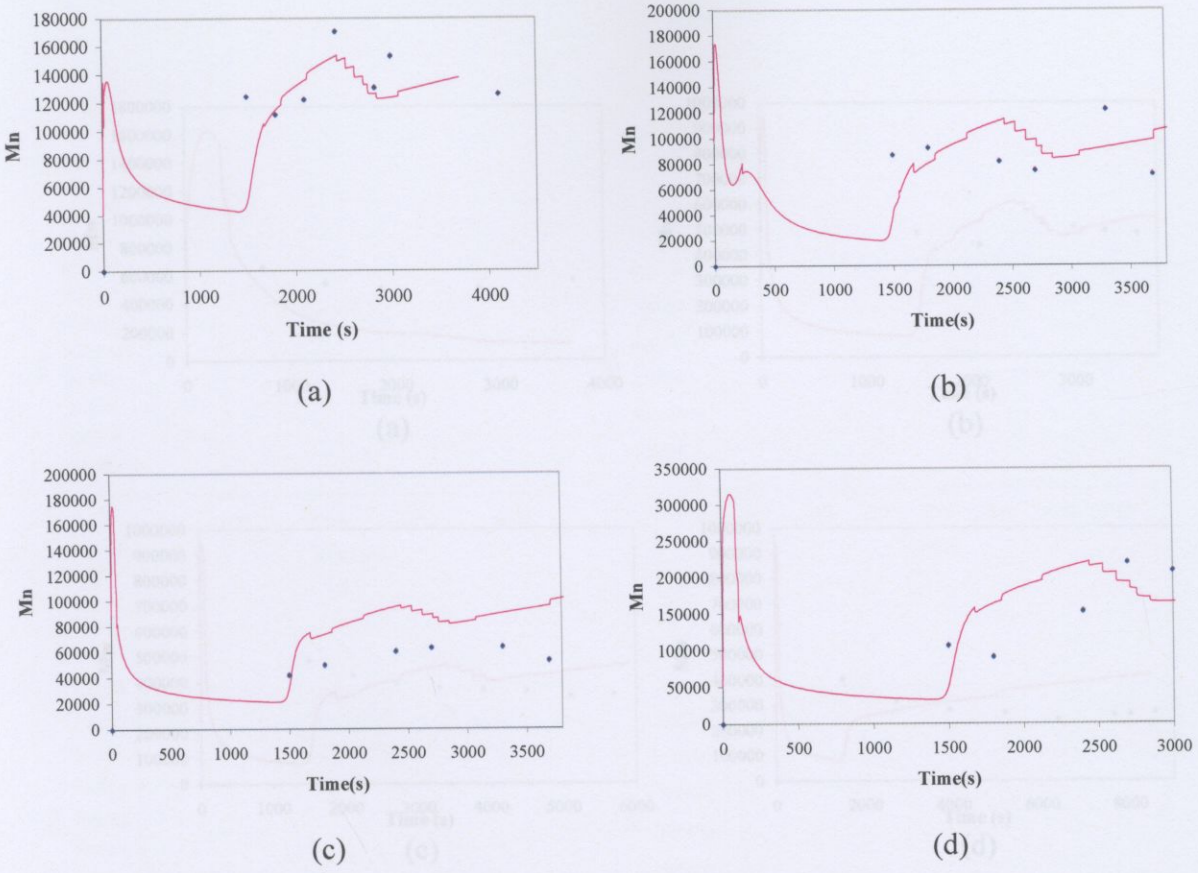

Figure 3.23 Number Average Molecular Weight obtained (M_n) in emulsion copolymerisation of styrene and MMA of a monomer feed rate of 0.064 g/s for a monomer feed ratio and temperature of:

(a) Temp = 75°C, 75/25 Styrene/MMA, (b) Temp = 75°C, 25/75 Styrene/MMA,

(c) Temp = 82°C, 50/50 Styrene/MMA, (d) Temp = 70, 50/50 Styrene/MMA

[Experimental ♦, Predictions —]

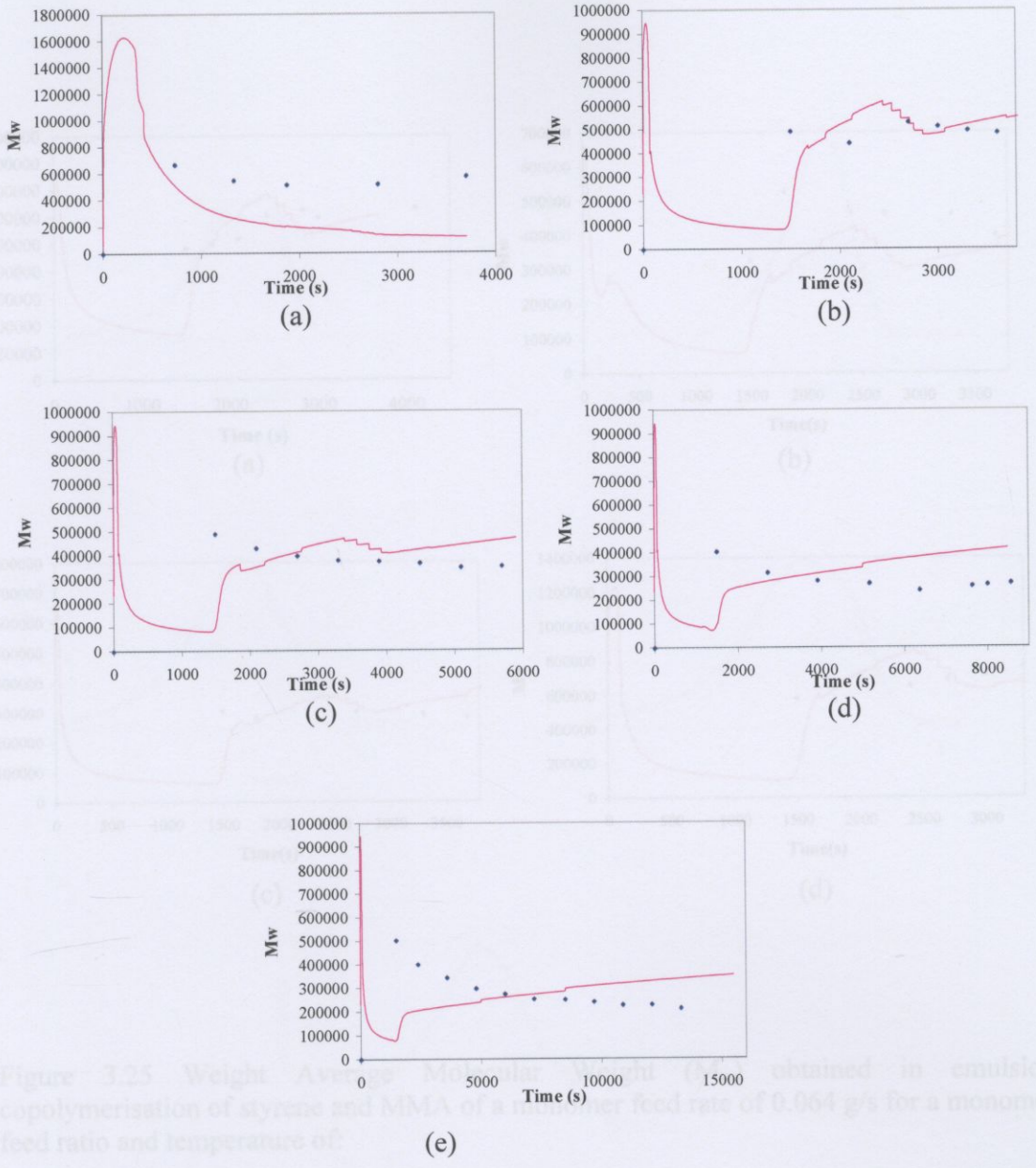

Figure 3.24 Weight Average Molecular Weight (M_w) obtained in emulsion copolymerisation of styrene and MMA (50/50) mixture at 75°C for monomer feed rates of: (a) Batch (0 g/s), (b) 0.064 g/s, (c) 0.032 g/s, (d) 0.016 g/s, (e) 0.008 g/s [Experimental ♦, Predictions –]

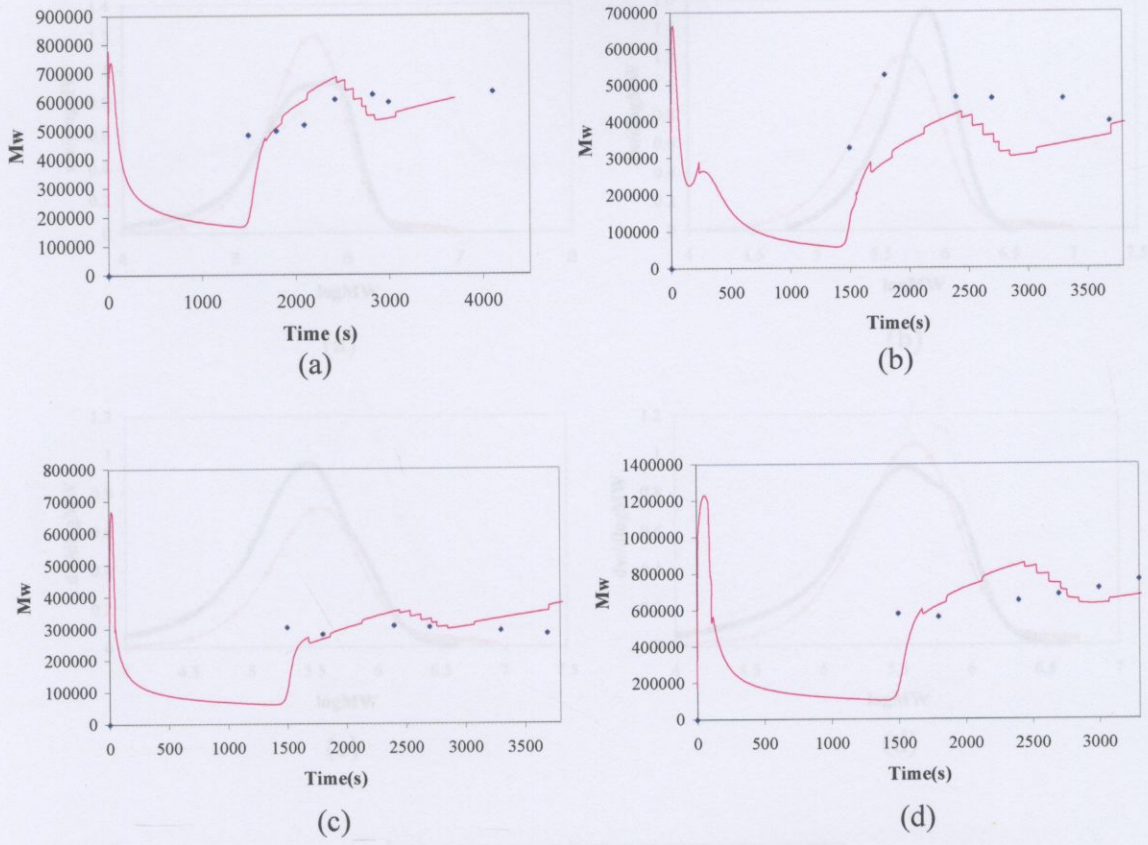

Figure 3.25 Weight Average Molecular Weight (M_w) obtained in emulsion copolymerisation of styrene and MMA of a monomer feed rate of 0.064 g/s for a monomer feed ratio and temperature of:

(a) Temp = 75°C, 75/25 Styrene/MMA, (b) Temp = 75°C, 25/75 Styrene/MMA,

(c) Temp = 82°C, 50/50 Styrene/MMA, (d) Temp = 70, 50/50 Styrene/MMA

[Experimental ♦, Predictions —]

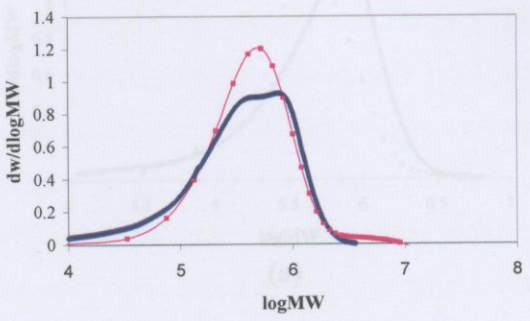

(a)

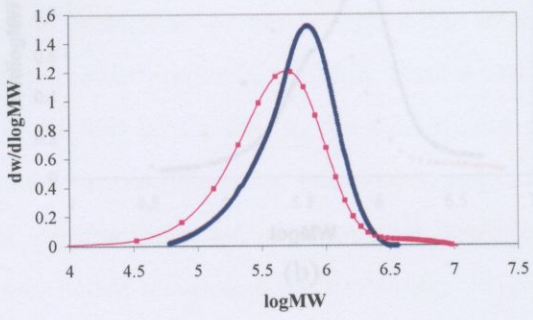

(b)

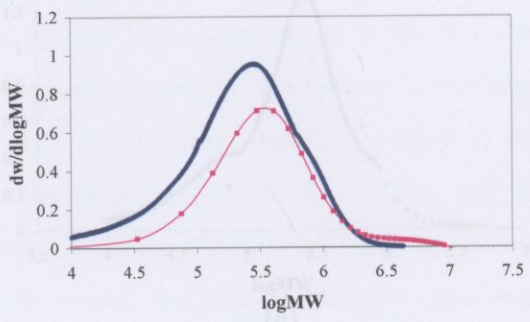

(c)

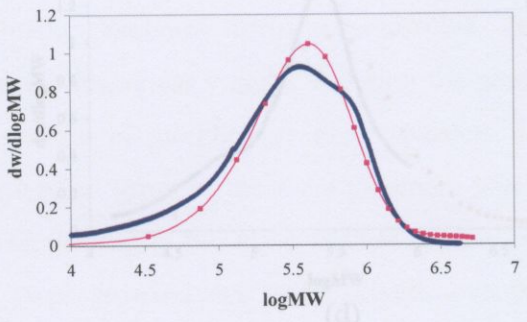

(d)

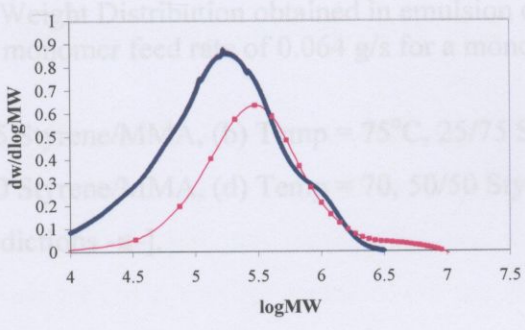

(e)

Figure 3.26 Molecular Weight Distribution obtained in emulsion copolymerisation of styrene and MMA (50/50) mixture at 75°C for monomer feed rates of: (a) Batch (0 g/s), (b) 0.064 g/s, (c) 0.032 g/s, (d) 0.016 g/s, (e) 0.008 g/s [Experimental -♦-, Predictions -■-].

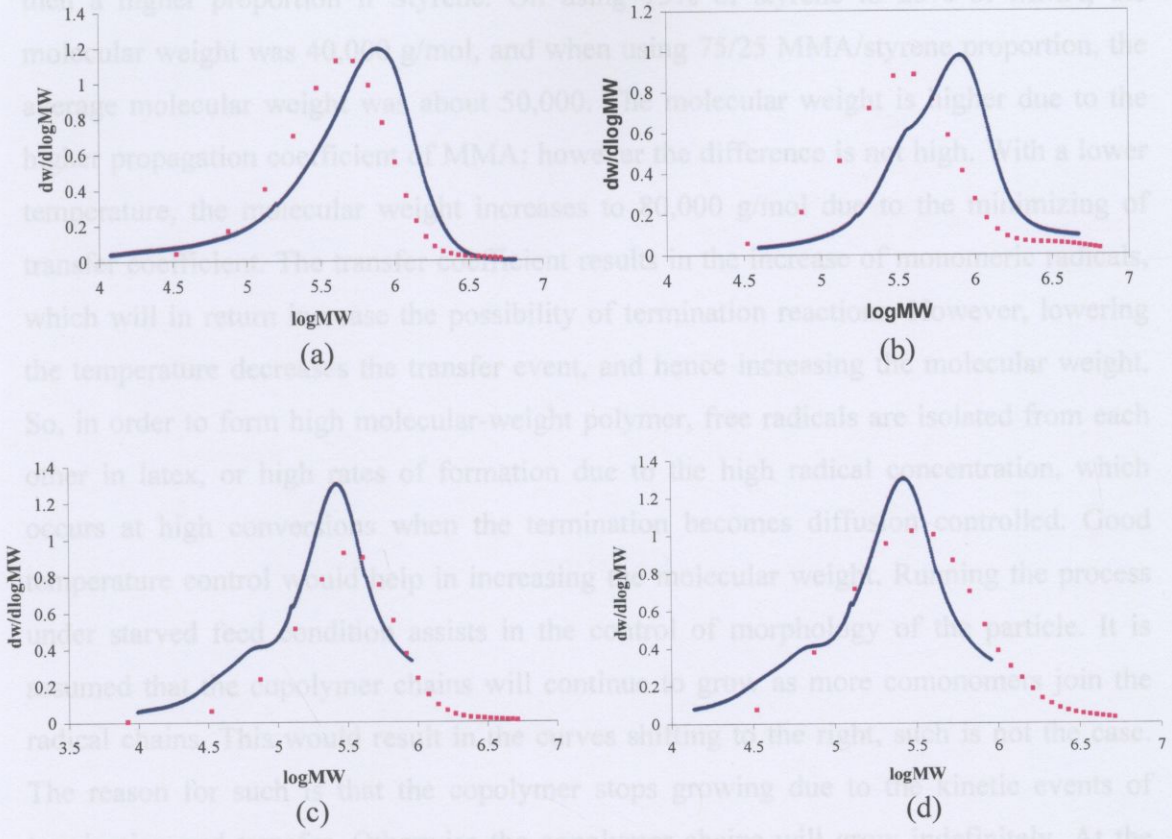

Figure 3.27 Molecular Weight Distribution obtained in emulsion copolymerisation of styrene and MMA of a monomer feed rate of 0.064 g/s for a monomer feed ratio and temperature of:

(a) Temp = 75°C, 75/25 Styrene/MMA, (b) Temp = 75°C, 25/75 Styrene/MMA,

(c) Temp = 82°C, 50/50 Styrene/MMA, (d) Temp = 70, 50/50 Styrene/MMA

[Experimental -♦-, Predictions -■-].

The kinetic events are all functions of Arrhenius equation. As the temperature increases, the kinetic events would increases, but more effectively is the transfer and termination kinetic events. The transfer and termination kinetic events or the chain brokage events act on stopping the increase in the molecular weight or in decreasing the molecular weight. In other words, the chain length decreases due to the transfer kinetic event. Moreover, the entry of radicals to the particles would result in instantaneous termination, and hence reducing the molecular weight. The chain growth event results from the effect of the

propagation coefficient. This clearly had appeared using a higher proportion of MMA, and then a higher proportion if Styrene. On using 75% of styrene to 25% of MMA, the molecular weight was 40,000 g/mol, and when using 75/25 MMA/styrene proportion, the average molecular weight was about 50,000. The molecular weight is higher due to the higher propagation coefficient of MMA; however the difference is not high. With a lower temperature, the molecular weight increases to 80,000 g/mol due to the minimizing of transfer coefficient. The transfer coefficient results in the increase of monomeric radicals, which will in return increase the possibility of termination reactions. However, lowering the temperature decreases the transfer event, and hence increasing the molecular weight. So, in order to form high molecular-weight polymer, free radicals are isolated from each other in latex, or high rates of formation due to the high radical concentration, which occurs at high conversions when the termination becomes diffusion controlled. Good temperature control would help in increasing the molecular weight. Running the process under starved feed condition assists in the control of morphology of the particle. It is assumed that the copolymer chains will continue to grow as more comonomers join the radical chains. This would result in the curves shifting to the right, such is not the case. The reason for such is that the copolymer stops growing due to the kinetic events of termination and transfer. Otherwise the copolymer chains will grow indefinitely. At the same time entry provides a source of radicals into the latex particles that increases the number of copolymer chains, accounting for the vertical shift in the graphs.

The number of radicals of a given polymer particle changes during polymerisation in a stochastic way as the latex particle gains free radicals by absorption or losses them by desorption and termination. If the polymer particle has one radical, a dead copolymer chain can only be formed by chain transfer reaction. On the other hand, if the polymer particle contains more than one radical, dead copolymer can be formed by both chain transfer reaction and bimolecular termination. Obviously, when the polymer particle contains no radicals, no copolymer is formed. Therefore, the length distribution of the copolymer chains depends on the number of radicals.

The results therefore add wealth of mechanistic information about the chain stoppage and chain growth events, which is the key to control the MWD of the desired copolymer.

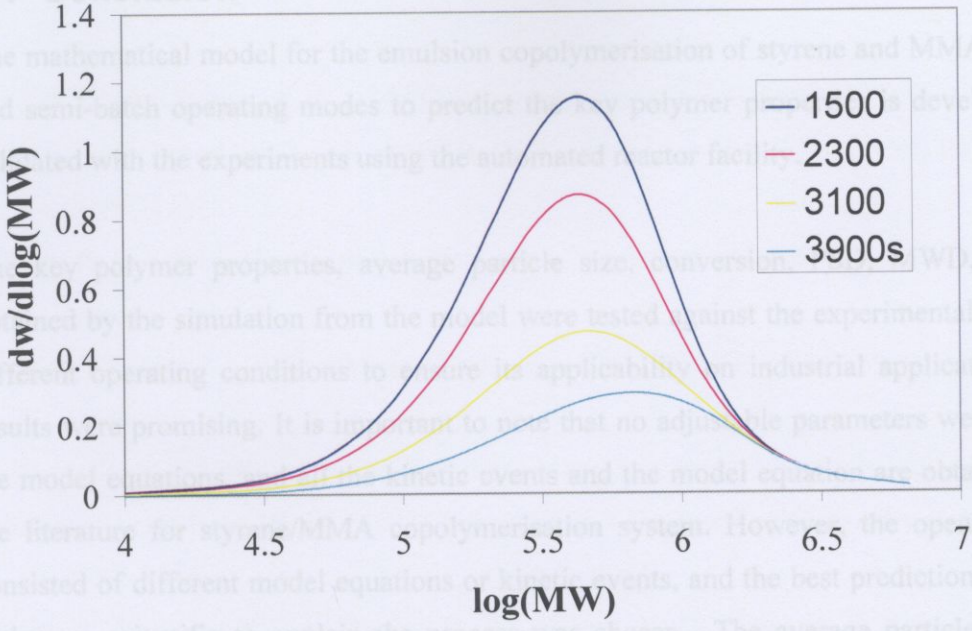

Figure 3.28. Predicted molecular weight distributions at 75°C.

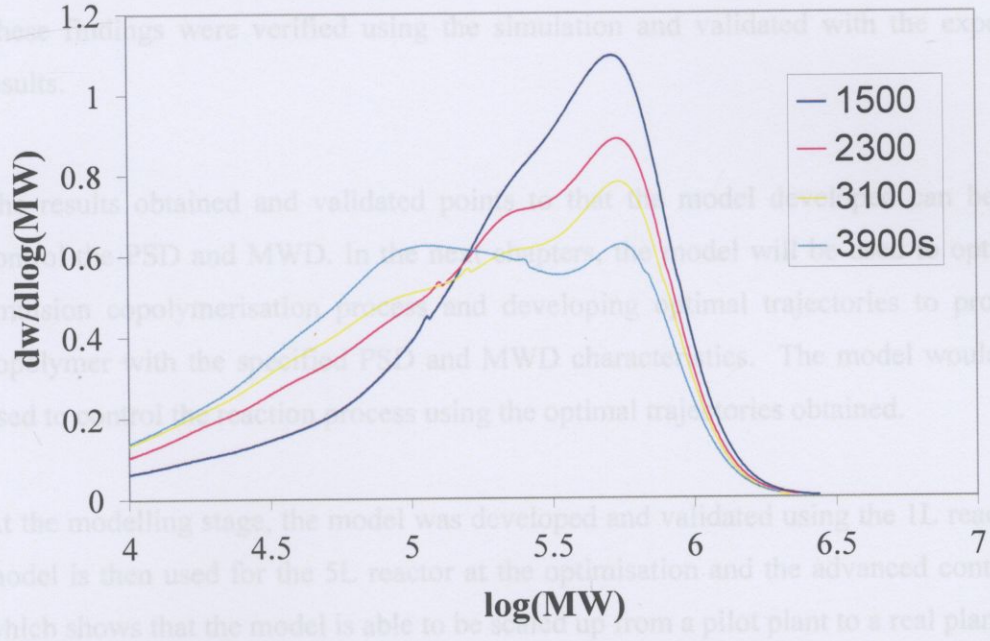

Figure 3.29. Experimental molecular weight distributions at 75°C.

3.4 Conclusion

The mathematical model for the emulsion copolymerisation of styrene and MMA in batch and semi-batch operating modes to predict the key polymer properties is developed and validated with the experiments using the automated reactor facility.

The key polymer properties, average particle size, conversion, PSD, MWD, M_n, M_w obtained by the simulation from the model were tested against the experimental results at different operating conditions to ensure its applicability on industrial applications. The results were promising. It is important to note that no adjustable parameters were used in the model equations, and all the kinetic events and the model equation are obtained from the literature for styrene/MMA copolymerisation system. However, the open literature consisted of different model equations or kinetic events, and the best prediction to results and more scientific to explain the process was chosen. The average particle size was found to increase with the increase in the monomer feed, and gave a larger particle size with the higher proportion of MMA, due to its higher propagation coefficient. The PSD followed a Gaussian distribution. On the other hand, the MWD was found to increase in the decrease of temperature, which affects the transfer rate and the termination kinetic events and lower entry rates. The monomer feed rates also had an influence in increasing the molecular weight, where a lower molecular weight was obtained for lower feed rates. These findings were verified using the simulation and validated with the experimental results.

The results obtained and validated points to that the model developed can be used to control the PSD and MWD. In the next chapters, the model will be used to optimise the emulsion copolymerisation process and developing optimal trajectories to produce the copolymer with the specified PSD and MWD characteristics. The model would then be used to control the reaction process using the optimal trajectories obtained.

At the modelling stage, the model was developed and validated using the 1L reactor. The model is then used for the 5L reactor at the optimisation and the advanced control stage, which shows that the model is able to be scaled up from a pilot plant to a real plant.

3.5 References

Clay, P. A. and Gilbert, R. G. (1995) Macromolecules, 28, 552-569.

Coen, E. M., Gilbert, R. G., Morrison, B. R., Leube, H. and Peach, S. (1998) Polymer, 39, 7099-7112.

Gilbert, R. G. (1995) Emulsion Polymerization: A mechanistic approach, Academic Press, London.

Nomura, M., Horie, I., Kubo, M. and Fujita, K. (1983) In AIChE Spring National Meeting, Houston.

Nomura, M., Kubo, M. and Fujita, K. (1981) Mem. Fac. Eng. Fukui Univ., 29, 167-174.

Saldívar, E. and Ray, W. H. (1997) Industrial and Engineering Chemistry Research, 36, 1322-1336.

Zeaiter, J., Romagnoli, J. A., Barton, G. W., Gomes, V. G., Hawkett, B. S. and Gilbert, R. G. (2002) In Chemical Engineering Science, Vol. 57 Elsevier Science Ltd, pp. 2955-2969.

Chapter 4

Process Optimisation

4.1 INTRODUCTION 4.2
4.2 OPTIMISATION: INTRODUCTION 4.3
4.2.1 Formulation of Optimization Problems 4.4
4.2.2 Topics in Optimization 4.5
4.2.3 Method of Attack 4.8
4.2.4 Dynamic Optimisation in gPROMS 4.9
4.2.4.1 The objective function 4.10
4.2.4.2 Bounds on the optimisation decision variables 4.10
4.2.4.3 Other constraint types 4.11
4.2.4.4 Classes of control variable profile 4.12
4.2.4.5 Optimisation report file 4.13
4.3 OPTIMISATION OF THE EMULSION COPOLYMERISATION PROCESS 4.14
4.3.1 Strategy Development 4.15
4.3.2 Experimental Validation of the Optimal Control Strategy 4.21
4.4 CONCLUSION 4.27
4.5 REFERENCES 4.28

4.1 Introduction

Desire for **optimality** (perfection) is inherent for humans. The search for extremes inspires mountaineers, scientists, mathematicians, and the rest of the human race. A beautiful and practical mathematical theory of optimisation (i.e. search-for-optimum strategies) is developed since the sixties when computers become available. Every new generation of computers allows for attacking new types of problems and calls for new methods. The goal of the theory is the creation of reliable methods to catch the extremum of a function by an intelligent arrangement of its evaluations (measurements). This theory is vitally important for modern engineering and planning that incorporate optimisation at every step of the complicated decision making process.

The model is able to predict adequately the key polymer properties, including PSD and MWD under different operating conditions. This is necessary for the model in order to be capable of optimising the emulsion copolymerisation process on maximising PSD and the M_n. The model is also efficient regarding the computation capabilities. This is also important, so that the model would be able to be used to optimise the process online, rather than offline. However, the optimal trajectories are obtained offline, and then used to run the process online on the optimised conditions.

Quality control of polymer latexes is becoming increasingly attractive as the production of more and more products involves emulsion copolymerisation processes. Advanced process optimisation techniques is a must need for the copolymerisation process. Process systems engineers through optimisation can meet these requirements (Quality and Profit) and achieve significant productivity and quality improvements to the reaction process. The model was used to optimise the emulsion copolymerisation process in order to maximize particle size polydispersity index (PSPI) and number average molecular weight (M_n). Five variables were used as manipulated variables, styrene monomer feed rate, MMA monomer feed rate, surfactant feed rate, initiator feed rate, and the temperature of the reaction by controlling the jacket temperature. The results from optimisation were validated against experimental and found to show good agreement. The optimisation strategy has been developed within a gOPT dynamic optimisation code. The optimal profiles are entered to the system by using a set point profile block in the Control Builder software.

In this chapter, the theory of process optimisation is explained and the techniques of the dynamic optimisation in gPROMS are discussed. Then the formulation of the optimisation problem is presented. The results of off-line optimisation in application to the emulsion copolymerisation process of styrene and MMA are investigated for the PSD and MWD control. The validation of the results are then shown, and finally the concluding remarks of the optimisation problem.

4.2 Optimisation: Introduction

The objective of optimization is to select the best possible decision for a given set of circumstances without having to enumerate all of the possibilities. From experience, designers learn to recognize good proportions and critical restrictions so their preliminary work will not require significant modification and improvement. The subject which formulates and explains this talent is a branch of applied mathematics known as optimization theory, a science that studies the best (Wilde, 1978). In recent years the subject of optimization has matured and is widely used in numerous applications, e.g., petroleum refining operations, routes for commercial aircraft, livestock feed blending and missile trajectories. Optimization methods take advantage of the mathematical structure of the problem to find the best values efficiently; and the size of the problems being solved has followed the growth in computer capability, especially in the case of linear programming.

The development of mathematical theory for optimization followed closely with the development of calculus, as pointed out by (Hancock and Harris, 1960).In fact, Hancock wrote the first modern book on the subject, entitled Theory of Maxima and Minima, which was published in 1917. This definitive work serves even today as an authoritative source.

There was a boost in First World War, where linear programming has moved from an interesting mathematical topic to probably the most important and widely applied optimization procedure. Its development followed closely the continually increasing capabilities of the digital computer. The ability to solve large sets of linear equations with the computer has permitted the application of linear programming to industrial problems, such as the optimization of a large petroleum refinery.

Another boost after the Second World War was that the optimal trajectory for a missile, which was one of a number of problems for which the methods of dynamic programming and the maximum principle were developed in this country and the U.S.S.R. These methods are now being used in areas that are not space-related.

4.2.1 Formulation of Optimization Problems

Three basic components are required to optimize an industrial process. First, the process or a mathematical model of the process must be available, and the process variables which can be manipulated and controlled must be known. Often, obtaining a satisfactory process model with known control variables is the most difficult task. Secondly, an economic model of the process is required. This is an equation that represents the profit made from the sale of products and costs associated with their production, such as raw materials, operating costs, fixed costs, taxes, etc. Finally, an optimization procedure must be selected which locates the values of the independent variables of the process to produce the maximum profit or minimum cost as measured by the economic model. Also, the constraints in materials, process equipment, manpower, etc. must be satisfied as specified in the process model.

Plant optimization finds the best operating conditions for a plant made up of process units manufacturing specified amounts of various products to maximize the company's profits within the constraints set by the available raw materials and how these raw materials can be transformed in the plant. Plant optimization usually approximates the individual process units in a relatively simple manner to obtain a satisfactory answer in a reasonable time. This requires that the optimal operating conditions of the individual process unit be known, and these results be used in the plant optimization to have the plant operating with the maximum profit. Also, due to the complexity of large industrial plants, individual process models are usually simplified by using simulation equations to keep the computer programming efforts and computer costs within reason. However, with individual process units, it is feasible to use more detailed models to determine more precisely the optimal operating conditions, e.g., temperatures, pressures, recycle rates, etc. to have minimum operating cost known as a function of these variables.

Simulation equations are obtained from process models. The procedure is to develop precise process models based on the fundamentals of mass and heat transfer, thermodynamics, kinetics and transport phenomena. This usually leads to process models which accurately represent the physical and chemical changes taking place over a wide range of conditions. However, these models usually are more complicated in mathematical form and may require the solution of differential equations. Consequently, these process models are usually exercised over the range of operation of the process, and simulation (regression) equations of a simplified mathematical form are developed, which are then used with the optimization method for the plant optimization. However, it may not be necessary to go through the simulation equations step if the equations that describe the key variables, i.e., the ones that affect the economic performance of the process or plant, are not complicated.

4.2.2 Topics in Optimization

The two areas of optimization theory are mathematical programming and variational methods, as shown in Table 4.1. Also, a number of techniques are listed under each of these areas. In mathematical programming, the objective is to locate a best point x $(x_1,x_2,...x_n)$ which optimizes (maximizes or minimizes) the economic model of the process. In variational methods, the objective is to locate the optimal function which maximizes or minimizes the economic model. Generally, mathematical programming methods are applicable to steady-state problems, and variational methods are applicable for dynamic problems.

Mathematical programming methods are of two types and are referred to as direct or indirect methods. Direct methods, such as multivariable search methods and linear programming, move from a starting point through consistently improved values of the economic model to arrive at the optimum. Indirect methods, such as analytical methods and geometric programming, solve a set of algebraic equations, and the solution to the set of equations may be the optimum of the economic model. For example, in analytical methods the algebraic equation set is obtained by differentiating the economic model with respect to each independent variable and setting the resulting equations equal to zero. The mathematical programming methods are listed in Table 4.1. These methods selected are the more widely used in industrial practice.

Optimisation	
Mathematical Programming	**Variational Methods**
Objective: Fine the best point that optimizes the economic model. Example: Optimum operating conditions for a petroleum refinery.	Objective: Find the best function that optimizes the economic model. Example: Best temperature profile that maximizes the conversion in a tubular chemical reactor.
Mathematical Formula:	**Mathematical Formulation:**
Optimize: y(x) Subject to: f i(x) > 0 i = 1,2,...m where x = (x1,x2...xn)	Optimize: I [y(x)] = IF[y(x),y'(x)]dx Subject to: Algebraic, integral or differential equation constraints.
Methods	**Methods**
Analytical Methods Geometric Programming Linear Programming Quadratic Programming Convex Programming Dynamic Programming (Discrete) Nonlinear Programming or Multivariable Search Methods Integer Programming Separable Programming Goal Programming or Multicriterion Optimization Combinatorial Programming Maximum Principle (Discrete) Heuristic Programming	Calculus of Variations Dynamic Programming(Continuous) Maximum Principle (Continuous)

Table 4.1 Areas and Topics in Optimisation

Linear programming requires that both the economic model and the set of constraint equations be linear, and the Simplex Method is the algorithm which locates the optimum by beginning at a feasible starting point (initially feasible basis). In quadratic programming, the model is a quadratic equation and the constraint equations are linear. Using analytical methods, this problem can be converted to a linear programming problem and solved by the Simplex Method. For convex programming, the economic model is a concave function, and the constraint equations are convex functions. Dynamic programming uses a series of partial optimizations by taking advantage of the stage structure in the problem and is effective for resource allocation and optimization through time. Nonlinear programming or multivariable search methods, as the theory and algorithms are called must begin at a feasible starting point and move toward the optimum in steps of improved values of the model. Integer programming is an extension of linear programming where the variables must take on discrete values. Separable programming is an extension of linear programming where a small number of nonlinear constraints are approximated by piecewise linear functions. Goal programming is an extension of linear programming also where multiple, conflicting objectives (or goals) are optimized using weights or rankings. Combinatorial programming has been described by Popadimitriou and Steiglitz (Papadimitriou and Steiglitz, 1982) as a body of mathematical programming knowledge including linear and integer programming, graph and network flows, dynamic programming and related topics. The maximum principle is comparable to dynamic programming in using the stage structure of the system, but it uses constrained derivatives that require piecewise continuously differentiable functions and successive approximations (Wilde and Beightler, 1967). Finally, the term heuristic programming has been used to describe rules-of-thumb that can be used for approximations to optimization.

In discussing the various topics in optimization, the economic model has been given several different names. These names arose in the literature as the optimization procedures were being developed. Regardless of the name, the economic model is the equation which expresses the economic return from the process for specified values of the control (manipulative, decision or independent) variables. The two most common names are the profit function or cost function. However, in linear programming the term objective function is used, and in dynamic programming the term return function is employed. Other synonymous names are: benefit function, criterion, measure of effectiveness and response surface.

4.2.3 Method of Attack

In solving an optimization problem, the structure and complexity of the equations for the economic model and process or plant constraints are very important, since most mathematical programming procedures take advantage of the mathematical form of these models. Examples are linear programming, where all of the equations must be linear, and geometric programming, where all of the equations must be polynomials. Consequently, it is extremely important to have the capabilities of the various optimization techniques in mind when the economic and process models are being formulated. For example, if a satisfactory representation of the economics and process performance can be obtained using all linear equations, the powerful techniques of linear programming can be applied, and this method guarantees that a global optimum is found. However, if one has to resort to nonlinear equations to represent the economics and process performance, it may be necessary to use a multivariable search method to locate the optimum. Unfortunately, these search techniques only find points that are better than the starting point, and they do not carry any guarantee that a global or a local maximum or minimum has been found.

It is necessary to determine if the problem requires an optimal point or function. If it is a point, mathematical programming is applicable; and if an optimal function, variational methods are applicable. If the equation for the economic model is relatively simple and there are no applicable constraints (process model), it is possible to locate the optimum by differentiating the economic model with respect to the independent variables, setting these equations equal to zero, and solving for the optimum. However, if there are constraints, and there usually are, but the equations are relatively simple, the method of Lagrange multipliers may be used. This converts the constrained problem to an unconstrained problem, and the previous procedure for unconstrained problems is used.

Now, if the problem has a large number of independent variables and the precision needed for the economic and process models can be obtained with linear equations, then linear programming may be used. However, if nonlinear equations are required and polynomial will suffice, it may be possible to determine the optimum rapidly and easily using geometric programming (Wilde, 1978).

Not having been successful to this point, it may be feasible to take advantage of the stage structure of the problem and apply dynamic programming with a series of partial

optimizations. However, if this is not successful it will be necessary to resort to multivariable search techniques and seek best values without having a guarantee of finding the global optimum.

4.2.4 Dynamic Optimisation in gPROMS

Dynamic optimisation is the process of optimising some aspects of process design and performance taking into account both steady-state and dynamic considerations. In contrast to steady-state optimisation, dynamic optimisation allows operability considerations to be taken into account at the design stage. Applicable to continuous, batch and semi-batch processes, it is the only meaningful way to optimise the latter two. Dynamic optimisation, in contrast with simulation, allows in formulating the problem to solve directly, and then use the start-of-the-art numerical and optimisation solvers within gPROMS to determine the optimal values or time profiles of the optimisation variables.

The processes of mixed differential and algebraic equations are described in gPROMS in the form of:

$$f(x(t);\dot{x}(t),y(t),u(t),v)=0 \qquad \text{(Eq. 4.1)}$$

Here *x(t)* and *y(t)* are the differential and algebraic variables in the model while $\dot{x}(t)$ are the time derivatives of the *x(t)* (i.e., $\dot{x}(t)=dx/dt$). *u(t)* are the control variables and v is the time invariant parameters to be determined by the optimisation

For initial conditions, gPROMS assumes that the initial ($t = 0$) condition of the system is described in terms of a set of general non-linear relations of the form:

$$I(x(0),\dot{x}(0),y(0),u(0),v)=0 \qquad \text{(Eq. 4.2)}$$

It is important to note that, once time variation of the controls is fixed, *u(t)* and the values of any time invariant parameters, *v*, the modelling equations together with the initial conditions completely determine the transient response of the system. In practice, one could determine this response by performing a gPROMS dynamic simulation.

4.2.4.1 The objective function

Dynamic optimisation in gPROMS seeks to determine

- the time horizon, t_f,
- the values of the time invariant parameters, v, and
- the time variation of the control variables, $u(t)$, over the entire time horizon $t \in [0, t_f]$, so as to minimise (or maximise) the final value of a single variable z.

This can be written mathematically as:

$$\min_{t_f, v, u(t), t \in [0, t_f]} z(t_f) \qquad \text{(Eq. 4.3)}$$

Here the objective function variable, z is one of either the differential variables x or the algebraic variables y. Maximisation can be carried out as well as minimisation. If it is required to optimise a function of several variables instead of a single variable, one simply adds an extra algebraic equation to the model. The additional computational cost incurred because of this model extension is usually negligible.

4.2.4.2 Bounds on the optimisation decision variables

In practice, the time horizon t_f will often be subject to certain lower and upper bounds:

$$t_f^{\min} \le t_f \le t_f^{\max} \qquad \text{(Eq. 4.4)}$$

In some cases, t_f will be fixed at a given value, t_f^*. This can be achieved simply by setting

$$t_f^{\min} = t_f = t_f^{\max} \qquad \text{(Eq. 4.5)}$$

The control variables and time invariant parameters will also be subject to lower and upper bounds:

$$u^{\min} \le u(t) \le u^{\max}, \forall t \in [0, t_f] \qquad \text{(Eq. 4.6)}$$

$$v^{\min} \le v \le v^{\max} \qquad \text{(Eq. 4.7)}$$

4.2.4.3 Other constraint types

4.2.4.3.1 End-point constraints

In some applications, it is necessary to impose certain conditions that the system must satisfy at the end of the operation. These are called end-point constraints. For instance, in the emulsion copolymerisation reactor, one may require:

- the final amount of material in the reactor to be at certain prescribed value;
- the final property, say molecular weight should to lie within given limits.

In the first case, it is an equality end-point constraint of the type:

$$w(t_f) = w^* \qquad \text{(Eq. 4.8)}$$

where w is one of the system variables (x *or* y). In the second case, it is an inequality end-point constraint:

$$w^{\min} \le w(t_f) \le w^{\max} \qquad \text{(Eq. 4.9)}$$

4.2.4.3.2 Interior point constraints

There are also other constraints that hold at one or more distinct times t_I during the time horizon (e.g. at the middle of the horizon). These are called interior-point constraints. These may be represented mathematically as:

$$w_I^{\min} \le w(t) \le w_I^{\max} \qquad \text{(Eq. 4.10)}$$

where w is a system variable, and t_I is a given time.

Both interior and end-point constraints are special cases of point constraints. However, gPROMS treats them separately. It also treats any constraints that have to be satisfied at the initial time t = 0 as interior-point constraints.

4.2.4.3.3 Path constraints

There are also certain constraints that must be satisfied at all times during the system operation. If these path constraints are equalities, then often they can simply be added to the system model effectively converting one of the control variables *u(t)* into an algebraic variable *y*. More often, they are inequalities of the form:

$$w^{\min} \le w(t) \le w^{\max}, \forall t \in [0, t_f] \qquad \text{(Eq. 4.11)}$$

For instance, in the emulsion copolymerization reactor, one would require that the temperature never exceeds a certain value so as to avoid some unwanted side-reactions that are not explicitly considered by the mathematical model.

4.2.4.4 Classes of control variable profile

For the dynamic optimisation problem to be well defined, it is required to be more specific regarding the type of the variation of the control variables over time that will be considered. The control variable profiles are shown in Figure 4.1.

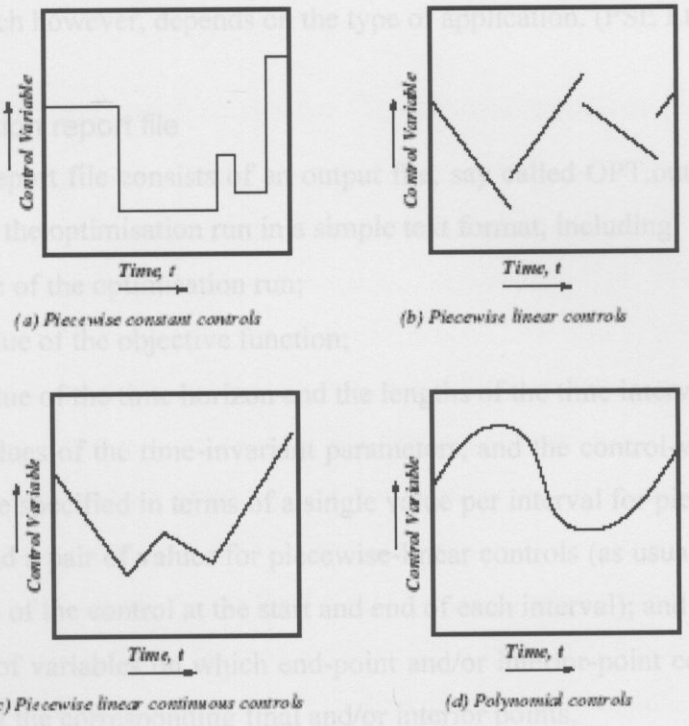

Figure 4.1: Profiles of typical classes of control variable (PSE, 2000a).

- Piecewise-constant controls; these remain constant at a certain value over a certain part of the time horizon before jumping discretely to a different value over the next interval (see Figure 2.2(a)).
- Piecewise-linear controls; these take a certain linear time variation over a certain part of the time horizon before jumping discretely to a different linear variation over the next interval (see Figure 2.2(b)).
- Piecewise-linear continuous controls; these are similar to the piecewise-linear controls described above, with the additional requirement that their values be continuous at the interval boundaries (see Figure 2.2(c)).
- Controls that vary smoothly over time; perhaps as polynomials of a given degree (see Figure 2.2(d)).

It is important to appreciate that, in most cases; the choice of the form of the control variables is engineering rather than a mathematical issue: it very much depends on the capabilities of the actual control system that we will eventually use to implement these controls on the real plant. For instance, piecewise constant controls may often be preferable to other types as they are much easier to implement, and still they perform the job efficiently, which however, depends on the type of application. (PSE Ltd., 2000a).

4.2.4.5 Optimisation report file

The optimisation report file consists of an output file, say called OPT.out file, contains a summary report on the optimisation run in a simple text format, including:

- the outcome of the optimisation run;
- the final value of the objective function;
- the final value of the time horizon and the lengths of the time intervals;
- the final values of the time-invariant parameters, and the control-variable profiles; the latter are specified in terms of a single value per interval for piecewise-constant controls, and a pair of values for piecewise-linear controls (as usual, corresponding to the value of the control at the start and end of each interval); and
- the values of variables on which end-point and/or interior-point constraints where specified, at the corresponding final and/or interior points.

The file also contains computational statistics on the performance of the numerical method. The optimization report also consists of the schedule file, say called OPT.SCHEDULE, which shows the most recent optimisation solution point in the form of a gPROMS SCHEDULE. The SCHEDULE file can be used to reproduce the detailed results of the optimisation by carrying out a simulation activity within gPROMS. This provides the access to the full facilities of the gPROMS Results Management System (gRMS). This also helps to confirm having a feasible solution to the problem.

However, the contents of the SCHEDULE file do not necessarily represent an optimal or even a feasible solution to the problem: if the optimisation run is interrupted by the user, or ends without finding a satisfactory solution, the file will simply show the point last considered by gPROMS. Only if a comment at the top of the file states the following, should the results be relied upon as a (locally) optimal solution:

Final Optimisation Status : Optimal Solution Found

A file is also saved in the optimization report called the *gOPT* file. This file is similar to the schedule file, where it contains the same information.

4.3 Optimisation of the Emulsion Copolymerisation Process

There is relatively little literature on the control of the full PSD, and it is even littler for the copolymerisation process. In contrast, there are a considerable number of studies reported in the literature on the control of lumped properties. (Semino and Ray, 1995b, Semino and Ray, 1995a) addressed the very pertinent issue of the controllability of population balance systems. They found in their system the controllability of the distributions for the unconstrained case is ensured by employing the feed concentration of surfactant, initiator and inhibitor as manipulated variables. (Kozub and Macgregor, 1992) applied the idea of a two-tier control strategy-open loop feed forward generation of an optimal recipe, which is then recomputed online based on feedback from process measurements to a semibatch emulsion polymerisation system , for the multivariable control of composition and average molecular weight. (Saldivar and Ray, 1997) studied the control of copolymer composition and averaged molecular weight for semi-continuous emulsion polymerisation. (Clarke-Pringle and MacGregor, 1998) presented a batch to batch adjustment strategy for the

control of molecular weight distribution (MWD) to re-optimise the inputs for the next batch based on end-point measurement of the MWD. (Crowley et al., 2001) used a hybrid modelling strategy in batch to batch optimisation for PSD control. (Crowley et al., 2000) are among the first researchers to address the control of the full particle size distribution. (Immanuel and Doyle, 2002) presented an open loop optimisation study for the control of the full PSD in the emulsion copolymerisation of vinyl acetate and butyl acrylate. (Zeaiter et al., 2002) developed a model for emulsion polymerisation of styrene to optimise and control the PSD.

The comprehensive dynamic model (validated and shown in Chapter 3) for the copolymerisation reactor developed by (Alhamad et al., 2003, Alhamad et al., 2004), allows the prediction of key polymer properties such as: average particle size, conversion, PSD, MWD, M_n, and M_w. A modified zero-one kinetic model is used in the formulation allowing prediction of secondary nucleation. In this work, based on this comprehensive model, a multi-layer model-based framework was developed and implemented within an industrial distributed control system environment, to optimise the PSPI and M_n.

The off-line approach to optimise the full PSD and M_n is reported. Later in this thesis, this off-line optimal trajectory will be used as a set point within an on-line multivariable model predictive control scheme to control the PSD and MWD.

4.3.1 Strategy Development

Emulsion Copolymerisation has three different phases, the particle, monomer and the water phase. All of the phases and the kinetic events should be taken into consideration. These phases results in the co-presence of a continuous phase and a dispersed phase. The first, most abundant phase is the aqueous or continuous phase. This phase initially contains the initiator, surfactant micelles and a small amount of the slightly soluble monomer and is present in all intervals of the reaction. The second phase consists of the emulsion/monomer droplets that are concentrated with the slightly insoluble monomer. It is from here that the reaction is fed with the required measure of monomer to facilitate propagation. The monomers droplets are present in intervals I and II only, after which the latex particles, which form the third phase, are found in high concentration. The latex

particles form early in the reaction and are present through the reaction in various sizes. They contain the formed polymer and some (Intervals I and II) or all (Interval III) of the unpolymerised monomer. The kinetic events from chain growth events including the propagation, and chain stoppage events including termination and transfer affect the PSD and MWD of the particles produced.

The number average molecular weight is affected by the propagation and transfer events. Those events are affected through the Arrhenius Equation, by the change in temperature. The propagation and transfer events are different for each monomer used, so the proportion of the monomer to the other would also affect the molecular weight. Moreover, the propagation is enhanced by the feed of the monomers. More radicals would cause more transfer in the process, and so the initiator feed would also affect M_n. The M_n changes also if surfactant is added, where micelle nucleation occurs, and the monomers are distributed into more particles, rather than been distributed into less particles and forming larger molecular weights. The monomer feed rate has a great effect in controlling the particle size and molecular weight, when running the process under starved conditions. The surfactant feed rate would increase the number of micelles. The initiator feed rate would increase the number of radicals. With these competing events, the process engineer should be able to maintain the copolymer properties. This demonstrates the importance of the mathematical model and its capability in optimising the process, and in controlling the pilot plant.

The PSD and MWD control would require knowing the measured process variables like temperature or conversion; however, these process variables that are usually used in the plant are not enough, and thus may result to fail in controlling the plant in real processes. Process engineers need to know all the process variables that are included in the control of PSD and MWD. Process engineers need to understand kinetic history of the process to know what to do, and to understand the process, and know how to develop it. Moreover, the plant is expected to face unprecedented disturbances in the operating conditions (e.g., temperature, pressure, flow rates, etc.) which directly may cause process disruptions and thus forming lower quality of products. In addition, the process engineer should know how each of the reactants (e.g. monomers, initiator, surfactant, etc.) incorporates in the shape of the copolymer.

The modelling of emulsion copolymerization must account for complex physico-chemical sub-processes involving particle formation mechanisms with two or more monomers under various reaction considerations, in a multi-phase environment, consisting of an aqueous phase, monomer droplets, surfactant, initiator and particulates.

Several objective functions were studied, in terms of both particle size and molecular weight. For the purpose of obtaining the desired broad PSD, a polydispersity index was chosen as an objective function to be maximized, where a bimodal distribution is expected. For molecular weight, maximising M_n was investigated as the objective function. The particle concentration densities, the particle diameter, reactor temperature and the temperature difference, copolymer composition, pump feed rates of the reactants, and the total amount of monomer to be added to the reactor were included as constraints.

The objective functions are optimised by using the five manipulated variables, styrene feed rate, MMA feed rate, surfactant feed rate, and initiator feed rate and temperature. The temperature was used as a manipulated variable for maximizing M_n, since the molecular weight is largely affected by the temperature, rather than the PSPI, which is not significantly affected by the temperature. The M_n was also maximized without the temperature as a manipulated variable investigating the actual effect of temperature.

The polymer particle size polydispersity index (PSPI), which is the ratio of the weight-average particle size to the number-average particle size, is directly related to the standard deviation of the polymer particle size distribution. Therefore, the polydispersity index can be used as a measure of the width of the particle size distribution.

$$PSPI = \frac{< r^2 >}{< r >^2} \qquad \text{(Eq. 4.12)}$$

The number average radius is defined as:

$$\langle r \rangle = \frac{\sum (r_{ms} \cdot n)}{\sum n} \qquad \text{(Eq. 4.13)}$$

The objective functions to be optimised were defined as: Max [PSPI(r, t_{final})] and Max[M_n(r, m, t_{final}] where: m is the molecular weight and t_{final} is the processing time. The monomers, surfactant, initiator feed rates and temperature (for molecular weight optimisation) were specified within the following upper and lower bounds due to operational reasons related to the power of the pumps used in the pilot plant.

$$0\ g/s \le F_{m,A} \le 0.2\ g/s \quad \text{(Eq. 4.14)}$$

$$0\ g/s \le F_{m,B} \le 0.2\ g/s \quad \text{(Eq. 4.15)}$$

$$0\ g/s \le F_S \le 0.2\ g/s \quad \text{(Eq. 4.16)}$$

$$0\ g/s \le F_I \le 0.2 g/s \quad \text{(Eq. 4.17)}$$

$$343\ ^oC \le T_{reac} \le 358\ ^oC \quad \text{(Eq. 4.18)}$$

The final PSD shape was included in the form of end point inequality constraints, which is formulated in terms of the final molar concentration density of particles.

$$n_{\min} \le n(r, t_{final}) \le n_{\max} \quad \text{(Eq. 4.19)}$$

where, n_{min} and n_{max} denote the lower and upper limits, respectively. The final copolymer composition required was 50/50, so a condition was specified as follows:

$$0.49 \le \overline{F} \le 0.51 \quad \text{(Eq. 4.20)}$$

The total amount of monomer in the recipe ($N_{m,T}$), and the total reaction time were added as end equality constraints, since a semibatch reaction is run, and there should be a limit for the monomers added to the reaction. These constraints are defined as follows:

$$N_{m,T} = 8 \text{ mol and } t_{\min} \le t \le t_{\max} \quad \text{(Eq. 4.21)}$$

The gOPT tool of gPROMS was used to perform the dynamic optimization calculations. The current implementation employs the corresponding routines from the general-purpose DAE solver DASOLV (Jarvis and Pantelides, 1992), although in principle any DAE solver that provides these three basic routines could be used. DASOLV pays particular attention

to problems that may become partially determined during solution and the integration of systems with very fast transients (Jarvis and Pantelides, 1991), but is currently restricted to equations of index not exceeding unity. The occurrence of an equation discontinuity leads to a request for a reinitialisation calculation and the return of control to the main simulation algorithm. However, initialisation and reinitialisation calculations are performed using the nonlinear algebraic equation solver SPARSE. This calculation, however, will not be performed until the consequences of any other simultaneous events have been implemented. All logical conditions relating to IF equations are checked at the beginning of each Newton step, and the current set of describing equations and the corresponding occurrence information are updated if necessary.

Five bounded time intervals were specified for the manipulated variables, $F_{m,A}$, $F_{m,B}$, F_S, F_I and T_{reac}, such that it remained constant over a certain time interval, before moving discretely to the value for the next interval. A violation over 0.1°C is put for the temperature, so that the temperature on a step change rises gradually. The time horizon is partitioned into five stages

A piecewise constant over equally spaced time intervals, 3910 seconds, is made for the inputs (Vassiliadis et al., 1994a). Given the initial conditions, the process equations are solved with a differential algebraic equation solver (DAES). This produces the value of the objective function, which the optimization routine then iteratively uses to find the optimal parameters in the control parameterization. The sequential method is of the *feasible path type,* that is, in every iteration, all process equations are feasible during the calculation of the objective value. This leads to a robust solution procedure if a first feasible solution is given first. The piecewise-constant control was set for the flow rates and temperature (manipulated variables), which means that it remains constant for the first period of time, and gets into another value to the second interval of time, and continues to the five intervals. The optimisation problem was run after 25 minutes of the pre-batch period, due to the reason that the first 25 minutes are meant for the seeds formation. The solution of the optimisation problem to maximise PSPI took over two days of operation, however for the molecular weight maximising, it took much less time of about 3 hours only. This relates to the sensitivity of each property to the changes in the inputs. Table 4.2 and Table 4.3 summarises the optimisation results of the particle size and molecular weight.

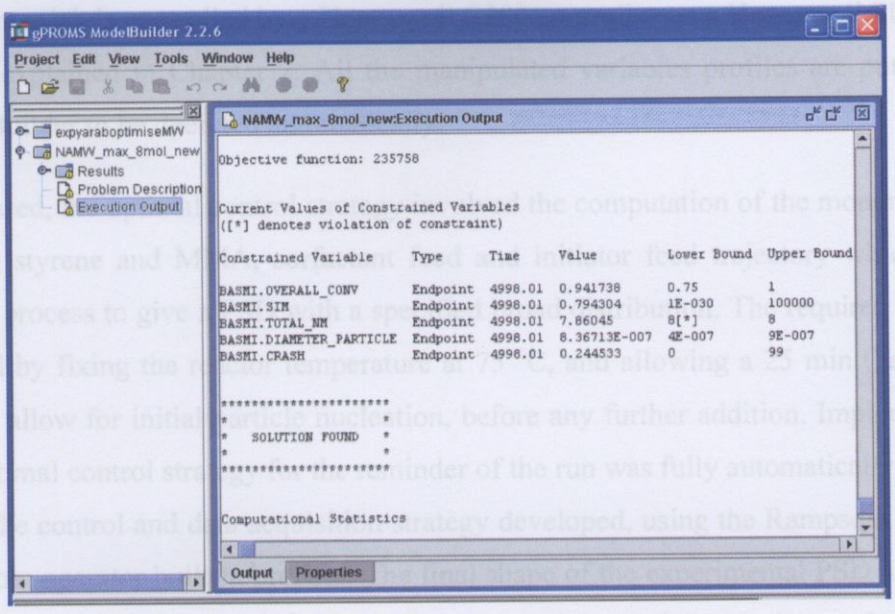

Table 4.2. Optimisation detailed results (Maximising M_n).

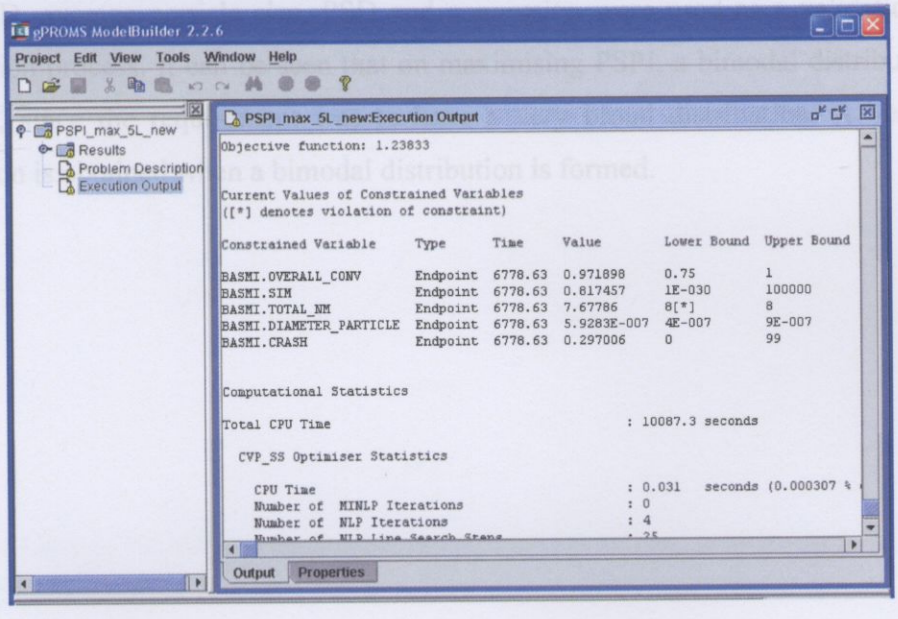

Table 4.3. Optimisation detailed results (Maximising PSPI).

4.3.2 Experimental Validation of the Optimal Control Strategy

The polymer lab is controlled by a Honeywell C200 controller on a Honeywell PlantScape DCS, as explained in Chapter 2. All the manipulated variables profiles are put into the Control Builder to be operated automatically.

As discussed, the optimal control strategy involved the computation of the monomers feed including styrene and MMA, surfactant feed and initiator feed trajectory which would drive the process to give a PSD with a specified broad distribution. The required PSD was generated by fixing the reactor temperature at 75 °C, and allowing a 25 min (batch) pre-period to allow for initial particle nucleation, before any further addition. Implementation of the optimal control strategy for the reminder of the run was fully automatically achieved through the control and data acquisition strategy developed, using the Rampsoak set-point option from operator built-in profiles. The final shape of the experimental PSD and MWD was in good agreement with the simulation results. Figure 4.2 shows the results obtained to maximise PSPI. Figure 4.3 shows the results obtained in order to maximize M_n using only the flow rates, that is, temperature was not used as a manipulated variable. Figure 4.4 displays the results to maximise M_n using the additional variable, which is the temperature. The MWD, average particle size, PSD and conversion were used as a validation to the optimisation process. It can be seen that on maximising PSPI, a bimodal distribution was produced, since the requirement was to have a very broad distribution. A very broad distribution is obtained when a bimodal distribution is formed.

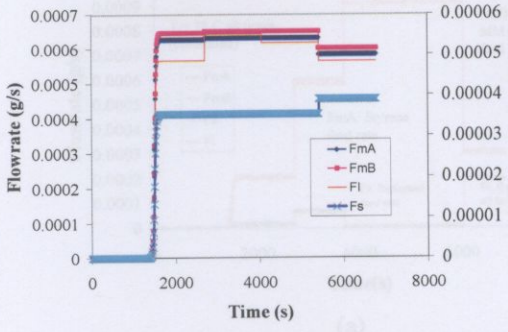

(a)

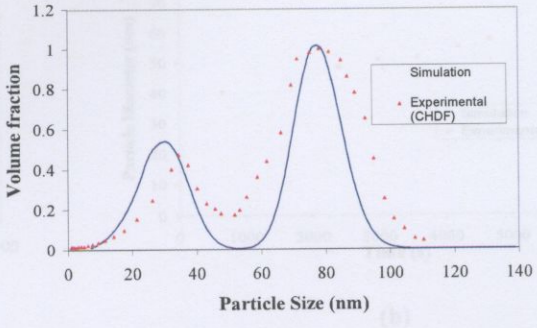

(b)

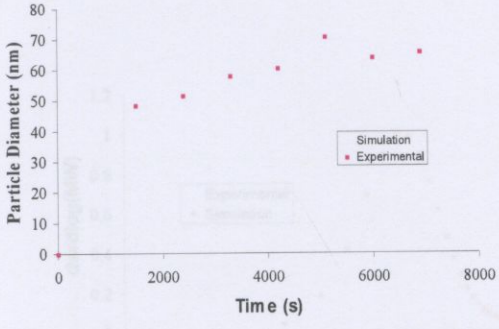

(c)

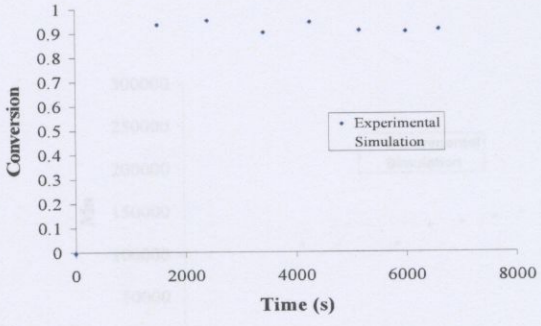

(d)

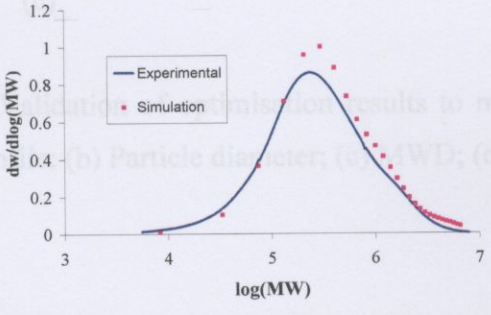

(e)

Figure 4.2 Case 1: Validation of optimisation results, (a) optimal profile, (b) PSD, (c) Particle Diameter, (d) Conversion, (e) MWD

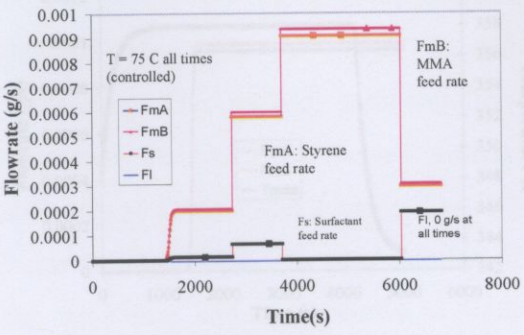

(a)

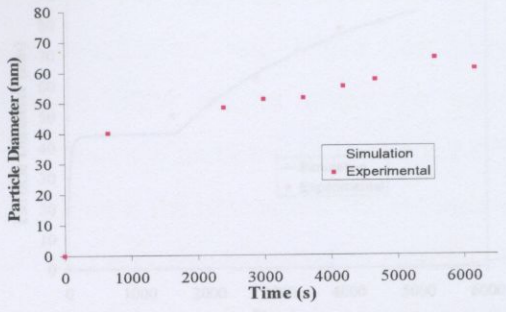

(b)

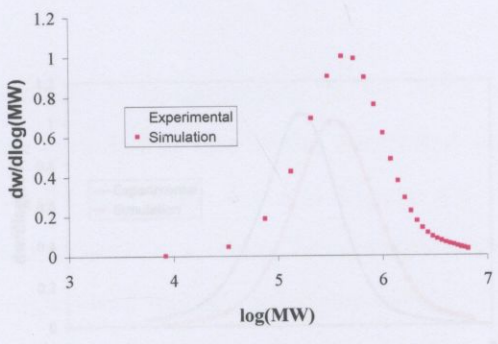

(c)

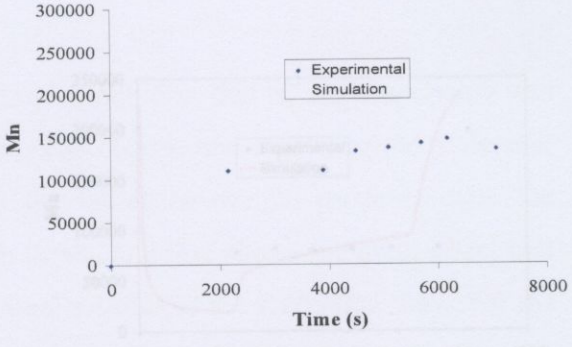

(d)

Figure 4.3 Case 2: Validation of optimisation results to maximize M_n (a) manipulated variables optimal profile; (b) Particle diameter; (c) MWD; (d) M_n

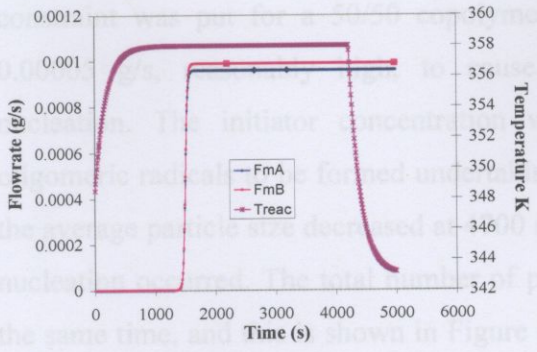

(a)

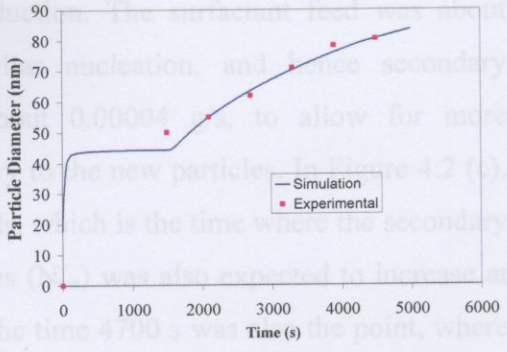

(b)

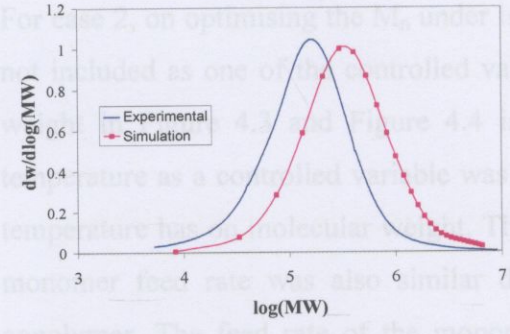

(c)

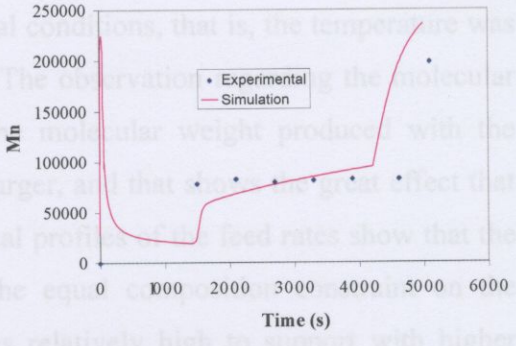

(d)

Figure 4.4 Case 3: Validation of optimisation results to maximize M_n. (a) manipulated variables optimal profile; (b) Particle Diameter; (c) MWD (d) M_n

The optimal duration to produce the desired copolymer was found to be two hours. The polydispersity was found to increase and then decrease sharply during the early stages of the simulation as shown in Figure 4.5 . This increase in the PSPI is due to the nucleation of particles during interval I. As Interval II starts particle formation ceases and the particles grow in size thus narrowing the distribution. From the optimal profiles in Figure

4.2 (a), it can be seen that the monomer feed of styrene and MMA were similar, since a constraint was put for a 50/50 copolymer production. The surfactant feed was about 0.00005 g/s, reasonably high, to cause micellar nucleation, and hence secondary nucleation. The initiator concentration was about 0.00004 g/s, to allow for more oligomeric radicals to be formed undertaking entry to the new particles. In Figure 4.2 (c), the average particle size decreased at 4700 seconds, which is the time where the secondary nucleation occurred. The total number of particles (N_{tot}) was also expected to increase at the same time, and this is shown in Figure 4.6. The time 4700 s was also the point, where the PSPI started increasing. The conversion in Figure 4.2 (d) was also used for the validation of the optimisation process, to ensure that the model is able to predict most of the key polymer properties at different conditions, and especially under optimised conditions.

For case 2, on optimising the M_n under isothermal conditions, that is, the temperature was not included as one of the controlled variables. The observation regarding the molecular weight in Figure 4.3 and Figure 4.4 is that the molecular weight produced with the temperature as a controlled variable was much larger, and that shows the great effect that temperature has on molecular weight. The optimal profiles of the feed rates show that the monomer feed rate was also similar due to the equal composition constraint on the copolymer. The feed rate of the monomers was relatively high to support with higher amount of monomers for the propagation increase, producing higher molecular weights. The surfactant feed rate was found to be very low. The reason is that adding surfactant would cause micellar nucleation, resulting in the decrease in the molecular weight. The surfactant was added at a very slow feed rate so that it stabilises the bigger particles formed, without producing any new micelles for micellar nucleation. The average radius was validated to this process to prove the validity of the model to act as a soft sensor under different conditions. From Figure 4.3, the agreement can be observed on obtaining the MWD, and on maximising the M_n. At case 3, the temperature profile was well compared with increase in the molecular weight, and the agreement was good. The value of M_n experimentally in Figure 4.4 (d) was a little lower than what is obtained from simulation, due to the slow cooling of the reactor temperature. The average size and the MWD were also analysed for case 3 as shown in Figure 4.4.

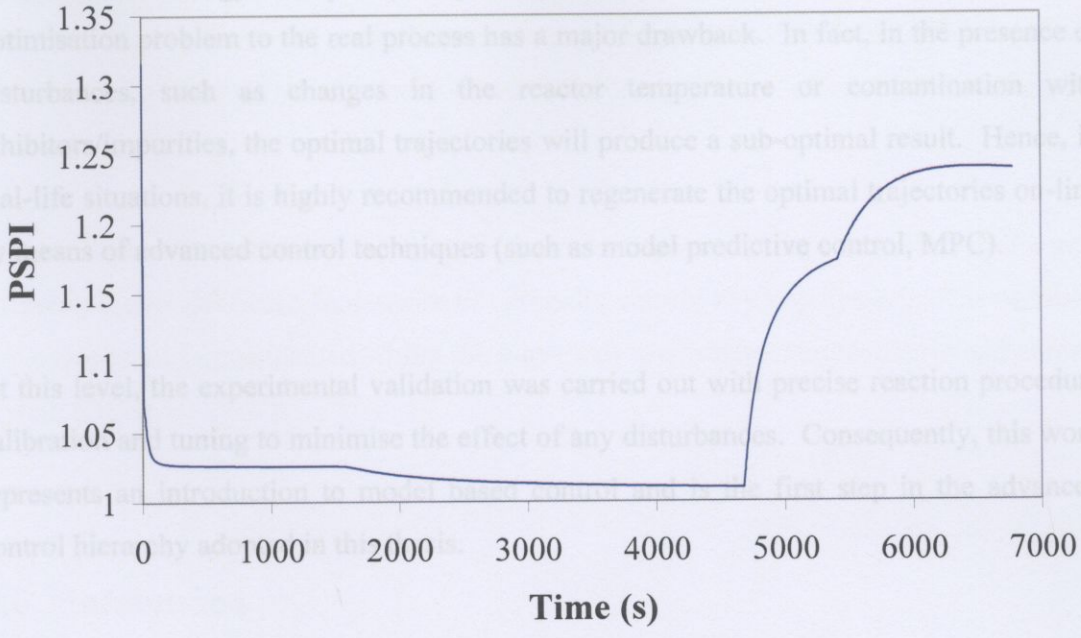

Figure 4.5 Case 1: Maximising PSPI

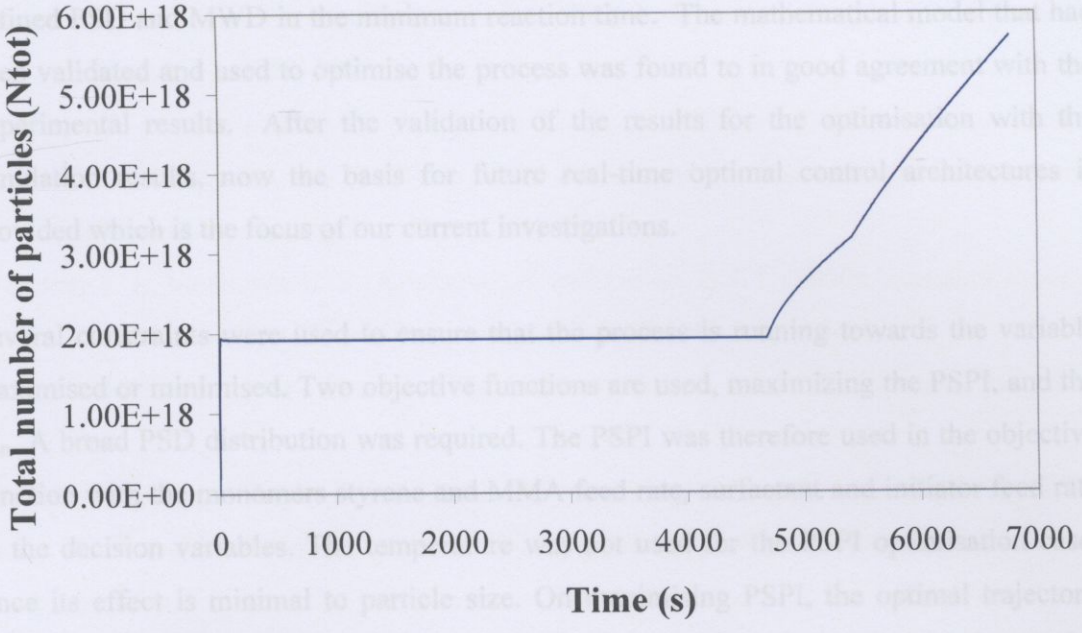

Figure 4.6. Profile of the particle number under optimum conditions.

However, the strategy of implementing the optimal trajectories obtained from the off-line optimisation problem to the real process has a major drawback. In fact, in the presence of disturbances, such as changes in the reactor temperature or contamination with inhibitors/impurities, the optimal trajectories will produce a sub-optimal result. Hence, in real-life situations, it is highly recommended to regenerate the optimal trajectories on-line by means of advanced control techniques (such as model predictive control, MPC).

At this level, the experimental validation was carried out with precise reaction procedure calibration and tuning to minimise the effect of any disturbances. Consequently, this work represents an introduction to model based control and is the first step in the advanced control hierarchy adopted in this thesis.

4.4 Conclusion

The optimisation strategy provided set-point trajectories for the manipulated variables (flow rates and reactor temperature) so as to ensure the production of a copolymer with a defined PSD and MWD in the minimum reaction time. The mathematical model that had been validated and used to optimise the process was found to in good agreement with the experimental results. After the validation of the results for the optimisation with the simulation results, now the basis for future real-time optimal control architectures is provided which is the focus of our current investigations.

Several constraints were used to ensure that the process is running towards the variable maximised or minimised. Two objective functions are used, maximizing the PSPI, and the M_n. A broad PSD distribution was required. The PSPI was therefore used in the objective function with the monomers styrene and MMA feed rate, surfactant and initiator feed rate as the decision variables. The temperature was not used for the PSPI optimisation case, since its effect is minimal to particle size. On maximising PSPI, the optimal trajectory generated produced a highly poly-dispersed polymer. The total number of particles increases at the time of secondary nucleation, where micellar nucleation takes place, and a bimodal distribution was obtained. Equality and inequality constraints were imposed to the system operation. For maximising M_n, all the five variables were chosen, since they all contribute to the maximisation process. The M_n was found to be higher at lower

temperatures. The temperature and the feed rates were used as the decision variables. The surfactant feed rate acted as a stabiliser to the growing particles. The initiator feed rate was set to zero by the optimiser, where it would have significant effect on decreasing the molecular weight.

In this chapter, the offline optimisation was run, and proved to be successful. In the next chapters, the model-based framework to optimally control key copolymerization variables is developed and implemented within the pilot-scale environment under distributed control system (DCS).

4.5 References

Alhamad, B., Romagnoli, J. A. and Gomes, V. G. (2003) In 31st Australasian Chemical Engineering Conference CHEMECA Adelaide, South Australia, pp. 138.

Alhamad, B., Willis, R., Romagnoli, J. A. and Gomes, V. G. (2004) In ESCAPE-14, Lisbon.

Clarke-Pringle, T. L. and MacGregor, J. F. (1998) Industrial & Engineering Chemistry Research, 37, 3660-3669.

Crowley, T. J., Harrison, C. A. and Doyle III, F. J. (2001) In 2001 American Control Conference, Jun 25-27 2001, Vol. 2 Institute of Electrical and Electronics Engineers Inc., Arlington, VA, pp. 981-986.

Crowley, T. J., Meadows, E. S., Kostoulas, E. and Doyle, F. J. I. (2000) Journal of Process Control 14th IFAC World Congress, Jul 5-Jul 9 1999, 10, 419-432.

Hancock and Harris (1960) Theory of Maxima and Minima, Dover Publications, Inc., New York.

Immanuel, C. D. and Doyle, F. J. I. (2002) Chemical Engineering Science, 57, 4415-4427.

Jarvis, R. B. and Pantelides, C. C. (1991) Presented at the AIChE Annual Meeting, Los Angeles.

Jarvis, R. B. and Pantelides, C. C. (1992) Technology and Medicine London SW7 2BZ, UK.

Kozub, D. and Macgregor, J. F. (1992) Chemical Engineering Science, 47, 929-942.

Papadimitriou, C. H. and Steiglitz, K. (1982) Combinatorial Optimization: Algorithms and Complexity, Prentice-Hall, Inc., Englewood Cliffs, New Jersey.

PSE (2000a) Process Systems Enterprise Ltd. (PSE), Release 1.8, United Kingdom.

Saldivar, E. and Ray, W. H. (1997) AIChE Journal, 43, 2021-2033.

Semino, D. and Ray, W. H. (1995a) Chemical Engineering Science, 50, 1805-1824.

Semino, D. and Ray, W. H. (1995b) Chemical Engineering Science, 50, 1825-1839.

Vassiliadis, V. S., Sargent, R. W. H. and Pantelidis, C. C. (1994a) Ind. Eng. Chem. Res., 33, 2111-2122.

Wilde, D. J. (1978) Globally Optimal Design, John Wiley and Sons, Inc., New York.

Wilde, D. J. and Beightler, C. S. (1967) Foundations of Optimization, Prentice Hall, Inc., Englewood Cliffs, New Jersey.

Zeaiter, J., Romagnoli, J. A., Barton, G. W., Gomes, V. G., Hawkett, B. S. and Gilbert, R. G. (2002) In Chemical Engineering Science, Vol. 57 Elsevier Science Ltd, pp. 2955-2969.

Chapter 5

Inferential Monitoring of Conversion

5.1 INTRODUCTION 5.2
5.2 CONVERSION MONITORING THROUGH REACTOR CALORIMETRY 5.3
5.2.1 Heat Transfer Analysis *5.6*
5.2.2 Data Acquisition and Parameter Estimation *5.11*
5.3 EXPERIMENTAL SETUP 5.12
5.4 RESULTS AND ANALYSIS 5.13
5.4.1 Relationship between overall conversion and process conditions *5.13*
5.4.2 Comparison between experiment and simulation result *5.14*
5.4.3 Optimisation results *5.15*
5.5 CONCLUSION 5.17
5.6 REFERENCES 5.18

5.1 Introduction

Having on-line sensors would push the polymer products to the lead. The quality of the products can be better by knowing the on-line key polymer properties and therefore can produce better products.

The polymer production always requires fulfilling the expectation from customer consistently, thus 'batch-to-batch' variation should be minimized. In order to produce the wanted key polymer properties, monitoring and controlling of polymerisation should be improved. However, it is difficult to find an existing reliable on-line device that gives an accurate measurement in real-time. Monitoring and controlling typical key polymer properties (conversion, particle size distribution and molecular weight) are very complicated. The mathematical model is a means towards developing a soft sensor on real time. However, there are other means to infer the conversion via the heat with reaction temperature, monomers feed rate and monomer composition. Fortunately, on-line calorimetry energy balance of the reaction temperature and jacket inlet and outlet temperature is a real time application to infer the conversion.

The investigation on calorimetry is very important. An accurate estimation of conversion and polymer property can use to improve the design and control emulsion polymerisation reactors in real industry. A good monitoring and controlling of reactor is essential for proper process operation and obtaining polymer with desired properties. So the studies on calorimetry in emulsion copolymerisation are very meaningful for the production of synthetic polymers.

In this chapter, the modelling studies are carried out by developing an on-line calorimetry. Conversion was estimated via the calorimetry model, which is based on the overall heat energy balance within the reactor and its jacket. To complete the calorimetric model, determination of heat transfer coefficient, heat loss and heat of polymerization reaction are required. All of them are based on the reaction temperature and the jacket inlet and outlet temperature.

5.2 Conversion Monitoring through Reactor Calorimetry

Emulsion Copolymerisation has grown to be one of the major means for the production of synthetic polymer product ranging from adhesives, inks, paints, coatings, drug delivery systems, medical assay kits, gloves, paper coatings, floor polish, films, carpet backing and foam mattresses to cosmetics. Due to this importance, technology is put into improving design and control of emulsion copolymerisation reactors (Schork et al., 1993, Fogler, 1992). However, the monitoring of such reactors is still a major challenge due to the lack of on-line sensors capable of monitoring the complex physio-chemical behaviour within such systems.

In emulsion copolymerisation, monitoring and control of monomer conversion is crucial both for proper process operation to reduce downstream separations, and for obtaining products with desired properties, due to the influence that conversion has on particle size and molecular weight. Current techniques implemented to determine conversion such as gravimetry indirectly through viscosity and density measurements, and gas chromatography, have notable drawbacks. Besides that, such techniques are implemented off-line, resulting in a measurement delay, which is undesirable for any form of real-time control. Thus, this work focuses on the development of an alternative approach to conversion monitoring that is suitable for on-line implementation.

It is possible to determine the reaction rate and monomer conversion via temperature measurements, since most polymerisation reactions are exothermic, and that is by operating the reactor in conjunction with an on-line calorimeter (Augustin et al., 1993, Fevotte and Klein, 1996, Hewitt et al., 1994, Litz, 1983, Lovell and El-Asser, 1997, Mckenna et al., 1996, Moritz, 1989, Rushton, 1952, Schuler and Schmidt, 1992, Wu, September, 1985, Zeaiter et al., 2002a). This method is certainly seen as promising for eventual industrial application. In this study, a detailed calorimetric model is developed for inferring monomer conversion in a batch/semibatch laboratory reactor where copolymer styrene-MMA is produced via emulsion copolymerisation. The significant advance here over existing calorimetric monitoring schemes is that the present development makes use of a dynamic model of the process. As will be shown, the calorimetric based results compared well with conversion data obtained off-line by gravimetric analysis.

On-line calorimetry is a straightforward technique combining measurements of temperature and flow rates with a dynamic energy balance of the reactor and its peripheral cooling systems. In the context of polymerisation, which is exothermic in nature, calorimetry can be used to determine the reaction rate and monomer conversion through temperature measurements by operating the reactor in conjunction with a calorimeter. This method is a promising candidate for industrial implementation of conversion monitoring and control. However, determining monomer conversion from temperature readings for different polymerisation processes, such as batch, semi-batch or continuous modes of operation, requires a thorough understanding of the heat transfer mechanisms occurring within the system.

Over the years, many researchers have spent a great deal of effort on the development of accurate calorimetric method for the purpose of on-line monitoring of a variety of processes.

(Schork et al., 1993) developed an approach to estimate the evolution of copolymer composition in emulsion polymerisation using calorimetric measurements. The strategy was tested for different copolymerisation batches, where a good agreement was achieved between the cumulative composition estimated by calorimetry and that determined by means of off-line measurements. (Fevotte and Klein, 1996) have applied on-line calorimetry to monitor the heat released during crystallisation of bifenox in methanol. Based upon the on-line identification of the differential heat of crystallisation, the authors were able to estimate, through simple calculations, the course of super-saturation and the concentration profile during reaction. (Fevotte and Klein, 1996) developed a strategy to accurately determine monomer conversion for different polymerisation batches. Off-line gravimetric data were used to track variations in the overall heat transfer coefficient. A general dynamic state-space formulation of the energy balance was proposed along with a Luenberger state-observer. (Mckenna et al., 1996) investigated the joint use of calorimetry with densimetry and gravimetry for the purpose of polymerisation on-line monitoring. Through a detailed sensitivity analysis, the authors concluded that calorimetry is easily adapted to polymerisation reactors, and could provide, along with infrequent gravimetric measurement updates, a good estimate of monomer conversion. (de Buruaga et al., 1997a, de Buruaga et al., 1997b, de Buruaga et al., 2000) used on-line calorimetry to estimate the conversion and copolymer composition in the emulsion copolymerisation of vinyle acetate

and butyl acrylate. The real-time feedback control of composition and conversion allowed the authors to avoid monomer accumulation in the reactor and maximised productivity without deteriorating the composition of the copolymer. Recently, (Zeaiter et al., 2002a) have used on-line calorimetry to estimate the heat of reaction and the heat transfer coefficient during polymerisation, and use the information of heat analysis to inferentially find the conversion.

Polymerisation heat is dependent on the rate of polymerisation of monomers (R_{pi}) and enthalpies of polymerisation of monomers (ΔH_i). (de Buruaga et al., 1997b, Gugliotta et al., 1995a, Gugliotta et al., 1995b) used the same approach to determine the rate of reaction. They assumed that the heats of cross-propagation are equal to those of homopolymerisation. Isabel Saenz de Burruaga et al. stated out a way to estimate the heat loss for industrial-scale reactor. The heat loss determination is possible to be carried out by filling the reactor with non-reacting mixture and solving the heat energy balance equation in steady state while the reactor temperature was kept constant.
Rate of polymerisation reaction is determined by obtaining the propagation rate constant, time-averaged probability of finding a free radical with ultimate unit of type j in the polymer particles, the concentration of monomer *i* the polymer particles, the average number of radicals per particle, total number of polymer particles and Avogadro's constant.

(Zeaiter et al., 2002a) used a simpler approach to estimate the polymerisation heat rate for homopolymerisation reaction. It did not involve the calculation of rate of homopolymerisation reaction. The heat of homopolymerisation reaction generated was estimated by determining the heat of polymerisation reaction.

In this work, a detailed calorimetric model is developed for inferring monomer conversion in the batch/semi-batch emulsion copolymerisation of styrene and MMA. The advance over the types of calorimetric monitoring in current use is that the present development includes an adaptive strategy to estimate the overall heat transfer coefficient and key evaporation/condensation parameters. The calorimetric results are compared to conversion data obtained offline by gravimetry. The other advance over other techniques is that it does not need the values of the kinetics through the reaction.

5.2.1 Heat Transfer Analysis

In principle, the calorimetry is based on the heat energy balance for the material inside the calorimeter, which was identified by the heat around the reactor, its peripheral equipment and heat of reaction. The dynamic heat balances equation is shown as follows (Zeaiter et al., 2002a):

$$MCp\frac{dT_e}{dt} = \sum_i F_i Cp_i (T_{amb} - T_e) + Q_f - Q_{loss} + Q_r + Q_s \qquad \text{(Eq. 5.1)}$$

where $\Sigma F_i Cp_i(T_{amb}-T_e)$ is the heat flow due to the reactor feed

Q_f is the heat flux across the reactor wall

Q_{loss} is heat loss to the surroundings

Q_r is the heat-generation rate due to the chemical reaction, and

Q_s is the heating due to stirring

where the heat flow due to the reactor feed term is identified as follows:

$$\sum_i F_i Cp_i (T_{amb} - T_e) = F_{m1,in} Mw_{m1} Cp_{m1} (T_{amb} - T_e) + F_{m2,in} Mw_{m2} Cp_{m2} (T_{amb} - T_e) \qquad \text{(Eq. 5.2)}$$

Since it is a semi-batch copolymerisation reaction, it would become significant when the monomer starts to be fed into the reactor. The monomers styrene and MMA added into the reactor are not preheated to the reactor temperature, therefore the monomer temperature was assumed to be ambient temperature. However, they are added drop-wise.

5.2.1.1 Jacket-side Dynamics

In principle, the calorimetry is based on the heat energy balance for the material inside the calorimeter, which was identified by the heat around the reactor, its peripheral equipment and heat of reaction. A high water flow rate was used to ensure a maximum inlet to outlet temperature differential of about 0.7°C for heating and cooling via the jacket. Thus, it could be assumed that the dynamics of the jacket system is negligible.

The heat flux across the reactor wall, Q_f is the defined as;

$$Q_f = UA(T_{j,out} - T_e) \quad \text{(Eq. 5.3)}$$

where the heat transfer coefficient can be determinated by obtaining data during the initial heating stage, when the reactor contents were being heated to the operation temperature. In this stage, there is no polymerisation reaction occurring and no monomer is fed in. The heat losses and heating due to stirring are neglected. So, the following equation is obtained as follows:

$$MCp\frac{dT_e}{dt} = Q_f = UA(T_{j,out} - T_e) \quad \text{(Eq. 5.4)}$$

Once heat transfer coefficient has been determined, heat loss from the reactor is then estimated. For simplifying the estimation, it was also done under the initial heating phase.

5.2.1.2 Determination of heat transfer coefficient

To determine the heat transfer coefficient, the heat of reaction, heat losses, heat of evaporation/condensation, heat energy due to stirring and kinetic energy. It is not easy to find all of these requirements. However, there are assumptions, which would reduce the amount of calculations and still gives a good prediction. The heat of stirring is considered negligible and is not included in further calculations. Moreover, water is about 90% of the reaction medium, which means to assume that the viscosity of the liquid does not change is valid. This also validates why the heat of stirrer is negligible.

The initial heat transfer coefficient, U_o, is determined by running the process with all ingredients (except the initiator, which is a small amount) charged into the reactor. Insulation is added to the jacket on the reactor to reduce the amount of heat looses to minimum.

The heat loss is a function of the reaction temperature and ambient temperature, so it was put into an empirical formula shown as follows:

$$Q_{loss} = \alpha(T_e - T_{amb})^{\beta} \quad \text{(Eq. 5.5)}$$

where α and β are constants, which are estimated by matching the measured thermal response of the reactor, shown as follows :

$$\alpha(T_e - T_{amb})^{\beta} = UA(T_{j,out} - T_e) - MCp\frac{dT_e}{dt} \quad \text{(Eq. 5.6)}$$

During a heating process, α and β are determined by least-squares method by rearranging the equation as follows:

$$\ln\alpha + \beta\ln(T_e - T_{amb}) = \ln\left[UA(T_{j,out} - T_e) - MCp\frac{dT_e}{dt}\right] \quad \text{(Eq. 5.7)}$$

Heating due to stirrer is neglected here to simplify the calculation, as it was estimated at about 0.5W

In determination of heat generated due to polymerisation, the reaction in aqueous phase was neglected. Assuming all the copolymerisation process was taken place within the micelle, the heat of reaction is defined as:

$$Q_r = R_{p1}V\Delta H_1 + R_{p2}V\Delta H_2 \quad \text{(Eq. 5.8)}$$

where R_{p1} and R_{p2} are reaction rate of styrene and MMA polymerisation in micelle respectively, while ΔH_1 and ΔH_2 are the enthalpy of homopolymerisation of styrene and MMA respectively. Q_r is found by the following equation:

$$Q_r = MCp\frac{dT_e}{dt} - \sum_i F_i Cp_i(T_{amb} - T_e) - Q_f + Q_{loss} - Q_s \quad \text{(Eq. 5.9)}$$

while other heat energy terms in the right hand side was accurately identified.

There are two unknowns (R_{p1} and R_{p2}) and one equation in Equation 5.8. Another equation was needed to solve for the two unknowns, and so an experiment was developed to obtain

the relation between the R_{p1} and R_{p2} as a function of time. The following relation was obtained.

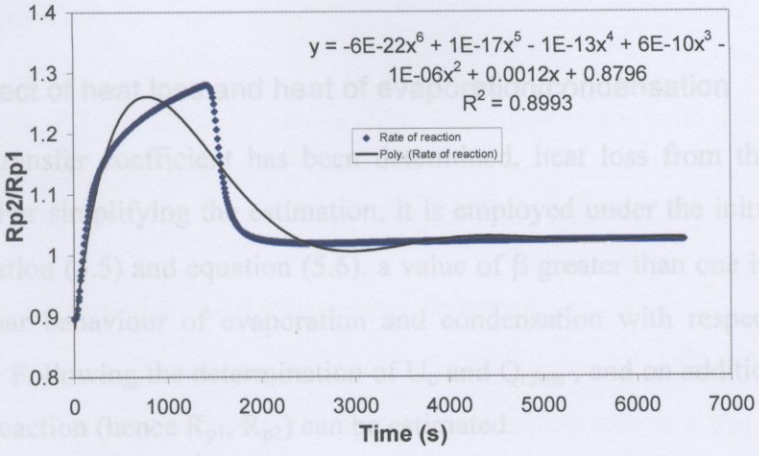

Figure 5.1 Relation between rate of reaction between styrene and MMA

From the relation obtained from Figure 5.1, it is clear that the deviation of the result is greater at 500 to 2000s, but it is more accurate on the rest of the points.

The heat transfer coefficient used for emulsion copolymerisation of styrene and MMA was estimated at about 85.59W/m^{2}K, which changes at different operating conditions, since Q_{loss} changes. The heat loss is expressed as $Q_{loss} = \alpha(T_e - T_{amb})^{\beta}$, where constant parameters, α and β were estimated as 2.05 W/^{o}C$^{\beta}$ and 1.03 respectively.

As time increases through the reaction, the rate of reaction is relatively high at the seeded process for the first 1500s. At the start of the semi batch process, the rate of reaction reduces slowly, since the amount added results partly in a reaction, which is less than the consumption of monomers to produce the particles.

P_s is the power input by stirring defined by:

$$P_s = K\rho N^3 d^5 \qquad \text{(Eq. 5.10)}$$

where K is a constant, N is the stirrer speed and d is the impeller diameter. ρ is the density of the latex calculated from:

$$\rho = \frac{N_m MW_m + N_p MW_m + V_{w0}\ \rho_w}{(N_m MW_m)/\rho_m + (N_p MW_m)/\rho_p + V_{w0}} \qquad \text{(Eq. 5.11)}$$

5.2.1.3 Effect of heat loss and heat of evaporation/condensation

Once heat transfer coefficient has been determined, heat loss from the reactor is then estimated. For simplifying the estimation, it is employed under the initial heating phase. For the equation (5.5) and equation (5.6), a value of β greater than one is expected due to the non-linear behaviour of evaporation and condensation with respect to temperature differential. Following the determination of U_o and $Q_{r,loss}$, and on addition of the initiator, the heat of reaction (hence R_{p1}, R_{p2}) can be estimated.

After solving for R_{pi}, the unreacted moles of styrene and MMA respectively can be defined as:

$$N_{unreacted,i} = \left(\frac{F_{mi}^{o} + F_{mi}}{Mw_{mi}} - R_{pi} \mathrm{V} \right) \times \Delta t \qquad \text{(Eq. 5.12)}$$

where F_{mi}^{o} is the initial mass of the monomer (g/s), F_{mi} is the feed rate of the monomer (g/s) and Mw_{mi} is the molecular weight of the monomer (g/mol).

The volume of the reactor contents, V, can be determined from:

$$V = \frac{N_m MW_m}{\rho_m} + \frac{N_p MW_m}{\rho_p} + V_{wo} \qquad \text{(Eq. 5.13)}$$

ρ_m and ρ_p are the monomer and polymer density respectively, MW_m the molecular weight of a monomer unit and V_{wo} the volume of water in the "recipe".

Conversion of styrene and MMA respectively was found to be:

$$X_i = 1 - \frac{N_{unreacted,i}}{N_{Total,i}} \times 100\% \quad \text{(Eq. 5.14)}$$

In batch mode, $F_{m,in}$ is equal to zero and $N_{m,T}$ is equal to the total amount of monomer (moles) charged initially into the reactor.

5.2.2 Data Acquisition and Parameter Estimation

The differential equations are discretised with respect of time. A link called dynamic data exchange (DDE) is used to connect to the data acquisition software. A program written in Microsoft Excel and Microsoft Visual Basic is then used to employ the calorimetric calculations on real time. In the heating process, α and β are determined by least-squares method (Zeaiter et al., 2002b). Recalling Equation 5.13, the following equation is obtained:

$$\ln\alpha + \beta\ln(T_e - T_{amb}) = \ln\left[UA(T_{j,out} - T_e) - MCp\frac{dT_e}{dt}\right] \quad \text{(Eq. 5.15)}$$

Putting Equation 5.15 into the form of an equation of a straight line $y=mx+c$

$$y = \ln\left[UA(T_{j,out} - T_e) - MCp\frac{dT_e}{dt}\right] \quad \text{(Eq. 5.16)}$$

$$m = \beta \quad \text{(Eq. 5.17)}$$

$$x = \ln(T_e - T_{amb}) \quad \text{(Eq. 5.18)}$$

$$c = \ln\alpha \quad \text{(Eq. 5.19)}$$

Using least-squares method, the slope of the line β is:

$$\beta = \frac{\sum x_i y_i - \frac{\sum x_i \sum y_i}{N}}{\sum x_i^2 - \frac{\left(\sum x_i\right)^2}{N}} \quad \text{(Eq. 5.20)}$$

The intercept $ln\alpha$ *is found as follows*:

$$\ln\alpha = \bar{y} - m\bar{x} \quad \text{(Eq. 5.21)}$$

$$\text{so, } \alpha = \exp(\bar{y} - m\bar{x}) \quad \text{(Eq. 5.22)}$$

where x_i, y_i are individual pairs of data for $ln(T_e\text{-}T_{amb})$ and $\ln\left[UA(T_{j,out} - T_e) - MCp\frac{dT_e}{dt}\right]$, n is the number of pairs of data used in preparing the calibration curve, and $\bar{x}$ and $\bar{y}$ are the average values for the variable, which is shown as follows:

$$\bar{x} = \frac{\sum x_i}{N} \quad \text{(Eq. 5.23)}$$

$$\bar{y} = \frac{\sum y_i}{N} \quad \text{(Eq. 5.24)}$$

A high agitation rate of 400 RPM is used to ensure a constant heat transfer coefficient throughout the reaction phase. The heat transfer area of the cylindrical jacket is calculated by knowing the reactor diameter, D, and the reaction volume. The equation is shown as follows:

$$A(t) = \frac{4V(t)}{D} \quad \text{(Eq. 5.25)}$$

5.3 Experimental setup

The experimental study of copolymerisation of styrene and methyl methacrylates (MMA) was carried out in the 1L reactor. The product from the copolymerisation was taken for conversion measurements by an off-line gravimeter. The heating jacket unit is circulated with water that was heated by an electrical heater. A computer-controlled system was used for data information recording and manipulation. The temperature within the reactor, inlet and outlet of the jacket and also monomer feed rate, which corresponded to the electronic balance and time, are all recorded in a database system, and so for calculating the heat

transfer coefficient, and therefore the monomer conversion. The reactor dimensions and the operation parameters are shown as follows:

Reactor height (m)	0.18
Reactor diameter (m)	0.085
Jacket height (m)	0.13
Jacket volume (ml)	350
Water flow rate through jacket (ml/s)	92
Agitation speed (rpm)	400

Table 5.1 Reactor dimensions and typical operating parameters

5.4 Results and Analysis

The result from both the experiment and simulation are presented in this section. Varying conditions were implemented to observe the effects of changing temperature and monomer composition on conversion and particle size (See Table 5.2). Factors such as total monomer feed rate, concentration of initiator and surfactant remained unchanged.

Experiment	Reaction Temperature (^{o}C)	Sty/MMA ratio
Run 1	75	25/75
Run 2	82.44	50/50
Run 3	70.34	50/50

Table 5.2 Operation process modes

5.4.1 Relationship between overall conversion and process conditions

In this Chapter, experimental overall conversion of copolymerisation was determined by gravimetry. A conversion of over 90% was obtained for the different runs. However, the instantaneous conversions at different time intervals are significantly different, which is

due to the different operation conditions and monomer composition. Factors enhancing for different results of conversion could be due to the rate of reaction which is higher at a higher temperature, and with the higher proportion of MMA. For a lower reaction temperature (<65°C), the copolymerisation reaction did not occur at all.

The rate of copolymerisation was calculated using the heat balance equations obtained from the experiment. The rate of copolymerisation was very high at the beginning of the reaction, since the smaller amount of the monomers (17.1%) of the total amount reacted, and as the seeds are formed, where most of the monomers reacted, the rate of polymerisation dropped. As the monomers were added as semibatch, unreacted monomers concentration increases in the aqueous phase, which induces an increasing of monomers concentration inside the particles. However, the polymerisation rate does not increase directly. Thus, unreacted monomers cause a drop of the conversion for an instant time, where more monomers are available. As the monomers are added as semi batch, the temperature also rises due to the exothermic reaction of the emulsion copolymerisation process. That increase in temperature caused the drop within the conversion predicted by the calorimetric model. The rate of copolymerisation propagation then increases gradually, and the accumulated unreacted monomers are consumed, and so overall conversion increases. The rate of copolymerisation increases with the addition of the monomer. The peak in the rate of reaction is the time where the monomers rate of change is constant for a short time, and then it decreases with the consumption of the rest of the monomers.

5.4.2 Comparison between experiment and simulation result

An agreement between experimental and simulated overall conversion under different process mode is described in this section. The experimental overall conversion was measured by gravimetry, while simulated ones were estimated by calorimetric model. The three overall conversion curves are plotted in the following figures. Figure 5.2 shows the comparison of overall conversions between experiment and simulations for Run 1, 2 and 3 respectively.

As it can be seen from the results, the deviation was expected to be within the time of 0 to 2000 s, but still predicting with a good agreement.

The conversion of each of the monomers is obtained through the reaction period, and what is obtained in the three runs above are the average conversion of both monomers. Figure 5.2 (d) shows the conversion of monomers, styrene and MMA.

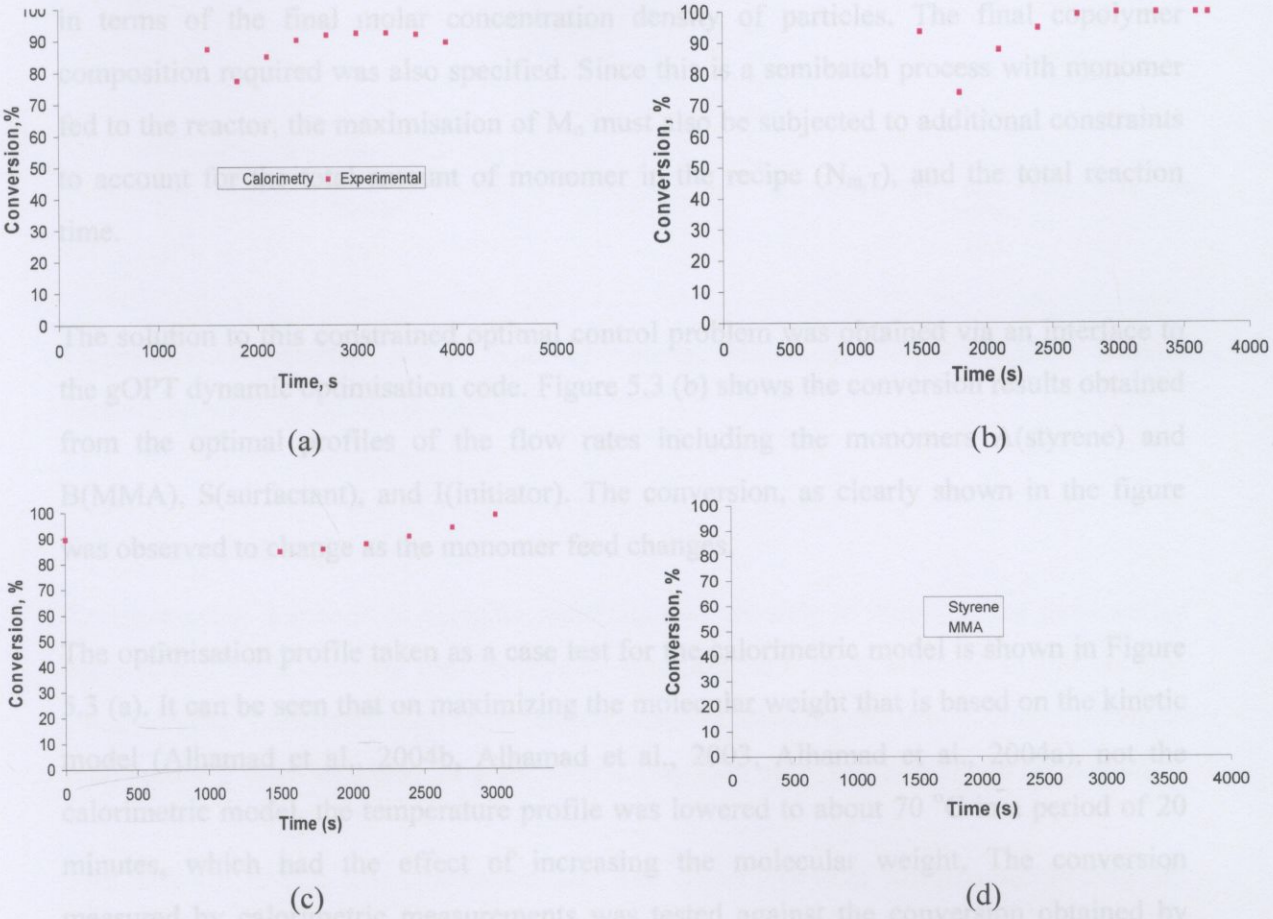

Figure 5.2. Comparison of overall conversion between experimental, and Calorimetry simulation for (a) run 1, (b) run 2, (c) run3 (d) run 3, conversion of each monomer

5.4.3 Optimisation results

The kinetic model developed by the author (Alhamad et al., 2003, Alhamad et al., 2004b, Alhamad et al., 2004a) was used to optimise the M_n. This optimisation system was used as a case study tested against the calorimetric model on obtaining the overall conversion. The objective functions to be optimised was defined as Max [MWPI(r, M_n, t_{final}], where MWPI

is the molecular weight polydispersity index, M_n is the number average molecular weight, r is the radius, and t_{final} is the processing time. For operational reasons, the monomers, surfactant, initiator feed rates and temperature (for molecular weight optimisation) were specified within upper and lower bounds. The final Particle Size Distribution (PSD) shape was included in this optimisation in the form of end point inequality constraints formulated in terms of the final molar concentration density of particles. The final copolymer composition required was also specified. Since this is a semibatch process with monomer fed to the reactor, the maximisation of M_n must also be subjected to additional constraints to account for the total amount of monomer in the recipe ($N_{m,T}$), and the total reaction time.

The solution to this constrained optimal control problem was obtained via an interface to the gOPT dynamic optimisation code. Figure 5.3 (b) shows the conversion results obtained from the optimal profiles of the flow rates including the monomers A(styrene) and B(MMA), S(surfactant), and I(initiator). The conversion, as clearly shown in the figure was observed to change as the monomer feed changes.

The optimisation profile taken as a case test for the calorimetric model is shown in Figure 5.3 (a). It can be seen that on maximizing the molecular weight that is based on the kinetic model (Alhamad et al., 2004b, Alhamad et al., 2003, Alhamad et al., 2004a), not the calorimetric model, the temperature profile was lowered to about 70 °C in a period of 20 minutes, which had the effect of increasing the molecular weight. The conversion measured by calorimetric measurements was tested against the conversion obtained by gravimetric measurements, and showed good agreement.

The main factors to control the accuracy of conversion predictions relying on calorimetric model are the heat transfer coefficient and heat loss, which change on the number of moles added and on the temperature profile. However, they are varying and it is difficult to estimate accurately during the copolymerisation reaction, since the property of the reactant content is changing, when the reaction is started. However, the assumptions taken would also affect the accuracy of the model developed. As expected, there was a small deviation within the first 2000 s as expected, but the rest of the reaction was well predicted.

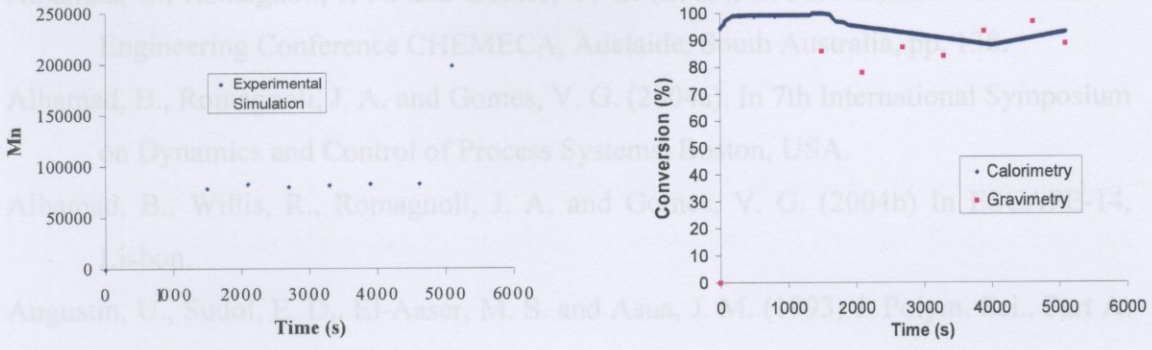

Figure 5.3. Optimisation run (a) Number Average Molecular Weight (M_n), (b) Overall conversion with the optimal profiles

5.5 Conclusion

The increasing demands of versatile materials that are able to adjust to the most varied applications are enhancing the importance that polymers have acquired in our society. Emulsion copolymerisation presents the advantage of allowing the production of polymers with unique properties, presenting more versatility than other polymerisation techniques.

The lack of on-line instrumentation was the main incentive towards developing the calorimetric model. The on-line soft sensor enables to predict the key polymer properties online and hence could control the reaction in order to obtain the product with the specified properties.

This chapter includes the experimental and calorimetric modelling studies of the semi-batch emulsion copolymerisation of styrene and MMA. The calorimetric model was found to be in good agreement with the offline gravimetric results. The copolymerisation reaction was carried out at three different reaction temperatures (70.34, 75 and 82.44°C) and two different monomer compositions (25styrene/75MMA and 50styrene/50MMA). The modelling studies are concerned with the development of heat balance based calorimetric model, with which the conversion was inferentially determined.

5.6 References

Alhamad, B., Romagnoli, J. A. and Gomes, V. G. (2003), In 31st Australasian Chemical Engineering Conference CHEMECA, Adelaide, South Australia, pp. 138.

Alhamad, B., Romagnoli, J. A. and Gomes, V. G. (2004a), In 7th International Symposium on Dynamics and Control of Process Systems, Boston, USA.

Alhamad, B., Willis, R., Romagnoli, J. A. and Gomes, V. G. (2004b) In ESCAPE-14, Lisbon.

Augustin, U., Sudol, E. D., El-Aaser, M. S. and Asua, J. M. (1993) J. Polym. Sci., Part A: Polym. Chem., 31, 2907-2913.

de Buruaga, I. S., Armitage, P. D., Leiza, J. R. and Asua, J. M. (1997a) Industrial & Engineering Chemistry Research, 36, 4243-4254.

de Buruaga, I. S., Echevarria, A., Armitage, P. D., de la Cal, J. C., Leiza, J. R. and Asua, J. M. (1997b) AIChE Journal, 43, 1069-1081.

de Buruaga, I. S., Leiza, J. R. and Asua, J. M. (2000) Polymer Reaction Engineering, 8, 39-75.

Fevotte, G. and Klein, J. P. (1996) Can. J. Chem. Eng., 74, 372-384.

Fogler, H. S. (1992) Elements of Chemical Reaction Engineering, Prentice Hall, Englewood Cliffs, NJ.

Gugliotta, L. M., Arotcarena, M., Leiza, J. R. and Asua, J. M. (1995a) Polymer, 36, 2019-2023.

Gugliotta, L. M., Leiza, J. R., Arotcarena, M., Armitage, P. D. and Asua, J. M. (1995b) Industrial & Engineering Chemistry Research, 34, 3899-3906.

Hewitt, G. F., Shires, G. L. and Bott, T. R. (1994) Process Heat Transfer, CRC Press, Boca Raton.

Litz, W. (1983) J. Thermal Anal., 27, 215-228.

Lovell, P. A. and El-Asser, M. S. (1997) Emulsion Polymerisation and Emulsion Polymers, Wiley, New York, NY.

Mckenna, T. F., Fevotte, G., Graillat, C. and Guillot, J. (1996) Trans. Instn. Chem. Eng. 47 (Part A), 340-348.

Moritz, H.-U. (1989) Polym. React. Eng., 248-266.

Rushton, J. H. (1952) Ind. Eng. Chem., 44, 2931-2936.

Schork, F. J., Deshpande, P. B. and Leffew, K. W. (1993) Control of Polymerisation Reactors, Dekker, New York, NY.

Schuler, H. and Schmidt, C.-U. (1992) Chem. Eng. Sci., 47, 899-915.

Wu, R. S. H. (September, 1985) Comput. Aided Eng., 57-61.

Zeaiter, J., Gomes, V. G., Romagnoli, J. A. and Barton, G. W. (2002a) Chemical Engineering Journal, 89, 37-45.

Zeaiter, J., Romagnoli, J. A., Barton, G. W., Gomes, V. G., Hawkett, B. S. and Gilbert, R. G. (2002b) In Chemical Engineering Science, Vol. 57 Elsevier Science Ltd, pp. 2955-2969.

Chapter 6

Real Time Optimal Control of Emulsion Copolymerisation

6.1 INTRODUCTION 6.2
6.2 OVERALL ARCHITECTURE 6.5
6.3 MODEL PREDICTIVE CONTROL ALGORITHM 6.7
6.3.1 Model Identification *6.8*
6.3.2 Multivariable Case (MIMO) *6.10*
6.3.3 Tuning in MPC *6.11*
6.3.4 MPC setup *6.12*
6.3.4.1 MPC Controller Block 6.14
6.4 REAL-TIME IMPLEMENTATION ARCHITECTURE 6.15
6.4.1 MATLAB – gPROMS – Honeywell Link *6.18*
6.4.1.1 MATLAB – gPROMS Link 6.18
6.4.1.2 MATLAB – Honeywell Link (DCS Interface Options) 6.18
6.4.2 Two Way Data Communication *6.20*
6.5 REAL TIME CONTROL OF SEMI-BATCH EMULSION COPOLYMERISATION REACTOR 6.21
6.5.1 MPC Application *6.22*
6.5.1.1 Multivariable Control: PSD and MWD (MIMO) 6.23
6.5.1.2 Multivariable MPC: MWD Control 6.33
6.6 CONCLUSION 6.40
6.7 REFERENCES 6.42

6.1 Introduction

Copolymerisation control is challenging due to its nonlinear and highly interactive behaviour. Copolymerisation reactors exhibit high complex nonlinear dynamic behaviour, because of the complexity of the physicochemical interactions and the kinetics of the copolymerisation reactions. In these reactors many important variables, often related to end-use polymer properties, cannot be measured on-line or can only be measured at very low sampling frequencies. Furthermore end-use polymer properties are usually related to the particle size, molecular weight and their distributions in the copolymerization reactor. Moreover, the typical industrial polymer reactor is used to manufacture a variety of grades of the same basic product necessitating frequent start-ups, online transitions, and shutdowns.

Because of these reasons, effective process monitoring and control of these reactors has been very challenging and has been the focus of active research programs in academia which has resulted in many publications. From an industrial perspective there are significant incentives for efficient polymer reactor monitoring and control which include the production of higher quality products, safer processes, minimisation of transition losses, and higher production rates. Increasing competition in the chemical industry requires a more agile plant operation in order to increase productivity under flexible operating conditions. Developing a model is the first step towards controlling the process. Problems occur on controlling the plant online by using the model. Moreover, the process would always face disturbances, which makes the optimal profiles to be sub-optimal; in this case, control of the process is essential to ensure having the operating conditions running on its optimal profiles.

(Dimitratos et al., 1994) stated that the control of the PSD and the MWD in emulsion polymerisation by means of closed-loop strategies is a challenging problem. For these reasons, experience and secret "recipes" industry are used to ensure a consistent quality product, but however not efficient. There had many studies for PSD control or MWD control, but very few works took into consideration the control of both PSD and MWD, using several variables to control the process. This is called multi-objective optimisation, and is very complicated to implement, which limits many researchers to fix the control to one of the key polymer properties.

More than 15 years after model predictive control (MPC) appeared in industry as an effective means to deal with multivariable constrained control problems, the on-line optimization, stability and performance are largely understood for systems described by linear models. Progress had been made on non-linear systems, but for practical applications, many questions remain, including the reliability and efficiency of the on-line computation scheme. Because of these reasons effective process monitoring and control of these reactors has been very challenging and has been the focus of active research programs in academia which has resulted in many publications.

(Garcia, 1984) employed an MPC strategy using the monomer addition rate and the cooling water flow rate as the manipulated variables to control the temperature of the reactor. The application was subjected to a semi-batch polymerization reaction. On the other hand, (Gordon and Weidner, 1981) used the monomer conversion to detect the formation of new particles in the emulsion polymerization of polyvinyl chloride, and used the surfactant as the manipulation variable to control the PSD.

In the literature, the topics of model-based control for emulsion polymerization systems are mostly implemented to control lumped parameters. Georgakis and coworkers have worked with a copolymerization system, and have applied adaptive Kalman filtering to estimate the average number of radicals per particle in an effort to control the ratio of mean particle diameters in a bi-disperse system (Dimitratos et al., 1991, Liotta et al., 1997). Additional secondary measurements were utilized, including density and monomer addition rate, to produce manipulations of the monomer feed for control. Other contributions to estimation and control of emulsion systems include the use of Luenberger observers (Fevotte et al., 1998) to estimate monomer conversion, and the combination of estimation and nonlinear control for an experimental styrene system. (Echevarria et al., 1998b) used a non-linear model-based controller to calculate the feed rates of chain transfer agent and monomer required to produce a polymer with desired MWD in styrene emulsion homopolymerisation. The control strategy was assessed by simulation and verified experimentally where a bimodal PSD was obtained. (Echevarria et al., 1998a). To end work on nonlinear synthesis for distribution control, one has to look to systems other than emulsion polymerization but which share a similar population balance structure. For example, Eaton and Rawlings (Eaton and Rawlings, 1990) posed and solved an interesting particle size distribution control problem for a batch crystallization process. Their

objective was to maximize the mass of seed crystals relative to nucleated crystals while achieving at least a minimum acceptable crystal yield. To solve this problem, they discretised the population balance equations describing crystal nucleation and growth, in time and in crystal size, using orthogonal collocation on finite elements. This reduced the partial differential equations to a set of algebraic equations which were then formulated as constraints in a nonlinear programming problem.

(Gobin et al., 1994) work aims at designing proper control strategies for this unstable train of reactors using a Dynamic Matrix Control (DMC) algorithm and to compare such a scheme with the use of conventional digital PID controllers. Their design of the DMC controller was based on a linearization of the dynamic model around an open-loop stable operating point. The implementation of the DMC algorithm was carried out using a standard formulation.

(Ozkan et al., 2002) presented an implementation of a model predictive control (MPC) algorithm using piecewise linear models on an industrial case study of solution copolymerization of methyl methacrylate and vinyl acetate. The control algorithm is a receding horizon scheme with a quasi-infinite horizon objective function which has finite and infinite horizon cost components. The finite horizon cost consists of free input variables that direct the system towards a terminal region which contains the desired operating point.

(Vicente et al., 2001) showed that copolymer composition and molecular-weight distribution of linear copolymers were controlled simultaneously by maintaining concentrations of the monomers and chain-transfer agent (CTA) at calculated values. (Vicente et al., 2002) also presented time optimal monomer and chain-transfer agent feed profiles computed and implemented experimentally for the simultaneous control of copolymer composition and molecular weight distribution.

(Immanuel and Doyle III, 2002) accomplished an open-loop generation of an optimal feed profile to attain a target particle size distribution (PSD) in the semi-batch emulsion co-polymerization of vinyl acetate and butyl acrylate. A nominal model of the process based on population balancing is utilised for this purpose. A Genetic Algorithm is employed as the optimization strategy. The optimal recipes generated in these studies are implemented

on an experimental emulsion polymerisation reactor. The end-point PSD obtained in these experiments closely matches the target in spite of the model uncertainties and process disturbances. Surfactant feed was used as one of the controlled variables.

Despite the recent publications, more work needs to be done in the area of on-line implementation of advanced multivariable control on emulsion copolymerization reactors. In order to apply advanced control techniques successfully, effective methods are needed to develop to accurately determine the PSD and MWD on-line. On the other hand, recent advances in process understanding, mathematical modelling, soft-sensor technology and model-based control techniques have been such as to offer copolymerization reactor operators the chance of achieving major improvements in process operation and product quality. A viable approach would be to involve combining these powerful tools into an effective model-based control strategy, as described in this chapter.

6.2 Overall Architecture

A detailed dynamic model is developed, which is applied to a system exhibiting zero-one kinetics in emulsion copolymerisation. This model (as shown in previous chapters) has the ability to predict the molecular weight distribution (MWD), number and weight average molecular weight (M_n and M_w), average particle size, the particle size distribution (PSD) and the conversion. The model had been tested to match the experimental results at variable different temperatures, different feed rates and variable co-monomer composition varying at 75/25, 50/50 and 25/75 feed composition. The model had been validated against the experimental results showing good agreement with the model.

The model was then used to determine the optimal feed rates to maximise the polydispersity index for particle size and molecular weight (PSPI and M_n). Monomers feed rate showed a small change on maximizing, but the surfactant and initiator feed rates and the temperature showed significance on maximizing the PSPI and M_n. Optimisation of the process showed good agreements with experimental validations.

Therefore, a multivariable model predictive control (MPC) is formulated to solve the control problems associated with a combination of regulation and targeting of terminal conditions. The simultaneous control of the PSD and MWD by manipulating the

monomers flow rates of styrene and MMA, surfactant flow rate, initiator flow rate and the reactor temperature is therefore considered. A 5×4 formulation is defined for the multi-constrained optimal control problem for maximising the breadth of the PSD while maintaining the number average molecular weight (M_n) at set point, and for maximizing the M_n. A major improvement in the process operation and polymer property control was evident upon the implementation of the multivariable MPC to the reactor. The manipulation of the four flow rates and the temperature increased the degree of freedom in the system and achieved better PSD and MWD control. The online MPC results are to be presented in this chapter.

An intelligent control hierarchy is formulated for such distributed parameter system incorporating three different levels; offline optimisation, on-line DMC and regulatory control successively. The novelty of this approach is the incorporation of a validated high order dynamic model as a soft sensor for on-line feedback of the PSD and MWD. Figure 6.1 shows the schematic diagram of the overall control hierarchy. The secondary set points are determined by the MPC to target the set points from the optimisation process. Knowledge based supervisory control, sits on the top of the levels.

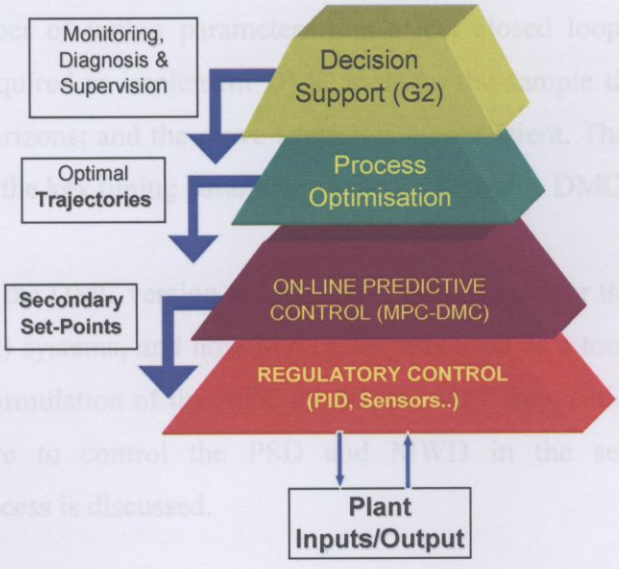

Figure 6.1 Model Framework

6.3 Model Predictive Control Algorithm

Model Predictive Control (MPC) is a methodology that refers to a class of control algorithms in which a dynamic model of the plant is used to predict and optimize the future behaviour of the process. At each control interval, the MPC algorithm computes an open-loop sequence of the manipulated variables in such a way to optimize the future behaviour of the plant. The first value in this optimal sequence is injected into the plant, and the optimization process is repeated at the subsequent control intervals.

Model Predictive Control (MPC) refers to a family of control algorithms that employ an explicit model to predict the future behavior of the process. A simple and common form of MPC control is the Smith predictor. The Smith predictor has been known to enhance control of processes with large dead times. The use of the original Smith predictor control structure with integrating processes will result in an offset problem during certain disturbance rejection scenarios. Another popular MPC algorithm, which is an unconstrained multivariable control algorithm (Culter and Ramaker, 1979) named Dynamic Matrix Control (DMC) was developed by engineers at Shell Oil brought forth. One of the limitations of classical DMC is that it requires the internal DMC step response process model to describe a stable plant. To allow for the differences in the dynamics of integrating processes over stable processes, the DMC algorithm is modified to account for this unstable behavior. Designing a Dynamic Matrix Controller (DMC) is challenging because of the number of tuning parameters that affect closed loop performance. The tuning parameters required to implement DMC include: the sample time; the prediction, model and control horizons; and the move suppression coefficient. The move suppression coefficient is used as the key tuning parameter to obtain desirable DMC performance.

Regarding this work, the DMC version of MPC form is presented for the MIMO (multiple-input multiple-output) systems, and how MATLAB was used as a tool to solve the MPC problem. After the formulation of the MPC model, the MPC application developed in the proposed architecture to control the PSD and MWD in the semi-batch emulsion copolymerisation process is discussed.

6.3.1 Model Identification

Model Predictive Control (MPC) is widely adopted in industry as an effective means to deal with large multivariable constrained control problems. The main idea of MPC is to choose the control action by repeatedly solving on line an optimal control problem. This aims at minimizing a performance criterion over a future horizon, possibly subject to constraints on the manipulated inputs and outputs, where the future behaviour is computed according to a model of the plant. Issues arise for guaranteeing closed-loop stability, to handle model uncertainty, and to reduce on-line computations.

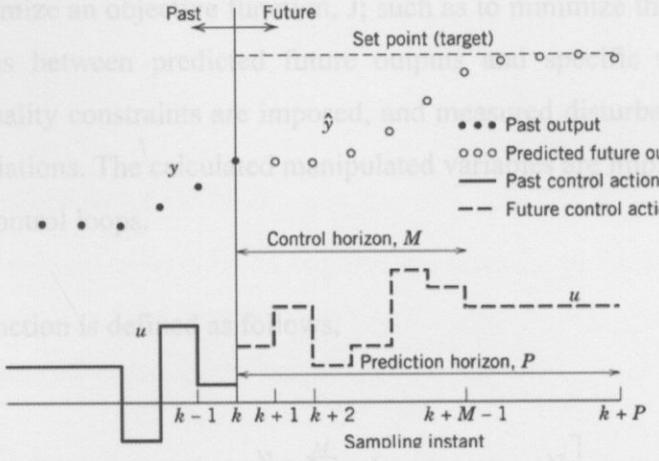

Figure 6.2. Basic Concept for Model Predictive Control

MPC receives an optimal steady-state operating point from an overlying optimizer or they may compute an optimal operating point using an internal steady-state optimizer. The general objectives of an MPC controller, in order of importance, are:

1. prevent violation of input and output constraints
2. drive the controlled variables to their steady-state optimal values (dynamic output optimization)
3. drive the manipulated variables to their steady-state optimal values using remaining degrees of freedom (dynamic input optimization)
4. prevent excessive movement of manipulated variables
5. when signals and actuators fail, control as much of the plant as possible.

The translation of these objectives into a mathematical problem statement involves a number of approximations and trade-offs that define the basic character of the controller. Like any design problem there are many possible solutions.

MPC has basic concepts in order to understand its way of control. Future values of output variables are predicted using a dynamic model of the process and current measurements. Unlike time delay compensation methods, the predictions are made for more than one time delay ahead. The control calculations are based on both future predictions and current measurements. The manipulated variables, $\boldsymbol{u}(k)$, at the k-th sampling instant are calculated so that they minimize an objective function, J; such as to minimize the sum of the squares of the deviations between predicted future outputs and specific reference trajectory. Inequality & equality constraints are imposed, and measured disturbances are included in the control calculations. The calculated manipulated variables are implemented as set point for lower level control loops.

The objective function is defined as follows,

$$J=\min_{\Delta u}\left[\sum_{i=1}^{P}\delta\left(y^{setpoint}(k+i)-y(k+i)\right)^2+\sum_{i=1}^{M}\lambda\left(\Delta u(k+X-i)\right)^2\right] \qquad \text{(Eq. 6.1)}$$

subject to:

constraints on the input moves: $\Delta u(k)\in[\Delta u_{min},\Delta u_{max}]$

constraints on the input: $u(k)\in[u_{min},u_{max}]$

constraints on the output: $y(k)\in[y_{min},y_{max}]$

where δ is the weight on the error, a W×W diagonal matrix, and λ is the weight on the input (suppression move), a X×X diagonal matrix. It is important to note that MPC control is used rather than PID controllers for certain reasons, stated:

1. Processes are difficult to control with standard PID algorithm (e.g., large time constants, substantial time delays, inverse response, etc.

2. There are significant process interactions between inputs (*u*) and outputs (*y*), i.e., more than one manipulated variable has a significant effect on an important process variable. Moreover, constraints (limits) on process variables and manipulated variables are important for normal control

Dynamic model for MPC can be either physical or empirical (but usually empirical). It could be linear or nonlinear (but usually linear). Typical linear models used in MPC are:

1. Transfer function models
2. State-space models
3. Step response models

6.3.2 Multivariable Case (MIMO)

In Equation 6.1, the objective function requires the model future predictions, $y(k+i)$. The model future predictions for a Single input-Single output (SISO) system are calculated at every sampling time using the following:

$$y(k+1)=\sum_{i=1}^{N} a_i \Delta u(k+1-i)+y^{ss}(k+1)+d(k+1) \qquad \text{(Eq. 6.2)}$$

The unmeasured disturbances are included in the last term on the right hand side of Equation (6.2). For MIMO systems, the model predictions are calculated as follows:

$$\mathbf{y}(k+L)=\sum_{i=1}^{N} \mathbf{a}_i \mathbf{\Delta u}(k+L-i)+\mathbf{y}^{ss}(k+L)+\mathbf{d}(k+L) \qquad \text{(Eq. 6.3)}$$

where y is a z-dimensioned vector of outputs, Δu is a w-dimensioned vector of control moves, a_i is a z×w matrix of step response coefficients at the i^{th} interval, , y^{ss} is the vector of initial conditions, and d the disturbance vector. Equation (6.3) reduces to Equation (6.2), when z = w = 1.

The step response coefficients for the SISO system in Equation (6.3), is calculated as follows:

$$a_i = \frac{y^{step}(k+i) - y^{ss}(k+i)}{u(k+i) - u^{ss}} \qquad \text{(Eq. 6.4)}$$

For the MIMO case, the dynamic matrix A is composed of W×X dimensions of step response coefficients matrices,

$$A = \begin{bmatrix} A_{11} & A_{12} \cdots\cdots A_{1w} \\ A_{21} & A_{22} \cdots\cdots A_{2w} \\ \vdots & \vdots \qquad\quad \vdots \\ A_{z1} & A_{z2} \cdots\cdots A_{zw} \end{bmatrix} \qquad \text{(Eq. 6.5)}$$

The weighting matrices in the MIMO case are defined as follows:

$$\boldsymbol{\lambda} = \underbrace{\mathrm{diag}(\lambda_1 \cdots \lambda_1 \; \lambda_2 \cdots \lambda_2 \cdots \lambda_w \cdots \lambda_w)}_{M} \qquad \text{(Eq. 6.6)}$$

and

$$\boldsymbol{\delta} = \underbrace{\mathrm{diag}(\delta_1 \cdots \delta_1 \; \delta_2 \cdots \delta_2 \cdots \delta_z \cdots \delta_z)}_{P} \qquad \text{(Eq. 6.7)}$$

6.3.3 Tuning in MPC

Tuning of unconstrained and constrained DMC for SISO and multivariable systems has been addressed by an array of researchers. In the past, systematic trial-and-error tuning procedures have been proposed(Cutler, 1983, Ricker, 1991). (Marchetti et al., 1983) presented a detailed sensitivity analysis of adjustable parameters and their effects on DMC performance. The method of principal component selection was presented by (Maurath et al., 1988, Maurath et al., 1985) as a method to compute an appropriate prediction horizon and a move suppression coefficient (Callaghan and Lee, 1988). Other tuning strategies for DMC have concentrated on specific aspects such as tuning for stability, robustness and performance. Although some of the methods provide a complete design of DMC, they also require fairly sophisticated analysis tools and an advanced knowledge of control concepts for their implementation. Hence, there still exists a need for easy-to-use tuning strategies

for DMC. Tuning of unconstrained SISO DMC is challenging because of the number of adjustable parameters that affect closed-loop performance. These include the following: a finite prediction horizon, P; a control horizon, M; a move suppression coefficient, λ; a model horizon, N; and a sample time, T. The first problem that needs to be addressed is the selection of an appropriate set of tuning parameters from among those available for DMC. Practical limitations often restrict the availability of sample time, T, as a tuning parameter (Franklin and Powell, 1980). The model horizon is also not an appropriate tuning parameter since truncation of the model horizon, N, misrepresents the effect of past moves in the predicted output and leads to unpredictable closed-loop performance (Lundstrom et al., 1995). In the case of multivariable optimisation, the number of parameters needed to be tuned is much higher.

6.3.4 MPC setup

MATLAB is a tool used to solve MPC problems. MATLAB is an abbreviation for MATrix LABoratory. MATLAB is a high-level programming environment that processes arrays and matrices and provides a powerful graphical environment.

The transfer functions were needed for the multiple input multiple output (MIMO) system between the five inputs and the four outputs. The inputs of the MIMO system are the manipulated variables, including the flow rates of monomers, styrene and MMA, the surfactant and initiator flow rate, along with the temperature of the reaction, giving a total of five inputs. The outputs are four in numbers, where the targets are the average radius, PSPI, M_n, and the conversion. On that MIMO system, twenty transfer functions were obtained to solve the MIMO control problem.

In order to obtain the transfer functions, the model of the plant is run to obtain the dynamic matrix control, between the five inputs, and the four outputs. The four outputs are represented as a matrix of set points. The DMC is used to obtain the transfer functions of the process, which are considered to be a linear representation of the model. The linear model used in the MPC Toolbox for prediction and optimization is depicted in Figure 6.3.

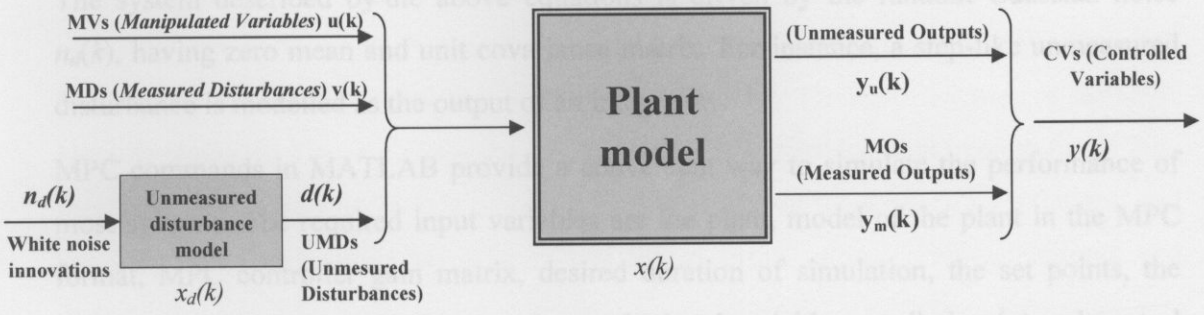

Figure 6.3 Model Used for MPC

The model consists of

- A model of the 'plant' to be controlled, whose inputs are the manipulated variables, the measured disturbances, and the unmeasured disturbances
- A model generating the unmeasured 'disturbances'

The model of the plant is a linear time-invariant (LTI) system described by the equations:

$$x(k+1) = Ax(k) + B_u u(k) + B_v v(k) + B_d d(k) \qquad \text{(Eq. 6.8)}$$

$$y_m(k) = C_m x(k) + D_{vm} v(k) + D_{dm} d(k) \qquad \text{(Eq. 6.9)}$$

$$y_u(k) = C_u x(k) + D_{vu} v(k) + D_{du} d(k) + D_{uu} u(k) \qquad \text{(Eq. 6.10)}$$

where $x(k)$ is the n_x-dimensional state vector of the plant, $u(k)$ is the n_u-dimensional vector of manipulated variables, i.e., the command inputs, $v(k)$ is the n_v-dimensional vector of measured disturbances, $d(k)$ is the n_d-dimensional vector of unmeasured disturbances entering the plant, $y_m(k)$ is the vector of measured outputs, and $y_u(k)$ is the vector of unmeasured outputs. The overall output vector $y(k)$ collects $y_m(k)$ and $y_u(k)$. In the above equations $d(k)$ collects both state ($Bd \neq 0$) disturbances and output disturbances ($Dd \neq 0$) . The unmeasured disturbance $d(k)$ is modelled as the output of the LTI system.

$$x_d(k+1) = \overline{A}x_d(k) + \overline{B}n_d(k) \qquad \text{(Eq. 6.11)}$$

$$d(k) = \overline{C}x_d(k) + \overline{D}n_d(k) \qquad \text{(Eq. 6.12)}$$

The system described by the above equations is driven by the random Gaussian noise $n_d(k)$, having zero mean and unit covariance matrix. For instance, a step-like unmeasured disturbance is modelled as the output of an integrator.

MPC commands in MATLAB provide a convenient way to simulate the performance of most systems. The required input variables are the plant, model of the plant in the MPC format, MPC controller gain matrix, desired duration of simulation, the set points, the limits onto the set points, limits onto the manipulated variables, prediction (p) and control (m) horizon, filter noise, the disturbance model and the initial conditions of the manipulated variables.

6.3.4.1 MPC Controller Block

Simulink is a platform for multi-domain simulation and model-based design of dynamic systems. It provides an interactive graphical environment and a customizable set of block libraries that let you accurately design, simulate, implement, and test control, signal processing, communications, and other time-varying systems.

The MPC Simulink Library provides a single block representing the MPC controller.

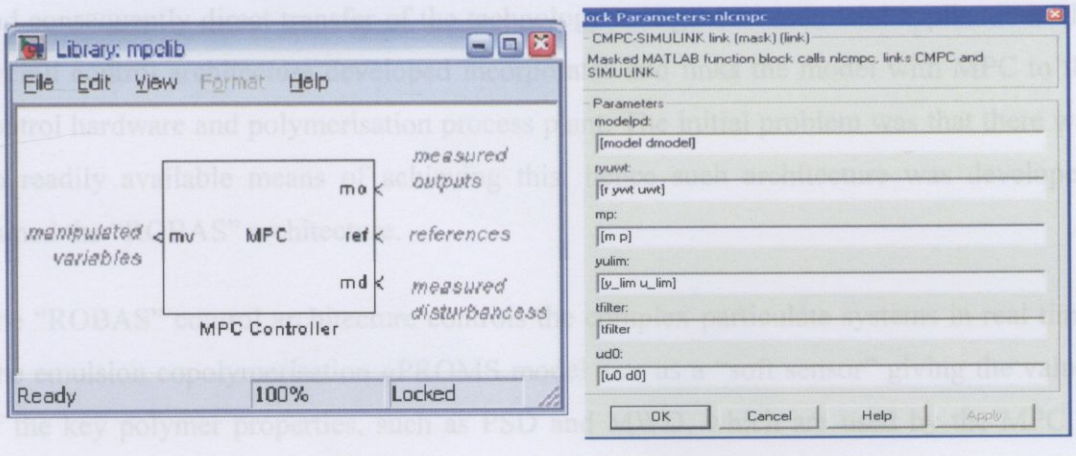

(a) (b)

Figure 6.4 MPC Simulink Library

The MPC block in Simulink would have the inputs as measured outputs, references or measured disturbances. Hard bounds on manipulated variables and/or controlled variables using linear models in the MPC step format for nonlinear plants must be determined. The outputs from MPC block are the values of the manipulated variables. Initial conditions for

the manipulated variables and the measured disturbances must be specified. The controlled variables sent to MPC block and the manipulated variables returned by MPC Simulink block are actual variables; they are not deviation variables. The representation of the MPC block is shown in Figure 6.4. Figure 6.4(b) shows the parameters that need to be defined including the setpoint (r), weight on output (ywt), weight on input (uwt), m, p (control and prediction horizon), limits on outputs and inputs (ylim, ulim), initial conditions and disturbances (u_o, d_o).

Closed-loop simulations can be run while the MPC controller is edited in the MPC Design Tool in MATLAB. In this case, the controller parameters used for simulating the Simulink diagram are those currently specified in the MPC Design Tool, so that the parameters of the controller can be more easily tuned. The designed controller must be exported to the workspace in order to be used in simulation within Simulink.

6.4 Real-Time Implementation Architecture

The whole online control application strategy has been developed within a gPROMS-API-DCS environment to allow for real-time implementation of a model-based control strategy and consequently direct transfer of the technology to a general industrial application. The overall control architecture developed incorporates and links the model with MPC to the control hardware and polymerisation process plant. The initial problem was that there was no readily available means of achieving this; hence such architecture was developed, named the "ROBAS" architecture.

The "ROBAS" control architecture controls the complex particulate systems in real time. The emulsion copolymerisation gPROMS model acts as a "soft sensor" giving the values of the key polymer properties, such as PSD and MWD, which are used by the MPC to determine the new secondary set points. The on-line "soft sensor" is embedded within Mathworks Simulink (http://www.mathworks.com) and works in conjunction with the MPC, which is also developed into Simulink. The link to the plants control system was developed in C++, and provides real time monitoring or manipulation of plant data within MATLAB or Simulink. Two of these links were developed, one which supports Honeywell PlantScape controllers, and another which supports any control system which has an OPC Server; the former one being faster and so more efficient.

The ROBAS Architecture applied to the polymerisation process controlled by a Honeywell PlantScape DCS is shown in Figure 6.6. The I/O module is the main interface between the DCS system and the process. It converts signals to digital form, and it also works for signal filtering. The local I/O Bus standards are the Ethernet and the Control Net. The controller modules receive the data; perform process calculations and sends actuator signals. The controller modules link data highway to controller modules and to user interfaces, which is a device to integrate displays and controls for operators. MATLAB – gPROMS – Honeywell Link are explained in the following section.

gPROMS and the MPC run within Mathworks Simulink and communicate with the polymerisation process by software bridges developed in C++ via either OPC or the Honeywell Network API interfaces. These interfaces communicate over TCP/IP over Ethernet to the PlantScape Server. The OPC server or Honeywell service then process the send and receive requests and forward them over ControlNet to the controller where from there they are processed to the I/O to interact with the plant.

The novelty of the real-time implementation architecture is that it controls the complex particulate systems on real time. Figure 6.5 shows the real-time implementation architecture.

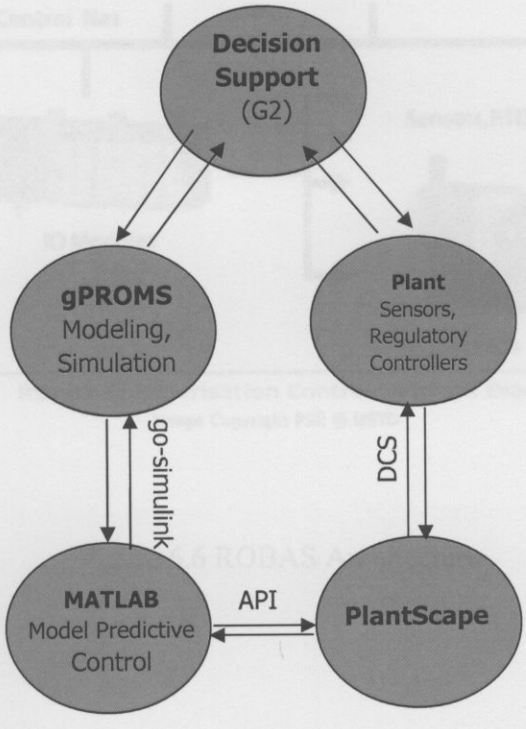

Figure 6.5 Real-time Implementation Architecture

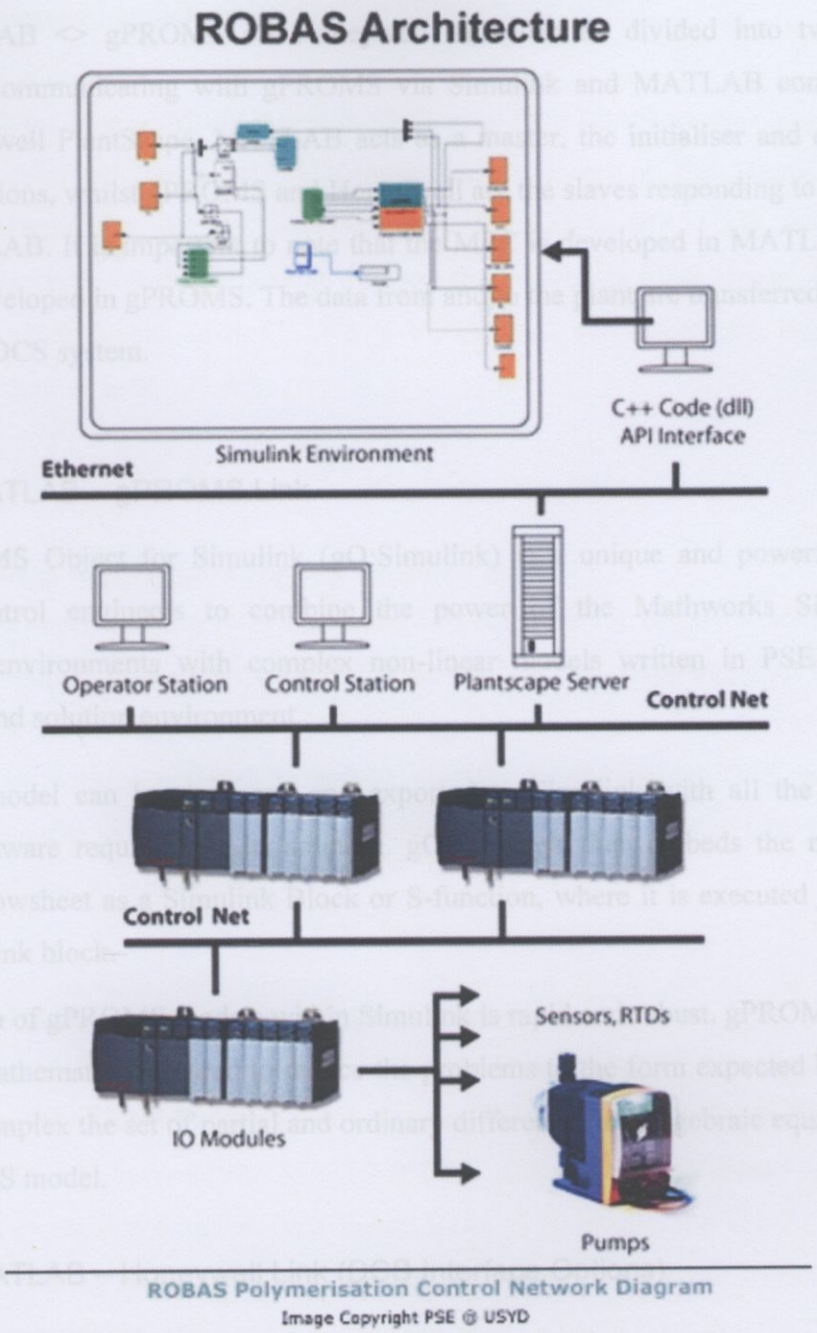

Figure 6.6 ROBAS Architecture

6.4.1 MATLAB – gPROMS – Honeywell Link

The MATLAB <> gPROMS <> Honeywell Link can be divided into two sections; MATLAB communicating with gPROMS via Simulink and MATLAB communicating with Honeywell PlantScape. MATLAB acts as a master, the initialiser and controller of communications, whilst gPROMS and Honeywell are the slaves responding to the requests from MATLAB. It is important to note that the MPC is developed in MATLAB, and the model is developed in gPROMS. The data from and to the plant are transferred through the Honeywell DCS system.

6.4.1.1 MATLAB – gPROMS Link

The gPROMS Object for Simulink (gO:Simulink) is a unique and powerful tool that enables control engineers to combine the power of the Mathworks Simulink and MATLAB environments with complex non-linear models written in PSE's gPROMS modelling and solution environment.

gPROMS model can be packaged and exported to Simulink with all the solvers and support software required for its solution. gO:Simulink then embeds the model in the Simulink flowsheet as a Simulink Block or S-function, where it is executed just like any other Simulink block.

The solution of gPROMS models within Simulink is rapid and robust. gPROMS takes care of all the mathematics required to reduce the problems to the form expected by Simulink, however complex the set of partial and ordinary differential and algebraic equations within the gPROMS model.

6.4.1.2 MATLAB – Honeywell Link (DCS Interface Options)

MATLAB provides DCS Interface technology that allows users to connect their dynamic models to external applications depending on the DCS hardware as well as your specific needs. MATLAB provides an API (Application Program Interface) that enables users to interface MATLAB with software or interfaces written in other programming languages, hardware devices using their own communication protocol, and clients or servers communicating via Component Object Model (COM) or Dynamic Data Exchange (DDE).

The interfaces, depending on their type, can be implemented in C, C++, FORTRAN, or Visual Basic programming languages.

The interface for linking MATLAB with C, C++ or FORTRAN routines is called a Mex file, and is compiled into a DLL (Dynamic Link Library) on the Microsoft Window Operating System. A mex file provides a mex function in MATLAB, which receives inputs and provides outputs. However the mex function takes these inputs and processes them in functions developed in C, C++ or FORTRAN, and returns the results of these functions as outputs in MATLAB.

There are two methods for implementing an interface to a DCS package.

6.4.1.2.1 Direct Application Program Interface (API)

This approach uses existing DCS hardware API software for linking external programs. All that is required is to create a DCS linking DLL which maps the MATLAB process information to the DCS. The primary advantage of this approach is that the MATLAB model can be locally updated to reflect changes to the actual DCS configuration. Additional benefits include a direct connection to the DCS hardware and the ability to take the entire platform to remote sites.

6.4.1.2.2 DCS Data Transfer via OLE Automation

This method makes use of the Process Data Table object in MATLAB. Process Variables contained in a MATLAB Process Data Table may be assigned tags. These tags are used to read and write data between the MATLAB OLE Automation Server and some external system. The external system can be a Visual Basic (VB) bridge to a vendor's DCS or an operator training simulator. This approach has similarities to both the Direct API and the middleware approaches. Vendor DCS API calls may be made from the VB Bridge similar to DCS API calls from a direct MATLAB DCS driver. The VB Bridge is similar to the middleware layer since there is a two step process to the data transfer.

The Direct Application Program Interface (API) was the method used to read and write to the plant through the DCS hardware between MATLAB (Simulink) and Honeywell. For online MPC, the mex function was created using C++, enabling MATLAB to

communicate with the Honeywell PlantScape DCS via means of the dynamic link library (DLL).

A simple form of the architecture can be shown in the following figure:

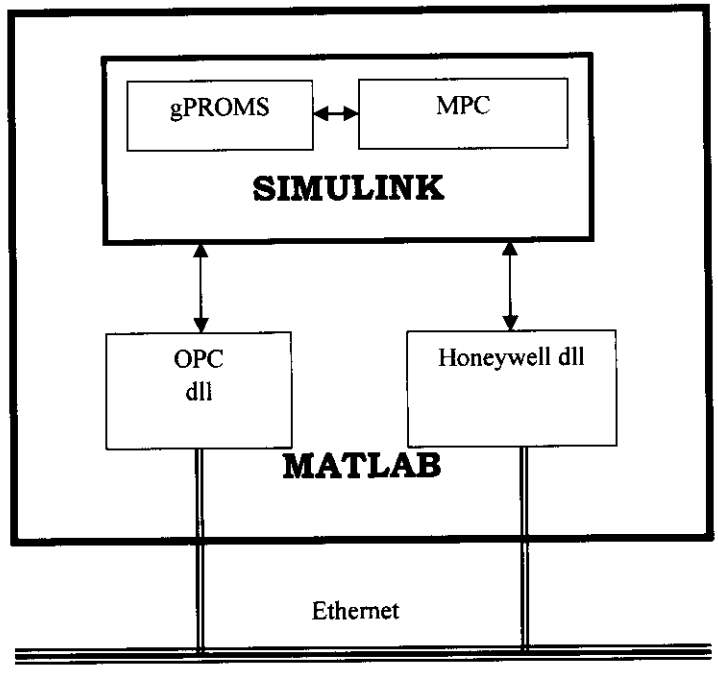

Figure 6.7 Simple form of ROBAS Architecture

6.4.2 Two Way Data Communication

The two way data communication of reading and writing from and to Honeywell, as explained is a mex function created using C++, enabling MATLAB to communicate with the Honeywell PlantScape DCS via means of a dynamic link library (dll). The syntax written in MATLAB is as follows:

write_Honeywell(*servername*, *point name*, *parameter name*, *parameter value*);

where:

servername is the name of the Honeywell server and is a string/char-array type

point name is the name of the point on the server and is a string/char-array type

***parameter** name* is the name of parameter within the point and is a string/char-array type

***parameter** value* is the value to be written to the parameter and is a double floating point type when writing numbers and a string/char-array type when writing text

For reading the data, one output is required. The syntax for reading from Honeywell is as follows:

"Output" = read_Honeywell(*servername*, *point name*, *parameter name*);

A user interface is used to ease the way of communication to the plant. The data is stored in MATLAB, and can be viewed in the MATLAB window, as well as in the Control Station software. Alarms are also shown in the Control Station software, as a supervisory control to ensure better performance.

6.5 Real time Control of Semi-Batch Emulsion Copolymerisation Reactor

The demand for online sensing for polymer properties in industry is increasing. The reasons behind the motivation towards online sensing are to be capable of controlling the process and to produce the product with consistent quality, and to able to adapt with the changes in the process due to the disturbances. On the other hand, the analysis time for PSD control using the CHDF and Zetasizer would require about a 2 hour analysis, and for the MWD control, the GPC would require for one sample, at least a period of 10 hours. This simply concludes that the data obtained from the analysis cannot be used for online sensing. The mathematical model developed predicts the key polymer properties, and in this section, it will be shown how the model works in the proposed architecture in order to control the process.

It is very important to note that the plant is run by just running the Simulink model, where it runs the model developed in gPROMS, and the MPC developed in MATLAB, as well as the reading and writing data from and to Honeywell on real time. The data includes the values of the temperature and the flow rates read by Simulink from the plant, and the

values calculated by MPC developed in Simulink sent to the plant as set point values. In order to calculate on-line the optimal trajectory an input/output model predictive controller (MPC) was developed as described in Section 6.3. In this control framework, the full dynamic model was run in parallel and used as a "soft sensor" to provide an on-line estimate of the PSD and MWD. The motive behind choosing MPC is the fact that it is the only strategy that can incorporate a number of performance criteria and is capable of utilising any available dynamic process model.

The operating conditions, which are used as manipulated variables in the MPC formulation include the four flow rates and reactor temperature. The manipulated variables are measured using on-line measurements connected to the DCS system, through Honeywell, to Simulink, and used by the dynamic model to estimate the PSD, MWD and conversion. Note that PlantScape Honeywell system interfaces the copolymerisation reactor to the computer running the MPC package, the latter being in MATLAB (Simulink).

The PSD, MWD and conversion measurements are obtained from the mathematical model, which is developed in gPROMS and embedded in Simulink, every 10 seconds and fed through the DCS system to the MPC (upper control layer) developed in MATLAB. The MPC would then calculate optimal trajectories, which are then sent as set point signals through the DCS system to the regulatory controllers (lower control layer). In order to validate the predicted results, off-line samples are also taken from the process for PSD, MWD and conversion measurements. The MPC formulation was very robust and handles any disturbances to the process.

The implementation of the MPC to two MIMO cases is tested: PSD control by using four manipulated variables including the monomers, styrene and MMA, surfactant and initiator flow rates. The 5×4 MIMO second case included five manipulated variables, using the reactor temperature as an addition manipulated variable, due to its significant effect on MWD.

6.5.1 MPC Application

There are two cases studied for the MPC of the semi-batch emulsion copolymerisation. However, owing to their distributed parameter nature, the PBE equations describing the full PSD cannot be directly used as the basis of synthesis and implementation of the

model-based controller. On the other hand, in order to determine control strategies which can be applied to the reactor, measurable or at least easily observable output variables have to be chosen. The first case was to control the PSD, where a MIMO system of 4 inputs and four outputs are investigated. The second case was to control the MWD, where 5 inputs and 4 outputs (5x4 DMC configuration) are investigated. As mentioned earlier, the second case had the temperature added as one of the manipulated variables, since it showed to have a large effect on the molecular weight. However, owing to their distributed parameter nature, the PBE equations describing the full PSD cannot be directly used as the basis of synthesis and implementation of the model-based controller. On the other hand, in order to determine control strategies which can be applied to the reactor, measurable or at least easily observable output variables have to be chosen.

6.5.1.1 Multivariable Control: PSD and MWD (MIMO)

The first multivariable study case was used to control the PSD, where a bimodal distribution is required. The off-line solution of the optimisation problem studied in chapter 4 is used as set points for the MPC control problem. So the optimal trajectory of the four outputs, including average particle size, PSPI, M_n and conversion was used. The MPC would in return determine the new optimal trajectories to achieve the four setpoints for the four outputs. The formulation was limited with constraints for operational reasons. These constraints are the maximum and minimum value of the operation of the pump. Other constraints were kept also for the polymer property, where a 50/50 copolymer is to be produced.

- The objective function can be defined as follows:

$$J = \min_{\Delta u}\left[\sum_{i=1}^{P}\delta\left(y^{setpoint}(k+i)-y(k+i)\right)^2+\sum_{i=1}^{M}\lambda\left(\Delta F_x(k+M-i)\right)^2\right] \qquad \text{(Eq. 6.13)}$$

It is important to note that $y^{setpoint}$ is a matrix of the set point values for the average radius, PSPI, M_n and conversion.

In this formulation, the outputs were calculated using the step response method. The prediction horizon, the control moves, and the sampling time were set at 30, 1 and 10

seconds, respectively. The (relatively large) magnitude of the sampling time is related to the speed of the process dynamics. As the average volume growth rate for particles in emulsion copolymerisation is very small (of the order 2×10^{-22} L/s), then a relatively long sampling time is needed for discernible changes to be observed.

The weights used on the outputs and the inputs are as follows:

ywt = [$5e^{16}$ 1 $7e^{8}$ 10] ; uwt = [1 1 $1e^{10}$ $1e^{15}$ 1]

The weights on the outputs support the action, while those on the inputs suppress it. For outputs (y_{wt}), the weights correspond to the order of particle average size, M_n, PSPI and conversion, respectively. The reason for the higher weights on the average size is that they are in the range of $1x10^{-8}$, while the M_n is in the range of $1x10^{6}$. A smaller weight is placed on conversion, because it is easier to control and is not significantly affected by the inputs. With respect to inputs, the weights are in the range of monomer flowrate of styrene (FmA), flowrate of MMA (FmB), flowrate of surfactant (Fs), flowrate of initiator (FI) and the reaction temperature (T_{reac}). The weight is greater for the surfactant and initiator concentration to suppress their effects, since they have substantial effects on the outputs. No constraints are imposed on changes in outputs, but constraints are placed on temperature, such that changes in temperature are bound by one-tenth degrees per second.

Other constraints are added to the MPC formulation by keeping the temperature moves within limitations. The constraints on the temperature moves are:

$$\Delta T_{reac} \leq 0.1 \qquad \text{(Eq. 6.14)}$$

Temperature constraints are added for process limitations,

$$T_{reac}(k) \in [70, \quad 85] \qquad \text{(Eq. 6.15)}$$

Initial conditions must be identified for the inputs and outputs of the system. For simplicity, and the strength of the model, the plant model was equal to the model itself.

The output of the set points for the manipulated variables was calculated using

$$[y,u] = cmpc[plant, model, ywt, uwt, m, p, tend, r, u\lim, y\lim]; \quad \text{(Eq. 6.16)}$$

The outputs of the set points are taken by the Simulink block. The MPC developed in Simulink is shown in Figure 6.8.

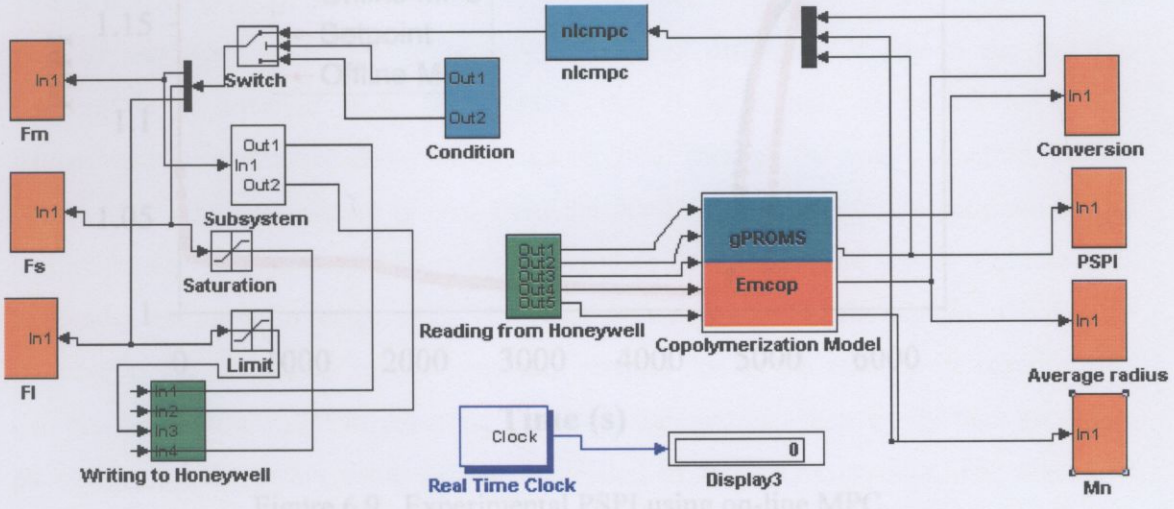

Figure 6.8 MPC of Emulsion Copolymerisation of Styrene and MMA

As shown in Figure 6.8, a real time block had been added, which a special function that had been developed to control the plant on real time. The performance of the control system was evaluated for set point tracking. The MPC controller was able to follow the desired product property trajectories with great accuracy. The PSPI was found to increase during the experiment and the average particle size was at set point for the whole experiment. The M_n was able to reach the desired set point, as well as the conversion. The control moves for both temperature and flow rates, were also kept within the constraints, as no controller saturations were observed during the whole experiment.

For the 1st case to maximise the PSPI, the MPC strategy was implemented to the semi-batch emulsion copolymerisation reactor operating at 75°C. It is important to note that the system was operated with no PSPI control during the batch pre-period of 1500 seconds,

however the system is run in Simulink, and the MPC is applied to the process with feedback from the soft-sensor at 1500s, automatically activated in Simulink. Note that also the temperature of the reaction is read by Simulink through the DCS system, as shown in Figure 6.8.

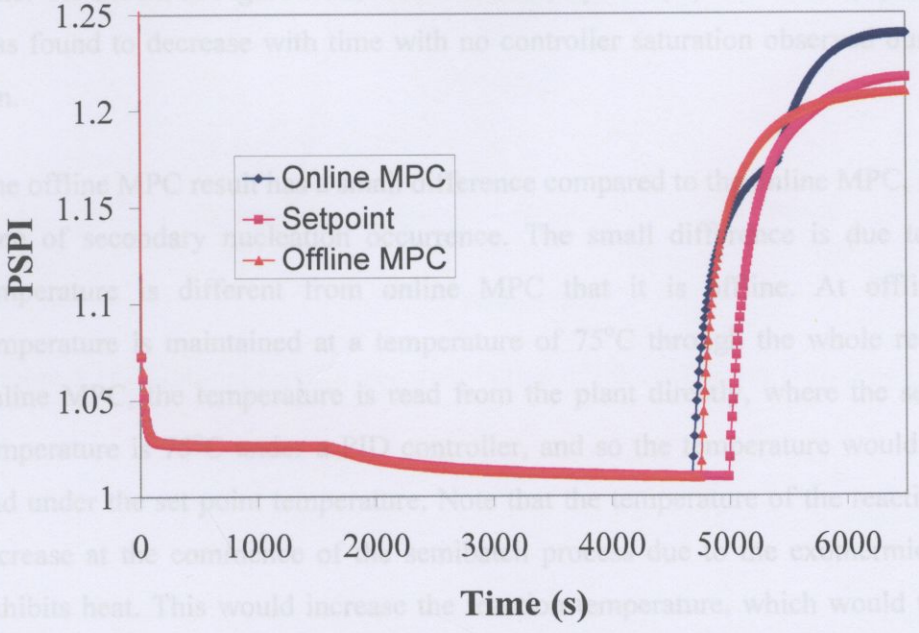

Figure 6.9. Experimental PSPI using on-line MPC.

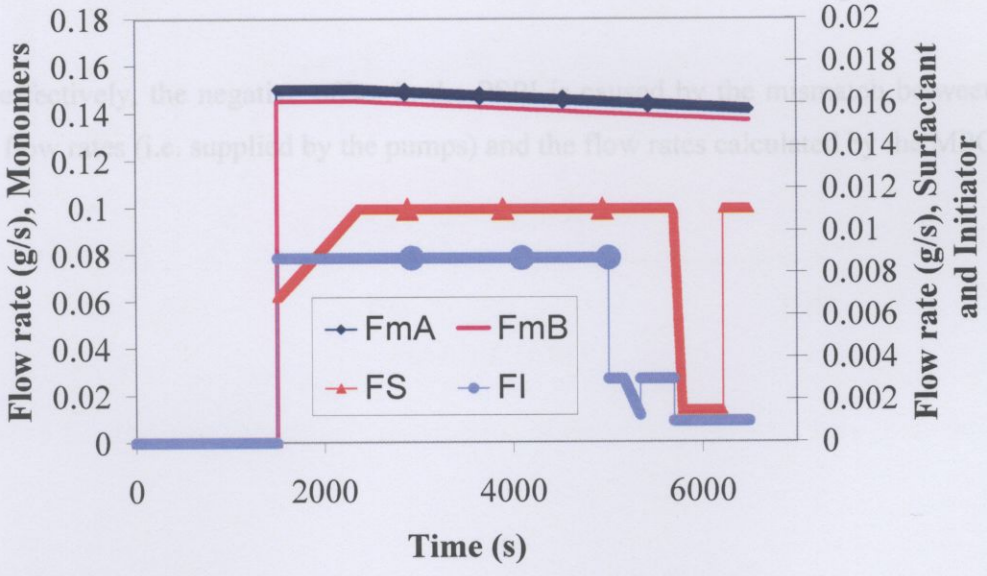

Figure 6.10. Optimal feed profile obtained by online MPC.

The results of the experiment are shown in Figure 6.9 and Figure 6.10. As it can be seen in Figure 6.9, the PSPI increased a 200 seconds delay from the set point. However, the PSPI increased to get closer to the optimal feed rate (and, consequently, the PSD continually broadened). An offset of variable magnitude was apparent at every sampling time. As shown in Figure 6.10, the monomers, styrene (A) and MMA (B) feed rate profile was found to decrease with time with no controller saturation observed during the entire run.

The offline MPC result has a small difference compared to the online MPC, in terms of the time of secondary nucleation occurrence. The small difference is due to the fact the temperature is different from online MPC that it is offline. At offline MPC, the temperature is maintained at a temperature of 75°C through the whole reaction, but on online MPC, the temperature is read from the plant directly, where the set point of the temperature is 75°C under a PID controller, and so the temperature would oscillate over and under the set point temperature. Note that the temperature of the reaction would also increase at the commence of the semibatch process due to the exothermic reaction that exhibits heat. This would increase the reaction temperature, which would then go down, by cooling up the jacket using Julabo, controlled by the PID controller. The mismatch from the flow rate values to the real values of the flow rate in the reaction has also the effect on the PSPI values that are been read by the model.

More effectively, the negative offset in the PSPI is caused by the mismatch between the actual flow rates (i.e. supplied by the pumps) and the flow rates calculated by the MPC.

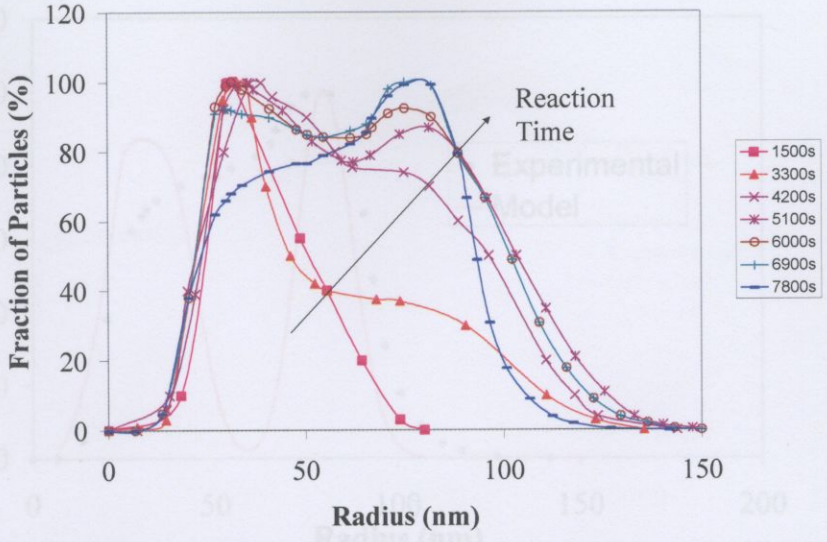

Figure 6.11. Optimal particle size distribution of the copolymer with time (Experimental)

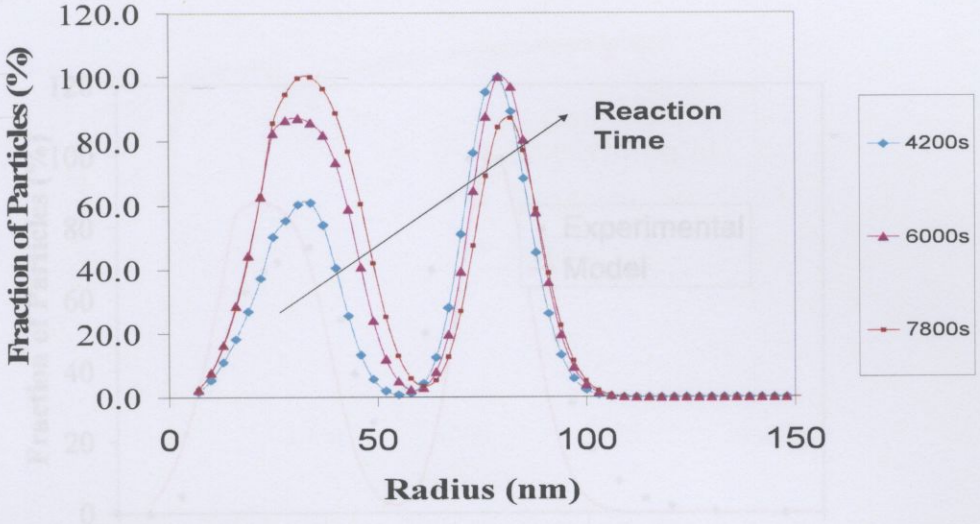

Figure 6.12. Optimal particle size distribution of the copolymer with time (Simulation)

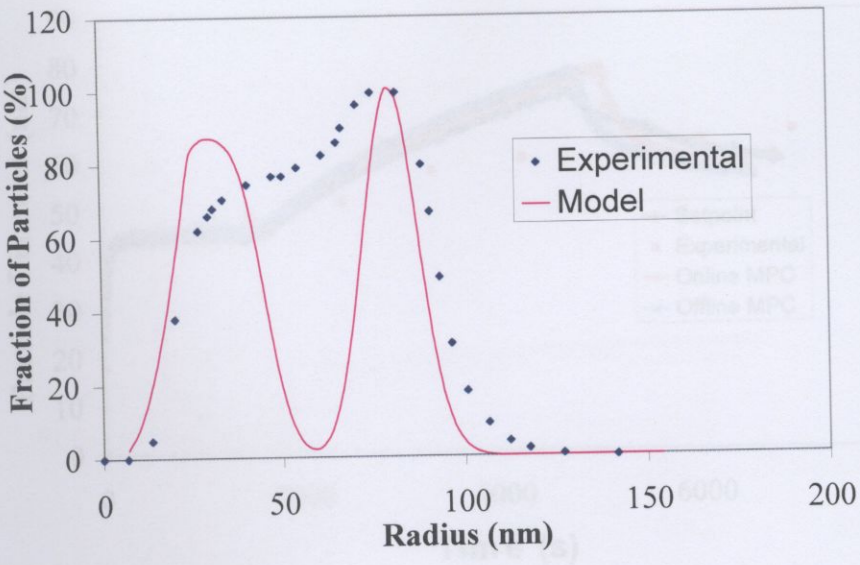

Figure 6.13. Optimal particle size distribution of the final product (Sodium Dodecyl Sulfate)

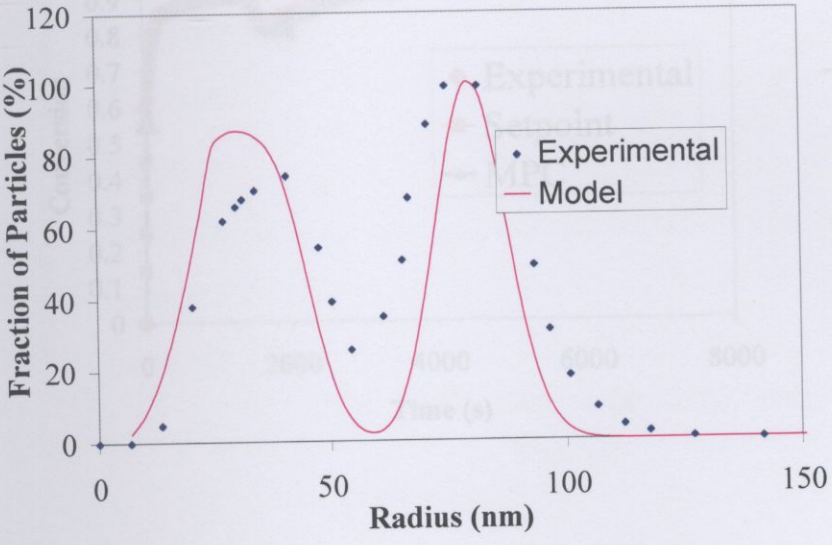

Figure 6.14. Optimal particle size distribution of the final product (AMA – Surfactant)

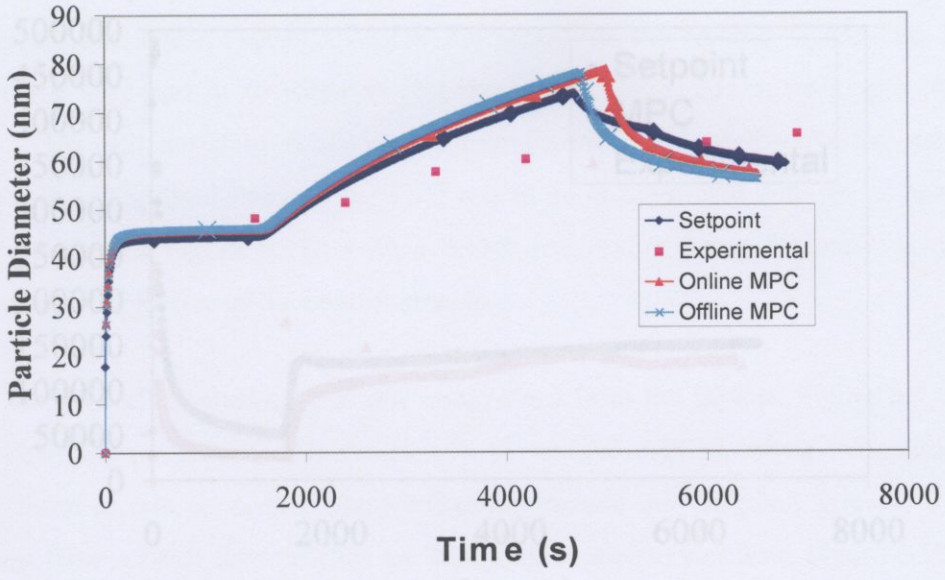

Figure 6.15. Particle size using on-line MPC.

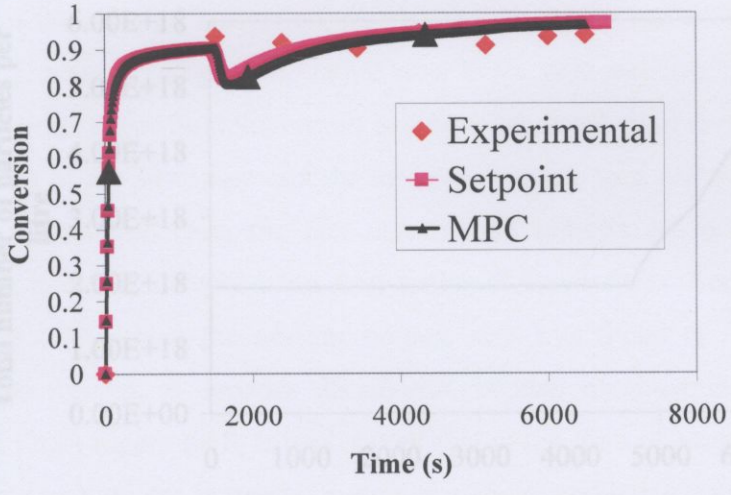

Figure 6.16. Overall Conversion using on-line MPC.

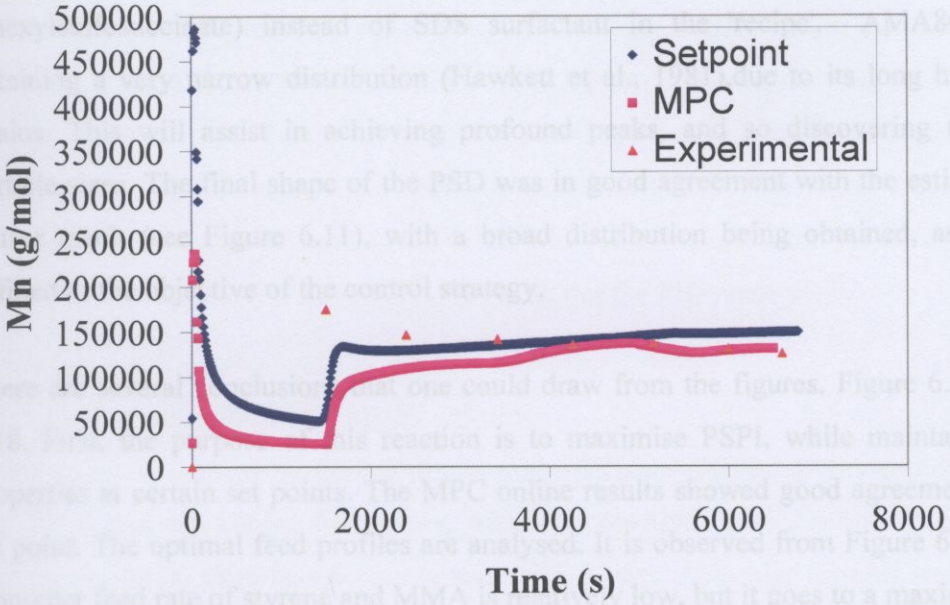

Figure 6.17. M_n using online MPC

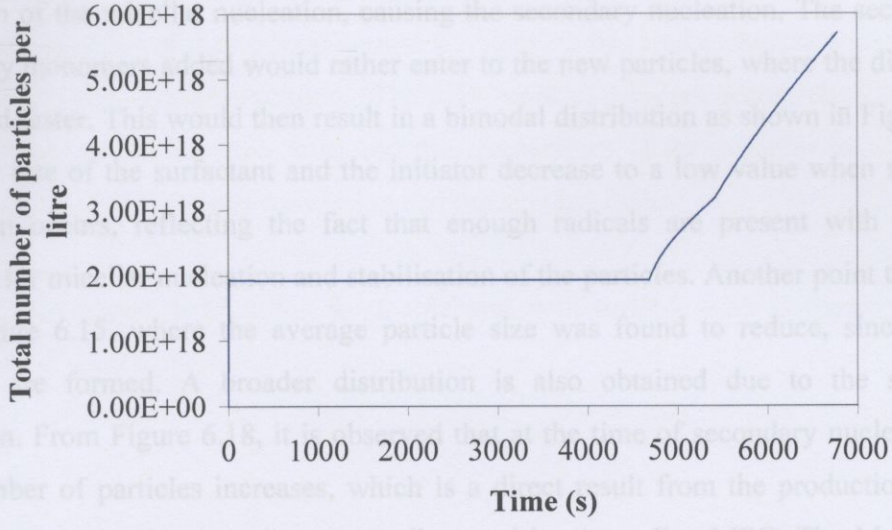

Figure 6.18. Total number of particles (Simulation)

Further investigation is undergone by replacing the using AMA80 (sodium dihexylsulfosuccinate) instead of SDS surfactant in the 'recipe'. AMA80 helps in obtaining a very narrow distribution (Hawkett et al., 1981),due to its long hydrocarbon chains. This will assist in achieving profound peaks, and so discovering the distinct particle sizes. The final shape of the PSD was in good agreement with the estimated soft-sensor result (see Figure 6.11), with a broad distribution being obtained, as originally defined as the objective of the control strategy.

There are several conclusions that one could draw from the figures, Figure 6.9 to Figure 6.18. First, the purpose of this reaction is to maximise PSPI, while maintaining other properties at certain set points. The MPC online results showed good agreement with the set point. The optimal feed profiles are analysed. It is observed from Figure 6.10 that the monomer feed rate of styrene and MMA is relatively low, but it goes to a maximum value, then it starts decreasing. The addition of monomer would result in forming larger particles. The addition of surfactant and initiator would cause two main issues. The first issue is that more radicals are occurring, plus that there more micelles present, which may allow an oligomeric radical to enter the micelle forming new particles. At that instant of time, where new particles are formed, the concentration of micelles increases, which is an indication of the micellar nucleation, causing the secondary nucleation. The second issue is that any monomers added would rather enter to the new particles, where the diffusion is easier and faster. This would then result in a bimodal distribution as shown in Figure 6.11. The flow rate of the surfactant and the initiator decrease to a low value when secondary nucleation occurs, reflecting the fact that enough radicals are present with sufficient micelles, for micellar nucleation and stabilisation of the particles. Another point to observe is in Figure 6.15, where the average particle size was found to reduce, since smaller particles are formed. A broader distribution is also obtained due to the secondary nucleation. From Figure 6.18, it is observed that at the time of secondary nucleation, the total number of particles increases, which is a direct result from the production of new particles. The overall conversion was well agreed by the online MPC. The M_n was also one of the set points in the matrix, and showed good agreement. Due to the addition of the surfactant, the M_n had a low value. In Figure 6.14, AMA surfactant was used to produce profound peaks to see the bimodal distribution. This was found to have very good agreement with the MPC online results.

The offline MPC results compared with online MPC results in Figure 6.15 showed a similar fashion to Figure 6.9, where the secondary nucleation occurred a litter later that what would be expected from the offline MPC results, but still following up the set point. As it was explained, the offset of offline to online results was due to the mismatch of the values of the four flow rates and reaction temperature. The mismatch was very small, since the pumps were calibrated, and so the offset was very small. The temperature mismatch is expected, and therefore, it is being controlled under the PID controller.

6.5.1.2 Multivariable MPC: MWD Control

A constraint is defined by the maximum and minimum operating temperatures, of 90°C and 70°C, due to process limitations, where no reaction occurs below 67 degrees and degradation occur above the higher temperature. Lower molecular weights were produced at higher temperatures. This is related to the change in transfer and termination kinetic events, as explained in previous chapters. A much lower temperature would increase the molecular, but to the extent where a reaction occurs.

The second multivariable case studied was used to mainly maximise the M_n, while maintaining the average particle size, overall conversion, and PSPI at specified set points. The off-line solution of the optimal control problem studied in the chapter 4 is used as set points for the MPC control problem. The MPC control problem accurately followed the optimal trajectory of the flow rates and the temperature of the reaction to achieve the setpoints of M_n, PSPI, overall conversion and the average radius.

The MPC developed in Simulink for the second multivariable case is shown in Figure 6.19.

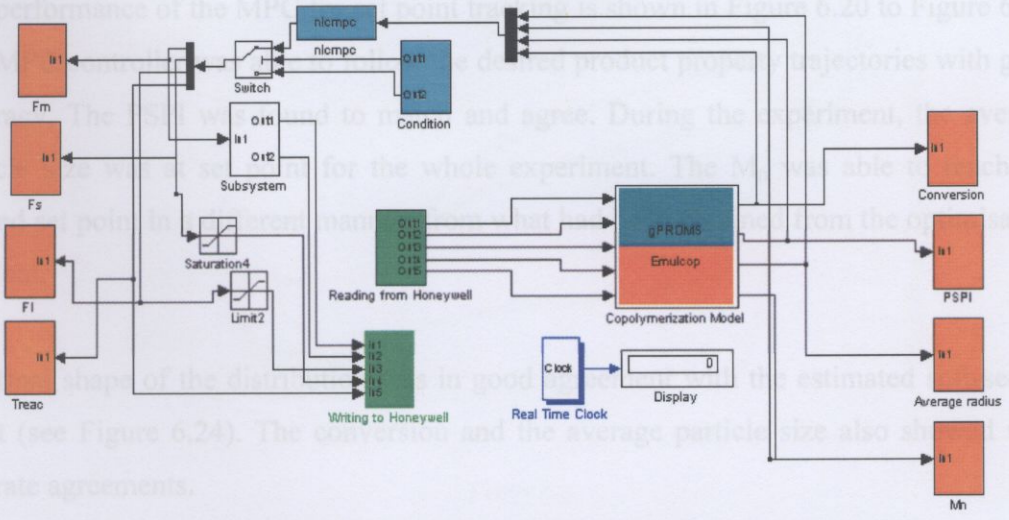

Figure 6.19 MPC of Emulsion Copolymerisation of Styrene and MMA

As shown in Figure 6.19, there are two blocks showing the reading and writing to the plant through the Honeywell system. The values of the new set points calculated by the MPC are sent to the plant. The gPROMS model in Simulink will then read the values of the manipulated variables from the plant. This will ensure that values obtained by the model will have no mismatch. A PID controller in the Control Builder software is used to control the temperature of the reaction. The PID controller is cascaded over the PID controller that is built in the heat circulator. It can also be observed from the figure that the values of the outputs, including the conversion, average particle size, M_n, and the PSPI are sent to the MPC as the set points of the outputs (in a matrix form).

The MPC controller was capable of achieving the desired optimal trajectories of the product. The control moves for both temperature and flow rates, were also kept within the constraints. It should be noted that there are twenty transfer functions, in a matrix of 5x4 was developed and investigated. The outputs of the "cmpc" MATLAB command are used by the MPC Simulink block "nlcmpc". The prediction horizon, the control moves, and the sampling time were kept at 60, 1 and 10 seconds, respectively. The formulation for MW control was less complicated due to the quick response of the MW to temperature changes and the non-transient behaviour exhibited by the M_n (which characterises the free-radical addition polymerisation).

The performance of the MPC for set point tracking is shown in Figure 6.20 to Figure 6.25. The MPC controller was able to follow the desired product property trajectories with great accuracy. The PSPI was found to match and agree. During the experiment, the average particle size was at set point for the whole experiment. The M_n was able to reach the desired set point in a different manner, from what had been obtained from the optimisation problem.

The final shape of the distribution was in good agreement with the estimated soft-sensor result (see Figure 6.24). The conversion and the average particle size also showed very accurate agreements.

The soft sensor supplies the online measurements of the outputs each second, relying in its calculations on the manipulated variables that are provided by the MPC. The MPC depends on its future predictions on comparing the value of the output calculated by the soft sensor, and the value of the setpoint profile to be achieved. The soft sensor plays a centre role in the architecture. The soft sensor developed (mathematical model) is embedded in Simulink, and the MPC formulation is put into Simulink as a block. Moreover, the writing and reading process to the DCS system is done in Simulink. This makes it easier for the process engineer to control the process. The display of the results can be seen online, in MATLAB, or in Honeywell. However, all of the data are saved in a file.

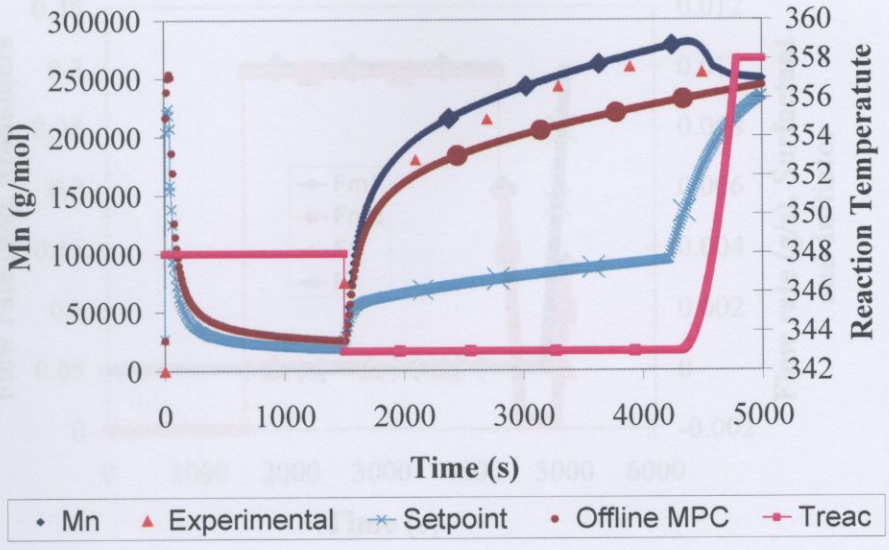

Figure 6.20. Experimental M_n using on-line multivariable constrained MPC.

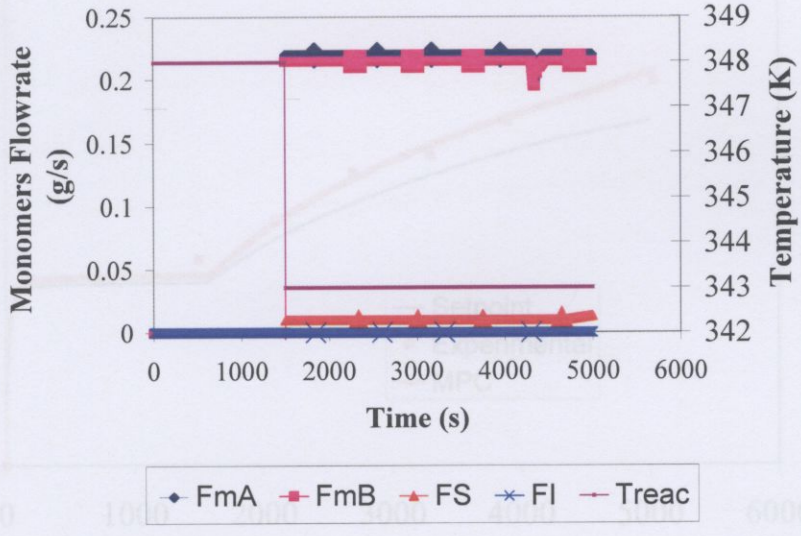

Figure 6.21. Optimal Feed Profile using off-line multivariable constrained MPC.

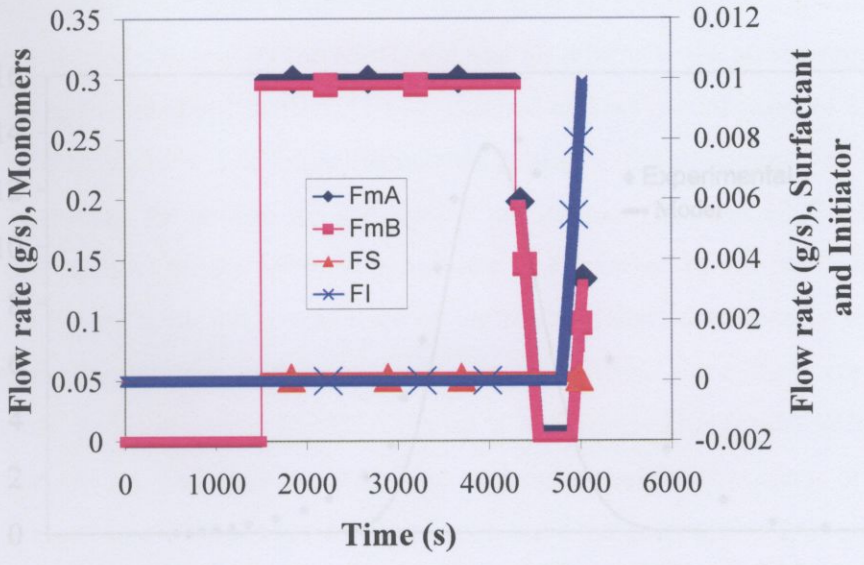

Figure 6.22. Optimal Feed Profile using on-line multivariable constrained MPC.

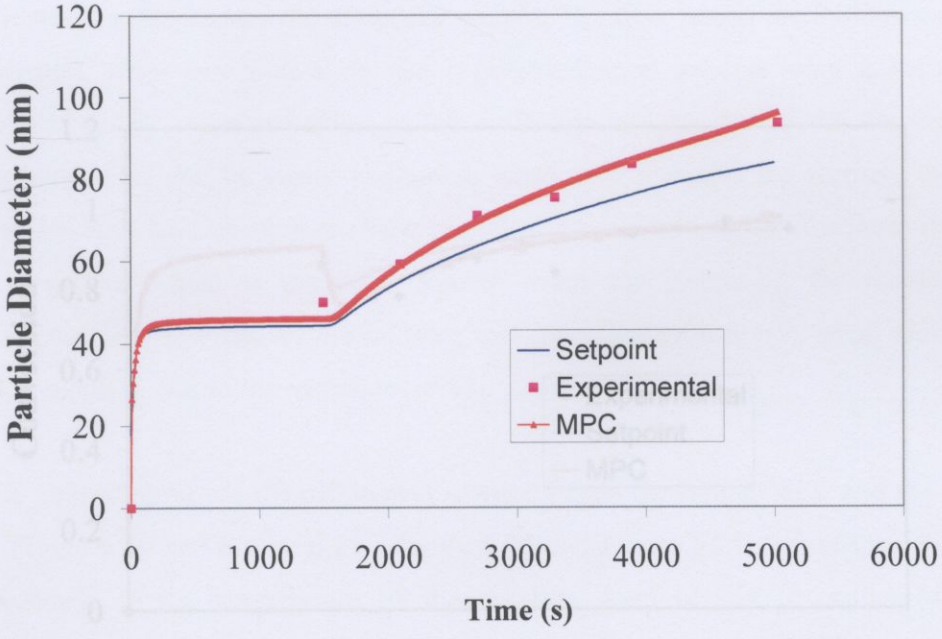

Figure 6.23. Experimental particle size using on-line multivariable constrained MPC.

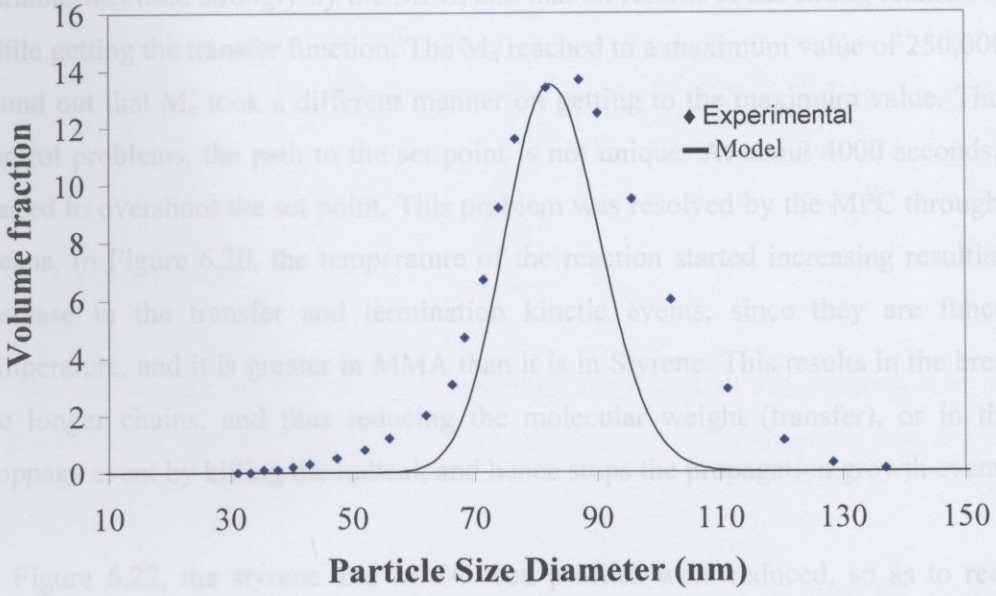

Figure 6.24. PSD under optimal operation (Constrained MIMO MPC).

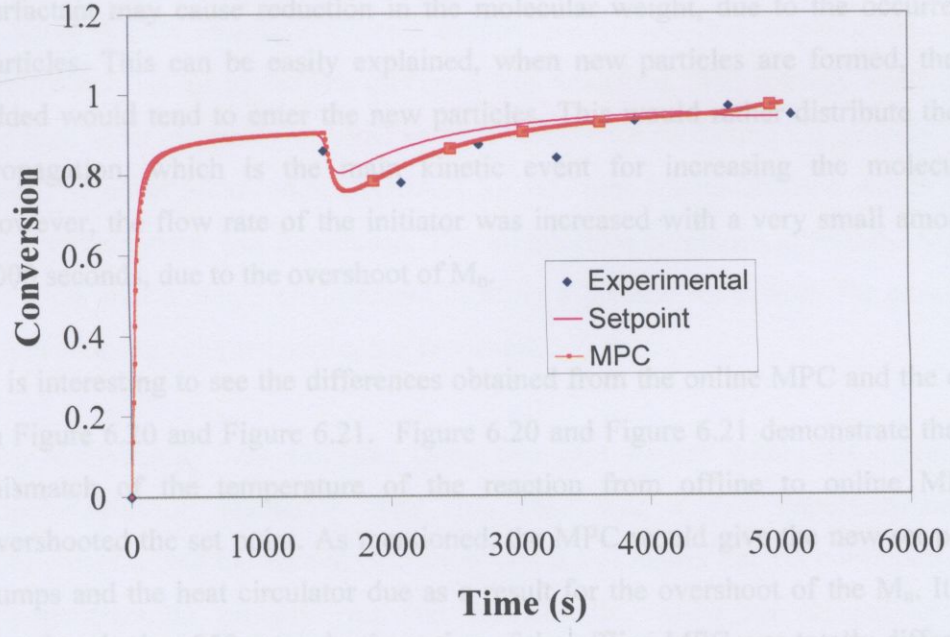

Figure 6.25. Experimental Overall Conversion using on-line multivariable constrained MPC.

It is clearly observed that the temperature had a great effect on the M_n, and the temperature variable was used strongly by the MPC, and that all returns to the strong relation obtained, while getting the transfer function. The M_n reached to a maximum value of 250,000. It was found out that M_n took a different manner on getting to the maximum value. Thus under control problems, the path to the set point is not unique. At about 4000 seconds, the M_n started to overshoot the set point. This problem was resolved by the MPC through several means. In Figure 6.20, the temperature of the reaction started increasing resulting in the increase in the transfer and termination kinetic events, since they are functions of temperature, and it is greater in MMA than it is in Styrene. This results in the break up of the longer chains, and thus reducing the molecular weight (transfer), or in the chain stoppage event by killing the radical, and hence stops the propagation growth event.

In Figure 6.22, the styrene and MMA feed profiles were reduced, so as to reduce the feeding process. This would consequently result in slowing up the process of increasing the molecular weight. The flow rate of the surfactant is very low, so as to provide micelles that will act in the stabilisation of the particles, and not to form any secondary nucleation that would rather reduce the molecular weight. The flow rate of the initiator was zero all of the time, since any radical in the copolymerisation process with a little amount of surfactant may cause reduction in the molecular weight, due to the occurrence of new particles. This can be easily explained, when new particles are formed, the monomers added would tend to enter the new particles. This would rather distribute the process of propagation, which is the main kinetic event for increasing the molecular weight. However, the flow rate of the initiator was increased with a very small amount at about 4000 seconds, due to the overshoot of M_n.

It is interesting to see the differences obtained from the online MPC and the offline MPC in Figure 6.20 and Figure 6.21. Figure 6.20 and Figure 6.21 demonstrate that due to the mismatch of the temperature of the reaction from offline to online MPC, the M_n overshooted the set point. As mentioned, the MPC would give the new set points for the pumps and the heat circulator due as a result for the overshoot of the M_n. It can also be seen in the last 950 seconds, the action of the offline MPC was totally different from the online MPC set points. For the offline MPC, the temperature of the reaction was put to the lowest value of the reaction at 343 K. For the online MPC, the temperature of the reaction was raised to compensate to the overshoot of the M_n.

The PSD and the conversion well agreed with the MPC online results. The conversion obtained by online MPC showed a larger drop at the feeding process at 1500 seconds, since a larger amount was added compared to the amount added in the optimisation process.

6.6 Conclusion

In this chapter, the on-line optimal control of the emulsion copolymerisation reactor is implemented. The strategy involved an MPC control scheme that was developed in MATLAB.

The novelty about the proposed strategy is the capability of the dynamic model for the semi-batch copolymerisation reactor (BASMI) to act as an on-line "soft sensor", and then incorporated with the MPC formulation embedded in Simulink for the PSD and MWD. Moreover, the full control of the copolymerisation plant was employed in one stage from Simulink. The soft sensor was running online to predict the PSD and MWD.

A novel generic multilayer control architecture for real-time implementation of optimal control policies for particulate processes was described. The strategy involved the use of the high order mechanistic model as "soft" sensor for predicting key process variables on-line. The novel architecture (ROBAS) for real-time implementation within an industrial DCS environment was introduced. The architecture combines gPROMS, MATLAB and the DCS into a single environment creating a generic framework for advanced control applications in complex particulate processes.

The methodology was validated using two case studies within the on-line control of copolymerization reactors. The first case was a 4x4 copolymerization control configuration, and the second case study was a 5x4 matrix control configuration. The first copolymerization process was run isothermally, while the second case used the temperature as an additional manipulated variable.

In the first case study, the MPC was successful in controlling the PSPI at the optimum trajectory and maintaining the conversion, M_n and the particle size on the specified setpoints. As a result, a broad PSD was obtained and the soft sensor results were in great accord with the experiment results.

In the second case study, the MPC was also successful in controlling the M_n at its optimum trajectory, while maintaining the average particle size, conversion and the PSPI on the optimal profiles. However, the M_n profile found by MPC was different from the optimal profile obtained from the optimisation problem, but still achieving the main goal in controlling the M_n and maintaining it to the optimum value.

The soft sensor values played a centre role in controlling the emulsion copolymerisation process, where it supplies with the online values of the conversion, M_n, average particle size and the PSPI. The soft sensor was again validated, on implementing it in the advanced control process.

Lastly, the achievement of this success in the proposed control strategy returns to the advanced techniques in the areas of process modelling (developed in gPROMS) and model based control (developed in MATLAB). However, the success of process modelling means the success of a well developed dynamic model, and the success of model based control in this context means the success of the overall architecture, so called "ROBAS architecture".

6.7 References

Callaghan, P. J. and Lee, P. L. (1988) Chem. Eng. Res. Des., 66, 345.

Culter, C. R. and Ramaker, B. L. (1979) Dynamic Matrix Control - A computer control algorithm, Houston, Texas.

Cutler, C. R. (1983) Ph.D. Dissertation, University of Houston, Houston, TX.

Dimitratos, J., Elicabe, G. and Georgakis, C. (1994) AIChE Journal, 40, 1993-2021.

Dimitratos, J., Georgakis, C., El-Aasser, M. S. and Klein, A. (1991) Chem. Eng. Sci., 46, 3203-3218.

Eaton, J. W. and Rawlings, J. B. (1990) Comput. Chem. Eng., 14, 469-479.

Echevarria, A., Leiza, J. R., Cal, J. C. d. l. and Asua, J. M. (1998a) AIChE J., 44, 1667-1679.

Echevarria, A., Leiza, J. R., de la Cal, J. C. and Asua, J. M. (1998b) AIChE Journal, 44, 1667-1679.

Fevotte, G., McKenna, T. F., Othman, S. and Santos, A. M. (1998) Comput. Chem. Eng, 22, 443-449.

Franklin, G. F. and Powell, J. D. (1980) Addison-Wesley Publishing Co.: Reading, MA.

Garcia, C. E. (1984) AIChE, Annual Meeting, San Francisco, CA.

Gobin, F., Zullo, L. C. and Calvet, J.-P. (1994) Computers & Chemical Engineering Proceedings of the 25th European Symposium of the Working Party on Computer Aided Process Engineering-3, Jul 5-7 1993, 18, 525-528.

Gordon, D. L. and Weidner, K. R. (1981) In ACS Symp. Series in Emulsion Polymers and Emulsion PolymerizationWashington, DC.

Hawkett, B. S., Napper, D. H. and Gilbert, R. G. (1981) Journal of the Chemical Society-Faraday Transactions I, 77, 2395-2404.

Immanuel, C. D. and Doyle III, F. J. (2002) Chemical Engineering Science, 57, 4415-4427.

Liotta, V., Georgakis, C. and El-Aasser, M. S. (1997) in: Proc. American Control Conf., Albuquerque, NM, 1172-1176.

Lundstrom, P., Lee, J. H., Morari, M. and Skogestad, S. (1995) Comput. Chem. Eng., 19, 409.

Marchetti, J. L., Mellichamp, D. A. and Seborg, D. E. (1983) Ind. Eng. Chem. Process Des. Dev., 22.

Mathworks, Simulink, http://www.mathworks.com

Maurath, P. R., Laub, A. J., Mellichamp, D. A. and Seborg, D. E. (1988) Ind. Eng. Chem. Res., 27, 1204.

Maurath, P. R., Mellichamp, D. A. and Seborg, D. E. (1985) Proc. Amer. Cont. Conf., IEEE Publications, 1059.

Ozkan, L., Kothare, M. V. and Georgakis, C. (2002) In 2002 American Control Conference, May 8-10 2002, Vol. 5 Institute of Electrical and Electronics Engineers Inc., Anchorage, AK, United States, pp. 3864-3869.

Ricker, N. L. (1991) Model Predictive Control: State of the Art, Amsterdam, Holland.

Vicente, M., Leiza, J. R. and Asua, J. M. (2001) AIChE Journal, 47, 1594-1606.

Vicente, M., Sayer, C., Leiza, J. R., Arzamendi, G., Lima, E. L., Pinto, J. C. and Asua, J. M. (2002) Chemical Engineering Journal, 85, 339-349.

Chapter 7

Conclusions and Future Directions

7.1 CONCLUSIONS 7.2
7.2 FUTURE WORK 7.3

7.1 Conclusions

This doctoral thesis findings are the development of a dynamic model for the advanced control of emulsion copolymerisation reactors, and the ability to predict the key polymer properties, which identify the physical and chemical properties of the copolymer produced, relying on customer's needs. This doctoral thesis addressed the development of the modelling of emulsion copolymerisation process, the automated reactor facility used for model validation, and the advanced control techniques employed to control the process and improve the performance of the reaction process.

The main conclusions are summarised in the following:

- **Dynamic Modelling and Optimisation:** The mathematical model, developed in gPROMS, is capable of predicting PSD, MWD, average particle size, M_n, M_w, conversion, comonomer composition and many other properties. Validation of the dynamic model was undergone with the experimental results, using the automated reactor facility at different operating conditions to ensure the capability of the dynamic model to be run online, that are to be able to predict the key polymer properties within the expected changes in the operating conditions. The dynamic model was then used to optimise the copolymerisation process. The optimal profiles were obtained, and the simulation results of the optimisation problem were validated.

- **Automated Reactor Facility, 1L/5L:** The 1L reactor with the automated facility was ready launched on starting the project, and was thus used to validate the simulation of the model with the experimental results, and that is within the model development stage. On the optimisation stage, the 5L reactor arrived. The 5L reactor was thus launched with the new automated facility. The 5L reactor was therefore used to validate the optimal results obtained by the mechanistic model.

- **Advanced Control:** The control of the copolymerisation process was employed using advanced control techniques. The control of the process is essential to take care of disturbances in the plant, change in operating conditions, shutdowns and startups. The DMC of the copolymerisation model was obtained. Using MATLAB,

the transfer functions relating the inputs with outputs were gained. The MPC formulation was then developed in MATLAB. Five inputs were used to control four outputs. Two MIMO systems were studied to control the PSD and MWD of the copolymer. The first case was to maximise the PSPI, where a broad PSD is required, and hence a bimodal distribution was obtained, besides maintaining the average particle size, M_n and conversion on their setpoints profiles. The second MIMO case was to maximise M_n, while maintaining PSPI, conversion and particle size on the specified setpoints. The MPC was able to follow the setpoint profiles. This was even clearer in the second MIMO case, where the M_n setpoint was achieved, but through a path different from what had been obtained from the optimisation problem.

Finally, one of the important outcomes of this thesis is development of the methodology of the *gPROMS – MATLAB/Simulink – Honeywell* link to control the plant online was implemented. The gPROMS model was embedded in Simulink as a block, and the MPC formulation was developed in MATLAB. The link to the DCS system was developed through dll files developed in C++. This means that running Simulink would let us control the plant on real time.

The architecture, so called "ROBAS" Architecture", is used to control the copolymerisation process. The architecture is a generic architecture that can be applied to most systems, especially to particle complex systems.

7.2 Future Work

The development of the mechanistic model is a success, but it is just the ignition and the start-up for a better understanding to copolymerisation processes. Hence, consideration is taken to future work.

- The most obvious area for future work is to extend into terpolymerisation processes, which will in return improve the characteristics and properties of the synthetic polymer produced; due to the addition monomer added incorporating new properties. The key polymer properties including PSD and MWD and conversion,

should be included in the modelling studies, since these properties mainly affect the final properties of the polymer to satisfy customer's needs.

- The model bases onto zero-one kinetics can be divided into two different regions, where the zero-one kinetics is applied in one region, and the pseudo bulk system is applied on the other region, especially that MMA has a part of its kinetics that obeys better in the pseudo bulk region, i.e., there is more than one radical that may enter the particle, without undergoing instant termination, and so the average number of radicals per particle could be greater than 0.5. So a model could be developed on the condition of the average number of radicals per particle.

- Coagulation studies should be included in future work. The velocity and shear distribution of the emulsion polymerisation process is being studied nowadays, and on success could be upgraded to study the copolymerisation case. The dynamic model could then be integrated with the coagulation model to achieve more accurate results, and better understanding of the process. However, there are softwares such as CFX, which is a Computational Fluid Dynamics (CFD) package, which provides the tools and means to model coagulation problems by predicting shear rates and velocities within the reactor. This integration would enable us to control the process better, and to improve the performance of the reactor.

- The incorporation of the model developed in gPROMS as a unit in Hysys, where the whole plant can be managed onto Hysys software. HYSYS is the only commercially available integrated simulation environment designed for complete user customization. This enables the seamless integration of proprietary unit operations, reactions and property packages, and interaction with other applications to create powerful hybrid programs, allowing companies to fully leverage engineering software investments.

- The code in gPROMS can be coded in C++, so that further benefit can be used like having the soft sensor on a chip that acts as a soft sensor to the copolymerisation process.

- The model developed for styrene-MMA copolymerisation can be used for other copolymerisation processes, to develop a package for the emulsion copolymerisation processes.

- An expert system can be developed for the semi-batch pilot scale emulsion copolymerisation reactor facility. This complex facility can be connected to the proprietary data acquisition system, Honeywell PlantScape. The expert system architecture will provide continuous support and rectification of product off-specs, monitoring and maintaining safety functionality. The knowledge-based system will be built under multiple layers of a proposed supervisory architecture. This expert system would be built using G2^{TM} (Gensym Corp). The expert system provides diagnostic and decision support to the operator. The whole framework is to be supervised by the expert system G2^{TM}, to have a good performance, which is reliable and robust.

- Better development can be brought to the polymerisation Lab, where mono-dispersed particles can be targeted using the model as a tool towards producing those type of particles. A final future development of the polymerisation lab is to add a GPC instrument, where the lab will be fully dependent on itself. An in-line particle size measurement is one of the main developments that could be done in future developments for the polymerisation lab. This means that the samples are going to be taken online, and measured. That information of the particle size would then be sent directly to the MPC of the copolymerisation reaction.

- Minor future developments could be added in the control room of the plant, where the polymer properties can all be seen on a large screen, while the copolymerisation reaction is running. Other future developments could be by adding transfer agents, and incorporating that in the model, and test the effect of adding transfer agents, and validating it through the experiments. The transfer agent can then be used as one of the controlled variables to control the MWD.